Industria Textilă

ISSN 1222–5347

4/2026

ISI rated** journal, included in the **ISI Master Journal List** of the Institute of Science Information, Philadelphia, USA, starting with vol. 58, no. 1/2007, with **impact factor 1.0 and AIS 0.091 in 2025.

The journal is indexed by CrossRef, starting with no. 1/2017 having the title DOI: https://doi.org/10.35530/IT.

Edited in 6 issues per year, indexed and abstracted in:

Science Citation Index Expanded (SCIE), Materials Science Citation Index®, Journal Citation Reports/Science Edition, World Textile Abstracts, Chemical Abstracts, VINITI, Scopus, Toga FIZ technik, EBSCO, ProQuest Central, Crossref

Scientific reviewers for the papers published in this number:

EDITORIAL STAFF

Aknowledged in Romania, in the Engineering sciences domain, by the National Council of the Scientific Research from the Higher Education (CNCSIS), in group A
Journal edited in colaboration with **Editura AGIR**, 118 Calea Victoriei, sector 1, Bucharest, tel./fax: 021-316.89.92; 021-316.89.93; e-mail: editura@agir.ro, www.edituraagir.ro

Design and development of an H-shaped wearable antenna for medical and wireless applications using textile materials

DOI: 10.35530/IT.077.04.202543

GURUPRASATH RENGARAJAN NAGARAJAN RAMALINGAM

ABSTRACT – REZUMAT

Design and development of an H-shaped wearable antenna for medical and wireless applications using textile materials

The main goal of this research is to design, develop, and fabricate a small H-stub antenna suitable for contemporary wireless communication systems. The antenna's 46 mm × 30 mm × 1.6 mm dimensions make it perfect for uses where weight and size are crucial limitations. By functioning well at 2.5 GHz to 12 GHz frequencies that correspond to important bands in modern wireless technologies, the suggested antenna exhibits triple-mode capability. The antenna employs innovative design techniques, including a parasitic strip and a reconfigurable ground plane slot, to accomplish efficient energy distribution across the antenna, incorporating H-shaped stubs that extend from the ground. Using a thick Teflon, yarns, and FR4 substrate ensures that the antenna meets the needs of modern wireless communication systems and also boosts bandwidth. Despite its small size, the antenna's adaptability comes from its ability to retain high efficiency and dependability over various frequency bands. Performance tests verify that the antenna can provide broad bandwidth, high radiation efficiency, and steady operation, all of which are in line with the changing needs of next-generation wireless communication. As Internet of Things (IoT) applications proliferate in today's communication networks, there is an increasing need for tiny antennas. IoT applications widely use microstrip patch antennas due to their compatibility. Because it is designed to function at a frequency of 2.5 GHz to 12 GHz, it may be used for IoT applications. It is designed to be used as an integrated antenna in an IoT device and is composed of a variety of H shapes. The main findings of this study show that, in comparison to a conventional antenna, the optimised shaped antenna enhanced bandwidth, gain, and return loss.

Keywords: *H-shaped, textile, gain, return loss, radiation pattern, VSWR*

Proiectarea și dezvoltarea unei antene purtabile în formă de H pentru aplicații medicale și wireless folosind materiale textile

Scopul principal al acestui studiu este proiectarea, dezvoltarea și fabricarea unei antene mici, în formă de H, potrivite pentru sistemele contemporane de comunicații wireless. Dimensiunile antenei de 46 mm × 30 mm × 1,6 mm o fac perfectă pentru utilizări în care greutatea și dimensiunea sunt limitări cruciale. Funcționând bine la frecvențe cuprinse între 2,5 GHz și 12 GHz, care corespund benzilor importante din tehnologiile wireless moderne, antena sugerată prezintă capacitate triplă de funcționare. Antena utilizează tehnici inovatoare de proiectare, inclusiv o bandă conductoare și un slot reconfigurabil în planul de masă, pentru a realiza o distribuție eficientă a energiei pe întreaga suprafață a antenei, încorporând ramificații în formă de H care se extind de la planul de masă. Utilizarea unui substrat gros de Teflon, fire și FR4 asigură faptul că antena îndeplinește cerințele sistemelor moderne de comunicații wireless și, de asemenea, sporește lățimea de bandă. În ciuda dimensiunilor sale mici, adaptabilitatea antenei provine din capacitatea sa de a menține o eficiență și o fiabilitate ridicate pe diverse benzi de frecvență. Testele de performanță confirmă faptul că antena poate oferi o lățime de bandă largă, o eficiență ridicată a radiațiilor și o funcționare constantă, toate acestea fiind în conformitate cu nevoile în continuă schimbare ale comunicațiilor wireless de ultimă generație. Pe măsură ce aplicațiile Internet of Things (IoT) proliferează în rețelele de comunicații actuale, există o nevoie tot mai mare de antene minuscule. Aplicațiile IoT utilizează pe scară largă antene microstrip de tip patch datorită compatibilității lor. Deoarece este proiectată să funcționeze la o frecvență cuprinsă între 2,5 GHz și 12 GHz, aceasta poate fi utilizată în aplicații IoT. Este concepută pentru a fi utilizată ca antenă integrată într-un dispozitiv IoT și este compusă dintr-o varietate de forme de tip H. Principalele concluzii ale acestui studiu arată că, în comparație cu o antenă convențională, antena cu formă optimizată a îmbunătățit lățimea de bandă, câștigul și pierderea de retur.

Cuvinte-cheie*: formă de H, textil, câștig, pierdere de retur, diagramă de radiație, VSWR*

INTRODUCTION

In order to provide wearable sensors more flexibility, flexible substrates such as polymers, plastics, paper, textiles, and fabrics are now required. The basic aim is to examine the bending, flexibility, and tendency to accept deformation of polymer materials. This research starts by providing a chronological summary of the flexible materials that have been used during the last several decades. To enable new applications via wireless connection, it is projected that the IoT will eventually support a wide variety of technologies. Materials need to be pliable and bendable for wearable IoTs to work. The mechanical, electrical, and physical properties of several popular polymer substrates are examined in this work. It also examines the effects of bending on the radiation performance of polymer-substrate antenna designs. Rogers RT/Duroid, liquid crystal polymer (LCP), polyimides (PI), polyethylene terephthalate (PET), polydimethylsiloxane (PDMS), and polytetrafluoroethylene (PTFE) are a few of the flexible materials that have been examined. These materials are used in the antennas of the IoTs. The S-parameters, resonant frequency deviation, and impedance mismatch with the feedline of flexible polymer substrate microstrip antennas are all closely examined in this work. These flexible polymer substrates may be used in general IoT applications and future wearable electronics. Flexible electronics are becoming essential for biological applications with complex curvilinear geometries and applications requiring flexible displays [1–5].

In response, researchers have tried to increase the flexibility of electrical devices by experimenting with a range of materials as substrates, such as polymers, plastic, paper, textiles, and fabrics. The capacity of various materials to bend, twist, and/or crumple is determined by their individual qualities. Because of their bendability and flexibility, these materials may be used in designs for future smart electronics systems as well as IoT applications. The bending properties of various materials are crucial for several electrical and communication applications. Examples of these include developments in flexible antennas, smart tags, and wearable technology [6–10].

In actuality, flexible displays and antenna systems are now widely used in business, healthcare, the military, and personal communication. These versatile devices are frequently used in aviation, RFID tagging applications, and health monitoring systems. Flexible circuits, such as thin sheets of carbon nanotubes on plastic substrates, provide a lightweight and conformal architecture. These flexible integrated circuits have a wide range of potential uses in embedded systems and other electronics domains, and several varieties of flexible RFID tags are currently widely used. Active-matrix displays, stretchy power sources, and stretchy organic solar cells, which may double as biological sensors, are recent examples of flexible electronics. Other novel applications recently introduced to the market include skin-like sensing robotic systems, electronic paper, flexible displays and touch screens [11–15]. Smart clothes and fashion are becoming increasingly popular. The past ten years have seen a rise in the popularity of smart attire. The electronic fibres that make up smart shirts and jackets enable the user to answer four out of twenty-five calls and listen to music and entertainment shows. With their smart clothing, the user can take pictures or videos using the built-in camera. Smart watches, smart jewellery, smart shoes, and wristbands are a few examples of wearable technology that are becoming more and more popular.

Since flexible communication systems are in great demand and wearable sensors and gadgets are evolving at an exponential pace, several new problems have arisen as a result of the exceptional performance requirements. The frequent example of wearable electronics with flexible antennas serves as a pertinent illustration for this work. The flexible antennas must thus be tiny, light, robust, heat and moisture-resistant, and above all extremely flexible without compromising the radiating properties. As a result, the primary focus of our study is on the seamless integrity and flexibility of flexible antennas. Conventional antennas are usually built by manufacturers using conductive wires or rigid substrates engraved with metal patterns. Stretching, folding, or twisting these antennas results in permanent deformation, if not shattered. This implies that they are not suitable for applications requiring a high degree of flexibility. Flexible antennas, due to their great degree of flexibility, have directly addressed this problem. Other advantages include their ease of integration with other microwave components, light weight, low energy consumption, ease of manufacturing, affordability, and widespread availability as substrate films. The concept of flexible wearable antennas emerged from the steady evolution of the Flexible Electronic System (FES). An increasing number of physical objects, wirelessly linked via antennas, form the IoT. The IoT affects transportation, the health and agriculture industries, industrial automation, and above all, emergency responses to natural disasters [16–20].

The IoT enables information sharing and decision-making based on objects connected to algorithms. IoT devices are now improving people's lives and expanding the scope of business uses. For instance, smart homes enable homeowners to switch on and off devices such as TVs, alarm systems, monitoring systems, and heating systems, as well as remotely and wirelessly control the temperature of particular rooms. Passive antennas, which are available in a range of materials, are used in almost all mobile electronic devices nowadays. Flexible antennas are becoming more and more popular because they provide a number of advantages over traditional rigid antennas. Their ability to combine conventionally sturdy materials with lightweight, thin, and low-profile designs is what makes them appealing. Standard antennas are 50–70% bigger and heavier than flexible antennas, rendering them less appropriate for small and lightweight applications. Flexible antennas provide a more efficient solution for contemporary wireless systems, particularly in portable and wearable devices where dimensions, weight, and flexibility are essential design factors. The size may be further reduced to around 90% of its initial size for a certain frequency by using a flexible substrate, such as a polymer, in place of hard printed boards. Flexible antennas are not only very lightweight and robust, but they can also tolerate high mechanical loads. Conductive materials can transfer electricity with little loss or emit energy in the form of electromagnetic (EM) waves. When the antenna has to be distorted from its typical straight posture, the materials must be able to withstand material deterioration and have bending capabilities, meaning they must be able to bend, crumple, and stretch without impairing the antenna's functionality [21–25].

The material utilised for the conductors must be able to withstand repeated pressure, and low resistance and high conductivity are still crucial components of these conductors' electrical characteristic qualities required for flexible wearable technology, such as RFID tags and flexible antennas, and for flexible electronic systems in general. The designed antenna with the support of conductive materials needs to be highly elastic, deformable, and conductive in addition to having a high bending, adhesion, and textile integration capability. They should simultaneously have minimal moisture absorption, resistance, and moisture content. Out of 50 experimental works that are studied on flexible antennas, we chose 20 for qualitative analysis in order to provide the reader with a comprehensive picture of the whole area for the range of various frequencies and applications. We carry out these investigations in a variety of settings and use a range of manufacturing and experimental methods.

However, considering the limitations, we grouped several experiments with almost equivalent physical characteristics and similar frequency ranges [26–30]. We also examine how previous studies compare the resonant frequency variations, gain, and reflection coefficients of antennas fabricated from flexible polymer substrates. Polymers from previous articles, such as PI, PET, PTFE, PDMS, and LCP, with certain modifications, are examined in this table. It also analyses the radiation characteristics for a specific application and illustrates the effects of bending on return loss, resonant frequency, and antenna gain. PI is the most often used of these five polymers as a flexible antenna substrate. Commercially, Kapton is a variant of PI. Because of its exceptional thermal stability and great electrical, chemical, and physical balance, we chose polyimide Kapton as the antenna's substrate. They discovered that there was an 80 MHz shift in the resonant frequency, or 0.36% of the 2.45 GHz resonant frequency. When compared to the flat example, the resonant frequency changes by the greatest 0.4% at the trial resonance frequency, which is less than 50 MHz.

When the antenna is bent to a smaller size of 9 mm, with silver nanoparticles serving as the conductor and Kapton (200 HN) as the base, it shifts frequencies by 1.1 GHz at maximum. The increase in directivity at 8.8 GHz results in a 3 dB increase in return loss.

Similarly, various flexible antennas employ Kapton (500 HN), which is roughly 130 mm thicker than Kapton (200 HN) but has a lower resistivity and a larger dissipation factor (209). A compact Kapton-based inkjet-printed multiband flexible antenna with convex and concave bending at a maximum level of 59 mm. The antenna operates in the following four wide frequency bands: 1.2 GHz, 2.0 GHz, 2.6 GHz and 3.4 GHz. Convex bending has no noticeable frequency shift, but concave bending exhibits a 3% frequency shift toward the lower end across all frequency bands. At higher centre frequencies, the gain rises with convex bending of up to 59 mm because of the increase in directivity that results from the antenna experiencing this greater curvature [31–33]. In Kapton 500 HN, a tiny, flexible antenna for WLAN and upper UWB applications, is coated with parylene-C to increase its flexibility without significantly altering its gain and return losses. Wearable flexible antennas have the potential to crumple, which might reduce their radiation effectiveness. Kapton 500 HN is an efficient polymer that can withstand high crumpling levels of up to 5.5 mm, according to this research.

DESIGN OF H-SHAPED ANTENNA

The performance of the suggested antenna at a high operating frequency of 2.5 to 12 GHz with a maximum gain of 8.2 dBi is the main focus of the research. Teflon and yarns have been used extensively in applications that need substrate flexibility and transparency. The antenna is bent; the frequency shift is minimal for flexible W-BAN antennas. The completely adjustable antennas with flexible antennas were created to function at 5.5 GHz and 10.5 GHz, proving.

The reflections are the same for bends of 60 degrees or greater. This extensive assessment emphasises a thorough comparative examination of both chemical and thermal characteristics of the flexible materials. The substrates of flexible antennas in the past provide a useful reference to better match their compatibility with certain wearable applications when choosing the right substrate for flexible antennas. One crucial feature of IoTs is their adaptability, which calls for adaptable antennas for communication. The article includes an overview of the bending process and an examination of the characteristics of several materials.

The article gives a summary of the bending process and presents the materials. This works well for adaptable IoT applications. Flexible antennas have the following properties: directivity, gain, and return losses. The performance of the suggested antenna is greatly impacted by degradation. Here, the behaviour of these flexible antennas with various substrates under various folding circumstances with the lowest curvature radiation was observed. There is a noticeable effect on the antenna. There is too much distortion in the radiation to get acceptable outcomes. It is determined that the radiation's properties have a specific amount of curvature and are too twisted to provide useful results. It could be beneficial to share the antenna's low-profile forward radiation, which takes advantage of the electromagnetic bandgap or subpar ground structure is shown in figure 1.

When utilised near angled surfaces, the antennas bend or flex, which might alter their reflecting qualities:

$$W = \frac{V_o}{2f_r}\sqrt{\frac{2}{\varepsilon_r + 1}} \tag{1}$$

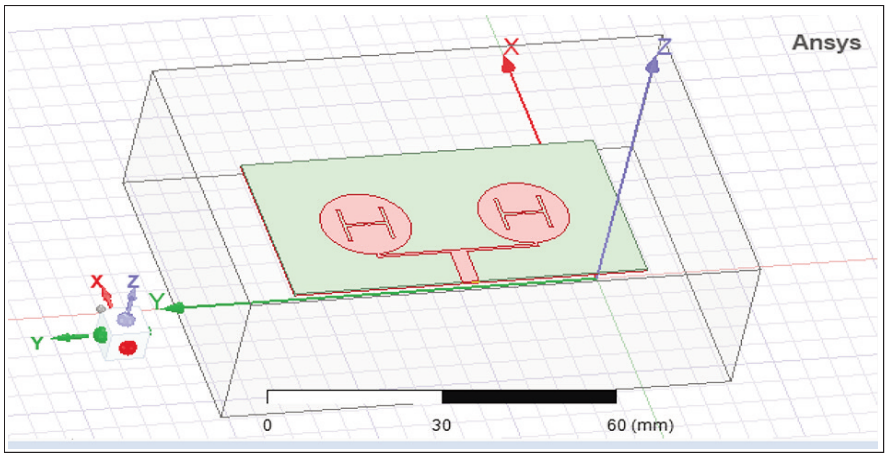

Fig. 1. H-shaped antenna structure

The antennas are tested for bending in a range of bending situations to make sure they work as intended, since they are made on flexible substrates. Antenna parameters are shown in table 1. The Teflon-based material commonly used in antenna design is polytetrafluoroethylene (PTFE), which is a high-quality insulating material known for its low dielectric constant, low loss tangent, and excellent heat resistance. PTFE is often augmented with glass fibres or ceramics to improve mechanical strength, particularly in printed circuit board (PCB) applications. In RF and antenna applications, conductive yarns, including silver-coated nylon, carbon-based fibres, and metallic threads, are often used. These threads function as conductive pathways or structural reinforcement in flexible or textile-based antennas.

$$L = \frac{V_o}{2f_r\sqrt{\varepsilon_{reff}}} - 2\Delta L \tag{2}$$

where V_o is the speed of light, ε_{reff} – effective permittivity, $2\Delta L$ – extension in length, W – width, f_r – resonating frequency and ε_{reff} – effective radiated power.

$$f_r = \frac{c}{2L\sqrt{\varepsilon_r}} = \frac{1}{2L\sqrt{\varepsilon_0\varepsilon_r\mu_0}} \tag{3}$$

Where ε_0 is the permittivity of free space, ε_r is the permittivity of the dielectric substrate, and μ_0 is the permeability of free space. The operating frequency of a patch antenna, considering L and W, is given by L – length of the patch and c – velocity of light:

$$f_r = \frac{c}{2\sqrt{\varepsilon_{reff}}}\left[\left(\frac{n}{L+2\Delta L}\right)^2 + \left(\frac{m}{w+2\Delta w}\right)^2\right]^{1/2} \tag{4}$$

where $n = 1$, $m = 0$.

$$f_{r(nm)} = \frac{c}{2(L+2\Delta L)\sqrt{\varepsilon_{reff}}} \tag{5}$$

$$\varepsilon_{reff} = \frac{\varepsilon_{r+1}}{2} + \frac{\varepsilon_{r-1}}{2}\left[1 + 12\frac{h}{w}\right]^{-1/2} \tag{6}$$

$$\Delta L = 0.412h\frac{\left(\varepsilon_{reff}+0.3\right)\left(\frac{w}{h}+0.264\right)}{\left(\varepsilon_{reff}-0.258\right)\left(\frac{w}{h}+0.8\right)} \tag{7}$$

$$W = \frac{(W_L - W_H)}{2}\cdot\frac{(W_L + W_H)}{2} \tag{8}$$

Table 1

ANTENNA PARAMETERS		
Sl. No	**Parameters**	**Range**
1	Antenna size (mm)	46 × 30 × 1.6
2	Length (mm)	9.403
3	Width (mm)	12.67
4	Input impedance (ohm)	50
5	Dielectric constant (mm)	4.8
6	Dielectric height (mm)	2.2
7	Substrate	Teflon, Yarn

It is crucial to test textile antennas under a range of bending situations to determine how their characteristics change as they are twisted, since they are likely to be bent or otherwise moulded to a certain surface throughout the activity. The substrate, backplane, front panel, and encapsulation are the four primary components that comprise flexible electronic devices (FES). FES is composed of flexible materials such as textiles, conductive foils, polymers, plastics, and laminates. Selecting the appropriate "substrate", the first part that forms the basis of the whole circuit, is essential. The second component is the backplane, which is a printed circuit board (PCB) with slots for connecting electrical components. The third section, the front panel, is usually a sheet of metal that secures the pieces and allows for certain adjustments to the system components.

In table 1, the dimensions 46 mm × 30 mm × 1.6 mm represent the overall antenna size, specifying its length, width, and thickness, respectively. The substrate is listed as Teflon and Yarn; it is important to specify the type of yarn used. The yarns incorporated are conductive, composed of metallic threads, which enhance the antenna's electrical performance and flexibility. Including these details in table 1 will provide clearer insight into the antenna's construction and material properties for better comprehension and reproducibility. The last component is an encapsulating layer that protects the electronics by covering them. Flexibility is necessary for all of the FES components; otherwise, it would disrupt their normal functioning. Devices worn on the person and those in the surroundings may communicate with the Wireless Body Area Network (WBAN). Flexible wearable antennas and smart tags, such as radio frequency identification (RFID) tags, are examples of these wearable devices. The WBAN, which combines FES with readily connected body-worn electronics, is evolving to allow users to wear antennas and smart tags instead of carrying them about. Thus, the development of flexible wearable electronics on a flexible substrate, including smart tags and antennas, is an interesting area that needs more investigation.

Due to their low weight, affordability, and tiny size, planar antennas are becoming an essential component of modern biomedical equipment. The deployment of medical technologies like body area networks, remote health monitoring, and microwave imaging systems depends on these antennas. The antennas used in the above-described applications need to meet certain specifications and be constructed from lightweight, human-safe materials. Wearable antennas are used to measure a person's health by attaching them to their body. Therefore, the performance of the antenna, including its radiation characteristics throughout the operating frequency bands, should not be affected by the proximity of a human body. This study aims to highlight the effects of human body proximity on wearable antenna performance. The several kinds of flexible antennas that have been suggested for use in biological applications are also examined in this study. It describes the challenges of developing wearable antennas, how to choose a flexible material that is suitable for their creation, and the proper manufacturing methods. The future directions in this quickly developing field are also highlighted in this study. Flexible antennas are the cornerstone for implementing next-generation wireless communication devices for monitoring and health safety applications. The total effectiveness of the antenna will be greatly impacted by the physical changes and water absorption of the body. The design of these antennas is influenced by the operating environment, transmission strength, and operational frequency range.

However, the antenna's total performance is entirely determined by the dielectric material. Based on its capacity to retain its characteristics under certain circumstances, including bending, crumpling, and stretching impacts, the dielectric material employed in the antenna design was selected. The conductive materials on the dielectric material's top and lower layers are very resilient to deterioration and mechanical deformation. Understanding the electromagnetic characteristics of the material, such as the substrate thickness, permittivity, and loss tangent, is crucial for the creation of wearable antennas. Both conductive and non-conductive textiles, also referred to as electro-textiles, are commonly found in wearable materials. Non-conductive textile materials, including felt, silk, nylon, leather, washed cotton, denim, polymer, fleece, and paper, are often utilised in the production of wearable antennas to minimise their weight and profile.

A high-performance antenna system that may be worn on or off the body and connect with nearby devices can be made possible using conductive fabric materials. To make conductive textile (e-textile) materials, we mix ordinary textiles with conductive metals or polymer threads. Taffeta, Shieldith, Zelt, Flectron, and pure copper are examples of conductive textiles. Because of their durability and flexibility, these materials are suitable for use on the body and provide a substantial contribution to the wearable context. To build a high-performance antenna system, we need a lightweight and flexible substrate. The AUWB [Aero Ultra-Wide Band] health monitoring system tracks a variety of daily activities that support a healthy lifestyle by using several wearable sensors at various locations and distances. Furthermore, polarisation mismatches are caused by human body movement, and most wearable antennas have linear polarisation.

The closeness of wearable antennas to the human body has an impact on the antenna's gain, bandwidth, driving point impedance, and efficiency.

The analysis of the polynomial regression:

$$Y = w_0 + w_1 t_1 + w_2 t_2 + \dots + w_n t_n \tag{9}$$

The analysis of the multivariate regression analysis:

$$Y = w_0 + \textstyle\sum_{a_1=1}^{t} w_1 t_1 a_1 + w_1 \sum_{a_1=1}^{t} w_2 t_2 a_2 + \dots + \\ + w_n \sum_{a_1=1}^{t} w_n t_n a_n \tag{10}$$

here w_1, w_2 are polynomial regression coefficient, a – input variable, Y – output variable, w_0 – intercept, w_n – weight matrix.

Second polynomial $T_1 = R_s$, $t_2 = K_s$ and $t_n = F_s$:

$$Y = w_0 + w_1 R_s + w_2 K_s + \dots + w_n F_s \tag{11}$$

Algorithm 1

Input x,y
Initialize $w_0[|W_t|_1=R_s]$, $W_1[|W_t|_2=R_s]$, $W_n[|W_t|_n=F_s]$
While |M|-|T|>M or |M|-|K|>N do
$A_1' = |W_t^T a_1'|$
While |M|-|F|>M-1 or |M|-|K|>N-1 do
$A_2' = |W_t^T a_2'|$
Set $W_{1,2}=0$
End while
Output w_t, w_n

This technique delineates a procedure for the iterative update and optimisation of weight parameters using conditional evaluations. Initially, three sets of weights are established: the first two using a reference state and the last one employing a final state condition. The program thereafter initiates an outer loop that persists as long as the disparity between certain data set sizes surpasses established criteria. This indicates that the algorithm is seeing convergence or equilibrium among variables like model size, training data, or critical performance metrics. Within the outer loop, a transformation or activation is performed on the existing weights, presumably to assess performance or intermediate outcomes. If further size criteria between sets remain unfulfilled, a nested loop is initiated. Within this inner loop, an additional transformation is calculated, presumably to further refine or optimise the model. At this level, two particular weights are recalibrated to mitigate bias or interference from preceding stages.

The loops guarantee that weight changes persist until the model stabilises or meets the specified criteria. Upon meeting all requirements, the algorithm terminates, yielding revised weight values. The approach is intended to repeatedly enhance a model's internal parameters to attain an optimum condition based on structural and performance restrictions. Algorithms are pivotal in the Internet of Things (IoT), facilitating data processing, decision-making, and efficient communication among smart devices. Algorithms in an IoT system often link to multiple physical and digital entities. This category encompasses sensors (e.g., temperature, motion, humidity), actuators (e.g., motors, switches), microcontrollers, communication modules (e.g., Wi-Fi, Bluetooth, Zigbee), cloud platforms, and data analytics instruments. Each component creates or utilises data that algorithms must evaluate, interpret, or reply to instantaneously.

To enhance clarity, the author could include a succinct description of IoT. The Internet of Things (IoT) is described as a network of networked devices that may gather and exchange data to execute intelligent activities autonomously, without direct human involvement. This concept elucidates that algorithms are not independent entities; they are integrated inside or associated with devices functioning in physical contexts. Defining the Internet of Things (IoT) aids in determining the components that must interface with the algorithm, including the sensors that provide data, the actuators it governs, and the means of communication with cloud services. This viewpoint facilitates a more lucid comprehension of the system's architecture and the function of each component in realising intelligent capabilities.

Wearable antennas have garnered a lot of attention recently because of their attractive features and the potential for creating wireless communication systems that are portable, lightweight, affordable, and multifunctional. The use of lightweight materials and revolutionary developments in nanomaterial research has enabled the widespread use of wearable antennas. One-dimensional (1-D) nanomaterials known for their exceptional electrical conductivity and mechanical strength are carbon nanotubes (CNTs). While maintaining some of the antenna's electromagnetic properties, CNTs may be utilised in wearable antennas to increase the mechanical stability and lifetime of the device. CNTs, for instance, provide a balance between mechanical strength and flexibility in sports and health monitoring systems. AgNWs combine the exceptional electrical conductivity of silver with the versatility of nanoscale dimensions. Wearable antennas frequently use AgNWs to improve electromagnetic performance, particularly in terms of gain and bandwidth.

High-frequency broadband communication applications, such as wireless sensor networks with high resolution and fast data transmission, are especially well-suited for AgNWs. Graphene, a two-dimensional (2-D) carbon material, is well recognised for its exceptional electromagnetic properties and mechanical strength. Graphene is the perfect material for uses that need both strong physical strength and excellent electromagnetic performance, like better environmental sensing and health monitoring systems. We have also introduced several wearable textile antennas to fully integrate wearable systems into protective apparel and smart clothing. Shieldit, Flectron, and non-conductive textile substrates, such as Cordura layers, felt, cotton/polyester, fleece fabric, and flexible pad foam, are frequently seen in protective clothing. There has been a lot of work put into antenna designs that don't have bad soldering connections and that use antenna topologies that are less affected by changes in the thickness of the non-conductive layer and the conductivity and permittivity of textile materials.

The field of sheet waveguides offers a novel communication technique. This research examines examples of sensor, personal, and body area network applications, to replace a portion of wired communication with a new field that relies on wireless communication, taking into account the communication range. Whether indoors or out, ubiquitous sensor networks that are usable at any time and location are gaining popularity. It is consequently challenging to establish a single network for everything, as the number of apps keeps growing. Infrastructure technology that supports wireless sensor networks is necessary because they vary depending on the applications. Applications that accept wearable material as a sheet-like waveguide enable effective transmission. Since multiple sensors can be affixed to the human body, a smart suit composed of conductive fabric is a fantastic option for an auxiliary BAN transmission line. This allows for simultaneous power supply and sensor data collection. This opens up the possibility of using it to transmit information for military and disaster relief purposes.

RESULTS AND DISCUSSION

Human body communication (HBC) systems use a wearable antenna made of electrodes that come into contact with the body's surface to excite radio-frequency impulses inside the body. Like other wireless circuits, these antennas' input impedance properties are crucial design factors for boosting transmission efficiency and lowering signal reflection. In this study, we address how variances among actual human subjects can affect the input impedance characteristics of a wearable antenna prototype. We compare the analytical results with data from real people in the 1–100 MHz range. For the simulations, we used a real human arm model. From simulations of input impedance characteristics from antennas worn on the wrists of male and female models with dry and wet skin, it looks like there isn't much difference in impedance between the sexes. For frequencies higher than a few MHz, the skin's moisture content has minimal effect. Additionally, we propose a simplified rectangular prism model to examine the thickness of the bodily tissues. Individual variations in impedance are mostly caused by variations in the thickness of the skin and fat layers, according to comparisons of measured input impedances. Additionally, the model allows us to design the antenna prototypes without experiments involving several subjects. The reflection coefficient of the proposed antenna was evaluated from 2.5, 6.3, 7.7 and 9.7 GHz and attained a return loss of –15.23, –22.02, –17.56 and –33.72 dB. Notably, the average radiation path of the antenna at the H-plane bends over the y-plane, deviating from the normal. The related antenna output, however, remained constant under bending circumstances. Additionally, there was a substantial difference between simulation and calculation due to the influence of the tiny ground plane on the feeding cable.

The VSWR of the proposed antenna was evaluated from 2.5, 6.3, 7.7 and 9.7 GHz and attained values of 1.62, 1.17, 1.3 and 1.02. The results showed that bending curvatures had a major effect on the cost and cumulative dispersion of radiation. Notably, the entire antenna architecture was examined in three general locations: the wrist, arm, and chest. The fact that the antenna's front-to-back radiation density drops with increasing bending curvature is a beneficial feature for WBAN applications. The bandwidth remained almost constant in every situation that was examined.

The results demonstrated that for all operational frequency ranges from 2.5 to 12 GHz and all bending radii of the wearable antenna, the realised reflection coefficients were less than 10 dB. For every bending radius, the conformal UWB antenna's reflection coefficient response was the same. Thus, the recommended antenna design is the ideal choice for UWB wearable applications because of its thickness, durability, and flexibility. However, a little change in the cardboard used to cover the antenna during the compatibility test might account for the calculated findings. Furthermore, there's a chance that the cardboard itself has certain dielectric properties, which would undoubtedly alter the operating frequency. The antenna achieves a gain of 8.27 dBi in the ISM medical range, with a value greater than 20 dB. It is clear that it has outstanding efficiency even under a range of bending situations and has no impact on human safety since the SAR value is less than 0.15 W/kg, which is much lower than the normal implementation level. The flow chart of the proposed antenna is shown in figure 2.

Researchers evaluated and compared how well complementary structures integrated with the human body. Two body-worn antennas were highlighted: a meandering slot antenna with an ungrounded surface and a printed patch antenna with a meandering ground. This work shows that magnetic antenna designs, including meandering slot printed antennas, are favoured for wearable systems, even if similar structures are practically the same in non-wearable systems. By making careful design decisions, the susceptibility of these antennas near the human body may be greatly decreased.

Wireless technology plays a key role in the development of flexible and elastic electronics, which has attracted attention in response to the rising need for devices that are compact, light, and comfortable. Microstrip antennas have emerged as desirable alternatives in the wireless technology sector due to their high degree of flexibility and complex bending electronics construction. However, the flexibility of microstrip antennas often leads to a decrease in their conductivity and radiation efficiency. To solve this problem, we suggested two designs: the arch-shaped microstrip antenna and the stretchy mesh microstrip antenna. Both antennas use conductive materials to cover a silicone substrate. Depending on the bending condition, the resonance frequency of the antennas varies. However, the variation is determined by the strain of the antenna element. The resonance frequency of the meshed microstrip antenna decreases as the antenna strain increases. The strain of the arching antenna must be greatly decreased in order to increase its resonance frequency. The microstrip antenna's resonance frequency rises 8.5 and 5.5 times, respectively, indicating that it is more susceptible to strain than the other one.

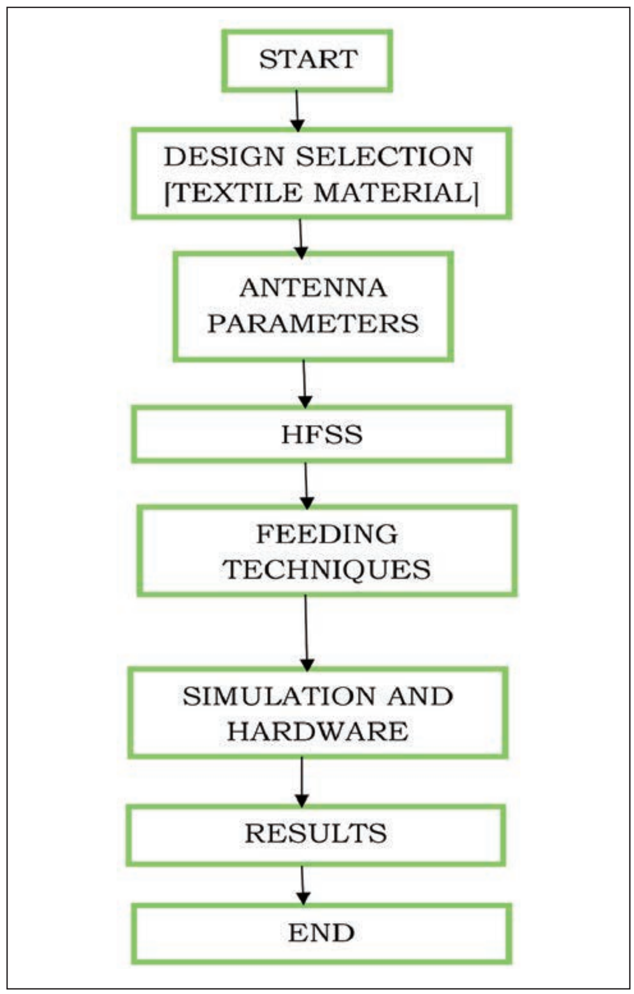

Fig. 2. Flow chart of the proposed antenna

Consequently, the following research questions and significant topics are enumerated for more investigation in this field: enhancing the present production and measurement processes' accuracy and effectiveness; introducing to the market novel yarns and conductive fabrics with reduced resistance or increased conductivity; introducing novel manufacturing methods or new flexible materials for embroidered apparel; Based on substrate materials, we are presenting new body-operated antenna sensors for a range of uses. Additional research in the domains of materials science and systems engineering is still required for the substantial practical deployment of wearable antennas. Biomedical applications may use novel materials like graphene compounds and conductive ink on textile substrates to enhance the functionality of antennas as sensors. These cutting-edge materials are fascinating components of the next generation of antenna designs. Flexible wearable antennas have received a great deal of interest from the scientific and business worlds. This presents certain research challenges. Researchers might focus their efforts on making the present manufacturing and measurement processes more accurate and efficient. Researchers can improve yarn and textile materials' conductivity by using innovative techniques. The simulated H-shaped antenna structure is shown in figure 3.

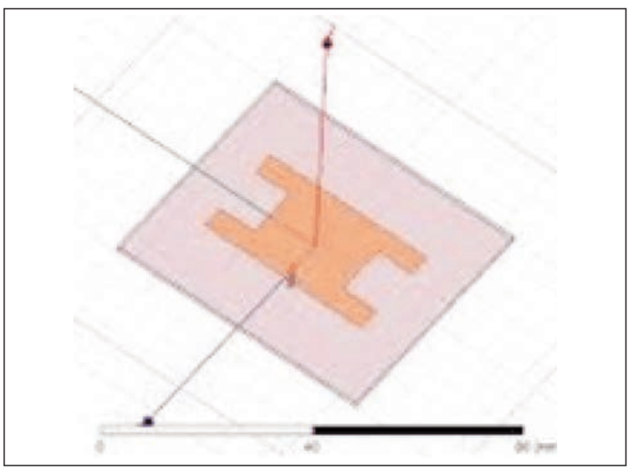

Fig. 3. H-shaped antenna structure

Wireless communication relies heavily on antennas as they facilitate the transmission and reception of signals across various frequency bands. These frequency bands include RFID (radio frequency identification), X-band, S-band, and the IoT. The antenna works well because it can be used with different frequencies, and the results from simulations and measurements agree very well. An interconnected network of physical objects that communicate online is known as the Internet of Things (IoT). Its goal is to enable intelligent, smooth communication and automation among devices for greater convenience and efficiency. Smart cities, wearable technology, industrial automation, smart homes, and healthcare monitoring are all examples of IoT applications. IoT devices operate in different frequency bands. Long-range, low-power communication (LPWAN) is made possible by sub-1 GHz frequencies like 433 MHz and 868 MHz; Zigbee and Bluetooth technologies allow for short-range communication using the 2.4 GHz band, and faster data rates and shorter-range applications use the 5.8 GHz spectrum. For worldwide IoT connectivity, cellular networks such as LTE-M, NB-IoT, and 5G function in several bands. Technologies like Sigfox and LoRa provide low-power, long-range solutions for particular Internet of Things applications by utilising a variety of sub-1 GHz bands.

The ideal technique for creating textile wearable antennas with superior production precision for wearable applications is screen and inkjet printing. A screen-printed interface layer was used to reduce the surface roughness of the polyester/cotton mixture, making it simpler to print a persistent conducting surface. Custom designs can still be generated rapidly for low-volume orders by doing away with the need for a screen and printing antennas straight from the finished design. Inkjet printing, a widely used technology, also enables an extremely fine resolution for improved production. The feeding mechanism of the antenna, in terms of compactness, is shown in figure 4.

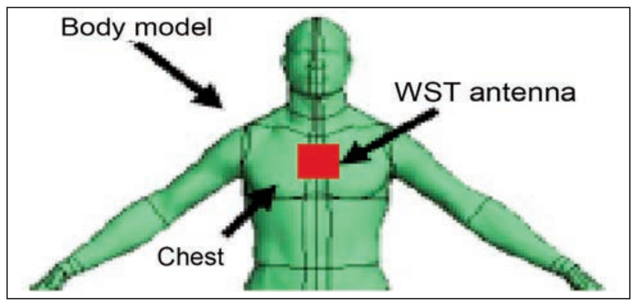

Fig. 4. Body model of the wearable devices

$X_{n,i}$ = Random(0, 1) . ($X_{n,i}^u$ – $X_{n,i}^L$) + $X_{n,i}^L$
i= 1,2,3,……..D and n = 1,2,3,……N
Where X_i^L is the lower bound of the variable X_i
Where X_i^U is the upper bound of the variable X_i
$V = X_{r1} + F(X_{r3} - X_{r2})$
Where F = Scaling factor
r1,r2,r3 are random solutions
Where (0<r1,r2,r3<N) And r1≠r2≠r3
Donor vectors are generated without involving the target vector.

Algorithm 2

Step 1: Set the generation counter G=0, and randomly initialise a population of NP individuals X. i Initialise the parameter F, CR.
Step 2: Evaluate the fitness for each individual in P.
Step 3: while the stopping criteria are not satisfied, do
for i= 1 to NP
select randomly a≠b≠c≠d≠i
for j=1 to D
j rand = rand (1,0) * D
if rand (0 ,1)≤CR or j= = jr and then
$U_{l,h} = X_{r1} + F(X_{r2} + X_{r3})$
else
$U_{l,h} = X_{l,h}$
end if

end for
end for
for i= 1 to N-1 do
Evaluate the offspring U I,h
if U I,h is better than P I,h then
P I,h = U I,h
end if
end for
Memorise the best solution achieved so far
Step 4: end while
End

Running comments

1. Bring in the necessary libraries.
2. Determine how many elements, or antennas, there are in the array.
3. Indicate the distance between the antenna array's components.
4. Indicate the components' phase angle.
5. The variables are allocated with array factor equations and design equations.
6. We provide plotting commands for outputs, patterns, or graphs.
7. Launch the software application.
8. If there are problems, debug them.
9. Examine the antenna array's dual-beam emission pattern.

The stages for the simulation are as follows:
Step 1: Installing Python software is step one.
Step 2: Launch Python IDLE shell version 3.9.
Step 3: Press Ctrl+N to create a new file.
Step 4: Import the necessary libraries, which are matplotlib from math, pylab, and pyplot.
Step 5: Set the settings to their starting values
– The quantity of components, or antennas
– The distance between the components (S)
– The components' phase angle (Phi)
Step 6: The variables are allocated to the array factor equations and design equations.
Step 7: Perform the directivity normalisation
Step 8: Plotting instructions are provided based on the syntax for the graphs and patterns.
Step 9: Give the program a name and save it in the designated place.
Step 10: Click Fn+F5 to launch the software application.
Step 11: Debug any issues that may have occurred.
Step 12: Examine the dual-beam radiation pattern to determine whether or not it has good directivity.
Step 13: If normalised directivity is not improved, optimise the patterns by varying the parameters, i.e., N, S, and Phi. This process is similar to a trial-and-error approach.
Step 14: The optimum output is achieved by repeatedly changing the settings until the best directivity is achieved.

This approach delineates the Differential Evolution (DE) process, a population-centric optimisation method extensively used for addressing intricate numerical challenges. The process starts with Step 1, whereby the generation counter G is set to zero, and a population of NP people is formed randomly. The mutation factor (F) and crossover rate (CR) are established at this phase. In Step 2, the fitness of each person is assessed according to a specified objective function. In Step 3, the fundamental evolutionary process begins and persists until a stopping requirement, such as a maximum number of generations or a convergence threshold, is satisfied. For each person, four unique people, a, b, c, and d, are randomly chosen from the population. A trial vector is produced by mutation and crossover operations. The progeny's fitness is then assessed. If the progeny outperforms its progenitor, it supplants it in the subsequent generation. This selection approach guarantees convergence to an optimum solution. The optimal answer is retained each generation for the final result.

When felt and Teflon are used on the antenna to improve performance, a deformed ground structure is added to the rectangular patch antenna to improve impedance matching. The reflection coefficient of the proposed antenna is shown in figure 5. Using Teflon as the antenna's substrate results in a better gain of 7.8 dB, but using felt yields a gain of 8.2 dB. These structures make the current path longer, which changes the frequency from a higher to a lower resonance. Bio-implantable device antennas employ Teflon fabric because of its precision and flexibility. The VSWR of the proposed antenna is shown in figure 6.

The method involves inserting H-shaped slots into a rectangular patch antenna to increase bandwidth. The slits and slots offer a modest bandwidth of <=1 GHz, according to the comparison study. By truncating the patch at the corners, this problem can be resolved, and bandwidth can be effectively increased from lower to higher than with conventional bandwidth improvement techniques. Systems for IoT, 5G, medical, and future communication require small, environmentally friendly, and effective broadband sensors and antennas. This article presents new dual-polarised and linear antennas for 5G, 6G, medical equipment, Internet of Things (IoT) systems, and healthcare monitoring sensors. Developing effective, small, affordable antennas and sensors is a key objective in the assessment of medical, 5G, and smart wireless communication devices. By attaching an energy-harvesting device to the antenna, passive and active sensors can also run on their own power by absorbing electromagnetic radiation and recharging the wearable sensor's battery.

The metamaterial technologies used in this work look at small, broadband, and useful antennas and sensors for 5G, 6G, and IoT, healthcare, and communication systems. The new, effective meta-fractal sensors and antennas optimise the system's dynamic range and electrical properties. Wearable medical sensors and equipment are used to monitor heartbeat, blood pressure, sugar levels, temperature, and other daily hospital tasks, including patient care and sleep habits. People use wearable technology to send, track, and monitor personal health information.

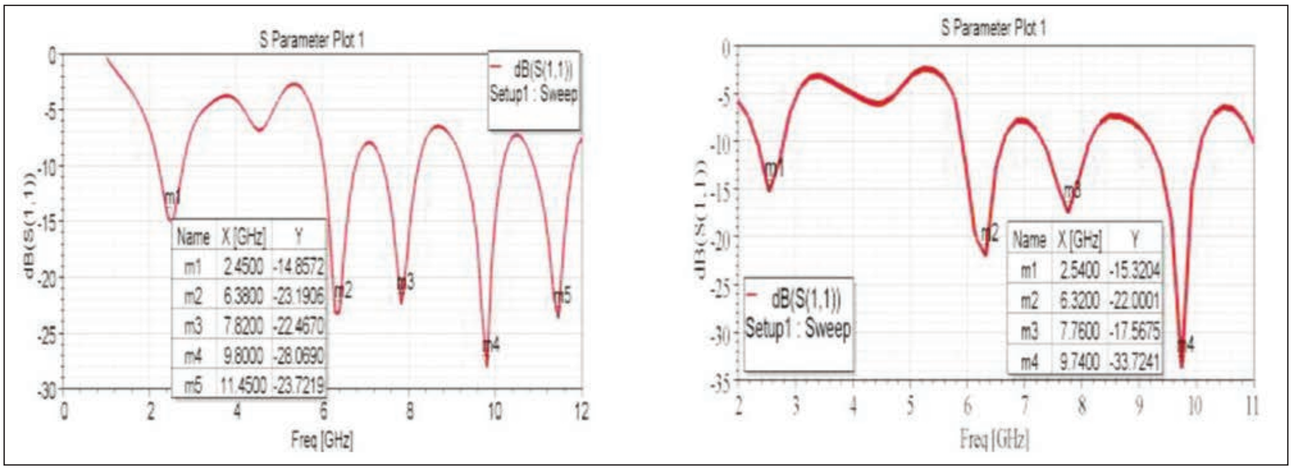

Fig. 5. Reflection coefficient of the proposed antenna

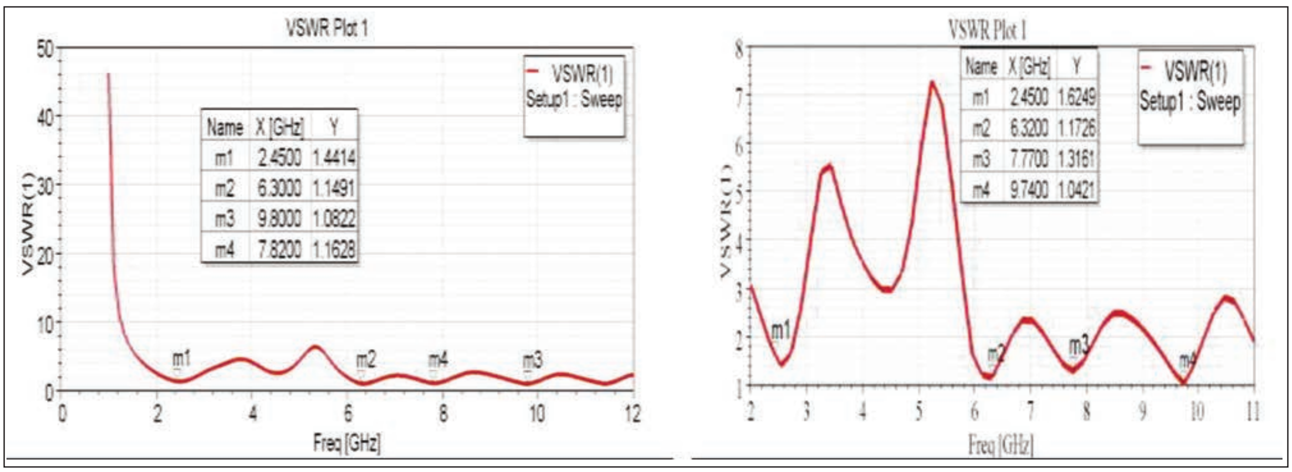

Fig. 6. VSWR of the proposed antenna

These medical devices are able to track vital signs like temperature, sweat, sleep patterns, and cardiac rate. To understand how well the proposed H-stub antenna works and operates on multiple frequencies, it's very important to look at how the current flows through it. The surface current is focused in various areas of the antenna structure at each resonant frequency, 7.5 GHz, demonstrating how well the design supports triple-mode operation. At 7.5 GHz, the main patch and the longer H-shaped stub segments, which serve as resonators at lower frequencies, are where the majority of the current is focused. This observation implies that resonance at this band is greatly influenced by the stubs' physical length. The current changes and intensify throughout the middle portions of the parasitic strip and the intermediate stub sections at 5.5 GHz. This experiment demonstrates how the ground plane adjustments and parasitic elements help to fine-tune the coupling processes and resonant behaviour. The current is mostly contained close to the feed line, patch edges, and open ends of the H-shaped slots at the higher frequency of 7.5 GHz, suggesting that these components are responsible for high-frequency resonance. A thick Teflon and FR4 substrate promotes improved electromagnetic coupling and wider bandwidth, which affects the current flow is shown in figure 7. The variance in current pathways at various frequencies demonstrates the antenna's capacity to isolate and control many resonances via compact design.

The colour gradient in the present distribution of the suggested antenna indicates the strength and amplitude of the surface current traversing the antenna's construction. Generally, warmer hues such as red and yellow signify areas of elevated current density, while cooler hues like blue and green denote regions of decreased current density. This picture facilitates

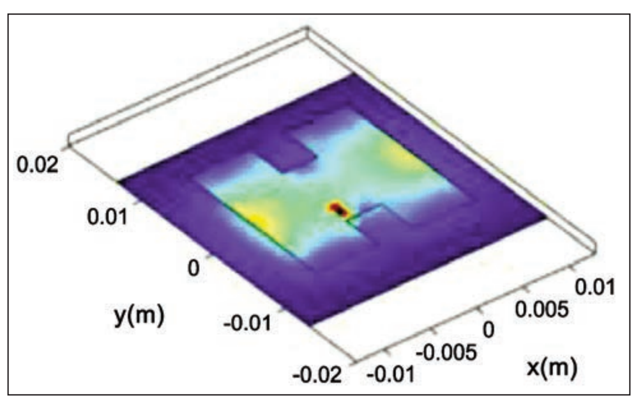

Fig. 7. Current distribution of the proposed antenna

the identification of active components of the antenna during operation, including the H-shaped stubs and parasitic elements where current is focused. Understanding the current distribution is important for improving antenna performance because it explains how well the antenna radiates energy and how the design affects bandwidth and efficiency.

There is a significant advancement in military wearable technology. Sensors and equipment that track soldiers are examples of wearable military technology. Soldiers can use boot inserts to measure their weapon grip effectiveness. In a variety of settings and climates, wearable sensors can track and evaluate soldiers' health and performance. They can also determine how geography influences soldiers' performance. Sports and fitness are important aspects of life. Professional and amateur athletes use sports equipment such as headgear, shoes, bats, and balls, along with wearable athletic sensors and devices. Sportswear can be made with wearable sports sensors integrated into the fabric. The GPS and Bluetooth-enabled gadgets give coaches access to real-time data so they can track and evaluate the athlete's performance. The gain plot of the proposed antenna is shown in figure 8.

An important performance metric that shows how well an antenna transforms input power into radio waves in a particular direction is its gain. The gain of the suggested H-shaped antenna has been assessed throughout its working frequencies, demonstrating reliable and effective radiation properties appropriate for contemporary wireless communication applications. The antenna attains a modest gain of around 5.5 to 8.5 dBi at 5.5 to 5.8 GHz, respectively, as shown in figure 9. Compact antennas that operate at lower frequencies and have tiny physical sizes in relation to wavelengths often have this amount of gain. For applications like GSM and IoT systems that need wide coverage, the H-shaped structure allows for efficient current distribution despite its small size, allowing for a respectable gain while preserving an omnidirectional radiation pattern. The H-shaped architecture, which more efficiently directs current over the radiating surface, supports the improved impedance matching and more efficient resonant behaviour that provides the increased gain at this frequency. As a result, the antenna is appropriate for mid-band uses, including mobile broadband, 3G, and 4G. This is explained by the directed character of the radiation pattern at this frequency, as well as the higher radiation effectiveness. Strong, concentrated radiation is made possible by the tiny but optimised H-shaped design, which is very advantageous for high-speed data applications like LTE and early 5G installations. The effectiveness and dependability of the suggested fabricated H-shaped antenna for multi-band wireless communication are shown in figure 10 by its constant gain performance across all three bands. It is a great option for tiny, high-performance wireless systems because of its capacity to sustain decent gain levels despite its small form size. The photocopy of the H-Shaped antenna is shown in figure 11.

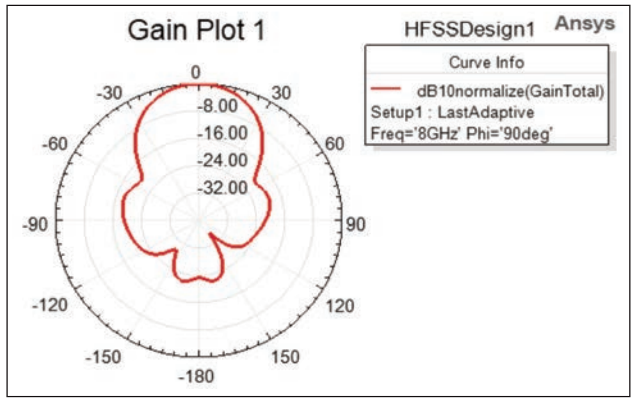

Fig. 8. Gain plot of the proposed antenna

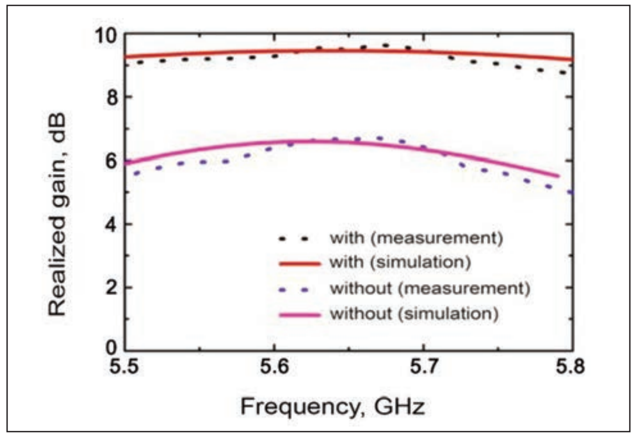

Fig. 9. Gain of the proposed antenna

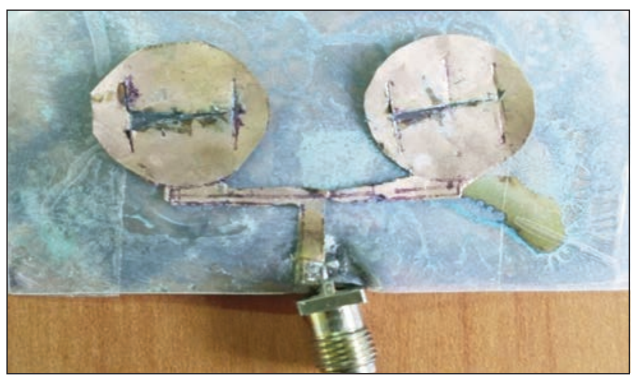

Fig. 10. Fabricated H-shaped antenna

The antenna has H-shaped stubs and a reconfigurable ground plane slot, which are metamaterial-inspired configurations that provide multi-band functionality and improved energy distribution. These metamaterial components modulate electromagnetic waves to enhance bandwidth, gain, and radiation efficiency within a compact design. Utilising novel materials and structural designs, the antenna fulfils the stringent requirements of next-generation wireless communication and sensing applications, providing improved flexibility and performance across many frequency bands.

Fig. 11. Photocopy of the H-shaped antenna

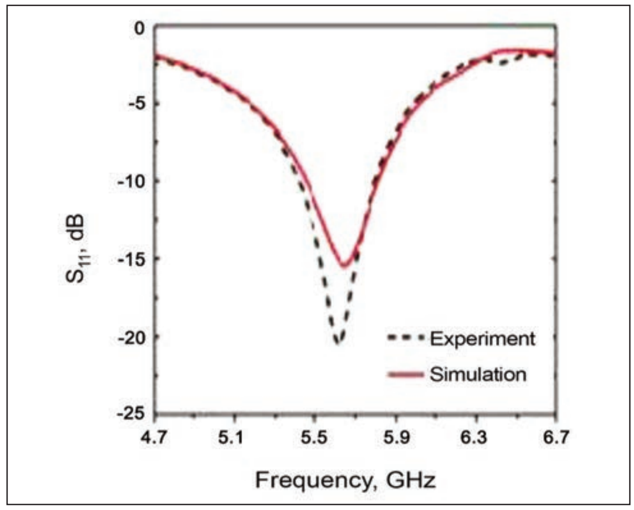

Fig. 12. Reflection coefficient of the experiment and simulation output

Copper foil is often used for antenna manufacturing owing to its superior electrical conductivity, flexibility, and simplicity of patterning. The use of copper foil guarantees effective signal transmission and reduces losses, which is crucial for sustaining high radiation efficiency across the antenna's operational frequency spectrum. Moreover, the compatibility of copper foil with substrates like Teflon and FR4 renders it optimal for the fabrication of small, dependable antennas. This selection enhances the antenna's performance objectives, including wide bandwidth and consistent operation for wireless communication applications.

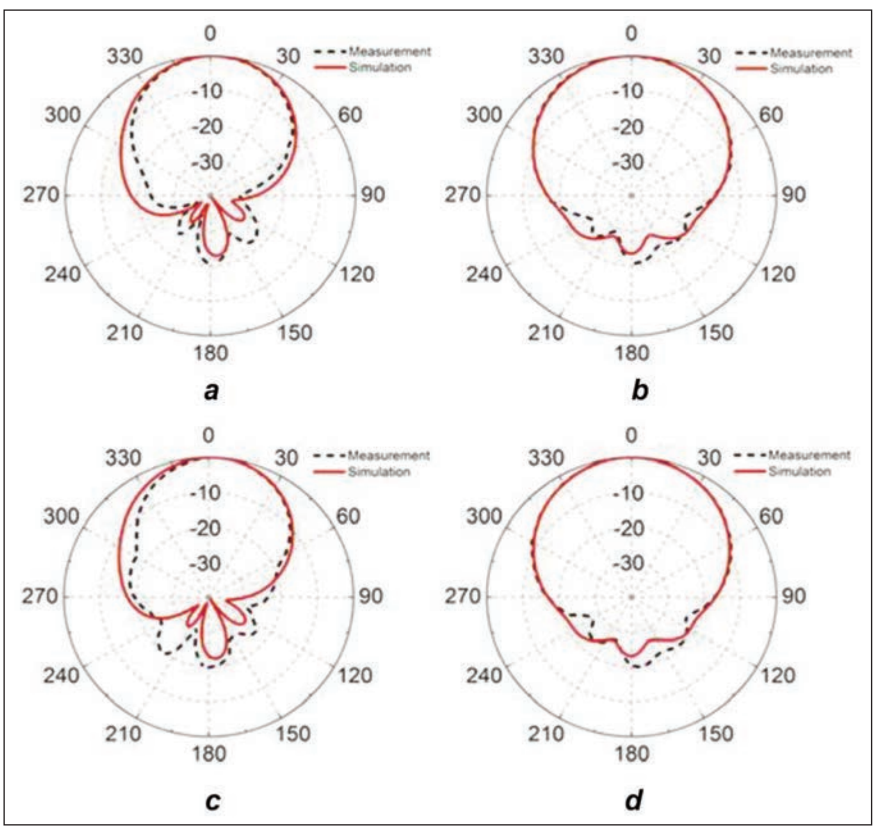

Fig. 13. Radiation pattern of the proposed antenna

The experimental and simulation output of the reflection coefficient is shown in figure 12. The radiation pattern of the proposed H-stub antenna is very important for how well it works at different frequencies and is key to determining if it is suitable for modern wireless communication systems. At its operational frequencies of 2.5, 6.3, 7.7 and 9.7 GHz, the antenna displays unique radiation characteristics that demonstrate its triple-mode capability and its well-optimised construction is shown in figure 13. For low-frequency wireless communication when broad coverage is crucial, the antenna's almost omnidirectional emission pattern in the H-plane (horizontal plane) at 9.7 GHz is perfect. Although the radiation is more directed in the E-plane (elevation plane), it still has a comparatively wide coverage area. This architecture supports applications like GSM and Internet of Things devices that require consistent signal delivery. The E-plane and H-plane radiation patterns begin to show a slight directionality, which helps improve signal strength and lessen interference. The changes to the parasitic strip and slot help direct the radiation to produce stronger and more controlled emission angles, resulting in better resonance effects and this behavior. Point-to-point communication and high-data-rate applications like LTE and 5G benefit from the antenna's more directional capabilities at 5.5 GHz, especially in the E-plane.

The improvement in gain and directivity at this frequency demonstrates efficient radiation despite the antenna's small size. The radiation pattern's stability and minimal distortion across all frequencies demonstrate good impedance matching and less back lobe radiation. These consistent, frequency-dependent radiation patterns demonstrate the outstanding adaptability of the suggested H-stub antenna, which makes it a strong contender for incorporation into broadband and portable wireless communication systems, as shown in figure 14.

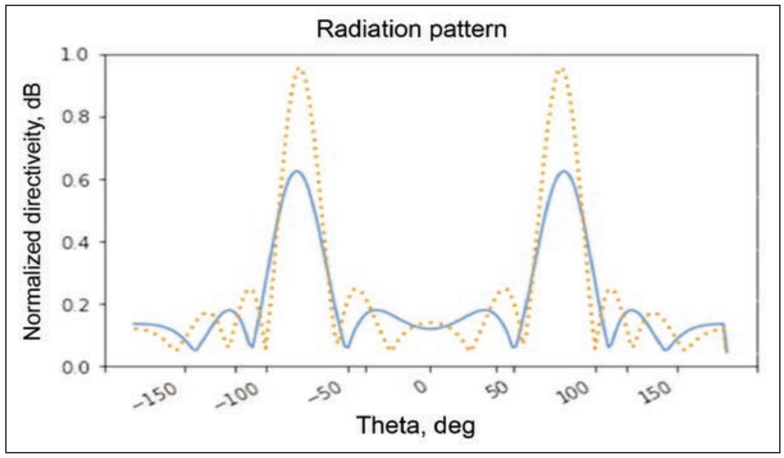

Fig. 14. Radiation pattern of the proposed antenna using Python

The changes in amplitude and phase of the proposed h-stub antenna are important features that reveal how it radiates signals, maintains signal quality, and performs overall at the frequencies of 2.5, 6.3, 7.7 and 9.7 GHz is shown in figure 15. These variances directly impact the antenna's efficiency, beam stability, and suitability for broadband and multi-band wireless applications. The suggested antenna's amplitude keeps its radiation strength comparatively constant across its operating frequencies. The amplitude distribution at 5.5 GHz is well distributed and smooth, suggesting low signal loss and excellent impedance matching. For wide coverage, this range produces a more consistent and omnidirectional radiation pattern. The amplitude starts to show somewhat more concentrated peaks as the frequency rises to 5.5 GHz and 9.5 GHz, especially in the primary radiation direction. Higher frequencies lead to better focus and stronger signals because of this improvement in amplitude response, which is helpful for applications that require high speeds and large amounts of data. To preserve beam coherence and reduce distortion, the phase variation over the radiating surface is also well-behaved. The antenna shows smooth phase transitions throughout the patch and stubs at all three resonant frequencies. The lack of sudden phase changes means the antenna helps reduce phase errors and allows waves to travel effectively. The H-stub antenna's well-controlled amplitude and phase features indicate that it can deliver reliable, high-quality radiation. Because of these characteristics, it may be integrated into contemporary wireless systems that need broadband, low-profile, and effective antenna solutions, guaranteeing reliable communication across many bands and excellent signal performance. The Reflection coefficient with the simulation and fabricated output of the proposed antenna is shown in table 2.

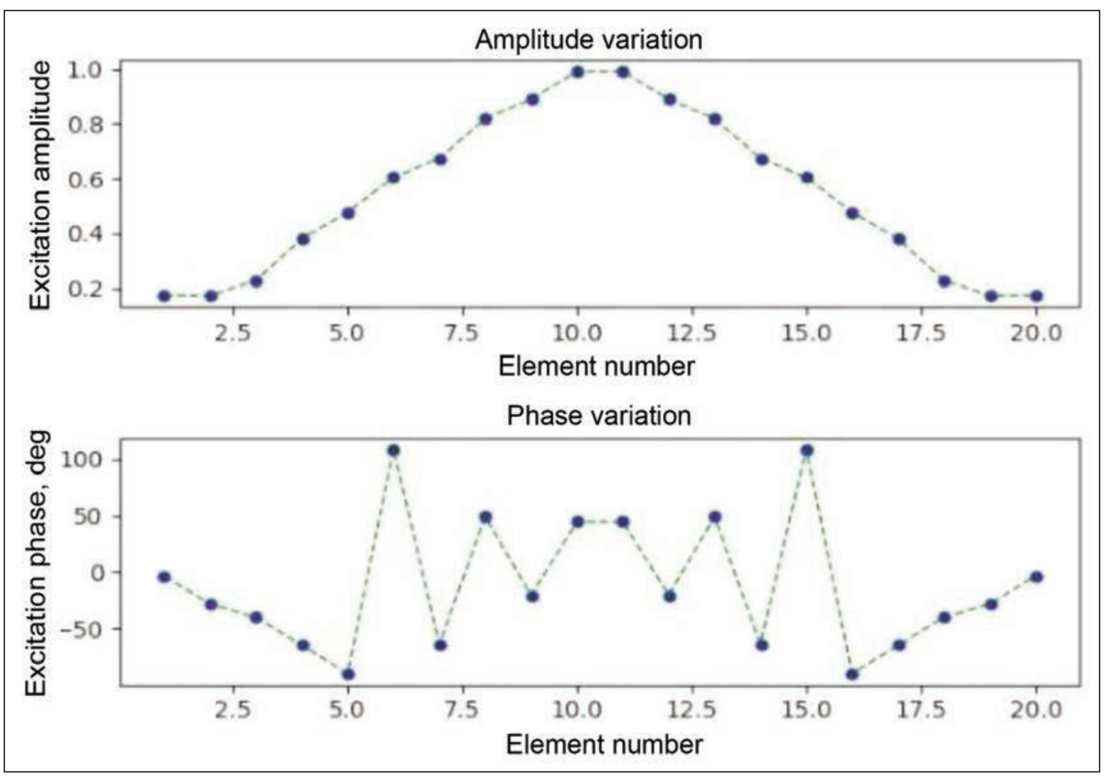

Fig. 15. Amplitude and phase variation of the proposed antenna using Python

Table 2

REFLECTION COEFFICIENT WITH SIMULATION AND FABRICATED OUTPUT OF PROPOSED ANTENNA		
Parameters	**Simulated output**	**Experiment output**
Reflection coefficient	–15.22 dB	–20.02 dB

Table 3

PERFORMANCE ANALYSIS OF THE H-SHAPED PROPOSED ANTENNA						
Frequency (GHz)	**Reflection coefficient (dB)**		**VSWR**		**Gain (dB)**	
	Proposed	**Existing**	**Proposed**	**Existing**	**Proposed**	**Existing**
2.5	–15.22	–12.25 [2]	1.62	1.12 [8]	3.5	2.5 [16]
6.3	–22.02	–20.25 [5]	1.17	1.02 [10]	5.5	3.0 [20]
7.7	–17.56	–15.25 [7]	1.13	1.05 [1]	7.5	4.5 [14]
9.7	–33.72	–2.25 [12]	1.04	1.00 [6]	8.5	5.2 [22]

Performance Analysis of the H-Shaped Proposed Antenna is shown in table 3.

The potential applications of the suggested tiny H-stub antenna in business are substantial, especially within the burgeoning fields of wireless communication and the Internet of Things (IoT). With the rising integration of smart gadgets, wearable technologies, and embedded systems in many sectors, there is an escalating need for compact, efficient antennas capable of functioning over broad frequency ranges. This antenna, measuring 46 mm x 30 mm x 1.6 mm and operating within a frequency range of 2.5 GHz to 12 GHz, is well-suited for incorporation into IoT devices, smart home systems, industrial automation, and healthcare monitoring applications. Consumer electronics use antennas in smartphones, tablets, and wireless headphones to enhance bandwidth and improve signal quality. In logistics and supply chain management, it facilitates asset monitoring and RFID systems, guaranteeing dependable data transfer even in congested conditions. Companies engaged in autonomous cars, drones, or robots may use their superior radiation efficiency and consistent performance for real-time communication. Moreover, the antenna's versatility and enhanced gain render it appropriate for 5G applications, smart city infrastructure, and remote sensing. The antenna offers a cost-efficient, high-performance solution that fosters innovation across several business sectors dependent on wireless communication.

CONCLUSION

In this research, we examine a wearable antenna's input impedance from the perspective of how the impedance varies depending on the body type of the user. First, a realistic human arm model wearing a wearable antenna prototype is used to calculate the input impedance characteristics. A similar trend was observed in both analytical and experimental results across the frequency range of 1 to 100 MHz. The gain is obtained at 8.2 dBi. The reflection coefficient of the proposed H-Shaped antenna is analysed at various frequencies, 2.5, 6.3, 7.7 and 9.7 GHz, and the values of –15.23, –22.02, –17.56 and –33.72 dB. The experiment determined the VSWR value to be less than two, a suitable value for most antenna systems. In addition, we made a simpler rectangular prism model to show how the different properties of each real human subject cause differences in input impedance. Furthermore, we may design the antenna prototype using the rectangular prism model without the need for multiple subject trials. The study's results show that HBC can work when looking at how resistant wearable antennas are to things like changes in skin moisture and tissue structure. The VSWR of the proposed H-Shaped antenna is analysed at various frequencies, 2.5, 6.3, 7.7 and 9.7 GHz, and the values of 1.62, 1.17, 1.3 and 1.04. The results also provide valuable insights for designing HBC systems, which include front-end circuits connected to an antenna and communication frequency bands. Future research will focus on enhancing the wearability of the antenna by investigating extremely flexible substrate materials such as denim, polyfoam, or jeans.

ACKNOWLEDGEMENTS

I want to express my gratitude to Dr. Nagarajan Ramalingam, my supervisor, who helped me with my research study.

REFERENCES

[1] Schmid, W., Fan, Y., Chi, T., Golanov, E., Regnier-Golanov, A.S., Austerman, R.J., Podell, K., Cherukuri, P., Bentley, T., Steele, C.T., *Review of Wearable Technologies and Machine Learning Methodologies for Systematic Detection of Mild Traumatic Brain Injuries*, In: J. Neural Eng., 2021, 18, 041006

[2] Steiner, L.A., Czosnyka, M., Piechnik, S.K., Smielewski, P., Chatfield, D., Menon, D.K., Pickard, J.D., *Continuous Monitoring of Cerebrovascular Pressure Reactivity Allows Determination of Optimal Cerebral Perfusion Pressure in Patients with Traumatic Brain Injury*, In: Crit. Care Med., 2002, 30, 733–738
[3] Schmid, M.B., Reister, F., Mayer, B., Hopfner, R.J., Fuchs, H., Hummler, H.D., *Prospective Risk Factor Monitoring Reduces Intracranial Hemorrhage Rates in Preterm Infants*, In: Dtsch. Ärzteblatt Int., 2013, 110, 489–496
[4] Chen, C.-J., Ding, D., Ironside, N., Buell, T.J., Southerland, A.M., Testai, F.D., Woo, D., Worrall, B.B., *Intracranial Pressure Monitoring in Patients with Spontaneous Intracerebral Hemorrhage*, In: J. Neurosurg., 2019, 132, 1854–1864
[5] Szwargulski, P., Wilmes, M., Javidi, E., Thieben, F., Graeser, M., Koch, M., Gruettner, C., Adam, G., Gerloff, C., Magnus, T., *Monitoring Intracranial Cerebral Hemorrhage Using Multicontrast Real-Time Magnetic Particle Imaging*, In: ACS Nano, 2020, 14, 13913–13923
[6] Karstensen, J.G., Ebigbo, A., Bhat, P., Dinis-Ribeiro, M., Gralnek, I., Guy, C., Le Moine, O., Vilmann, P., Antonelli, G., Ijoma, U., *Endoscopic Treatment of Variceal Upper Gastrointestinal Bleeding: European Society of Gastrointestinal Endoscopy (ESGE) Cascade Guideline*, In: Endosc. Int. Open, 2020, 8, E990–E997
[7] Peng, X., Xia, X., Xu, X., Yang, X., Yang, B., Zhao, P., Yuan, W., Chiu, P.W.Y., Bian, L., *Ultrafast Self-Gelling Powder Mediates Robust Wet Adhesion to Promote Healing of Gastrointestinal Perforations*, In: Sci. Adv., 2021, 7, eabe8739
[8] El Gharbi, M., Fernández-García, R., Ahyoud, S., Gil, I., *A Review of Flexible Wearable Antenna Sensors: Design, Fabrication Methods, and Applications*, In: Materials, 2020, 13, 3781
[9] Mahmood, S.N., Ishak, A.J., Saeidi, T., Alsariera, H., Alani, S., Ismail, A., Soh, A.C., *Recent Advances in Wearable Antenna Technologies: A Review*, In: Prog. Electromagn. Res. B, 2020, 89, 1–27
[10] Yang, M., Ye, Z., Ren, Y., Farhat, M., Chen, P.-Y., *Recent Advances in Nanomaterials Used for Wearable Electronics*, In: Micromachines, 2023, 14, 603
[11] Won, P., Jeong, S., Majidi, C., Ko, S.H., *Recent Advances in Liquid-Metal-Based Wearable Electronics and Materials*, In: iScience, 2021, 24, 102698
[12] Ates, H.C., Nguyen, P.Q., Gonzalez-Macia, L., Morales-Narváez, E., Güder, F., Collins, J.J., Dincer, C., *End-to-End Design of Wearable Sensors*, In: Nat. Rev. Mater., 2022, 7, 887–907
[13] Ling, Y., An, T., Yap, L.W., Zhu, B., Gong, S., Cheng, W., *Disruptive, Soft, Wearable Sensors*, In: Adv. Mater., 2020, 32, 1904664
[14] Jan, M.A., Khan, F., Khan, R., Mastorakis, S., Menon, V.G., Alazab, M., Watters, P., *Lightweight Mutual Authentication and Privacy-Preservation Scheme for Intelligent Wearable Devices in Industrial-CPS*, In: IEEE Trans. Ind. Inform., 2020, 17, 5829–5839
[15] Hashim, F.F., Mahadi, W.N.L.B., Abdul Latef, T.B., Othman, M., *Bin Key Factors in the Implementation of Wearable Antennas for WBNs and ISM Applications: A Review WBNs and ISM Applications: A Review*, In: Electronics, 2022, 11, 5270
[16] Alhayajneh, A., Baccarini, A.N., Weiss, G.M., Hayajneh, T., Farajidavar, A., *Biometric authentication and verification for medical cyber physical systems*, In: Electronics, 2018, 7, 436
[17] Abbasi, Q.H., Rehman, M.U., Qaraqe, K., Alomainy, A., *Advances in Body-Centric Wireless Communication: Applications and State-of-the-Art*, In: Institution of Engineering and Technology: Stevenage, UK, ISBN 1849199892, 2016
[18] Negra, R., Jemili, I., Belghith, A., *Wireless body area networks: Applications and technologies*, In: Procedia Comput. Sci., 2016, 83, 1274–1281
[19] Hadjidj, A., Souil, M., Bouabdallah, A., Challal, Y., Owen, H., *Wireless sensor networks for rehabilitation applications: Challenges and opportunities*, In: J. Netw. Comput. Appl., 2013, 36, 1–15
[20] Isa, M.S.M., Azmi, A.N.L., Isa, A.A.M., Zin, M.S.I.M., Saat, S., Zakaria, Z., Ibrahim, I.M., Abu, M., Ahmad, A., *Textile dual band circular ring patch antenna under bending condition*, In: J. Telecommun. Electron. Comput. Eng., 2017, 9, 37–43
[21] Mersani, A., Bouamara, W., Osman, L., Ribero, J.M., *Dielectric resonator antenna button textile antenna for off-body applications*, In: Microw. Opt. Technol. Lett., 2020, 62, 2910–2918
[22] Marterer, V., Radouchová, M., Soukup, R., Hipp, S., Blecha, T., *Wearable textile antennas: Investigation on material variants, fabrication methods, design and application*, In: Fash. Text, 2024, 11, 9
[23] Abdulla, F.A.A., Demirkol, A., *A novel textile-based UWB patch antenna for breast cancer imaging*, In: Phys. Eng. Sci. Med., 2024, 47, 851–861
[24] Ibrahim, N.F., Dzabletey, P.A., Kim, H., Chung, J.Y., *An all-textile dual-band antenna for ble and lora wireless communications*, In: Electronics, 2021, 10, 2967
[25] Parameswari, S., Chitra, C., *Textile UWB antenna with metamaterial for healthcare monitoring,* In: Int. J. Antennas Propag., 2021, 2021, 5855626
[26] Ullah, U., Mabrouk, I.B., Koziel, S., *A compact circularly polarized antenna with a directional pattern for wearable off-body communications*, In: IEEE Antennas and Wireless Propagation Letters, 2019, 18, 12, 2523–2527, https://doi.org/10.1109/lawp.2019.2942147
[27] Sabban, *Small new wearable metamaterials antennas for IoT medical and 5G applications*, In: 14th IEEE European Conference on Antennas and Propagation, EuCAP, 2020, 1–5, https://doi.org/10.23919/EuCAP48036.2020.9136003
[28] Ouyang, Y., Chappell, W.J., *High-frequency properties of electro-textiles for wearable antenna applications*, In: IEEE Transactions on Antennas and Propagation, 2008, 56, 2, 381–389, https://doi.org/10.1109/tap.2007.915435
[29] Ashyap, Y., Zainal Abidin, Z., Dahlan, S.H., et al., *Compact and low-profile textile EBG-based antenna for wearable medical applications*, In: IEEE Antennas and Wireless Propagation Letters, 2017, 16, 2550–2553, https://doi.org/10.1109/lawp.2017.2732355

[30] Raed, S., Daraghma, M., *Design of Microstrip Patch H-Notch Antenna for Vehicle Using Array Systems*, In: Journal of Communications, 2024, 19, 4, 204-210
[31] Vital, D., Bhardwaj, S., Volakis, J.L., *Textile-based large area RF-power harvesting system for wearable applications*, In: IEEE Transactions on Antennas and Propagation, 2019, 68, 3, 2323–2331, https://doi.org/10.1109/tap.2019.2948521
[32] Pathan, T., Karn, R.A., *Compact circular polarized metamaterial-inspired fabric antenna for WBAN applications*, In: Microwave and Optical Technology Letters, 2021, 63, 2651–2655, https://doi.org/10.1002/mop.32958
[33] Mersani, A., Lotfi, O., Ribero, J.M., *Design of a textile antenna with artificial magnetic conductor for wearable applications*, In: Microwave and Optical Technology Letters, 2018, 60, 6, 1343–1349, https://doi.org/10.1002/mop.31158

Authors:

GURUPRASATH RENGARAJAN[1], NAGARAJAN RAMALINGAM[2]

[1]Assistant Professor, Department of Electronics and Communication Engineering,
Gnanamani College of Technology, Tamil Nadu, India

[2]Professor, Department of Electrical and Electronics Engineering,
Gnanamani College of Technology, Tamil Nadu, India
e-mail: krnaga71@yahoo.com
ORCID: https://orcid.org/0000-0002-4990-5869

Corresponding author:

GURUPRASATH RENGARAJAN
e-mail: jcetguru@gmail.com, guruprasathr@gct.org.in
ORCID: https://orcid.org/0000-0001-6654-1860

Sustainability, reliability, and safety assessment of microchannel heat sinks in electronic cooling applications: a detailed study with a focus on smart fabrics and wearable electronics

DOI: 10.35530/IT.077.04.2025147

SANTOSH KUMAR RAI
MAHESH KUMAR GUPTA
GYANENDRA PRASAD BAGRI
ARUN UNIYAL
ASHWANI KUMAR
RAMONA BIRAU
IULIANA CARMEN BĂRBĂCIORU
CRISTINA FELICIA IONICI

ABSTRACT – REZUMAT

Sustainability, reliability, and safety assessment of microchannel heat sinks in electronic cooling applications: a detailed study with a focus on smart fabrics and wearable electronics

The ongoing miniaturisation of electronics poses significant thermal management challenges due to rising power densities within constrained volumes. This study addresses the critical need for efficient heat dissipation to ensure the sustainability, reliability, and safety of these systems. We present a detailed assessment of microchannel (MICH) heat sinks, a high-performance cooling technology particularly relevant for advanced electronic applications. The core of this work is a comprehensive review and analysis of MICH classifications, fabrication methods, and performance metrics. A primary focus is placed on a sustainability assessment, including the optimisation of material usage, enhancement of energy efficiency, and reduction of the environmental impact of coolants, all of which contribute to a longer product lifecycle. The paper also explores how MICH technology improves system reliability by maintaining components within safe operating temperature ranges, thereby preventing performance degradation and premature failure. We pay special attention to the emerging application of integrating MICH technology into smart fabrics and wearable electronics, a domain where thermal management is a critical and complex challenge. By examining this specific use case, we demonstrate the versatility and potential of MICH heat sinks. The paper concludes by outlining future research directions and innovations necessary for the widespread commercial viability and adoption of MICH-based cooling solutions in both traditional and next-generation electronic devices.

Keywords: *smart fabrics, wearable electronics, microchannel, reliability, safety, electronic devices cooling, MEMS*

Evaluarea sustenabilității, fiabilității și siguranței radiatoarelor cu microcanale în aplicațiile de răcire electronică: un studiu detaliat cu accent pe materiale textile inteligente și electronice purtabile

Miniaturizarea continuă a componentelor electronice ridică provocări semnificative în ceea ce privește gestionarea termică, din cauza densităților de putere în creștere în volume limitate. Acest studiu abordează nevoia critică de disipare eficientă a căldurii pentru a asigura sustenabilitatea, fiabilitatea și siguranța acestor sisteme. Prezentăm o evaluare detaliată a radiatoarelor cu microcanale (MICH), o tehnologie de răcire de înaltă performanță, deosebit de relevantă pentru aplicațiile electronice avansate. Elementul central al acestei lucrări îl constituie o trecere în revistă și o analiză cuprinzătoare a clasificărilor MICH, a metodelor de fabricație și a indicatorilor de performanță. Un accent principal este pus pe evaluarea sustenabilității, incluzând optimizarea utilizării materialelor, îmbunătățirea eficienței energetice și reducerea impactului asupra mediului al agenților de răcire, toate acestea contribuind la un ciclu de viață mai lung al produsului. Studiul explorează, de asemenea, modul în care tehnologia MICH îmbunătățește fiabilitatea sistemului prin menținerea componentelor în intervale de temperatură de funcționare sigure, prevenind astfel degradarea performanței și defectarea prematură. Acordăm o atenție specială aplicației emergente a integrării tehnologiei MICH în materialele textile inteligente și în dispozitivele electronice purtabile, un domeniu în care gestionarea termică reprezintă o provocare critică și complexă. Prin examinarea acestui caz de utilizare specific, demonstrăm versatilitatea și potențialul radiatoarelor MICH. Studiul se încheie cu o prezentare a direcțiilor viitoare de cercetare și a inovațiilor necesare pentru asigurarea viabilității comerciale pe scară largă și a adoptării soluțiilor de răcire bazate pe tehnologia MICH, atât în dispozitivele electronice tradiționale, cât și în cele de nouă generație.

Cuvinte-cheie*: materiale textile inteligente, dispozitive electronice purtabile, microcanale, fiabilitate, siguranță, răcirea dispozitivelor electronice, MEMS*

INTRODUCTION

In the past two decades, the drastic growth of miniaturisation of electronic devices such as MEMS, microfluidic devices, biomedical devices, and high-density electronics has revolutionised engineering, research, and technology in several areas. As devices decrease in compactness in size to microscopic and nanoscopic dimensions, they more and more produce increasingly substantial high heat fluxes as a result of high power densities, imposing drastic requirements on thermal management. Inadequate heat dissipation from the devices or system makes the devices much less reliable and sustainable, as well as increases the safety risks for both users and devices when utilised in some applications [1, 2]. However, conventional cooling methods like mini-channel heat sinks [3–6], natural circulation loops [7–9], passive airflow, and fine configurations are not sufficient for these small, high-power systems and MEMS and electronics devices. To resolve these issues, microchannel heat sinks (MCHSs) have proven to be a very effective option, with high heat transfer because of their large surface-area-to-volume ratios, compactness, low coolant usage, and high coefficients of heat transfer. Furthermore, MCHSs provide efficient thermal management and enable devices to function safely within acceptable temperature ranges [10].

Also, several fabrication and design techniques have been investigated to enhance MCHS performance. Passive augmentations such as adding ribs, cutting grooves, pin fins, and different cross-sectional geometries increase turbulence, disturb thermal boundary layers, and enhance heat dissipation from the device to the environment. Furthermore, various applications of nanofluids, phase-change fluids and materials are used to enhance thermal capability, with enhanced thermal conductivity above that of standard fluids. However, apart from the passive method, some active methods are also available, which improve the heat transfer rate. These active methods are flowing pulsation, electrostatic modulation, magnetic fields, and acoustic or vibrational stimulation that have come into play for improving the heat transfer by externally caused effects.

Simultaneously, some important numerical and experimental methods are more frequently being used to optimise microchannel geometry [11, 12]. Topology optimisation and surrogate modelling are some methods that expedite design cycles while providing drastic enhancements in thermal resistance and pumping power efficiency.

Design and fabrication of the MICHs are progressively advancing with innovations to improve the heat dissipation rate for increasing sustainability, reliability, and safety of the devices. Some of the design is inspired by bionic topologies, non-traditional cross-sections (trapezoidal or triangular), and interrupted flow structures like cavities and ribs that optimise heat removal by maximising surface area and inducing mixing and uniform cooling. Additionally, through-chip MICH embedded in 3D stacked circuits is a leading area of thermal management with direct, internal cooling and huge performance potential.

Sustainability aspects form an intrinsic part of cooling system development. MCHS is used for improving energy-efficient, compact designs with minimal material requirements and environmental footprint. Their durability and flexibility with sustainable industrial principles minimise waste and maximise lifecycle performance. Future research places as much emphasis on sustainable operation, considering eco-friendly coolants, materials, processes, and system lifecycle effects as thermal performance [13–15]. Based on the several advantages of the MICHs for heat transfer from the device to the environment, there are still various problems and disadvantages of the MICHs that require improvement for the sustainability, reliability, and safety of the electronic devices. Also, there are many problems that occur in producing and fabricating MICHs. Producing intricate MICHs in volume and packaging them economically into production lines is still not trivial. Creating coolants that are both high-performance and environmentally friendly is a two-way obligation.

Maintaining design consistency so MICHs provide uniform cooling among devices is critical to prevent hotspots, which can significantly compromise reliability. In this context, the paper presents a comprehensive literature review of MICHs that is based on the safety, reliability and thermal management in miniaturised electronics devices such as electronic devices, MEMS, microfluid devices, sensors, etc., which are used in several wearable electronic devices as well as in fabric to remove the heat. The review covers categorisation of microchannel geometries, optimisation of heat transfer in single and two phases, heat transfer mechanism through microchannel, and implementation in device safety improvement and reliability enhancement in a systematic manner. The review also incorporates environmentally conscious design factors such as energy efficiency, material optimisation, coolant environmental responsibility, and lifecycle performance. Further, promising directions for future research focused on developing MICH-based cooling technologies are proposed for improving the safety and reliability of electronic devices.

LITERATURE REVIEW

MICH's sustainability and reliability are important factors in their use across a wide range of industries, from petrochemicals and electronics to thermal management. MICHs provide improved heat transfer and energy efficiency, but also face special reliability and safety challenges at their small scale and operating conditions. The literature review, a comprehensive study of literature, has led to a detailed investigation into the aspects of reliability, sustainability, and safety of MICHs in terms of classification of the channel, fabrication, materials used for fabrication, thermal management, and cooling of electronic devices. The literature review primarily covers the period from 2000 to 2025, providing a contemporary perspective on the field, followed by an investigation of the different fabrication methods and heat transfer methods to enhance the reliability, sustainability, and safety of MICHs.

Methodology for reviewing literature

This study follows a structured literature review methodology to evaluate the sustainability, reliability, and safety performance of MICH for electronic cooling that is used in smart fabrics and wearable electronic systems, such as biosensors, microfluidics, etc. The review centres on comprehending MICH classifications, fabrication methodologies, material and coolant selection, environmental ramifications, thermal performance metrics, and the viability of integration into flexible substrates. Previously published articles were searched across Scopus, Web of Science, IEEE Xplore, ScienceDirect, Google scholar, Elsevier, and Springer, etc. Various important keywords were used, such as Micro-channel, signal and two-phase, sensor, biosensor, microchannel heat sink, microfluidic cooling, sustainable cooling, energy-efficient electronics, wearable thermal management, smart fabrics cooling, and reliability in electronic cooling. We used Boolean operators (AND/OR) and only looked at literature from 2000 to 2025, with a focus on more recent work to find the most up-to-date progress.

Criteria for inclusion and exclusion of the article in this study

In this study, several papers were included based on the peer-reviewed papers about MICH design, thermal modelling, choosing materials, cooling fluids, evaluating sustainability, and wearable integration. Studies that are analytical, experimental, numerical, and review. Works that report thermal performance metrics like the heat transfer coefficient, pressure drop, pumping power, Nusselt number, and temperature drop. Also, some articles are excluded from the present study based on the studies on cooling that don't use microchannels unless they are comparative. Articles that don't include a performance evaluation or don't give enough details about the methodology. Patents, preprints without technical data, and publications that aren't in English. Also, we have used some traditional processes to include and exclude in this study based on the screening, classifying, and putting together. We looked at the titles and abstracts to see if they were relevant, and then we looked at the whole text.

Based on the selected articles, we put the chosen articles into three groups based on their themes such as geometries (rectangular, trapezoidal, fractal, wavy, porous), MEMS/AM fabrication, and nano-enhanced coolants, aspects of sustainability, reliability, and safety include material efficiency, the effect of the coolant on the environment, lifecycle assessment, and preventing overheating failures and use in smart fabrics and wearable electronics which limits on flexibility, biocompatibility, mechanical durability, comfort, and thermal load distribution.

Fundamental principle of the microchannel and mechanism of heat dissipation through the microchannel

MCHs work based on the principle of convective heat transfer, wherein a working fluid absorbs heat from the surface of an electronic component as it travels through narrow channels within the MCH (figure 1). Because of the high surface area-to-volume ratio and minimal diffusion paths within microchannels, MCHs provide significantly more heat transfer than traditional cooling techniques. When a fluid (liquid or nanofluid) is going through microchannels, heat from the electronic device is dissipated to the fluid through conduction through the heat sink material and convection along the channel walls. The heated fluid is transported away from the device at a safe operating temperature. These are mainly two types of force convection and free convection. But mostly forced convection methods were used to remove the heat from the electronic devices to enhance their reliability, sustainability, and safety. Figure 1 depicts the schematic diagram of the working of the MCHs [16].

From figure 2, it can be seen that the heat transfer mechanism through the MCH works by moving fluid from the reservoir through a saline tube that is controlled by a fluid regulator before entering the MCH test section. The power supply unit powers and controls the heated surface, which is where the fluid flows through the MCH and absorbs heat. To keep an eye on heat distribution and thermal performance, several thermocouples (B1–B6, A1, A2) are placed along the channel to measure temperature changes at different points. A digital temperature indicator shows the temperature readings, which help to determine the temperature of the wall and fluid of the channel and transfers of heat through convection. The fluid goes through the microchannel, where it

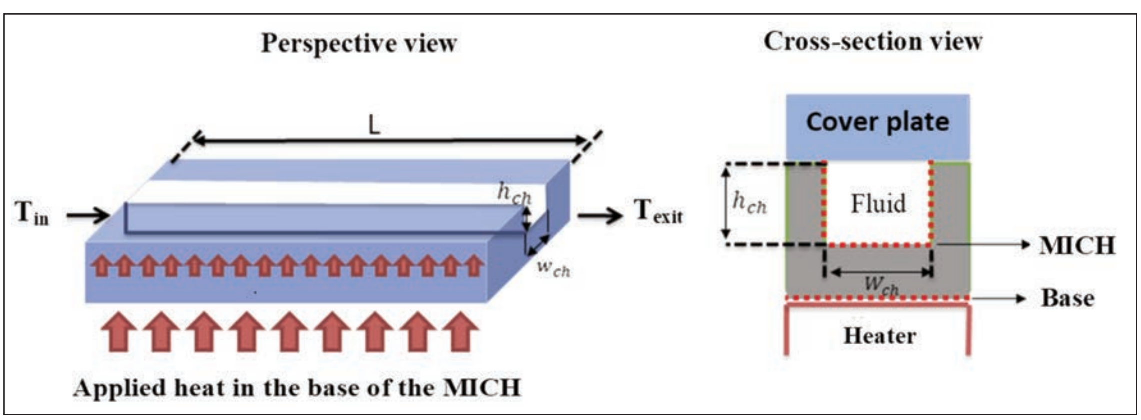

Fig. 1. Schematic diagram of the microchannel

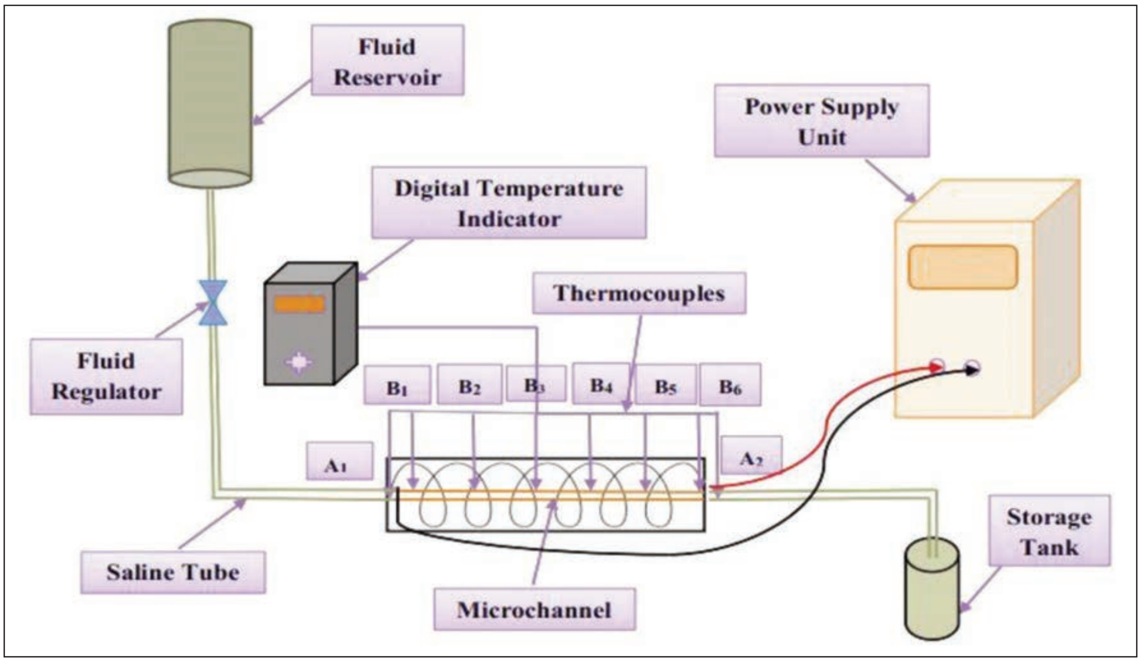

Fig. 2. Schematic diagram of the heat transfer through a microchannel

picks up heat, then leaves and is stored in the storage tank. This completes the flow loop and depicts the heat transfer mechanism in the experimental setup.

Classification of microchannel and materials and coolant used in this for improving the safety of the devices

MCHs are developed in various designs, such as single and manifold channels, serpentine channels, pin fins, interrupted channels, etc., that are made of different materials for improving the heat transfer from the electronic devices by employing several coolants for the safety of the device. Figure 3, *a* shows the classification of the MICH based on the optimising heat transfer criteria and THP, which provides significant safety of the electronic devices as well as improves the life span.

Based on the previously reported research, MICHs are classified into three categories: cross-sectional geometry optimisation, complex geometry optimisation, and wall geometry optimisation. Similarly, various materials are used to fabricate the MICHs to prevent damage to the channels and improve the thermal performance, structural integrity, and corrosion resistance, as well as to choose the materials based on their high thermal conductivity and light weight. Mainly, copper, aluminium, silicon ceramics, and polymers (with fillers) are used, which improve the THP of the channel and provide higher safety to the electronic devices. Similarly, selection of the working fluid is a critical parameter of MICHs for improving the cooling effect and preventing the devices from burning and damage. The THP and pressure drop in the channel are affected by the

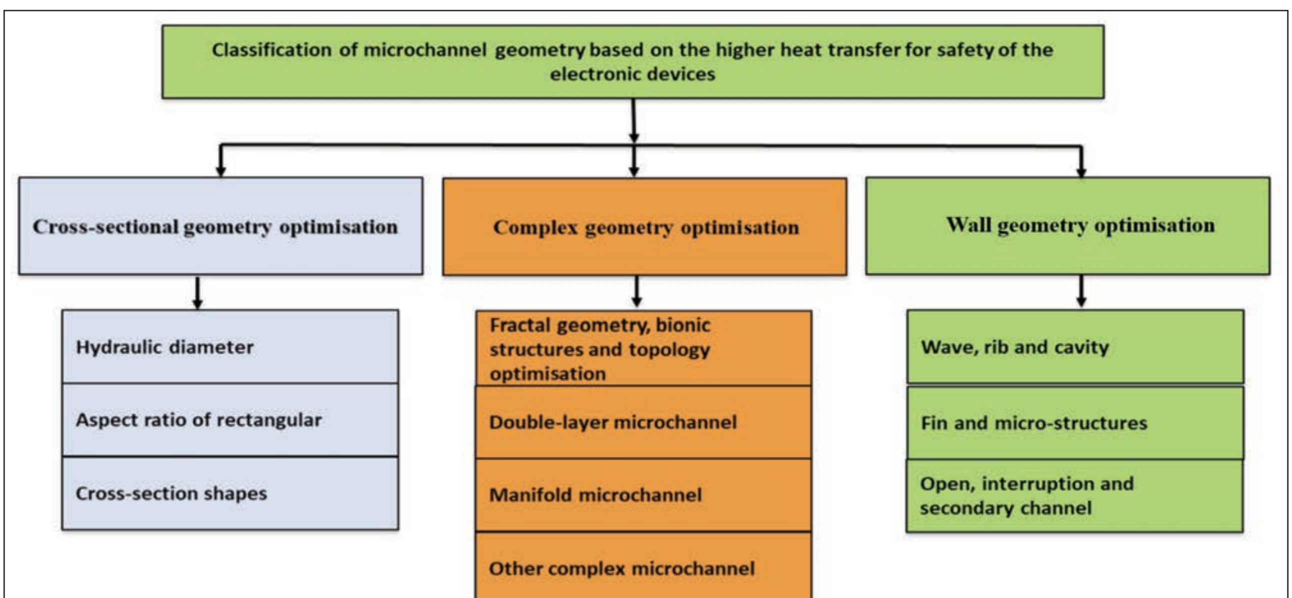

a

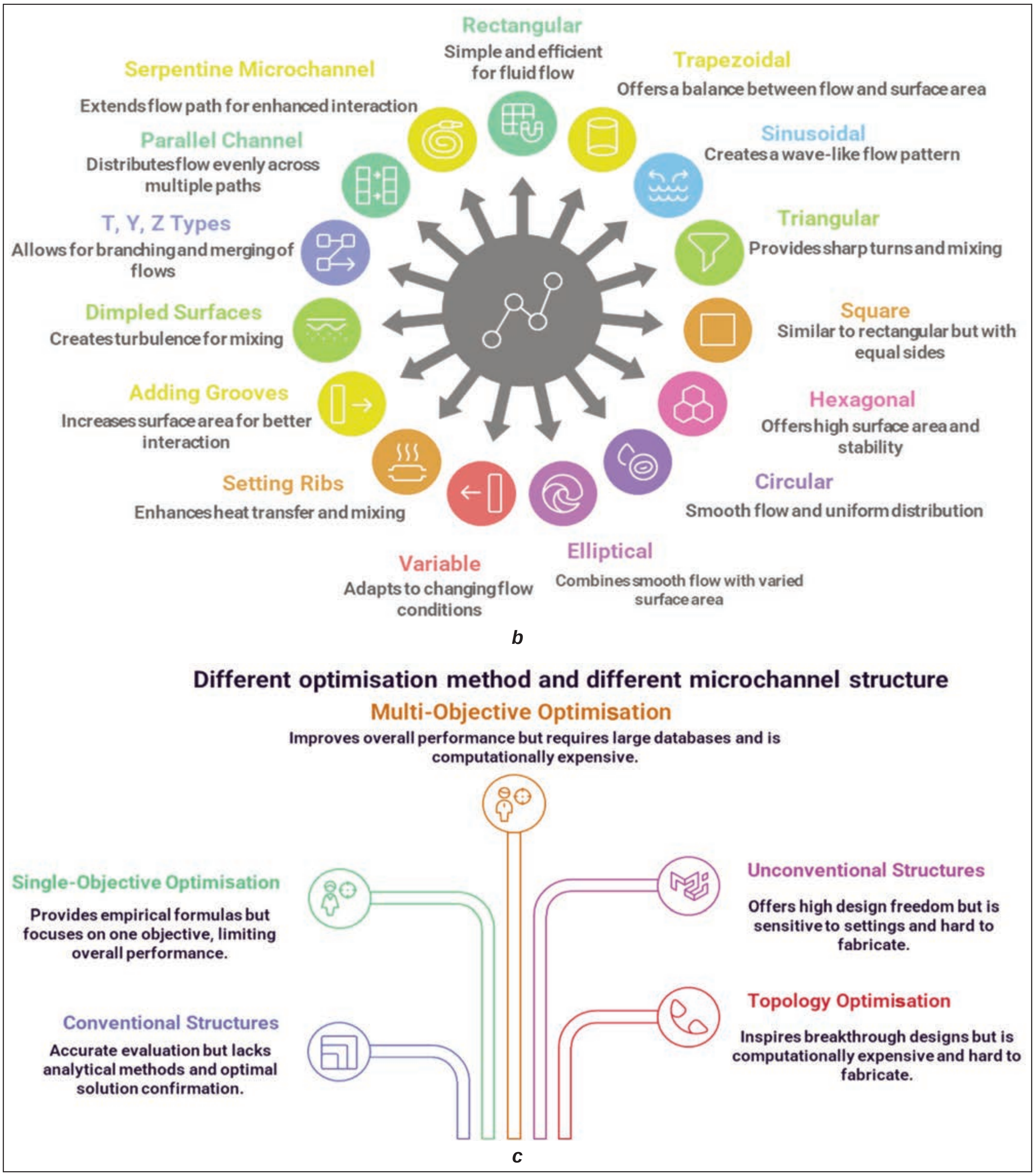

Fig. 3. Representation of: *a* – classification of the microchannel based on the higher heat transfer for improving the safety of the electronics devices; *b* – classification of the microchannel based on different microchannel structures; *c* – advantages and disadvantages of different optimisation methods and structure of MCHs

thermal properties, electrical conductivity, and chemical stability of the coolant, which directly affect system efficiency and safety.

Several coolants are used in MICHs to improve the sustainability, reliability, and safety of the electronic devices. Mainly deionised water, nanofluids, dielectric fluids (i.e., Fluorinert, Novec), refrigerants, mixtures of two different fluids, etc., due to high specific heat, higher thermal conductivity, and electrical non-conductivity, as well as the capability of improving the THP and reducing the friction loss in the channels [17–19]. Also, various shapes, geometries, and their modification of MCH were developed with time to improve the heat transfer rate and reduce the pressure drop in the application of wearable electronic devices, which is given in figure 3, *b*. Further, it is very useful to optimise possible thermal improvement methods for MCHSs by changing configuration and shapes, sizes and their surface microstructures. Their advantages and disadvantages, and the method of MCHs depicted in figure 3, *c*.

SUSTAINABILITY ASPECTS, THERMAL SAFETY AND OVERHEATING RISKS, MECHANICAL AND THERMAL RELIABILITY OF THE DEVICES

As electronic devices rapidly miniaturise and become more power-dense and thermally demanding, the sustainability, reliability, and safety of thermal management solutions become very important. MICHs are used in various electronic devices due to their compact size and higher THP. Therefore, it must be evaluated not only for THP and efficiency but also for its long-term environmental and resource impacts and small-scale, complex flow dynamics and integration with sensitive electronics, as well as ensuring safety in operation for protecting both devices and users from hazards.

Wang et al. [20] optimised the thermal hydraulic performance (THP) of an MCHS using numerical and artificial neural networks (ANNs) methods. With the drastic demand for high-performance electronic devices, rapid cooling of these devices is essential to work under the limiting temperature of the device, which provides safety as well as ensures the reliability of the devices. They used a numerical model with hexagonal fins, which was developed in COMSOL, while other ANN models were trained to accurately predict Nusselt number and pressure drop with high accuracy (R^2 = 0.999). The outcomes revealed that the distance of fins from sidewalls has depicted a significant effect and increased the Nu by 66.3% and ΔP by 37.6%. Three optimal configuration parameters were identified, such as Nu = 27.596, ΔP = 282.3 Pa, and an overall efficiency of 1.491, and compared to the benchmark result, the optimised design enhanced total performance by 49.1% and concluded that ANN-based optimisation is an effective tool for designing high-performance MCHSs, which are capable of optimising the safe and reliable parameters of MCHS for dissipating heat from electronic devices to the surroundings.

Elbadawy et al. [21] numerically investigated the THP of offset strip finned MCHSs with various MICH cross-sectional shapes, such as rectangular, trapezoidal, triangular, and circular, to provide the safety of the electronic devices. They optimised the Nu, pressure drop, and overall efficiency to identify optimal geometry shapes and sizes for providing efficient cooling of electronic devices to increase the life span of the devices. Its results showed that the MICH shape significantly affects the safety and reliability of the devices. It was observed that trapezoidal and triangular shapes provided higher heat transfer as compared to rectangular and circular shapes. However, trapezoidal and triangular shapes gave higher pressure drops. The correlation between Nu and pressure drop was developed using a performance evaluation criterion (PEC), which showed that the trapezoidal channel is the effective configuration that provides a higher heat dissipation rate as compared to the others, as well as provides the safety of the electronic devices at less friction loss.

Shakir et al. [22] numerically and experimentally investigated single-phase and two-phase boiling heat transfer in aluminium MICH using R113 as the working fluid. A square cross-section of the test setup was developed with dimensions of 0.5 mm and 0.5 mm, and a constant heat flux was applied to the bottom of the channel, which varied from 40 to 600 W at three different mass flow rates, such as 0.0125 kg/s, 0.015 kg/s, and 0.0175 kg/s. In this, they analysed heat transfer coefficients (HTC), exit quality, and pressure drops for both subcooled and saturated boiling regimes to provide the safety and reliability of the electronic devices. Its outcome showed that single-phase flow at laminar and fully developed characteristics with HTCs increase with increasing the mass flux, whereas fluid temperature decreases with increasing the mass flux. However, in two-phase flow, HTC was significantly affected by heat flux, mass flow rate, and vapour quality. Onset of boiling was seen around 47°C, and pressure drop behaviour showed two different regimes for single- and two-phase flow, which was also shown both numerically and experimentally, and developed empirical correlations for the safety of the electronic devices. Furthermore, the effect of MICH geometry and operating conditions on boiling heat transfer and instabilities was investigated to accurately provide a robust condition for providing the safety and reliability of the electronic devices.

Chen et al. [23] conducted numerical simulation combined with response surface methodology (RSM) to investigate the thermal–hydraulic optimisation of trapezoidal MCHSs by incorporating different rib geometries to protect the failure of electronic devices. In this study, they used four different rib shapes, such as triangular, rectangular, semicircular, and trapezoidal, with varying rib height and pitch to predict the effects on Nusselt number (Nu), friction factor (FF), and performance evaluation criterion (PEC) to enhance the safety of the electronic devices. Its results demonstrated that rib structures significantly improve HTC and Nu due to flow disturbance and secondary vortices. However, pressure drop is increased, which reduces the reliability of the device wall. Furthermore, trapezoidal ribs provided significant HTC and minimum pressure drop, which provided the highest safety and reliability of the electronic devices during cooling among all other shapes of the test ribs. Furthermore, RSM-based optimisation identified the optimal rib geometry and its arrangement for higher safety of the devices by improving the heat dissipation rates. Zhang et al. [24] numerically examined the effect of different MICH cross-sectional geometries, such as rectangular, trapezoidal, triangular, and circular, on the heat transfer rate and THP performance of MCHSs. Also, they were evaluated for Nu, FF, and performance evaluation criteria to ensure the safety of the electronic devices. Its results revealed that trapezoidal and triangular channels had significantly improved heat transfer compared to rectangular and circular-shaped channels. However, the pressure drop was observed to be maximal. The trapezoidal-shaped MICH gave a higher heat transfer rate at minimum pressure drop, which is similar to Chen et al. [23]. This finding suggested that optimising the MICH cross-sectional shape is a crucial parameter for improving and enhancing the safety of the electronic devices, as well as for use in various advanced thermal management applications, particularly for microelectronic device cooling. Further, Wunderle et al. [25] extensively reviewed and summarised advancements in MCHS designs with various channel cross-sectional geometries to improve the heat transfer rate in the microelectronic devices. They suggested that rectangular MICH is widely used for cooling the electronic devices, which experience higher pressure drop and relatively lower heat transfer performance compared to non-rectangular geometries such as trapezoidal, triangular, and circular shapes. Researchers demonstrated that non-rectangular channels enhance heat transfer through the promotion of secondary flows and larger surface areas, often at the cost of higher pressure drops. They concluded that trapezoidal and triangular geometries provide higher heat transfer rates, as well as experience higher pressure drops. Also, Sidik et al. [26] examined the effect of several different cross-section geometries, such as rectangular, triangular, semicircular, and trapezoidal shapes, on the THP of MCHSs using the 3D-CFD tool ANSYS and reported that Nu, ff, and THP varied at varying Reynolds numbers. Also, they suggested that the heat transfer rate increases with increased Reynolds numbers at low friction loss and pressure drop, as well as rectangular cross-section. MICH had the least heat transfer and the highest-pressure drop, which makes electronic devices less safe and reliable.

Mudawar in 2002 [27] conducted numerical investigations to determine the THP of MCHSs, including different designs of the MICH, such as zigzag, sinusoidal, and wavy designs, as well as combining the effect of the structure or improving the cooling efficiency to provide safety of the electronic devices. Simulations were conducted to evaluate Nu and pressure drop (ΔP) at various Reynolds numbers. Its outcome showed that using a zig-zag channel significantly improves heat transfer due to fluid mixing and changing the flow boundary layers, as well as increasing the pressure drop. Among all designs, zigzag and sinusoidal structures showed higher heat dissipation rates, which provide better safety for electronic devices as well as improve their lifespan. Similarly, Spizzichino et al. [28] presented a numerical analysis of the THP of wavy MCHSs with different wave structures, such as sinusoidal, triangular, and trapezoidal profiles, and they suggested that wavy MICH showed maximum heat transfer as compared to other designs with a higher-pressure drop.

Furthermore, Ko et al. [29] developed a low-temperature MEMS fabrication method for MICH and integrated it with temperature sensors and micro-heaters to measure local heat transfer during the operation of the electronic devices. In this study, they used low-thermal-conductivity materials such as epoxy, Pyrex, PMMA, SU-8, and a two-stage process. Air is used as a working fluid in the channel for cooling the HTC revealed that HTC is significantly affected by using the MICH for heat transfer from the electronic device, which can improve the safety and life of the devices. Also, they suggested the impact of size effects and wall properties and demonstrated the feasibility of micro-channel cooling for high-power devices such as future CPU chips.

Tiseljet al. [30] experimentally investigated heat transfer in silicon-based MICHs. In this study, they used MEMS sensors to accurately predict the wall temperature of the electronic devices as well as HTC. Also, a fabrication method that allows for the accurate positioning of heaters and thermocouples within high-aspect-ratio MICHs, thereby reducing conduction losses and enhancing measurement precision. Experimental findings for single-phase liquid flow demonstrate that traditional macroscale heat transfer correlations tend to overestimate microchannel performance, highlighting notable scale effects. Its outcomes identify variations in local Nusselt number trends, indicating diminished heat transfer rates and uneven distributions along the channel. The findings suggested that MICHs have a compact design and high-performance cooling systems for microelectronics and demonstrate that microscale heat transfer necessitates advanced theoretical models that extend beyond classical assumptions.

Ding et al. [31] studied both experimentally and numerically to analyse heat transfer through MCHS at different aspect ratios using water as a working fluid. Its results revealed that intermediate channel widths improve the flow inside the channel due to less frictional pressure drop, variation of wall temperature along the length, and THP. Based on this, a correlation of heat transfer and the width of the channel was developed to maintain the working temperature under the limiting temperature.

Lorenzo Consolini and Thome [32] reported heat transfer through MICH from electronic devices in single- and two-phase flow using three different working fluids (R-134a, R-236fa, and R-245fa) and two different hydraulic diameters (510 and 790 μm) of the channels. Also, a parametric study was performed to determine the two-phase flow instability, which develops a thermal fatigue load that is harmful for devices as well as MICH. Its results revealed that the HTC of R-134a and R-236fa are significantly dependent on the heat flux and mass flow rate at low and high dryness fractions. However, R245fa showed the opposite of the other fluid, which developed instability in the channel and degraded the lifespan of the channel.

Jahar Sarkar [33] suggested that heat transfer through MICH significantly improved using supercritical carbon dioxide as a working fluid in electronic devices. Also, parametric studies were performed for two different fluids, supercritical carbon dioxide and water, to examine which fluid gives higher heat transfer at lower resistance. Its results showed that heat transfer was improved by 30% as compared to water at low thermal resistance, which provides higher safety to the electronic devices.

Xiang et al. [34] numerically investigated the MCHS using a thermal resistance model to accurately predict the heat transfer rate from the electronic devices. In this study, they fabricated the MCHS and tested for heat transfer. Its result showed that developed MCHS hives have higher heat transfer as compared to conventional metal made of MCHS, which is recorded for heat transfer from LED applications.

Bello-Ochende et al. [35] numerically investigated the heat transfer through MICH using the 3D model finite volume method to reduce the wall temperature of the MICH from the working fluids. The results indicated that the maximum temperature of the MICH is significantly reduced by increasing the working fluid flow rate in the channel, as well as increasing the aspect ratio of the channel.

Li et al. [36] suggest a correlation to distinguish between mini and MICH for heat transfer from electronic devices. In this study, they used single and manifold types of MICH as well as single and two-phase flow. Also, in this study, seven pre-developed correlations were used to predict and verify the heat transfer of the 4228 databases. Based on this correlation, they proposed a new correlation, Bo*Re0.5 = 200, to accurately predict the heat transfer rate through MICH.

Spizzichino et al. [37] investigated heat transfer and flow characteristics of parallel MICH (i.e., 10 channels) using both experiments and numerical simulation methods, and deionised water was used as the working fluid. Results show that uniform-width channels cause higher pressure drops and mass flow in intermediate channels, leading to uneven base temperatures, while refining intermediate channel widths produces more uniform flow and wall temperature distributions. A new Performance Evaluation Criterion for Non-uniform Channels (PECNC) was proposed to assess designs, with structure VI emerging as the optimal configuration. Additionally, a mathematical expression was developed to guide the design of width distributions that promote uniform temperature fields.

Qu and Mudawar [38] investigated the heat transportation phenomenon of two-phase in MICH to improve the safety and reliability of the electronic cooling devices. In this study, they suggested the basic reliable operation of a two-phase MICH transport phenomenon integrated with convective boiling in single and parallel channels. They used high-speed photographic methods to accurately predict hydrodynamic instability, two-phase flow patterns, pressure drop, and convective boiling heat transfer. The study's findings indicate that MICH primarily experiences two types of instability: a drastic pressure drop and a mild parallel channel.

Sehgal et al. [39] conducted several experiments to examine the effect of the inlet and outlet plenums in different arrangements of various MICH shapes, such as U, P, and S types, on improving the cooling of electronic devices as well as enhancing their thermal–hydraulic performance (THP). A heat input ranging from 125 W to 375 W was applied to the wall of the MICH, with Reynolds numbers (Re) varying from 224 to 1121, to assess THP. Higher heat dissipation was observed in the U-shaped MICH, while a greater pressure drop occurred in the S-type MICH among other channels, which improves the reliability and safety for electronic devices.

Xia et al. [40] numerically investigated the effect of the position of the MICH on the 3D-IC in heat transfer for improving the performance and safety of the devices, as well as thermal management of the electronic devices. In this study, two types of cavities are considered, namely triangular reentrant cavities (TRC) and fan-shaped reentrant cavities (FRC) having a pitch and height of 1/0.2 mm and 0.2 mm, respectively. The effect of both cavities of MICH was compared with that of rectangular MICH. Its results revealed that the distribution of the heat rate and pressure drop was uniform along the length of each layer, as well as the pitch of 0.1 mm of MICH. Higher heat transfer and THP were observed at a higher pressure drop and pumping power, which significantly affected the safety of the devices as well as reduced their life span.

Several recent experimental and numerical research works were reported to improve the safety and reliability of electronic devices by improving the heat transfer rate from these devices due to their compact size.

Table 1 shows a comparative summary of recently reported research to improve the safety of electronic devices using different designs, shapes, and working fluids. It can be seen from table 1 that MCHS is mainly used for electronics devices cooling and is significantly suggested by the numerous researchers to use hybrid designs and integrated optimisation to increase heat dissipation at a low volume-to-area ratio. Markal et al. [41] developed MICH, which consists of MICH with pin-type fins, which gives higher heat dissipation by optimising the design and geometry sizes of the channel and fins to minimise the thermal resistance and pressure drops to increase the safety of the electronic devices. Similarly, Li et al. [36] developed lattice-interconnected channels and nanofluid in the MICH to improve the cooling rate of the devices and reported that heat transfer is increased by using the nanoparticle in the coolant, and the pressure drop is reduced in the channel. Also, Huang et al. [42] implanted phase-change materials (PCMs) with graphite foam to absorb cyclically generated heat from electronic devices, which reduced the limiting temperature of the chips and electronic devices and provided better safety and reliability of the devices. Xiang et al. [34] also developed a vacuum-assisted two-phase honeycomb heat sink to reduce the electronic device temperature by approximately 15°C at 90 W and validated performance through both experiments and numerical analysis. Further, Rai et al. [43] conducted several single- and two-phase numerical and experimental studies in single- and two-phase flow through MICH

Table 1

SUMMARY OF DIFFERENT METHODS AND WORKING FLUIDS USED TO IMPROVE THE SAFETY OF THE ELECTRONIC DEVICES			
Author	**Design / Method**	**Working fluids**	**Main findings**
Markal et al. [41]	MICH with pin-fin heat sink	Deionized water	• Higher heat transfer but increased pressure drop. • Optimal fin height and channel width significantly improved the THP. • Thermal resistance reduced by approximately 15–20% and pressure drops increased by 30–40% as compared to plain MICH.
Li et al. [36]	MICH with nanofluid	Water + Al_2O_3 nanofluid	• Best lattice geometry improved THP. • Peak temperature drops up to 12°C and pressure drops approximately 20% compared to straight MICH.
Huang et al. [42]	Phase-change material (PCM) with graphite foam embedded in the walls	Water (base) + PCM for transient loads	• PCM and high-conductivity foam maximised THP. • Peak temperature of the reduced approximately 15°C vs. solid plate at 90 W. • Reduced peak chip temperature under cyclic heat input from the devices. • PCM absorbed heat generated from the devices.
Xiang et al. [34]	Vacuum-assisted two-phase honeycomb MICH	Water + R134a (two-phase mix)	• Optimal regular hexagon, 2 mm pitch, 0.5 mm depth, 8 mm radius. • Max chip temp reduced from 85°C to 70°C at 90 W with ± 1°C.
Rai et al. [43]	Single MICH (Single and Two Phase)	Deionised water (single and two-phase)	• Working temperature of the device is to be maintained under 40°C. • Experimental and numerical validation showed ±6.04 errors.
Husain et al. [44]	Different designs of MICHs (Square, rectangular and trapezoidal and different boundary conditions)	Deionised water (H methods)	• Optimising the design of the MICH and applying 2H and 4H boundary conditions to enhance the heat transfer rate and improve the safety of the electronic devices.

for improving the safety and reliability of the electronic devices. They used deionised water as a working fluid and three different MICH geometries. They developed a correlation between mass flow rate and generated heat power from the electronic devices to reduce the working temperature of the device to under 40°C, which improves the safety and reliability of the electronic devices. Also, in numerical studies, they optimised the geometry for higher heat transfer in rectangular, square, and trapezoidal shapes and reported that trapezoidal geometry provides high heat transfer. To enhance the safety and reliability of the electronic devices, hybrid methods are employed alongside geometry optimisation, which is necessary to prevent drastic pressure changes inside the MICH.

Heat transfer in single and two-phase microchannels

Several researchers have carried out various experimental and numerical studies to predict the heat transfer and Nusselt (Nu) number at different mass flow rates, inlet velocity and Reynolds (Re) number. Wu et al. [45] developed MCHs with widths of 130–200 μm and depths of 30–60 μm using a photolithographic technique and predicted the Nu at different Re numbers. Similarly, Hao et al. [46], Gnielinski et al. [47] and Admas et al. [48] developed MCHs to predict the heat transfer rate through MCHs. However, they modified the hydraulic diameter. It can be seen from figure 4 that Wu et al. [45], Hao et al. [46], and Gnielinski et al. [47] predicted Nu correlation showed a similar profile. However, the quantitative values depicted higher different to each other. Also, Admas et al. [48] used Gnielinski's correlation [47] with certain modifications of Re and Dh to

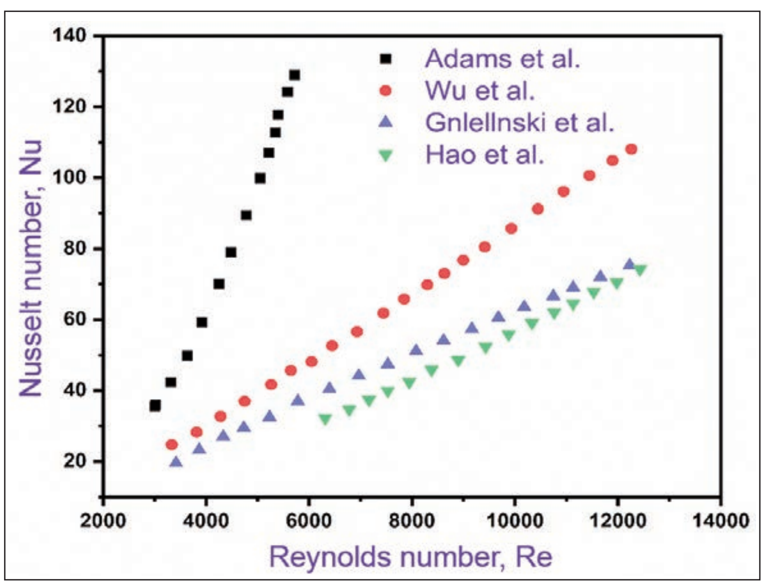

Fig. 4. Variation of Nusselt numbers at different Reynolds numbers

predict the Nu and HTC in MICH and found that at Re numbers 3000 to 6000, Nu and HTC were observed to be higher as compared to other proposed correlations.

Advanced textile microfluidic systems for sweat analysis, cooling, and wearable healthcare monitoring

Textile-based microfluidic biosensors, microchannel- and nanochannel-based devices, and sensors exemplify a novel integration of multiple interdisciplinary domains, encompassing bioelectronics, materials science, and microfluidics. Their potential in biomedicine is considerable, as they utilise textiles to meet the stringent requirements of biocompatibility with the human body and adapt to its uneven surfaces. In microfluidics, a fabric treated with hydrophobic substances functions as a conduit for the accurate transmission of liquids to the sensing element, specifically a biosensor [49–55]. Khosravi et al. [56] developed wearable sweat biosensors for detecting health parameters, which are fabricated in a textile that is easily mounted over a human in a very easy manner. It can be mounted on the daily use cloth and operated for a long time. However, after operating for a long time, the sensor gets heated, and its life span decreases. Therefore, MCHs are used to remove heat from the sensor to the environment to maintain the working temperature under working limits. Yin et al. [57] introduce wearable sweat biosensors that utilise MCHs and nanochannels to detect human health. These types of channels are capable of easily absorbing the heat and sweat from the human body to detect the body temperature, and with the help of sweat sensors, they are able to detect human health to provide safety. Zhang et al. [58] presented a fabric-based microfluidic device that is integrated with cloth to monitor the health of humans for providing safety. They have performed experimental and numerical tests using MCH to properly absorb and deliver the sweat in the sensors, which showed that it is more efficient. Kim et al. [59] presented a flexible textile-based hybrid microbial–enzymatic biofuel cell using a Y-shaped screen-printed MCH and optimised electrode/catalyst configurations to enhance performance. Achieving high power and current densities, the device demonstrates a safe, wearable microscale power platform superior to previous textile or paper microfuel cells. Similarly, Chen et al. [60] suggested a laser-engraved textile microfluidic design using fractal, tree-like bifurcating channels to enable rapid, leakage-free sweat collection with high wicking efficiency. The optimised geometry provides fast induction (<1 min) and high sweat flux, ensuring complete droplet capture for reliable sampling. Integrated with printed sensors and microchips, the system enables real-time wireless monitoring of sweat rate and electrolyte levels, demonstrating strong practicality in field tests. Also, Lingling et al. [61] demonstrated a simple, sustainable method for fabricating moist-electric generators (MEGs) using biomass Juncus effusus fibres, whose natural 3D microchannel networks and LiCl loading enhance moisture capture and continuous energy generation. The resulting JE-based MEG delivers stable long-term output (306.2 mV, 1.11 mA, 13.60 mWcm^{-2}) with strong durability under bending and abrasion.

Demonstrations powering LEDs and a watch highlight its potential as a wearable, textile-integrated power source for portable electronics. Laha et al. [62] experimentally investigated viscoelastic polymer solutions interacting with deformable microchannels, revealing a strong dependence of flow-induced deformation on polymer concentration and molecular weight. Higher concentrations and elastic effects intensify wall deformation, alter local pressure-drop behaviour, and produce nonlinear fluid–structure interactions. Theoretical modelling further confirms the coupled rheology–deformation mechanisms, offering insights for designing adaptive microfluidic devices handling complex fluids. Furthermore, Askar et al. [63] suggested a skin-strain-actuated microfluidic pump (SAMP) that records human activity using asymmetric aspect-ratio microchannels, enabling passive, image-based data capture. The device changes the hydraulic resistance in a way that turns cyclic skin strain into one-way liquid flow. This has been shown to work in both analytical modelling and benchtop tests. Fabricated using PDMS soft lithography, the SAMP reliably tracks repetitive wrist motions and distinguishes between different shoulder movements. The equivalent electrical circuit model accurately predicts pumping efficiency, confirming strain-dependent asymmetric channel behaviour as the core mechanism. Overall, the SAMP functions as a fluidic memory device for summarising human activity, offering a simple, low-power alternative to conventional electronic wearables.

RESEARCH GAPS

After extensively reviewing the previously reported works of several researchers, some concise observations regarding the use of different single- and two-phase cooling methodologies, as well as various designs used to improve the safety and reliability of the electronic devices, are as follows:

- Traditional cooling methods, such as air-cooled heat sinks and fans, are not sufficient to provide enough safety to the high-performance electronic devices, such as chips, integrated chips, high-frequency processors, laser diodes, and power electronics, due to their compact sizes. Therefore, a robust design with higher THP of MICHs is required, which can remove higher heat flux from the devices to improve the safety and reliability of the electronic devices [64].
- One of the major challenges is the fabrication of the MICHs, which requires precision machining, etching, micro-milling, etc., that are costly and time-consuming, as well as high-precision sealing and assembly processes to completely seal channels, which can protect the electronic devices from short circuits during operation.

- Very limited studies on the manifold and serpentine types of MICHs are available in the literature, which can be needed to extensively study for improving the THP as well as the safety of the electronic devices.
- Very limited working fluids are used in the MICHs for improving the THP and efficiency of the channel. Supercritical fluids can be used to improve the THP and safety of the electronic devices.
- There is significant potential for the integration of MCHs and nanochannels in the textile industry, particularly for thermal management in wearable electronics and microfluidic devices embedded within fabrics and clothing, which are very limited.

CONCLUSION AND FUTURE SCOPE

In this present work, an extensive literature review is conducted on the available literature related to the sustainability, reliability, and safety of MICHs in the application of electronics devices, which are used in various industries such as electronics, aerospace, automotive, biomedical and microfluid devices, etc. Several important findings are observed from this extensive literature review, which are given below.

- Day by day, electronic devices are drastically increasing with miniaturisation, minimising their sizes and increasing their power densities. Therefore, effective thermal management is required as well as a determinant of system longevity, energy efficiency, and operational safety. MICH and MCHSs can remove a significant amount of heat from the electronic devices, which improves the sustainability of the electronic devices. Also, MICH reduces energy consumption and improves device lifespans and does not affect the environment. However, careful selection of materials and coolants is necessary to ensure recyclability and minimise environmental risks.
- MICH is a better solution for improving the safety of electronic devices as compared to traditional cooling methods.
- The cyclic heat load can be removed by using the PCM in the MICHs, which increases the safety of the electronic devices by absorbing temperatures of 10°C to 15°C.
- The trapezoidal design of MICHs provides higher heat transfer than other designs, such as rectangular, square, and circular types of MICHs.
- MCHs are increasingly utilised in textile-based systems to integrate wearable biosensors and microfluidic devices for real-time human health monitoring.
- Two-phase and boiling methods provide higher heat transfer as compared to single-phase cooling methods and improve the safety and reliability of the electronic devices.

By using the MICHs, various problems have been resolved to improve safety and increase the lifespan of electronic devices. However, there are still several issues that have remained open to be resolved for improving the safety of the MICHs during use in the electronic cooling devices. 3D modelling using different designs and shapes of the MICHs cab can improve the safety of the devices. 3D printers can be used to fabricate the MICHs. Also, for real-time monitoring of temperature, flow rate, pressure, and THP of the MICHs, a combined system (including sensors, IoT devices, and machine learning) can be used. Furthermore, robust pressure control, leak-proof design, and accurate heat input prediction are required to improve the sustainability, reliability, and safety of electronic devices.

REFERENCES

[1] Yu, Z., Q., Li, M.T., Cao, B.-Y., *A comprehensive review of microchannel heat sinks for electronics cooling*, In: International Journal of Extreme Manufacturing, 2024, 6, 022005

[2] Rai, S.K., Sharma, R., Saifi, M., Tyagi, R., Singh, D., Gupta, H., *Review of recent applications of micro channel in MEMS devices*, In: International Journal of Applied Engineering Research, 2018, 13, 9, 64–69

[3] Tuckerman, D.B., Pease, R.F.W., *High-performance heat sinking for VLSI*, In: IEEE Electron Device Letters, 2005, 2, 5, 126–129

[4] Lu, K., Wang, C., Wang, C., Fan, X., Qi, F., He, H., *Topological structures for microchannel heat sink applications – a review*, In: Manufacturing Review, 2023, 10, 2

[5] Japar, W.M.A.A., Sidik, N.A.C., Saidur, R., Asako, Y., Nurul Akmal Yusof, S., *A review of passive methods in microchannel heat sink application through advanced geometric structure and nanofluids: Current advancements and challenges*, In: Nanotechnology Reviews, 2020, 9, 1, 1192–1216

[6] Ayatollahi, S.M., Ahmadpour, A., Hajmohammadi, M.R., *Performance evaluation and optimization of flattened microchannel heat sinks for the electronic cooling application*, In: Journal of Thermal Analysis and Calorimetry, 2022, 147, 4, 3267–3281

[7] Rai, S.K., Kumar, P., Tiwari, M., Panwar, V., Kumar, D., Sharma, V.K., *A comprehensive overview of advancements, applications, and impact of supercritical fluid natural circulation loops*, In: Annals of Nuclear Energy, 2025, 211, 110971

[8] Suman, S., Upadhyaya, R., Raghuvanshi, N.S., Gupta, M.K., Shah, S., Alam, S., *A state of art review of instability in parallel channels of supercritical fluid in nuclear applications*, In: Materials Today: Proceedings, 2022, 62, 226–232

[9] Rai, S.K., Kumar, P., Panwar, V., *Computational analysis of static flow instabilities in supercritical natural circulation loop*, In: Proceedings of International Conference on Thermofluids: KIIT Thermo 2020, Singapore: Springer Singapore, 2020, 387–395

[10] Mala, G.M., Li, D., Dale, J.D., *Heat transfer and fluid flow in microchannels*, In: International Journal of Heat and Mass Transfer, 1997, 40, 13, 3079–3088

[11] Kandlikar, S., *Heat transfer and fluid flow in minichannels and microchannels*, Elsevier, 2006

[12] Cova, P., Santoro, D., Spaggiari, D., Portesine, F., Vaccaro, F., Delmonte, N., *CFD modeling of additive manufacturing liquid cold plates for more reliable power press-pack assemblies*, In: Microelectronics Reliability, 2020, 114, 113734
[13] Sidik, N.A.C., Muhamad, M.N.A.W., Japar, W.M.A.A., Rasid, Z.A., *An overview of passive techniques for heat transfer augmentation in microchannel heat sink*, In: International Communications in Heat and Mass Transfer, 2017, 88, 74–83
[14] Gupta, H.K., Rai, S.K., &Sheorey, T., *Boiling flow heat transfer in microchannel: Experimental and numerical investigation*, In: Proceedings of the 23rd National Heat and Mass Transfer Conference and 1st International ISHMT-ASTFE Heat and Mass Transfer Conference IHMTC-2015, 2015, 1–8
[15] Singh, D., Rai, S., Shukla, S., *Numerical analysis of two phase flow boiling heat transfer through microchannel*, In: IJERT, 2017, 6, 1–6
[16] Ohadi, M., Choo, K., Dessiatoun, S., Cetegen, E., *Fundamentals of microchannels. In Next Generation Microchannel Heat Exchangers,* New York, NY: Springer New York, 2012, 1–32
[17] Tullius, J.F., Vajtai, R., Bayazitoglu, Y., *A review of cooling in microchannels*, In: Heat Transfer Engineering, 2011, 32, 7–8, 527–541
[18] Yu, Z.Q., Li, M.T., Cao, B.Y., *A comprehensive review on microchannel heat sinks for electronics cooling*, In: International Journal of Extreme Manufacturing, 2024, 6, 2, 022005
[19] Dixit, A., Maithani, R., Sharma, S., *Enhancing electronic system cooling: exploring minichannel heat sink solutions*, In: Journal of Thermal Analysis and Calorimetry, 2025, 1–51
[20] Wang, X., Su, Z., Mansir, I.B., Singh, P.K., Othman, N.A., Zhang, L., Deifalla, A., *Thermal and hydrodynamic management of a finned-microchannel heat sink applying artificial neural network*, In: Case Studies in Thermal Engineering, 2023, 45, 102996
[21] Elbadawy, I., Alhajri, A., Doust, M., Almulla, Y., Fayed, M., Dinc, A., Al-Kouz, W., *Reliability of different nanofluids and different micro-channel configurations on the heat transfer augmentation*, In: Processes, 2023, 11, 3, 652
[22] Shakir, R., *Boiling heat transfer in a micro-channel complex geometry*, In: IOP Conference Series: Materials Science and Engineering, IOP Publishing, 2020, 928, 2, 022129
[23] Chen, L., Zhang, X.R., Okajima, J., Komiya, A., Maruyama, S., *Numerical simulation of stability behaviors and heat transfer characteristics for near-critical fluid microchannel flows*, In: Energy Conversion and Management, 2016, 110, 407–418
[24] Zhang, X., Jaluria, Y., *Reliability-based optimization and design limits of microchannel cooling systems*, In: International Journal of Heat and Mass Transfer, 2020, 149, 119202
[25] Wunderle, B., Schacht, R., Wittler, O., Michel, B., Reichl, H., *Performance and thermo-mechanical reliability of micro-channel coolers-a parametric study*, In: The Ninth Intersociety Conference on Thermal and Thermomechanical Phenomena in Electronic Systems (IEEE Cat. No. 04CH37543), IEEE, 2004, 2, 11–16
[26] Sidik, N.A.C., Muhamad, M.N.A.W., Japar, W.M.A.A., Rasid, Z.A., *An overview of passive techniques for heat transfer augmentation in microchannel heat sink*, In: International Communications in Heat and Mass Transfer, 2017, 88, 74–83
[27] Mudawar, I., *Assessment of high-heat-flux thermal management schemes*, In: IEEE Transactions on Components and Packaging Technologies, 2002, 24, 2, 122–141
[28] Spizzichino, M., Sinibaldi, G., Romano, G.P., *Experimental investigation on fluid mechanics of micro-channel heat transfer devices*, In: Experimental Thermal and Fluid Science, 2020, 118, 110141
[29] Ko, H.S., Liu, C.W., Gau, C., Yang, C.S., *Fabrication and design of a heat transfer micro-channel system by a low temperature MEMS technique,* In: Journal of Micromechanics and Microengineering, 2007, 17, 5, 983
[30] Tiselj, I., Hetsroni, G., Mavko, B., Mosyak, A., Pogrebnyak, E., Segal, Z., *Effect of axial conduction on the heat transfer in micro-channels,* In: International Journal of Heat and Mass Transfer, 2004, 47, 12-13, 2551–2565
[31] Ding, Y.Y., Liu, M.G., Jin, Q., *Experimental and numerical investigation of the influence of varying micro-channel width on flow and heat transfer uniformity*, In: International Journal of Thermal Sciences, 2025, 208, 109394
[32] Consolini, L., Thome, J.R., *Micro-channel flow boiling heat transfer of R-134a, R-236fa, and R-245fa*, In: Microfluid Nanofluid, 2009, 6, 731–746
[33] Sarkar, J., *Improving thermal performance of micro-channel electronic heat sink using supercritical CO2 as coolant*, In: Thermal Science, 2019, 23, 1, 243–253
[34] Xiang, J., Deng, L., Zhou, C., Zhao, H., Huang, J., Tao, S., *Heat transfer performance and structural optimization of a novel micro-channel heat sink*, In: Chinese Journal of Mechanical Engineering, 2022, 35, 1, 38
[35] Bello-Ochende, T., Liebenberg, L., Meyer, J.P., *Constructal cooling channels for micro-channel heat sinks*, In: International Journal of Heat and Mass Transfer, 2007, 50, 21–22, 4141–4150
[36] Li, W., Wu, Z., *A general criterion for evaporative heat transfer in micro/mini-channels*, In: International Journal of Heat and Mass Transfer, 2010, 53, 9–10, 1967–1976
[37] Spizzichino, M., Sinibaldi, G., Romano, G.P., *Experimental investigation on fluid mechanics of micro-channel heat transfer devices*, In: Experimental Thermal and Fluid Science, 2020, 118, 110141
[38] Qu, W., Mudawar, I., *Transport phenomena in two-phase micro-channel heat sinks*, In: Journal of Electronic Packaging, 2004, 126, 2, 213–224
[39] Sehgal, S.S., Murugesan, K., Mohapatra, S.K., *Experimental investigation of the effect of flow arrangements on the performance of a micro-channel heat sink*, In: Experimental Heat Transfer, 2011, 24, 3, 215–233
[40] Xia, G.D., Ma, D.D., Wang, W., Zhai, Y.L., *Effects of different structures and allocations on fluid flow and heat transfer performance in 3D-IC integrated micro-channel interlayer cooling*, In: International Journal of Heat and Mass Transfer, 2015, 91, 1167–1175
[41] Markal, B., Evcimen, A., *Investigation of flow boiling phenomenon in micro-pin-fin heat sinks adapted to actively direction-changing moving systems*, In: International Communications in Heat and Mass Transfer, 2024, 159, 108310
[42] Huang, S., Long, C., Hu, Z., Xu, Y., Zhang, B., Zhi, C., *Thermal Performance of Heat Sink Filled with Double-Porosity Porous Aluminum Skeleton/Paraffin Phase Change Material*, In: Micromachines, 2024, 15, 6, 806
[43] Rai, S.K., Goyat, V., Gupta, M.K., Ghangas, G., Bhatt, D., Uniyal, A., Shrivas, N.V., *Numerical and experimental heat transfer analysis of two-phase flow through microchannel for development of heat dissipation correlation*, In: Journal of Non-Equilibrium Thermodynamics, 2025

[44] Hussain, M.E., Rai, S.K., Suman, S., Gupta, P., Gupta, M.K., *Computational Analysis of Transfer of Heat in Micro Size Channels Using Different Boundary Condition in Laminar Flow*, In: Biennial International Conference on Future Learning Aspects of Mechanical Engineering, Singapore: Springer Nature Singapore, 2022, 445–455
[45] Peiyi, W., Little, W.A., *Measurement of friction factors for the flow of gases in very fine channels used for microminiature Joule-Thomson refrigerators,* In: Cryogenics, 1983, 23, 5, 273–277
[46] Hao, P.F., He, F., Zhu, K.Q., *Flow characteristics in a trapezoidal silicon microchannel*, In: Journal of Micromechanics and Microengineering, 2005, 15, 6, 1362
[47] Gnielinski, V., *New equations for heat and mass transfer in turbulent pipe and channel flow*, In: International Chemical Engineering, 1976, 16, 2, 359–367
[48] Adams, T.M., Abdel-Khalik, S.I., Jeter, S.M., Qureshi, Z.H., *An experimental investigation of single-phase forced convection in microchannels*, In: International Journal of Heat and Mass Transfer, 1998, 41, 6–7, 851–-857
[49] Sun, X., Zhao, C., Li, H., Yu, H., Zhang, J., Qiu, H., Liang, J., Wu, J., Su, M., Shi, Y., Pan, L., *Wearable near-field communication sensors for healthcare: Materials, fabrication and application*, In: Micromachines, 2022, 13, 5, 784, https://doi.org/10.3390/mi13050784
[50] Milić, L., Zambry, N.S., Ibrahim, F.B., Petrović, B., Kojić, S., Thiha, A., Stojanović, G.M., *Advances in textile-based microfluidics for biomolecule sensing*, In: Biomicrofluidics, 2024, 18, 5
[51] Hanze, M., Piper, A., Hamedi, M.M., *Stitched textile-based microfluidics for wearable devices,* In: Lab on a Chip, 2025, 25, 1, 28–40
[52] Watel, Q., Cayla, A., Aubert, V., Salaün, F., Viovy, J.L., Boussu, F., *Fully woven textile-based closed microfluidic system design*, In: The Journal of The Textile Institute, 2025, 116, 7, 1358–1367
[53] Yu, W., Li, Q., Zhao, Z., Gong, J., Li, Z., Zhang, J., *A yarn/fabric-based microfluidic patch for sweat sensing and monitoring*, In: The Journal of The Textile Institute, 2024, 115, 11, 2331–2342
[54] Akter, A., Apu, M.M.H., Veeranki, Y.R., Baroud, T.N., Posada-Quintero, H.F., *Recent studies on smart textile-based wearable sweat sensors for medical monitoring: a systematic review*, In: Journal of Sensor and Actuator Networks, 2024, 13, 4, 40
[55] Galliani, M., Ismailova, E., Azizian, P., Makhinia, A., Cabot, J.M., *Vertical textile microfluidics: advancing on-garment sweat sampling for real-time biosensing*. In: Flexible Electronics, 2025, 9, 1, 38
[56] Khosravi, S., Soltanian, S., Servati, A., Khademhosseini, A., Zhu, Y., Servati, P., *Screen-printed textile-based electrochemical biosensor for noninvasive monitoring of glucose in sweat*, In: Biosensors, 2023, 13, 7, 684, https://doi.org/10.3390/bios13070684
[57] Yin, J., Li, J., Reddy, V.S., Ji, D., Ramakrishna, S., Xu, L., *Flexible textile-based sweat sensors for wearable applications*, In: Biosensors, 2023, 13, 1, 127, https://doi.org/10.3390/bios13010127
[58] Zhang, T., Ratajczak, A., Chen, H., Terrell, J.A., Chen, C., *A step forward for smart clothes: Fabric-based microfluidic sensors for wearable health monitoring*, In: ACS Sensors, 2022, https://doi.org/10.1021/acssensors.2c01827
[59] Kim, J., Kong, H.G., Ahn, Y., *Textile-Based Membraneless Microfluidic Double-Inlet Hybrid Microbial–Enzymatic Biofuel Cell*, In: ACS Applied Materials & Interfaces, 2024, 16, 33, 43661-43669
[60] Chen, Y.C., Shan, S.S., Liao, Y.T., Liao, Y.C., *Bio-inspired fractal textile device for rapid sweat collection and monitoring*, In: Lab on a Chip, 2021, 21, 13, 2524–2533
[61] Su, L., Zhang, C., Tang, W., Fu, Z., Gong, J., Qin, J., Xu, W., *Moist-electric generators using biomass Juncus effusus fibers with 3D microchannels for wearable applications*, In: Chemical Engineering Journal, 2024, 499, 156106
[62] Laha, S., Mukherjee, S., Chakraborty, S., *Dynamical Response of Deformable Microchannels under Pressure-Driven Flow of Aqueous Polymer Solutions*, arXiv preprint, 2025, arXiv:2509.21343
[63] Askar, C.B., Cmager, N., Altay, R., Araci, I.E., *Human Activity Recording Based on Skin-Strain-Actuated Microfluidic Pumping in Asymmetrically Designed Micro-Channels*, In: Sensors, 2024, 24, 13, 4207
[64] Kumar, P., Kumar, D., Chalisgaonkar, R., Sharma, V.K., Rai, S.K., *A Critical Review of Ram Methodology: Analysis and Performance Evaluation in Industrial Complexities*, In: Reliability: Theory & Applications, 2024, 19, 4, 80, 83–89

Authors:

SANTOSH KUMAR RAI[1], MAHESH KUMAR GUPTA[1], GYANENDRA PRASAD BAGRI[1], ARUN UNIYAL[2], ASHWANI KUMAR[3], RAMONA BIRAU[4], IULIANA CARMEN BĂRBĂCIORU[5], CRISTINA FELICIA IONICI[5]

[1]Department of Mechanical Engineering, Faculty of Engineering and Technology, SRM Institute of Science and Technology, Delhi NCR Campus, Ghaziabad, UP 201204, India
e-mail: 08rai.santosh@gmail.com, maheshgupta59@gmail.com, gpbagri@gmail.com

[2]Department of Mechanical Engineering, COER University, Roorkee, Uttarakhand, 247664, India
e-mail:arun.uniyal1990@gmail.com

[3]Department of Mechanical Engineering,Technical Education Department, Uttar Pradesh Kanpur, 208024, India & Department of Mechanical Engineering, Graphic Era deemed to be University Dehradun 248001, Uttarakhand India

[4]University of Craiova, "Eugeniu Carada" Doctoral School of Economic Sciences, Craiova, Romania & ”Constantin Brâncuși” University of Târgu Jiu, Faculty of Economic Science, Târgu Jiu, Romania

[5]Constantin Brâncuși” University of Târgu Jiu, Faculty of Engineering, Târgu Jiu, Romania
e-mail: cbarbacioru@gmail.com, feliciaionici@gmail.com

Corresponding author:

RAMONA BIRAU
e-mail: ramona.f.birau@gmail.com

Optimised flexible thermoelectric generators manufactured by metallic threads sewn on fabrics

DOI: 10.35530/IT.077.04.202535

ION RAZVAN RADULESCU
DOINA TOMA
ELENA PERDUM
ADRIAN MARIN
LAURENTIU DINCA
RALUCA MARIA AILENI

ABSTRACT – REZUMAT

Optimised flexible thermoelectric generators manufactured by metallic threads sewn on fabrics

Autonomous energy harvesting sources in wearables enable supply for sensors, antennas and transmission lines, with powers in the range of mW. Thermoelectric generators (TEGs) based on the Seebeck effect are noiseless and have a relatively good energy harvesting efficiency when compared to other sources. Flexible TEGs (F-TEGs) are made of metallic threads and coatings applied on textile substrates that can be integrated into wearable systems. This paper relies on previously manufactured prototypes of T-type and J-type F-TEGs by applying metallic threads onto textile substrates, with the new goal of optimising the harvested voltage, based on a mathematical relation from the scientific literature. This relation yields an optimal ratio of the cross-sectional areas of the n- and p-legs of the F-TEG with respect to their thermic and electric conductivities. The J-type F-TEG was selected for optimisation, and the ratio of the Constantan and Stainless Steel threads was modified from 2:2 to 1:3, according to the mathematical relation. The optimised prototype was designed, manufactured, and measured under the same physical conditions as the initial prototype, yielding better voltage-harvesting values: the slope between temperature difference and harvested voltage increased from 0.0646 to 0.0832.

Keywords: *thermocouples, textiles, energy harvesting, wearables*

Optimizarea generatoarelor termoelectrice flexibile realizate din fire metalice cusute pe materiale textile plane

Sursele autonome de generare a energiei în articole purtabile permit alimentarea senzorilor, antenelor și liniilor de transmisie cu puteri în domeniul mW. Generatoarele termoelectrice (TEGs) care funcționează în baza efectului Seebeck sunt silențioase și au o eficiență energetică relativ mare comparativ cu alte surse autonome de energie. Generatoarele termoelectrice flexibile (F-TEGs) sunt realizate din fire sau acoperiri metalice pe substraturi textile, care se pot integra în sisteme purtabile. Această lucrare continuă studiul prototipurilor F-TEG de tip T și de tip J, prin aplicarea de fire metalice pe substraturi textile, cu obiectivul nou de a optimiza tensiunea electrică generată, în baza unei relații din literatura de specialitate. Din relație rezultă un raport optim între aria secțiunii elementelor de tip n și a elementelor de tip p, în funcție de conductivitatea termică și electrică a acestora. F-TEG de tip J a fost selectat pentru optimizare, iar raportul între firele de constantan și inox a fost modificat de la 2:2 la 1:3, în conformitate cu relația analitică. Prototipul optimizat a fost proiectat, fabricat și măsurat în aceleași condiții ca prototipul inițial, cu valori mai bune pentru tensiunea electrică generată: coeficientul curbei între diferența de temperatură și tensiunea generată a crescut de la 0,0646 la 0,0832.

Cuvinte-cheie: *termocupluri, textile, generare energie, articole purtabile*

INTRODUCTION

Wearable products encompass a strong trend in the field of textiles and clothing, with main applications in the monitoring of vital signs for sports and medicine [1, 2]. While many of the technical issues related to wearables have found proper solutions (transmission lines via metallic threads [3], embedded antennas [4], sensors via metallic coatings [5]), the energy supply of such textile-electronic systems (textronics) still encounters difficulties [6]. The main goal is to ensure an integrated and autonomous energy supply of textronics, having in view that the electric power needed for the sensors, antennas and transmission lines is relatively low, in the range of mW.

Considering these aspects, many research studies deal with the energy harvesting of autonomous sources for powering the textronic systems, based on various physical principles. These autonomous energy harvesting sources replace the heavy, bulky and un-washable batteries [7]. The following sources of autonomous energy harvesting and their related technological solutions were identified [8]: photovoltaic cells (solar light), electrodynamic transducers (motion, force), piezoelectric transducers (mechanical vibration) and thermoelectric generators (temperature gradient). Each of these sources has advantages and drawbacks to be considered when implementing into a textronic system [8].

Thermoelectric generators (TEGs) rely on the Seebeck effect and are used for electric energy harvesting from a temperature gradient. The physical principle describes pairs of two different metallic legs, with connections at the hot and cold junctions. One pair builds a thermocouple leg, while several thermocouples connected in series build a thermopile. The harvested energy of a thermopile is the sum of the energy of the series thermocouples. This is usually needed due to the relatively low electric power, in the range of mW, harvested by TEGs. The pairs have to include one p-material (generating positive holes) and one n-material (generating negative electrons). The heat at a junction disperses both holes of the p-material and electrons of the n-material, with the generation of a small electric current [9].

When considering TEGs, the main advantages are the high amount of power compared to other sources and their noiselessness [8]. TEGs require a temperature gradient; they require many legs connected in series; they are relatively expensive; and they generate low output voltage and high currents, requiring stabilisation via Boost converters [10].

Several technical solutions were proposed to apply flexible TEGs (F-TEG) in wearables and textronics [11–14].

Lund et al. [11] have a comprehensive paper on a F-TEG, manufactured on a felted wool fabric with pairs of silver threads as n-type material and PEDOT:PSS coated thread as p-type material. The horizontal geometry of the F-TEG describes the upper part of the fabric as the hot junction and the lower part as the cold junction, while the conductive threads are sewn through the fabric. Manufacturing, modelling and optimisation are tackled in the paper, with a description of all the required physical parameters. The generated voltage was 2.3 mV at 30 K.

Allison et al. [12] bring valuable results with an F-TEG achieved by deposition of PEDOT:CL as p-type material and Carbon threads as n-type material on a cotton substrate. The vertical geometry of the fabric is meant for bending, so that one side of the fabric is the outdoor cold junction and the other side is the inner hot junction. The harvested voltage of 1.1 mV at a temperature difference of 30 K represents a promising result.

Hardianto and the team of UGent [13] studied in depth the supply of e-textiles via F-TEGs. Various pairs of legs were achieved, mainly Nickel and Carbon Fibers on the same thread, with the Nickel on one side of the fabric and the Carbon Fibers on the other side. The geometry consists of a hot junction at the upper part of the fabric and the cold junction at the lower part, which enables measurement by an experimental setup composed of a hotplate, thermometer and nano-voltmeter. Results encompass voltages of 700 μV at a temperature gradient of 30 K.

Another contribution of the UGent and the UWB teams [14] describes pairs of n-type and p-type legs of different metallic threads, embroidered on a fabric with left-right geometry: the cold junction is on the left part of the fabric, while the hot junction is at the right part. The harvested electric power had good results, with values of 1.2 mV at 60°K temperature gradient.

More recent research contributions focused on advanced geometries for integrating TEGs into smart garments [15–21]. Vertical thermoelectric elements were integrated into a smart glove with n-type material of SWCNT doped with Polyethylene-imine and p-type material with SWCNT doped with PEDOT:PSS. Performance outlined values of 23.2 mV generated voltage and 2.6 μW generated power were outlined at a 48°C temperature difference [15]. COMSOL simulations were performed to assess the F-TEG's optimal dimensions in relation to the generated voltage. For the thermocouple legs, silver was applied as n-type material, while PEDOT:PSS was used as p-type material, according to the simulation [16]. A silicone rubber sheet with horizontal geometry and elements of Ni-doped Bi_2Te_3 as n-type material and $Bi_{0.3}Sb_{1.7}Te_3$ as p-type material had outstanding energy harvesting performance with a voltage of 1 V and a power of 77.41 mW at a 60°C temperature difference [17]. An F-TEG built with graphene and copper legs reached a power of 11 μW at a temperature difference of 75°C [18]. One bracelet for monitoring vital signs of the human body was autonomously powered by miniaturised TEGs [19]. Another F-TEG used PANI/graphite and bismuth telluride composites for the thermocouple legs [20], while Single-Wall Carbon Nanotubes were used in another similar application [21–23].

Our paper proposes an F-TEG designed on a textile substrate with metallic threads, by applying the T- and J-Type thermocouple pairs, with a geometry of the fabric similar to contribution [14]. By considering the initial prototypes of T- and J-type thermocouples presented in our paper [22], an optimisation of the prototypes based on the relation of the legs' cross-section area and their electric/thermic conductivity is tackled within the current paper [11]:

$$\frac{A_n}{A_p} = \sqrt{\frac{\sigma_p \lambda_p}{\sigma_n \lambda_n}} \tag{1}$$

where $A_{n/p}$ is the cross-section area and $\sigma_{n/p}$ and $\lambda_{n/p}$ are the electric/thermic conductivity of the thermocouple legs.

DESIGN OF THE F-TEGS

Concept

Two main design concepts were identified from the scientific literature regarding F-TEGs:

– the horizontal geometry with the hot and cold junction on the upper and lower part of the fabric [11];
– the vertical geometry with the hot and cold junction on the left and right part of the fabric [12].

Figures 1 and 2 showcase the identified geometries. The F-TEGs presented in this paper were designed and manufactured according to the vertical geometry, by adapting the concept from contribution [14]. The distance between the parallel legs was 20 mm, while the length of a leg was 100 mm, considering the need for dielectric isolation between the legs as well as a

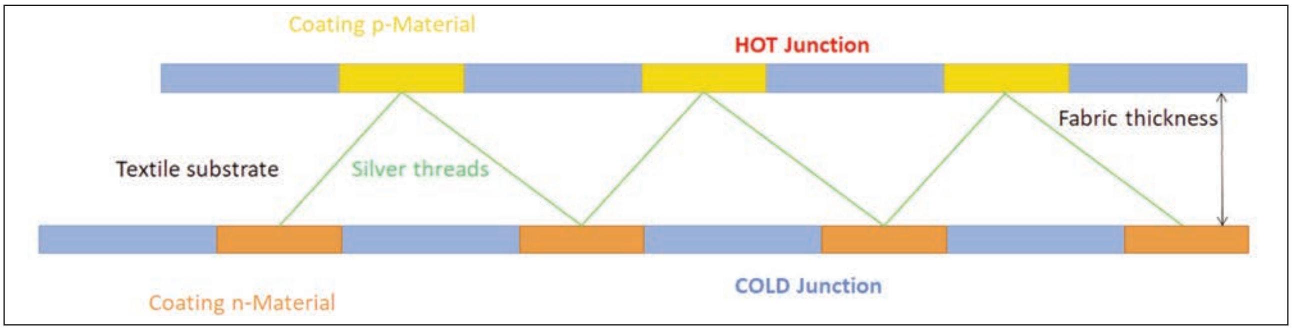

Fig. 1. The horizontal geometry of the F-TEG

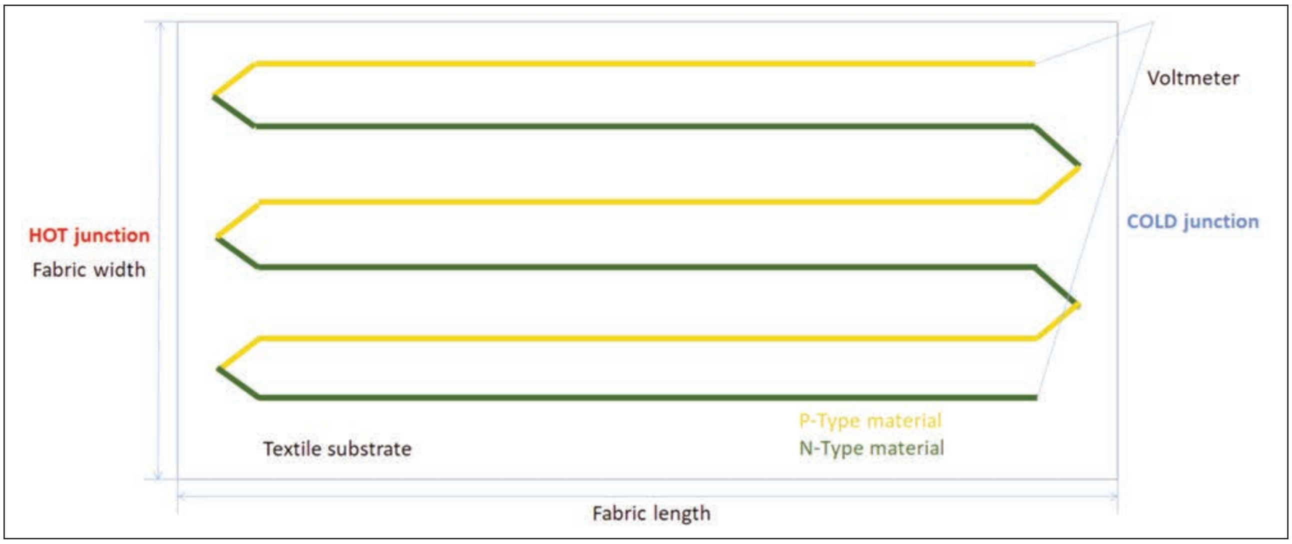

Fig. 2. The vertical geometry of the F-TEG

feasible distance between the hot and the cold junction. Multi-filamentary threads with metallic and PES filaments were sewn onto the 100% PES textile substrate.

Materials

Our previous attempts to achieve F-TEGs based on metallic threads yielded results in the range of 7.2 mV for T-type thermocouples and 4 mV for J-type thermocouples, at a temperature difference of 60 K [24]. Figures 3 and 4 present the initial manufactured F-TEGs [24].

Table 1 includes the design and the physical-mechanical properties of the textile substrate for the F-TEG. The copper, constantan and stainless steel threads have a multifilament structure of 100% PES with

Fig. 3. F-TEG type T
Pairs of legs of Constantan and Copper threads
Junctions consolidated by Silver threads
Electric circuit Ohmic resistance: 55 Ω

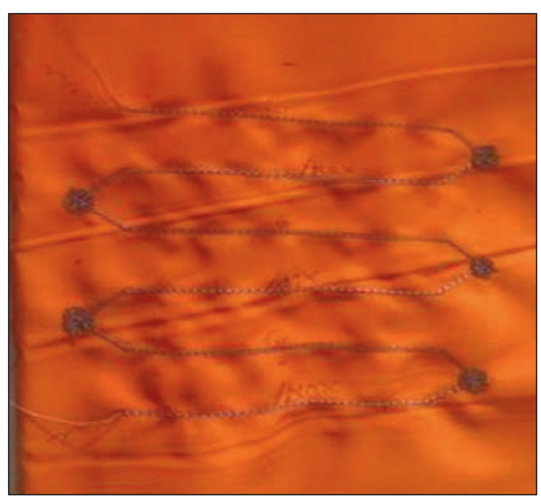

Fig. 4. F-TEG type J
Pairs of legs of Constantan and Steel threads
Junctions consolidated by Silver threads
Electric circuit Ohmic resistance: 375 Ω

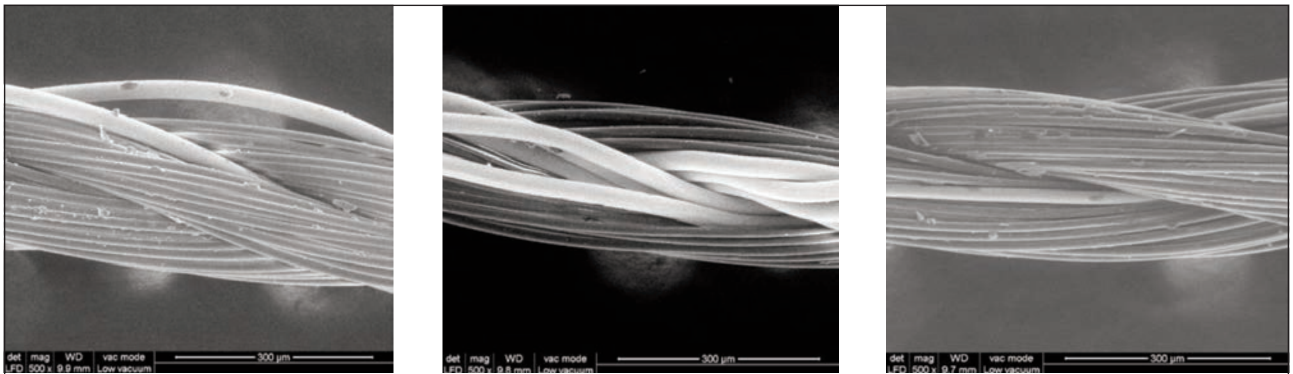

a *b* *c*

Fig. 5. SEM image of the multifilament metallic thread, mag 500x:
a – Constantan; *b* – Copper–Silver; *c* – Stainless steel

Table 1

DESIGN AND PHYSICAL-MECHANICAL PROPERTIES OF THE TEXTILE SUBSTRATE		
No.	**Design structure/ Physical-mechanical property**	**Value**
1	Fibrous composition (%)	100% PES
2	Weave	Plain weave
3	Specific mass (g/m^2)	258
4	Tensile strength Warp/Weft (N)	2400/1070
5	Elongation at break Warp/Weft (%)	48.4/25.8
6	Tear strength Warp/Weft (N)	60/26
7	Air permeability (l/m^{2}s)	27.5

metallic insertions and were purchased from Clevertex, Czech Republic. Figure 5, *a–c* presents the SEM images of the multifilament thread with metallic insertions of Constantan, Copper-Silver, and Stainless steel. Every two threads were sewn in parallel for the conductive F-TEGs legs.

Methods

The main aim of this paper is to optimise the performance of the F-TEGs based on relation 1, namely to tailor the cross-section area of the threads in relation to their electric/thermic conductivity. The electric conductivity was computed according to relation 2 from the specification of the threads regarding linear resistance and optical diameter [25], in table 2:

$$\sigma = \frac{1}{R_L}\,\frac{L}{A} = \frac{1}{R_L}\,\frac{4L}{\pi D^2} \tag{2}$$

with A – the cross-sectional area, L – the length of the thread and R_L – the linear electric resistance [Ω].

The next step was to compute the thermic conductivities of the metallic threads based on analytical relations 3:

$$\lambda_{eff} = \sum \lambda_i v_i \tag{3}$$

with v_i – volume fraction of each component and λ_i – thermic conductivity of each component. The volume fraction of metallic multifilament/PES multifilament was determined from the SEM images of the yarns

Table 2

ELECTRIC CONDUCTIVITY OF THE METALLIC THREADS			
Type of metallic thread	**Linear electric resistance R_L (Ω/m)**	**Optical diameter D (µm)**	**Electric conductivity σ (S/m)**
Copper/Silver	3	160	17580000
Constantan	210	220	125000
Stainless steel	1150	250	17730

Table 3

THERMIC CONDUCTIVITY OF THE METALLIC THREADS			
Type of metallic thread	**Thermic conductivity PES, v_{PES} = 5:6 (W/mK)**	**Thermic conductivity metals, v_{metal} = 1:6 (W/mK)**	**Thermic conductivity (W/mK)**
Copper/Silver		415	70
Constantan	0.19	22	3.83
Stainless steel		20	3.49

Table 4

OPTIMAL RATIO CROSS SECTION AREA COMPUTED FOR THE TWO TYPES OF F-TEGs – RELATION 1			
F-TEG Type	**Electric conductivity (S/m)**	**Thermic conductivity (W/mK)**	**Optimal ratio cross section**
T-type Constantan Copper/Silver	 125000 17580000	 3.83 70	$A_{Constantan} = 50 \times A_{CopperSilver}$
J-type Constantan Stainless steel	 125000 17730	 3.83 3.49	$A_{StainlessSteel} = 2.8 \times A_{Constantan}$

and from the EDS elemental composition, as to 1:6 of metallic content to PES.

RESULTS

The optimal ratio between the cross-section areas of the thermocouple legs was computed according to optimisation relation 1 and presented in table 4.
Since the T-type F-TEG requires a very high ratio between the cross-sectional area of the two legs (1:50), with no practical feasibility, we have drawn our attention towards the J-type F-TEG with a ratio of (2.8:1).
In order to technically meet the demand of the optimisation ratio (2.8:1) between the Stainless Steel and the Constantan F-TEG legs, a new prototype was manufactured with 3 Stainless steel threads in parallel and a single one Constantan thread, keeping the same design pattern and the same electric/thermic conductivities of the legs. The optimisation relation makes sense when the sum of the cross-sectional area is kept constant: $A_n + A_p = const.$ The new J-type F-TEG is displayed in figure 6.

Fig. 6. Optimised J-type F-TEG with Stainless steel: Constantan threads ratio 3:1
Electric circuit Ohmic resistance: 300 Ω

The optimised J-type F-TEG prototype has an internal electric resistance of 300 Ω, when compared to the initial prototype with 375 Ω. The two J-type F-TEG prototypes were once again measured via the experimental setup, consisting of a hotplate with variable temperature (hot junction), an ice bath (cold junction), an IR thermometer and a voltmeter.

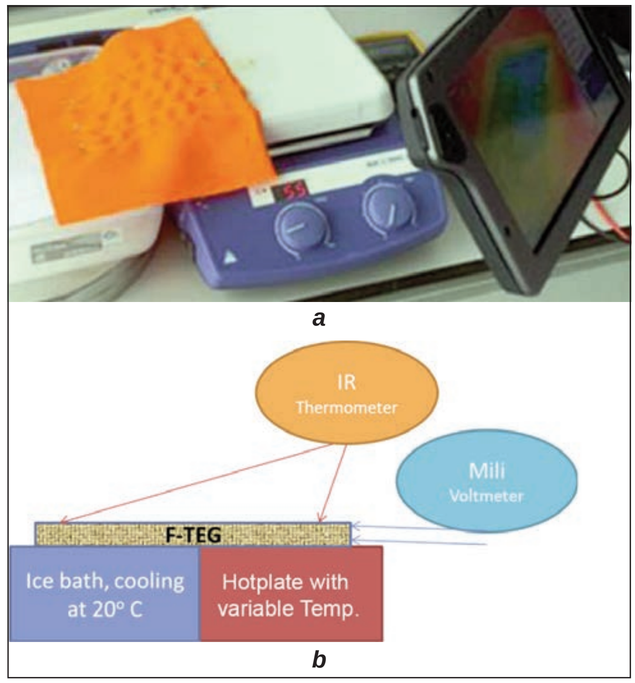

Fig. 7. Graphical representation of: *a* – image of the experimental setup; *b* – scheme of the experimental setup

Figure 7 presents the experimental setup, and figure 8 presents the achieved results.
The linear increase of the generated voltage with the temperature difference is the first good result of the J-type F-TEGs.

DISCUSSION

Two linear trend lines were added to the voltage as a function of temperature difference, with the slope increasing from 0.0646 for the initial prototype to 0.0832 for the optimised prototype. A maximum of 6.6 mV was harvested at a 70°C temperature difference by the optimised F-TEG. Once again, the optimisation relation makes sense, single if $A_n + A_p = const.$ One statistical indicator was computed to evidence the fulfilment of the optimisation condition (1), considering the constant thermic and electric conductivities of the applied threads (table 5).
A smaller statistical indicator shows a better fulfilment of the analytic condition. Whereas in the case of the initial F-TEG the indicator is 1.14, in the case of the optimised F-TEG this indicator is 0.27, showing a better fulfilment of the optimisation condition. The

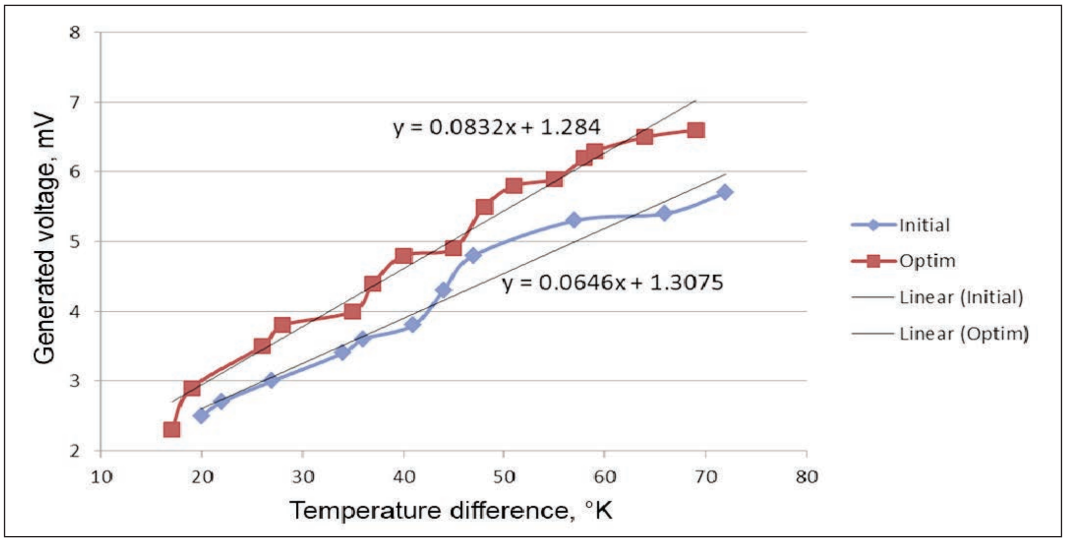

Fig. 8. Graph of the achieved voltages with the initial and the optimised J-type F-TEG

Table 5

STATISTICAL INDICATOR COMPUTED FOR THE INITIAL AND OPTIMIZED F-TEG			
Optimization relation		**Optimized F-TEG**	**Initial F-TEG**
Electric and thermic conductivities	$\sqrt{\frac{\sigma_p \lambda_p}{\sigma_n \lambda_n}} (= X_{norm})$	0.36	0.36
Cross-section area	$\frac{A_n}{A_p} (= X)$	0.26	0.77
Statistical indicator	$\frac{\lvert X - X_{norm} \rvert}{X_{norm}}$	0.27	1.14

optimised prototype harvested better voltages than the initial prototype by designing the cross-section area of the legs according to relation 1.

CONCLUSIONS

The paper tackled the design optimisation of a flexible thermoelectric generator type J, based on an analytic relation. Both the initial and the optimised prototypes were manufactured and measured, with an increase of the slope between temperature and voltage from 0.0646 to 0.0832, proving the better voltage harvesting values for the optimised prototype. Stainless steel and Constantan threads were used for the J-type F-TEG, while considering the cross-sectional area within the optimisation process. Future optimisation work will follow the integration of boost converters for balancing the ratio between current and voltage, as well as applying larger dimensions of legs onto the wearable system, to achieve a voltage of 1.8 V, typically needed to supply most sensors and microcontrollers used for wearable systems.

ACKNOLEDGEMENTS

This work was carried out through the Core Programme within the National R&D&I Plan 2022-2027, carried out with the support of the Ministry of Education and Research, project no. 6N/2023, PN 23 26 01 03, project 3D-WearIoT.

REFERENCES

[1] Simegnaw, A.A., Malengier, B., Rotich, G.K., Tadesse, M.G., Van Langenhove, L., *Review on the Integration of Microelectronics for E-textile*, In: Materials, 2021, 14, 5113, https://doi.org/10.3390/ma14175113

[2] Grancaric, A.M., Jerkovic, I., Koncar, V., Cochrane, C., Kelly, F.M., Soulat, D., Legrand, X., *Conductive polymers for smart textile applications*, In: Journal of Industrial Textiles, 2018, 48, 3, 612–642, https://doi.org/10.1177/1528083717699368

[3] Marterer, V., Radouchova, M., Soukup, R., Hipp, S., Blecha, T., *Wearable textile antennas: investigation on material variants, fabrication methods, design and application*, In: Fashion and Textiles, 2024, 11, 9, https://doi.org/10.1186/s40691-023-00369-1

[4] Burgnies, L., Huppe, C., Ducournau, G., Cochrane, C., Rault, F., Koncar, V., Lheurtte, E., *High-Pass Sub-mmWave Filtering by Woven Textile Metamaterials*, In: IEEE Transactions on Terahertz Science and Technology, 2018, 8, 4, 427–433, https://doi.org/10.1109/TTHZ.2018.2844096

[5] Aileni, R.M., Chiriac, L., *Conductive Membranes Based on Cotton Fabric Coated with Polymers for Electrode Applications*, In: Materials, 2022, 15, 7286, https://doi.org/10.3390/ma15207286
[6] Van Langenhove, L., *Smart textiles for protection: an overview*, chapter in book: Smart textiles for protection, edited by R. A. Chapman, Woodhead Publishing Limited, 2013
[7] Dolez, P.I., *Energy Harvesting Materials and Structures for Smart Textile Applications: Recent Progress and Path Forward*, In: Sensors, 2021, 21, 6297, https://doi.org/10.3390/s21186297
[8] Wiesmeier, J., *Energy Harvesting for Passive Smart Devices*, Master Thesis, TU Graz, 2013
[9] Wang, L., Zhang, K., *Textile-Based Thermoelectric Generators and Their Applications*, In: Energy & Environmental Materials, 2019, https://doi.org/10.1002/eem2.12045
[10] Zaid Samih, M.H., *Energy Harvesting Using Thermoelectric Generators*, Master Thesis, German Jordanian University, 2016
[11] Lund, A., Tian, Y., Darabi, S., Müller, Ch., *A polymer-based textile thermoelectric generator for wearable energy harvesting*, In: Journal of Power Sources, 2020, 480, 228836, https://doi.org/10.1016/j.jpowsour.2020.228836
[12] Allison, L.K., Andrew, T.L., *A Wearable All-Fabric Thermoelectric Generator*, In: Advanced Materials Technologies, 2019, 4, 5, 1800615, https://doi.org/10.1002/admt.201800615
[13] Hardianto, H., Mey, G.D., Malengier, B., VanLangenhove, L., *Textile-based thermoelectric generator fabricated from carbon fibers*, In: Journal of Industrial Textiles, 2020, https://doi.org/10.1177/1528083720910686
[14] Kalcik, J., Soukup, R., Malengier, B., Radouchova, M., Rous, P., *Towards Textile Thermopiles*, In: 46th International Spring Seminar on Electronics Technology (ISSE), Timisoara, Romania, 2023, 1–4, https://doi.org/10.1109/ISSE57496.2023.10168518
[15] Xia, B. et al., *Vertically designed high-performance and flexible thermoelectric generator based on optimized PEDOT:PSS/SWCNTs composite films*, In: Chemical Engineering Journal, 2024, 486, 150305, https://doi.org/10.1016/j.cej.2024.150305
[16] Jabri, M., et al, *Flexible thin-film thermoelectric generators for human skin-heat harvesting: A numerical study*, In: Nano Energy, 2024, 129, 110001, https://doi.org/10.1016/j.nanoen.2024.110001
[17] Van Toan, N. et al., *Ultra-flexible thermoelectric generator based on silicone rubber sheet and electrodeposited thermoelectric material for waste heat harvesting*, In: Energy Reports, 2022, 8, 5026–5037, https://doi.org/10.1016/j.egyr.2022.03.121
[18] Chen, W.H., et al., *Optimization of material properties and performance of flexible thermoelectric generators with/without graphene*, In: Energy Conversion and Management, 2024, X, 24, 100741, https://doi.org/10.1016/j.ecmx.2024.100741
[19] Liang, L. et al., *A wearable multimodal health monitoring bracelet powered by high-power-density flexible thermoelectric generators*, In: Device, 2025, 3, 100748, https://doi.org/10.1016/j.device.2025.100748
[20] Yoshitha, P.A., et al., *Fabrication and characterisation of a flexible thermoelectric generator using PANI/graphite/bismuth telluride composites*, In: RSC Adv., 2024, 14, 40117, https://doi.org/10.1039/d4ra04565c
[21] Mytafides, C.K., *Additive manufacturing of highly conductive carbon nanotube architectures towards carbon-based flexible thermoelectric generators*, In: Energy Adv., 2024, 3, 1642, https://doi.org/10.1039/d4ya00182f
[22] Visileanu, E., Ene, A.G., Radulescu, R., Dondea, F., Dinca, L., Salistean, A., *Development and characterisation of conductive knitted fabrics as humidity sensors for automatic hemostasis detection*, In: Industria Textila, 2025, 76, 6, 739–748, https://doi.org/10.35530/IT.076.06.202536
[23] Grosu, C., Blaga, M., Seghedin, N.-E., Avădanei, M.-L., Perdevară, M., Marmarali, A., *Knitted linings for protective equipment against vibrations*, In: Industria Textila, 2025, 76, 1, 44–51, http://doi.org/10.35530/IT.076.01.2023142
[24] Rădulescu, I.R., Dincă, L., Perdum, E., Marin, A., Aileni, R.M., *Dezvoltarea generatoarelor termoelectrice flexibile – o soluție pentru alimentarea autonomă cu energie electrică a componentelor pentru e-textile (Development of F-TEGs – a solution for autonomous energy harvesting of e-textile components)*, In: Buletinul AGIR, 2025, 2
[25] Clevertex, *Metallic threads acquired from Clevertex.cz Czech Republic*, Available at: https://www.clevertex.cz/en/homepage [Accessed on March 3, 2025]

Authors:

ION RAZVAN RADULESCU, DOINA TOMA, ELENA PERDUM, ADRIAN MARIN, LAURENTIU DINCA, RALUCA MARIA AILENI

National Research and Development Institute for Textiles and Leather,
16 Lucretiu Patrascanu Street, 030508, Bucharest, Romania
e-mail: office@incdtp.ro

Corresponding author:

ION RAZVAN RADULESCU
e-mail: razvan.radulescu@incdtp.ro

Development of high-performance ZnO nanoparticles using *Olea europaea* leaf extract: potential for multifunctional textile finishing and dye degradation

DOI: 10.35530/IT.077.04.2025175

NEDRA ABBES
THOURAYA BARHOUMI
SANA FRIDJINE
NEJIB SEJRI
BOUBAKER JAOUACHI
JUN XU
HONGLUAN LIU
IMENE BEKRI-ABBES

ABSTRACT – REZUMAT

Development of high-performance ZnO nanoparticles using *Olea europaea* leaf extract: potential for multifunctional textile finishing and dye degradation

Zinc oxide nanoparticles were sustainably synthesised using Olea europaea leaf extract as a high-performance candidate for functional textile finishing. These green-synthesised nanoparticles were compared to conventional chemical ZnO to evaluate their suitability for textile-related applications. SEM analysis revealed that Green ZnO consists of well-defined hexagonal prisms with a primary size of 200–500 nm, providing a high density of active surface sites. The material exhibited a reduced band gap (2.6 eV) and enhanced visible-light absorption attributed to carbon incorporation and induced oxygen vacancies during thermal treatment. These characteristics are particularly advantageous for the development of self-cleaning textiles under natural sunlight. Green ZnO exhibited superior methylene blue adsorption (52 mg/g, 21% higher than chemical ZnO) and achieved 94% photocatalytic degradation within 3 h. The results indicate that these nanoparticles can effectively degrade textile dye effluents and provide self-cleaning properties to treated substrates. Furthermore, antimicrobial testing showed significant inhibition against Staphylococcus aureus (16 mm) and Candida albicans (28 mm). This eco-friendly, scalable ZnO presents a multifunctional finishing agent capable of providing simultaneous dye removal, self-cleaning, and disinfection, offering a sustainable pathway for the production of smart, bioactive textiles.

Keywords: *green ZnO, textile dye, adsorption, antimicrobial, photocatalytic activity*

Dezvoltarea unor nanoparticule de ZnO de înaltă performanță folosind extractul din frunze de *Olea europaea*: potențial pentru finisarea textilelor multifuncționale și degradarea coloranților

Nanoparticulele de oxid de zinc au fost sintetizate în mod durabil folosind extractul din frunze de Olea europaea ca material cu performanțe ridicate pentru finisarea textilelor funcționale. Aceste nanoparticule sintetizate ecologic au fost comparate cu ZnO chimic convențional pentru a evalua utilizarea lor în aplicații din domeniul textil. Analiza SEM a relevat că ZnO ecologic este format din prisme hexagonale bine definite, cu o dimensiune primară de 200–500 nm, oferind o densitate ridicată de zone active la suprafață. Materialul a prezentat o bandă interzisă redusă (2,6 eV) și o absorbție îmbunătățită a luminii vizibile, atribuite încorporării de carbon și apariției de lacune de oxigen induse în timpul tratamentului termic. Aceste caracteristici sunt deosebit de avantajoase pentru dezvoltarea de materiale textile cu autocurățare sub lumina naturală a soarelui. ZnO ecologic a prezentat o adsorbție superioară a albastrului de metilen (52 mg/g, cu 21% mai mare decât ZnO chimic) și a atins o degradare fotocatalitică de 94% în decurs de 3 ore. Rezultatele indică faptul că aceste nanoparticule pot degrada eficient efluenții de coloranți textili și pot conferi proprietăți de autocurățare substraturilor tratate. În plus, testele antimicrobiene au evidențiat o inhibare semnificativă împotriva Staphylococcus aureus (16 mm) și Candida albicans (28 mm). Acest ZnO ecologic și scalabil reprezintă un agent de finisare multifuncțional capabil să asigure simultan îndepărtarea coloranților, autocurățarea și dezinfectarea, oferind o cale durabilă pentru producția de textile inteligente și bioactive.

Cuvinte-cheie: *ZnO ecologic, colorant textil, adsorbție, proprietăți antimicrobiene, activitate fotocatalitică*

INTRODUCTION

The textile industry is currently undergoing a paradigm shift toward sustainable functionalization, driven by the global demand for “smart” fabrics that possess self-cleaning, antimicrobial, and UV-protective properties [1, 2]. Conventional textile finishing often relies on synthetic binders and hazardous chemical agents that contribute to environmental degradation and toxic dye effluents [3, 4]. Consequently, the development of multifunctional, eco-friendly nanomaterials that can facilitate both the remediation of dye-polluted water and the bio-activation of textile surfaces has become a primary research frontier [5, 6].

Among various metal oxides, Zinc Oxide (ZnO) nanoparticles have emerged as a leading candidate for textile applications due to their high chemical stability, non-toxicity, and significant photocatalytic potential [7]. Traditional chemical synthesis routes for

ZnO, such as sol-gel and hydrothermal methods, frequently involve the use of toxic reducing agents like sodium borohydride or hydrazine, which limit their "green" credentials [8–11].

To address this, plant-mediated "green" synthesis has gained traction, utilising the bioactive secondary metabolites of flora such as polyphenols, flavonoids, and terpenoids to act as natural reducing and capping agents [2, 12, 13]. Specifically, Olea europaea (olive) leaf extract is a promising bio-resource due to its high concentration of oleuropein and hydroxytyrosol, which have been shown to influence the morphology and optical properties of metallic nanoparticles [14–16].

However, a critical analysis of current literature reveals a significant research gap. Most green synthesis protocols for ZnO utilise low-temperature calcination (below 600°C), which often results in unstable organic surface residues that may leach or degrade, potentially compromising the long-term durability required for industrial textile finishing [17]. Furthermore, while the narrowing of the ZnO band gap via plant extracts is well-documented [18, 19], there is a scarcity of research investigating how high-temperature thermal treatment (900°C), while removing primary organic fractions, can induce stable, in situ carbon-doped defect states. These states are vital for extending the photocatalytic response into the visible light spectrum, which is a prerequisite for efficient self-cleaning functionality under natural sunlight [20, 21].

This study addresses these limitations by reporting the green synthesis of ZnO nanoparticles using Olea europaea leaf extract at a high calcination temperature of 900°C. The work provides a rigorous comparison between the green-synthesised ZnO and conventional chemical ZnO regarding their structural, optical, and morphological characteristics.

The performance of these nanoparticles is evaluated through two critical lenses for the textile industry: the adsorption and photocatalytic degradation of Methylene Blue (MB) dye under natural sunlight, and broad-spectrum antimicrobial efficacy against *Staphylococcus aureus* and *Candida albicans*. By establishing the superior visible-light activity and adsorption capacity of this carbon-modified green ZnO, this research provides a sustainable pathway for the next generation of bioactive and self-cleaning textile finishes.

METHODS AND MATERIALS

ZnO synthesis

Olive (*Olea europaea*) leaves were collected, rinsed repeatedly with tap and distilled water to remove dust, shade-dried at room temperature for 10–12 days, and ground into coarse powder. The aqueous extract was prepared by boiling 10 g of powder in 100 mL double-distilled water at 80°C for 60 min, followed by filtration and storage at –4°C. Green ZnO nanoparticles were synthesised by dissolving 10 g zinc acetate dihydrate (Sigma-Aldrich) in 100 mL olive leaf extract and stirring at 80°C for 2 h, forming a pale yellow precipitate. The product was centrifuged, washed thoroughly with deionised water, dried at 80°C for 24 h, and calcined at 900°C for 2 h to yield fine ZnO powder. For comparison, conventional ZnO was prepared via NaOH precipitation. A 0.1 M zinc acetate dihydrate solution was heated to 80°C under stirring, and 0.2 M NaOH (Novachem) solution was added dropwise to form a zinc hydroxide precipitate. After 1 h of stirring, the precipitate was cooled, repeatedly washed with distilled water, dried, and calcined at 450°C for 2 h to obtain ZnO powder. Both synthesis routes produced white ZnO nanoparticles suitable for textile finishing applications.

Antimicrobial activity

The antimicrobial activity of green-synthesised ZnO nanoparticles was assessed against *Staphylococcus aureus* (ATCC 25923) and *Candida albicans* (ATCC 10231) using the disk diffusion method. Overnight cultures were adjusted to 0.5 McFarland standard (~1.5 × 10^8 CFU/mL) in nutrient broth. Microbial suspensions were lawn-spread on Mueller-Hinton agar plates. Sterile 6-mm filter paper disks were loaded with ZnO suspension (50 µL) and placed on the agar. Distilled water served as a negative control, while ampicillin (10 µg) and fluconazole (25 µg) were positive controls for bacteria and fungus, respectively. Plates were incubated at 37°C for 24 h (bacteria) or 48 h (*C. albicans*). Inhibition zone diameters were measured in millimetres using a digital calliper. Clear zones indicated effective antimicrobial action of the green ZnO nanoparticles.

Adsorption and photocatalytic properties

Methylene blue (MB, Sigma-Aldrich) was selected as a model textile dye due to its widespread use and environmental relevance. Adsorption isotherms were studied by contacting 80 mg of ZnO adsorbent (green or chemical) with 20 mL MB solutions (10–500 mg/L) at natural pH. Suspensions were agitated at 150 rpm for 24 h to reach equilibrium. Kinetic studies used 25 mg of adsorbent in 50 mL of 25 mg/L MB, with sampling from 15 to 240 min. Photocatalytic degradation was evaluated under natural sunlight in Borj Cedria, Tunisia (36°43′04″N, 10°25′41″E) on 22 July 2025, between 12:00–15:00 CET (GHI 800–1000 W/m^2). 50 mg of ZnO was dispersed in 50 mL of 25 mg/L MB solution. After 24 h of dark equilibration to achieve adsorption–desorption balance, suspensions were exposed to direct sunlight without stirring. Aliquots (3 mL) were collected periodically, centrifuged (10,000 rpm, 5 min), and analysed by UV–Vis spectrophotometry at λmax = 664 nm.

Characterization techniques

X-ray diffraction (XRD) patterns were recorded using an X'Pert Pro Panalytical diffractometer and a Bruker D8 ADVANCE system (USA), with a 0.02° step size and analysed via X'Pert HighScore Plus software. Functional groups were identified by attenuated total reflection Fourier-transform infrared (ATR-FTIR) spectroscopy (PerkinElmer Spectrum, 400–4000 cm^{-1}) equipped with an ATR accessory.

Dynamic Light Scattering was determined using a Zeta meter (Zetasizer ZS90, Malvern, UK). 0.1 g of SA was introduced into 100 mL of ultrapure water under ultrasonic stirring at 500 rpm for 5 min. Then, 0.75 mL was injected into the ZP measuring cell in the zeta meter instrument.

Surface morphology was examined by scanning electron microscopy (SEM) using a Quanta 650 microscope (30× to 200,000× magnification, 0.2–30 kV accelerating voltage). Optical properties were investigated with a Shimadzu UV-1800 spectrophotometer (Kyoto, Japan). A scanning electron microscope (SEM), specifically the FEI Quanta 650, was used for surface examination.

RESULTS AND DISCUSSION

XRD

The X-ray diffraction (XRD) pattern of the synthesised Zn nanoparticles, prepared using olive leaf extract, was recorded to investigate their crystallographic structure. The pattern exhibits characteristic peaks corresponding to the wurtzite (hexagonal) phase of ZnO, confirming the successful synthesis of crystalline zinc oxide. Prominent reflection peaks were observed at 2θ = 31.3° (100), 34° (002), and 35.8° (101), which are consistent with the hexagonal wurtzite structure of ZnO [29, 30]. These findings are in agreement with previous studies on plant-mediated synthesis of ZnO nanoparticles [22]. Additional peaks, if present, at 47.1° (102), 56.2° (103), or 62.5° (110), further support the wurtzite phase, though their intensities may vary depending on synthesis conditions such as the 80°C extraction temperature used in this study. No significant peaks corresponding to impurities ($Zn(OH)_2$ or unreacted Zn precursors) were observed, indicating a high purity of the ZnO phase.

FTIR

The successful formation of zinc oxide was further confirmed by the Fourier transform infrared spectrum, as illustrated in figure 2. The spectrum revealed characteristic absorption peaks at 3376, 1582, 1400, 1020, 747, 664, and 483 cm^{-1}. The broad bands observed at 3376 cm^{-1} are attributed to O-H stretching vibrations, indicating the presence of adsorbed water molecules and/or surface hydroxyl groups on the material [23], which serve as active sites for photocatalytic radical generation. Crucially, the peaks at 1582 cm^{-1} and 1400 cm^{-1} are assigned to the asymmetric stretching (v3) of carbonate (CO_3^{2-}) species [24]. These inorganic carbonates, along with the C–O stretching at 1020 cm^{-1}, represent a stable carbonaceous framework resulting from the high-temperature (900°C) thermal decomposition of the Olea europaea extract [25]. Finally, the strong absorption bands at 664 cm^{-1} and 483 cm^{-1} are characteristic of the metal-oxygen (Zn-O) stretching vibrations in the hexagonal wurtzite structure of zinc oxide [22].

DLS

The Dynamic Light Scattering (DLS) analysis of Zinc Oxide nanoparticles synthesised using Olive Leaf Extract provides crucial insight into their colloidal characteristics (figure 3). The analysis shows a bimodal size distribution characterised by two distinct peaks: the primary peak at 973.1 nm representing 66.5% of the intensity distribution, and a secondary

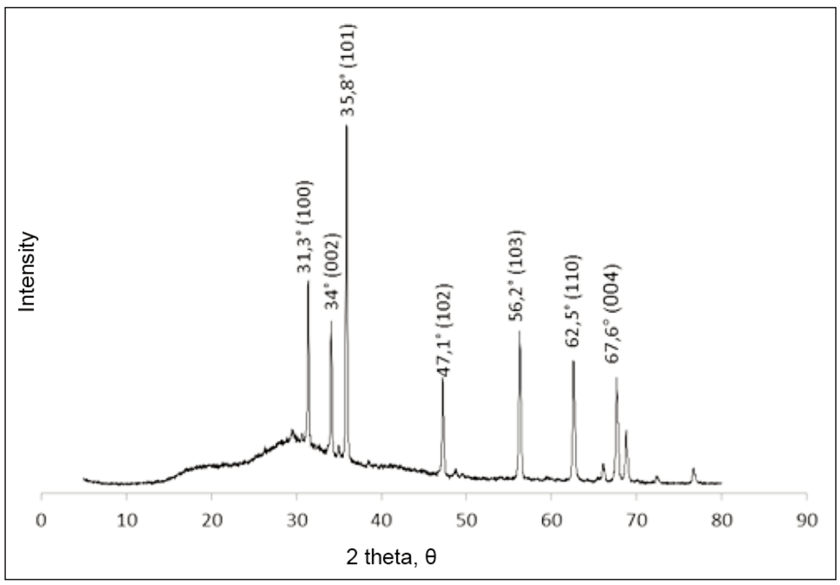

Fig. 1. XRD pattern of Zn nanoparticles synthesised using olive leaf extract

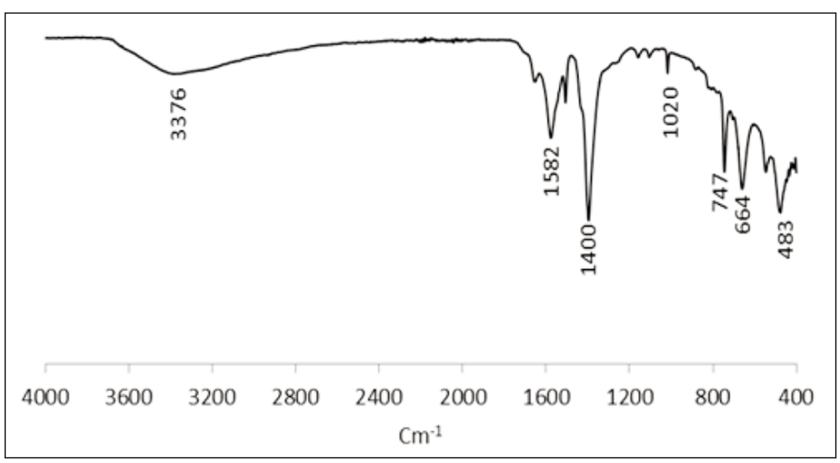

Fig. 2. FTIR spectrum of the synthesised ZnO nanoparticles

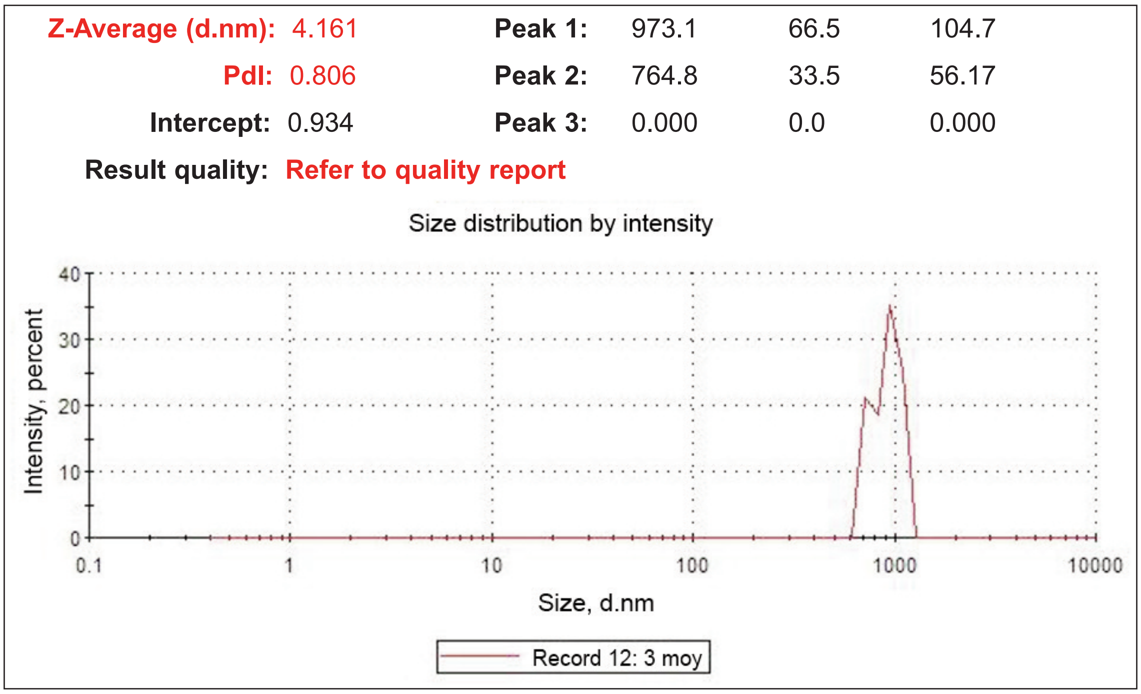

Fig. 3. Dynamic Light Scattering (DLS) analysis of Zinc Oxide nanoparticles synthesised using olive leaf extract

peak at 764.8 nm accounting for 33.5% of the intensity. This bimodal pattern suggests the coexistence of two different populations of particle aggregates in the suspension.

SEM

Figure 4 displays SEM images of ZnO nanostructures synthesised via conventional chemical precipitation and green synthesis using Olea europaea leaf extract. Conventional ZnO (figure 4, *a*) exhibits irregularly shaped, highly agglomerated particles forming rough, coral-like porous clusters (200–800 nm). The heterogeneous surface, covered with fused granules lacking defined facets, results from rapid NaOH-induced supersaturation, homogeneous nucleation, and uncontrolled dehydration of $Zn(OH)_2$ without capping agents. This morphology is typical of chemical routes favouring bulk growth over shape control [24].

The morphological characteristics were further investigated using SEM and DLS to distinguish between primary crystal size and colloidal behaviour. SEM analysis (figure 4, *b*) reveals that green ZnO consists of well-defined hexagonal plates with primary lateral dimensions of 200–500 nm [25] with thicknesses estimated between 100 and 200 nanometers. DLS showed a Z-average diameter of 4161 nm with a bimodal distribution (peaks at 973.1 nm and 764.8 nm). This discrepancy is common in green synthesis; while SEM captures the “dry” inorganic core, DLS measures the hydrodynamic diameter, which includes the solvation shell and the carbonaceous framework surrounding the particles. The larger DLS values indicate that in aqueous suspension, these hexagonal plates form stable, loosely bound agglomerated clusters. For textile applications, such clusters are often beneficial as they facilitate better entrapment within the microfiber networks of cotton during the dip-coating process.

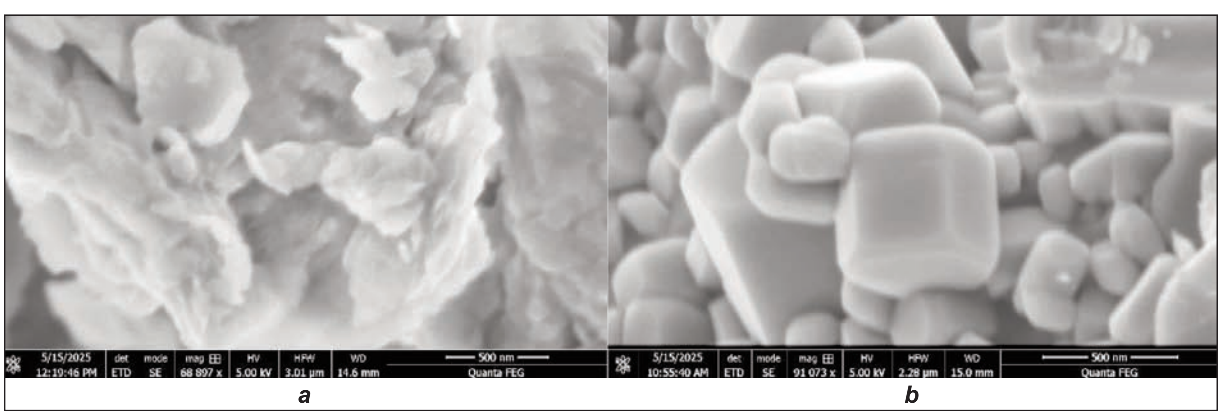

Fig. 4. SEM image of: *a* – chemically synthesised ZnO; *b* – olive leaf extract mediated ZnO

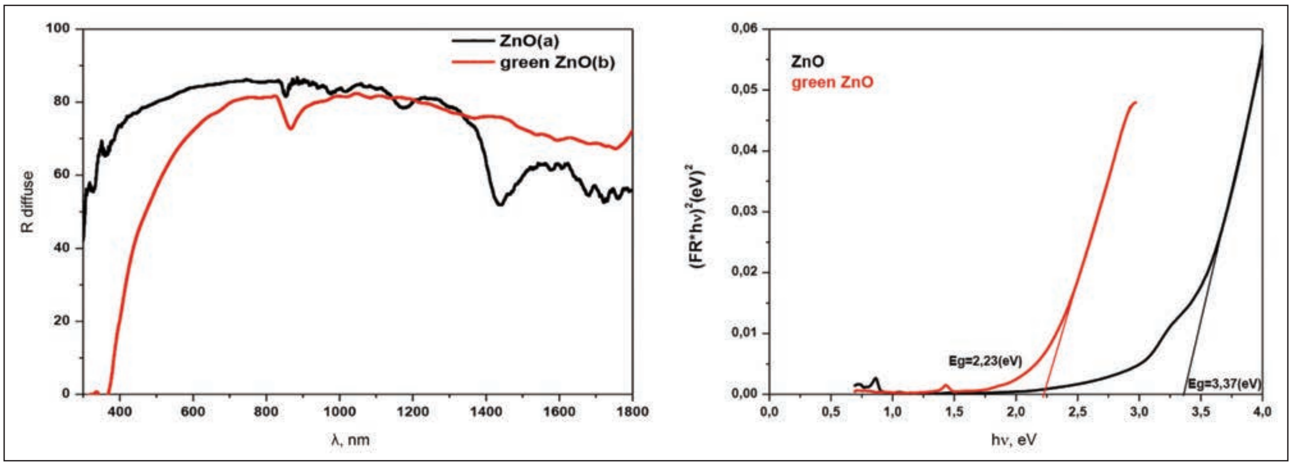

Fig. 5. Reflectance spectra and determination of the band gap of green and chemically synthesised ZnO

Reflectance spectroscopy and determination of band gap using Kubelka-Munk model

Figure 5 presents the reflectance spectra of green-synthesised and conventional ZnO across the UV-Vis-NIR range, revealing distinct optical behaviours. Conventional ZnO exhibits high reflectance (~80%) in the visible region, characteristic of high crystalline quality and low defect density. In contrast, green ZnO displays significantly lower reflectance and a pronounced absorption tail extending into the visible region, indicating enhanced light-harvesting capability. Band gap energies were determined using the Kubelka-Munk function combined with Tauc plots (figure 5).

Conventional ZnO shows a direct band gap of 3.37 eV, typical for pure ZnO. Remarkably, green ZnO exhibits a reduced band gap of 2.26 eV, representing a 33% narrowing. This substantial red-shift arises from the in situ incorporation of carbon and heteroatoms (N, O) resulting from the thermal decomposition of *Olea europaea* leaf extract during the 900°C calcination process. These species, along with induced oxygen vacancies, introduce mid-gap states and carbon-based defect levels within the ZnO lattice. The lowered band gap enables green ZnO to absorb a broader portion of the solar spectrum, particularly in the visible range, making it far more efficient for sunlight-driven photocatalytic applications compared to conventional ZnO, which is primarily UV-active. This optical tuning, achieved solely through eco-friendly precursors, eliminates the need for doping with rare-earth or transition metals, preserving the non-toxic nature of the material.

Antimicrobial activity

The antimicrobial activity of green-synthesised ZnO nanoparticles was investigated against two microorganisms: *Candida albicans* (C.a) and *Staphylococcus aureus* (S.a), employing the standard disk diffusion method as presented in figure 6. As shown, both microbial strains revealed clear zones of inhibition around the ZnO-loaded disk, confirming the broad-spectrum antimicrobial potential of the biosynthesised nanoparticles. *C. albicans* demonstrated a substantially larger inhibition zone with a diameter of 28 mm compared to *S. aureus* (16 mm in diameter), suggesting greater susceptibility of the fungal pathogen to ZnO nanoparticles. The observed inhibition zones suggest that the green-synthesised ZnO nanoparticles exert their antimicrobial effects through multiple mechanisms, including membrane disruption and interference with cellular metabolic processes. These results show the promising potential of eco-friendly synthesised ZnO nanoparticles as effective antimicrobial agents against both fungal and bacterial pathogens, investigation for biomedical and pharmaceutical applications.

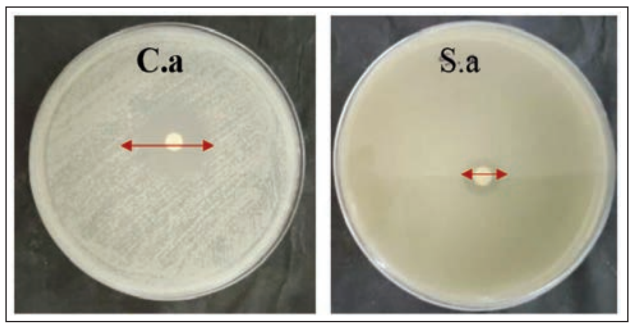

Fig. 6. Antimicrobial activity for *Candida albicans* (C.a) and *Staphylococcus aureus* (S.a)

Adsorption and photocatalytic properties

Figure 7 compares the adsorption performance of green-synthesised ZnO and chemically synthesised ZnO toward MB. The kinetic profile reveals rapid initial uptake within 50 min for both materials, reaching equilibrium by ~60 min. Green ZnO achieves a significantly higher equilibrium capacity ($q_e \approx 52$ mg/g) than chemical ZnO ($q_e \approx 43$ mg/g), representing a 21% enhancement. This superiority stems from polyphenolic capping layers on green ZnO, which provide additional hydroxyl and aromatic groups for electrostatic attraction, hydrogen bonding, and π–π stacking with cationic MB. The adsorption isotherm, conducted at equilibrium, shows that green ZnO maintains higher uptake across the entire concentration range (5–60 mg/L). At 50 mg/L initial MB, green

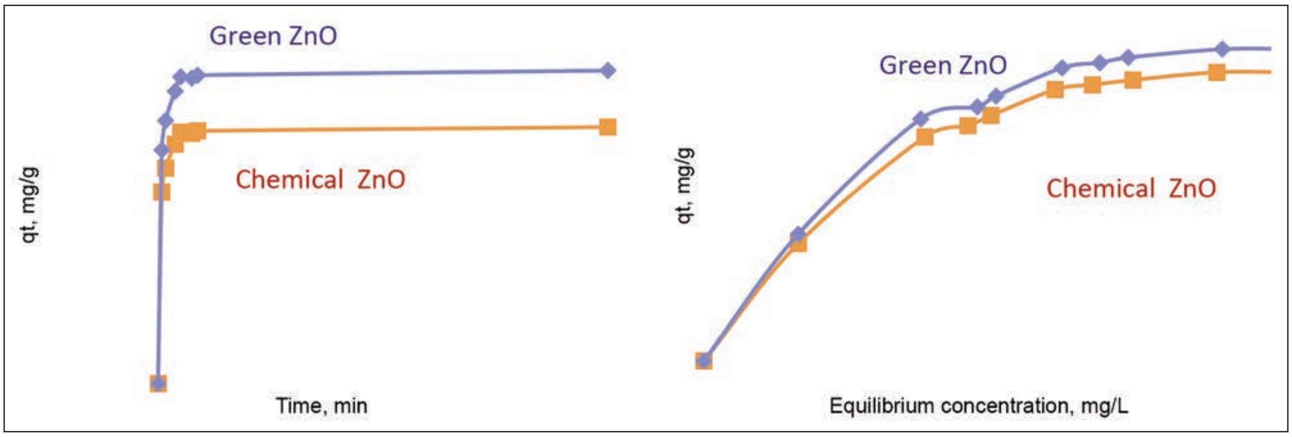

Fig. 7. Kinetic and adsorption isotherm for MB of green and chemical synthetized ZnO

ZnO removes ~94% of the dye, compared to ~78% by chemical ZnO. The steeper initial slope for green ZnO indicates stronger affinity, while the plateau suggests monolayer coverage consistent with Langmuir behaviour. The organic residues not only increase active binding sites but also create surface defects that improve dispersibility and prevent aggregation, ensuring more accessible surface area. Figure 8 compares the photocatalytic degradation of MB under natural sunlight using green-synthesised and conventional ZnO nanoparticles. The process includes a 24-h dark adsorption phase followed by solar exposure, ensuring that observed decolourisation reflects true photocatalysis rather than mere adsorption. Green ZnO demonstrates superior performance, achieving 94% MB degradation within 3 h under static conditions, compared to 88% for chemical ZnO. This enhanced activity stems from its narrowed band gap (2.6 eV) caused by phytochemical-induced defects and mid-gap states, extending absorption into the visible region (up to ~477 nm) and enabling efficient utilisation of the solar spectrum. Conversely, chemical ZnO, with a wider band gap (3.37 eV), relies primarily on UV light (<368 nm). Although its highly crystalline structure promotes charge separation and ROS generation, limited visible-light absorption restricts overall efficiency.

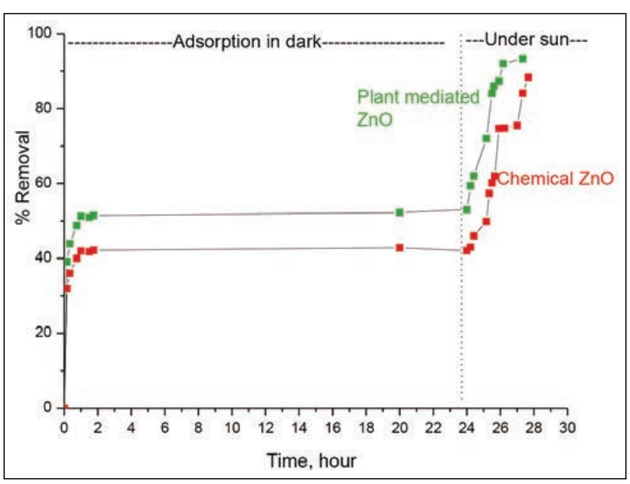

Fig. 8. MB removal using chemical ZnO and plant-mediated ZnO adsorption in dark and photocatalytic degradation under sunlight

Proposed mechanism

Figure 9 presents sunlight photocatalytic activity enhancement and mechanism of green ZnO prepared with olive leaf extract. The green synthesis method yields ZnO with superior photocatalytic performance compared to conventional ZnO's wurtzite structure. Chemical synthesis using NaOH yields near-stoichiometric ZnO with band gaps around 3.37 eV, due to minimal defects and high crystallinity. In contrast, green synthesis employing olive leaf extract results in a reduced band gap of ~2.6 eV, enhancing photocatalytic and antimicrobial applications by extending absorption into the visible spectrum. The proposed mechanism centres on the multifaceted role of olive leaf phytochemicals, primarily polyphenols like oleuropein, hydroxytyrosol, and flavonoids, which serve as bioreductants, stabilisers, and inadvertent dopants. During synthesis, Zn^{2+} ions from zinc acetate are reduced to ZnO nuclei via electron donation from phenolic -OH groups, forming

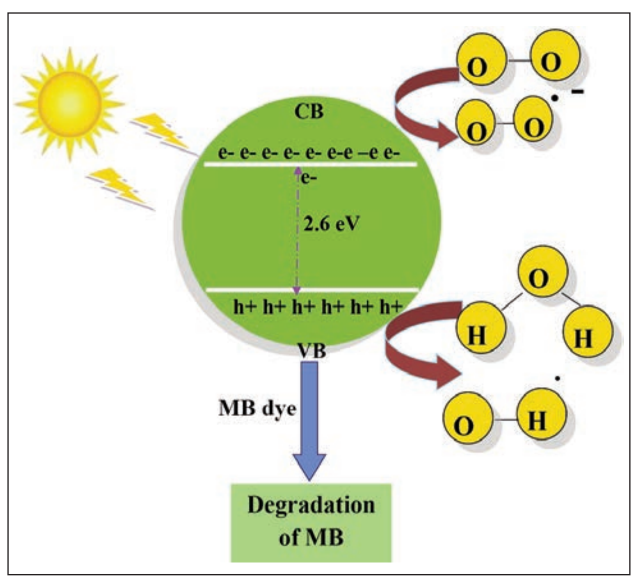

Fig. 9. Sunlight photodegradation of MB by green ZnO prepared with olive leaf extract

Zn-O-C bonds at the surface. This capping prevents agglomeration but introduces organic residues. Upon partial decomposition of these organics, oxygen vacancies and interstitial oxygen defects are generated, which contribute to narrowing the band gap by ~0.7 eV. Simultaneously, carbon from decomposed phenolics forms impurity bands that overlap with valence/conduction bands.

Implications for textile functionalization

While this study primarily focuses on the synthesis and physicochemical optimisation of green-synthesised ZnO, the findings have significant implications for the development of bioactive textiles. The hexagonal prismatic morphology (200–500 nm) and the resulting high surface area to volume ratio are critical for increasing the density of active sites available for dye adsorption and bacterial interaction [26].

Furthermore, the in situ carbon-doped framework and stable carbonate species products of the 900 °C thermal treatment enable high photocatalytic efficiency (94%) under natural solar irradiation.

From a processing perspective, the bimodal cluster distribution observed in DLS is expected to facilitate better mechanical interlocking within the porous cotton microfiber matrix during standard dip-dry-cure applications [27, 28]. This provides a distinct advantage over conventional chemical ZnO, which lacks these specific surface modifications. Future research will investigate the wash-fastness and laundering durability of these particles when immobilised using green cross-linking agents, such as citric acid, to ensure long-term functionality in smart textile substrates [29].

CONCLUSION

This study successfully demonstrates a fully green, scalable synthesis of ZnO nanoparticles using *Olea europaea* leaf extract as a precursor and template, offering a sustainable alternative to conventional chemical routes. The resulting green ZnO exhibits superior physicochemical properties, hexagonal prismatic morphology, a narrowed band gap (2.6 eV), and abundant surface defects, marking it as a highly promising multifunctional textile finishing agent. Compared to chemical ZnO, the green variant achieves 21% higher methylene blue adsorption (52 mg/g), 94% photocatalytic degradation within 3 h under natural sunlight, and stronger antimicrobial activity against *Staphylococcus aureus* and *Candida albicans*. These improvements stem from the in situ carbon modification and induced oxygen vacancies resulting from the thermal treatment of the plant-based precursors, which increase active sites and extend visible-light responsiveness. By proposing the replacement of multiple toxic finishes with a single bio-derived nanomaterial, this approach significantly reduces environmental impact, aligns with circular economy principles, and meets the textile industry's demand for eco-friendly, high-performance solutions for future smart fabric development. By bridging the gap between waste-derived green synthesis and high-performance textile finishing, this study demonstrates a sustainable pathway for producing multifunctional, bioactive fabrics with significant industrial potential.

REFERENCES

[1] Kalaba, M.H., Moghannem, S.A., El-Hawary, A.S., Radwan, A.A., Sharaf, M.H., Shaban, A.S., *Green Synthesized ZnO Nanoparticles Mediated by Streptomyces plicatus: Characterizations, Antimicrobial and Nematicidal Activities and Cytogenetic Effects*, In: Plants, 2011, 10, 9, 1760, https://doi.org/10.3390/plants10091760

[2] Al-Dhabi, N.A., Valan Arasu, M., *Environmentally-Friendly Green Approach for the Production of Zinc Oxide Nanoparticles and Their Anti-Fungal, Ovicidal, and Larvicidal Properties*, In: Nanomaterials, 2018, 8, 7, 500, https://doi.org/10.3390/nano8070500

[3] Ahmad, W., Kalra, D., *Green synthesis, characterization and anti microbial activities of ZnO nanoparticles using Euphorbia hirta leaf extract,* In: Journal of King Saud University – Science, 2020, 32, 4, 2358–2364, https://doi.org/10.1016/j.jksus.2020.03.014

[4] Maatoq, S.L., Ali, H., *Green Fabrication of Silica with Zinc Oxide as Nanocomposite for Adsorption of Methylene Blue Dye from Aqueous Solution,* In: Indones. J. Chem., 2025, 25, 5, 1451, https://doi.org/10.22146/ijc.104761

[5] Ramesh, M., Anbuvannan, M., Viruthagiri, G., *Green synthesis of ZnO nanoparticles using Solanum nigrum leaf extract and their antibacterial activity*, In: Spectrochimica Acta Part A: Molecular and Biomolecular Spectroscopy, 2015, 136, 864–870, https://doi.org/10.1016/j.saa.2014.09.105

[6] Ezealisiji, K.M., Siwe-Noundou, X., Maduelosi, B., Nwachukwu, N., Krause, R.W.M., *Green synthesis of zinc oxide nanoparticles using Solanum torvum (L) leaf extract and evaluation of the toxicological profile of the ZnO nanoparticles–hydrogel composite in Wistar albino rats*, In: Int Nano Lett, 2019, 9, 2, 99–107, https://doi.org/10.1007/s40089-018-0263-1

[7] Tien H.N., et al., *One-pot synthesis of a reduced graphene oxide–zinc oxide sphere composite and its use as a visible light photocatalyst*, In: Chemical Engineering Journal, 2013, 229, 126–133, https://doi.org/10.1016/j.cej.2013.05.110

[8] Chao L.-C. et al., *Zinc oxide nanodonut prepared by vapor-phase transport process*, In: Applied Physics Letters, 2006, 88, 25, 251111, https://doi.org/10.1063/1.2214146

[9] Liu S., et al., *Fabrication of palladium-copper nanoparticles with controllable size and chemical composition*, In: Journal of Colloid and Interface Science, 2018, 526, 201–206, https://doi.org/10.1016/j.jcis.2018.04.109

[10] Hu, S.-H., Chen, Y.-C., Hwang, C.-C., Peng, C.-H., Gong, D.-C., *Development of a wet chemical method for the synthesis of arrayed ZnO nanorods*, In: Journal of Alloys and Compounds, 2010, 500, 2, L17–L21, https://doi.org/10.1016/j.jallcom.2010.03.235

[11] Kadinskaya, S., et al., *Deep-Level Emission Tailoring in ZnO Nanostructures Grown via Hydrothermal Synthesis,* In: Nanomaterials, 2022, 13, 1, 58, https://doi.org/10.3390/nano13010058

[12] Vella Durai, S.C., Kumar, E., Indira, R., *Green route to prepare zinc oxide nanoparticles using Moringa oleifera leaf extracts and their structural, optical and impedance spectral properties,* In: SPQEO, 2024, 27, 01, 064–069, https://doi.org/10.15407/spqeo27.01.064

[13] Padalia, H., Chanda, S., *Characterization, antifungal and cytotoxic evaluation of green synthesized zinc oxide nanoparticles using Ziziphus nummularia leaf extract*, In: Artificial Cells, Nanomedicine, and Biotechnology, 2017, 45, 8, 1751–1761, https://doi.org/10.1080/21691401.2017.1282868

[14] Tripathi, R.M., Bhadwal, A.S., Gupta, R.K., Singh, P., Shrivastav, A., Shrivastav, B.R., *ZnO nanoflowers: Novel biogenic synthesis and enhanced photocatalytic activity*, In: Journal of Photochemistry and Photobiology B: Biology, 2014, 141, 288–295, https://doi.org/10.1016/j.jphotobiol.2014.10.001

[15] Singh, B.N., Rawat, A.K.S., Khan, W., Naqvi, A.H., Singh, B.R., *Biosynthesis of Stable Antioxidant ZnO Nanoparticles by Pseudomonas aeruginosa Rhamnolipids*, In: PLoS ONE, 2014, 9, 9, e106937, https://doi.org/10.1371/journal.pone.0106937

[16] Pavithra, N.S., Lingaraju, K., Raghu, G.K., Nagaraju, G., *Citrus maxima (Pomelo) juice mediated eco-friendly synthesis of ZnO nanoparticles: Applications to photocatalytic, electrochemical sensor and antibacterial activities,* In: Spectrochimica Acta Part A: Molecular and Biomolecular Spectroscopy, 2017, 185, 11–19, https://doi.org/10.1016/j.saa.2017.05.032

[17] Abdelbaky, A.S., Abd El-Mageed, T.A., Babalghith, A.O., Selim, S., Mohamed, A.M.H.A., *Green Synthesis and Characterization of ZnO Nanoparticles Using Pelargonium odoratissimum (L.) Aqueous Leaf Extract and Their Antioxidant, Antibacterial and Anti-inflammatory Activities,* In: Antioxidants, 2022, 11, 8, 1444, https://doi.org/10.3390/antiox11081444

[18] Abdelmigid, H.M., Hussien, N.A., Alyamani, A.A., Morsi, M.M., AlSufyani, N.M., Kadi, H.A., *Green Synthesis of Zinc Oxide Nanoparticles Using Pomegranate Fruit Peel and Solid Coffee Grounds vs. Chmical Method of Synthesis, with Their Biocompatibility and Antibacterial Properties Investigation*, In: Molecules, 2022, 27, 4, 1236, https://doi.org/10.3390/molecules27041236

[19] Shahack-Gross, R., Ayalon, A., *Stable carbon and oxygen isotopic compositions of wood ash: an experimental study with archaeological implications*, In: Journal of Archaeological Science, 2013, 40, 1, 570–578, https://doi.org/10.1016/j.jas.2012.06.036

[20] Hanna, A.L., et al., *Biosynthesis and Characterization of Silver Nanoparticles Produced by Phormidium ambiguum and Desertifilum tharense Cyanobacteria*, In: Bioinorganic Chemistry and Applications, 2022, 2022, 1, 9072508, https://doi.org/10.1155/2022/9072508

[21] Fazlzadeh, M., Khosravi, R., Zarei, A., *Green synthesis of zinc oxide nanoparticles using Peganum harmala seed extract, and loaded on Peganum harmala seed powdered activated carbon as new adsorbent for removal of Cr(VI) from aqueous solution*, In: Ecological Engineering, 2017, 103, 180–190, https://doi.org/10.1016/j.ecoleng.2017.02.052

[22] Frost, R. L., Dickfos, M.J., *Raman spectroscopy of halogen-containing carbonates*, In: J Raman Spectroscopy, 2007, 38, 11, 1516–1522, https://doi.org/10.1002/jrs.1806

[23] Yuvakkumar, R., Suresh, J., Saravanakumar, B., Joseph Nathanael, A., Hong, S.I., Rajendran, V., *Rambutan peels promoted biomimetic synthesis of bioinspired zinc oxide nanochains for biomedical applications*, In: Spectrochimica Acta Part A: Molecular and Biomolecular Spectroscopy, 2015, 137, 250–258, https://doi.org/10.1016/j.saa.2014.08.022

[24] Pascariu, P., Gherasim, C., Airinei, A., *Metal Oxide Nanostructures (MONs) as Photocatalysts for Ciprofloxacin Degradation,* In: IJMS, 2023, 24, 11, 9564, https://doi.org/10.3390/ijms24119564

[25] Ogunyemi, S.O., et al., *Green synthesis of zinc oxide nanoparticles using different plant extracts and their antibacterial activity against Xanthomonas oryzae pv. oryzae*, In: Artificial Cells, Nanomedicine, and Biotechnology, 2019, 47, 1, 341–352, https://doi.org/10.1080/21691401.2018.1557671

[26] Saleem, H., Zaidi, S.J., *Sustainable Use of Nanomaterials in Textiles and Their Environmental Impact,* In: Materials, 2020, 13, 22, 5134, https://doi.org/10.3390/ma13225134

[27] Saleemi, S., Naveed, T., Riaz, T., Memon, H., Awan, J.A., Siyal, M.I., Xu, F., Bae, J., Surface Functionalization of Cotton and PC Fabrics Using SiO2 and ZnO Nanoparticles for Durable Flame Retardant Properties, In: Coatings, 2020, 10, 124, https://doi.org/10.3390/coatings10020124

[28] Yadav, A., Prasad, V., Kathe, A.A. et al., *Functional finishing in cotton fabrics using zinc oxide nanoparticles*, In: Bull Mater Sci, 2006, 29, 641–645, https://doi.org/10.1007/s12034-006-0017-y

[29] Xu, H., Yang, C., Song, H.-y., *Eco-Friendly Dyeing and Functional Finishing of Organic Cotton Using Optimized Oolong Tea Stems (Agricultural Waste) Through Response Surface Methodology*, In: Molecules, 2025, 30, 509, https://doi.org/10.3390/molecules30030509

Authors:

NEDRA ABBES[1,2], THOURAYA BARHOUMI[3], SANA FRIDJINE[3], NEJIB SEJRI[3], BOUBAKER JAOUACHI[2], JUN XU[1*], HONGLUAN LIU[1*], IMENE BEKRI-ABBES[5]

[1]School of Textile Science and Engineering, Tiangong University, Tianjin, China

[2]University of Monastir, Textile Engineering Laboratory (LGTex), Monastir 5000, Tunisia
e-mail: nedraabbes2@gmail.com, boubaker.jaouachi@enim.u-monastir.tn

[3]Physical Chemistry Laboratory for Mineral Materials and Their Applications, National Centre for Research in Materials Sciences, Borj Cedria Technopark, Soliman 8027, Tunisia
e-mail: thourayabarhoumi186@gmail.com, sanafridjine@gmail.com, sejri.nejib@gmail.com

[4]University of Monastir, National School of Engineers of Monastir (ENIM), Monastir 5000, Tunisia

[5]National Center of Materials Science, Techno-pole, Borj Cedria, Slimene 2084, Tunisia
e-mail: bekrimene@gmail.com

*These authors contributed equally to this work and share corresponding authorship.

Corresponding authors:

HONGLUAN LIU
e-mail: liuhongluan@tiangong.edu.cn
JUN XU
e-mail: xujun@tiangong.edu.cn

Can digital transformation become a new engine for the development of the textile industry? Evidence from China

DOI: 10.35530/IT.077.04.2025139

SHICHAO GAO QIANKAI JIANG

ABSTRACT – REZUMAT

Can digital transformation become a new engine for the development of the textile industry? Evidence from China

At present, China is undergoing a major transition from an industrial economy to a digital economy, particularly as enterprises that demonstrated resilience during the pandemic were predominantly those at the forefront of comprehensive digital transformation and online-offline integration. Recently, Shandong Municipality placed significant emphasis on the transformation and upgrading of its textile industry, which played a crucial role in the digital economy. Based on the contemporary implications of the digital economy and high-quality development, this study selected relevant indicator data from Shandong Province for the period 2014–2023 and constructed a coupling coordination model to measure the coupling coordination level between the two systems. The findings indicated that the coupling coordination development demonstrated a favourable trend, which was conducive to the healthy development of the textile industry. This research aimed to promote the deep integration of the textile industry with the digital economy and create a "strong engine" for high-quality development in the face of new historical opportunities.

Keywords: *coupling coordination model, digital economy, entropy method, green development*

Transformarea digitală poate deveni un nou motor al dezvoltării industriei textile? Date din China

În prezent, China se află în plin proces de tranziție de la o economie industrială la o economie digitală, în special datorită faptului că întreprinderile care au dat dovadă de reziliență în timpul pandemiei au fost, în mare parte, cele aflate în avangarda transformării digitale cuprinzătoare și a integrării dintre mediul online și cel offline. Recent, municipalitatea Shandong a acordat o importanță deosebită transformării și modernizării industriei textile, care a jucat un rol crucial în economia digitală. Pe baza implicațiilor contemporane ale economiei digitale și ale dezvoltării de înaltă calitate, acest studiu a selectat date privind indicatorii relevanți din provincia Shandong pentru perioada 2014–2023 și a construit un model de coordonare a cuplării pentru a măsura nivelul de coordonare a cuplării dintre cele două sisteme. Rezultatele au indicat că evoluția coordonării de cuplare a demonstrat o tendință favorabilă, care a contribuit la dezvoltarea sănătoasă a industriei textile. Acest studiu a avut ca scop promovarea integrării profunde a industriei textile cu economia digitală și crearea unui „motor puternic" pentru dezvoltarea de înaltă calitate în contextul noilor oportunități istorice.

Cuvinte-cheie: *model de coordonare a cuplării, economia digitală, metoda entropiei, dezvoltarea ecologică*

INTRODUCTION

China's textile industry has a long history, from hemp and silk weaving in the Neolithic Age to modern high-tech fibres and functional fabrics; it has always been an important pillar of China's economy [1]. As the world's largest textile producer and exporter, China possesses a complete industrial chain, covering multiple stages such as cotton cultivation, fibre processing, fabric weaving, and garment manufacturing [2, 3]. In recent years, China's textile industry has made significant progress in technological innovation, sustainable development, and international cooperation, driving industrial upgrading and green transformation [4, 5]. In the future, China's textile industry will continue to develop toward high-end, intelligent, and green directions, strengthen international cooperation, meet the upgrading of domestic consumption and diverse market demands, and contribute more to the prosperity of the global textile industry [6].

By 2024, China's digital economy had continued to grow and had become a key force driving economic progress [7]. According to the latest data from the "Research Report on China's Digital Economy Development (2024)", China's digital economy reached 53.9 trillion yuan in 2023, accounting for 42.8% of GDP, representing an increase of 1.3 percentage points from the previous year, with the digital economy's contribution to GDP growth reaching 66.45% [8].

The digital economy's resilient growth during challenging circumstances further highlighted its important position in the national economy, effectively supporting pandemic prevention and control as well as economic and social development [9, 10]. Scholars Si et al. found that the deep integration of the digital economy with manufacturing could drive manufacturing to achieve quality transformation, efficiency transformation, and dynamic transformation [11]. Scholars

Heping and Fuxiang employed a "micro-meso-macro" analytical framework to investigate the intrinsic mechanisms by which the digital economy drove high-quality economic development [12]. Scholars Fromhold-Eisebith et al. contended that it was essential to vigorously enhance the deep integration of informatisation and industrialisation, advance the widespread application of digital technology in various textile processes, and construct new manufacturing models such as intelligent production and digital management [13].

Under the influence of the digitalised economy, the textile industry was progressing towards intelligent production, management, and operations [14]. However, few scholars had analysed the coordinated development level and mutual interaction effects between the digitalised economy and the textile industry. Against this broader backdrop, this study was dedicated to exploring the coupling coordination relationship between the digitalised economy and the progress of the textile industry, to identify opportunities for the progress of Shandong Province's textile industry.

The innovations could be summarised as follows: First, by selecting textile industry and digital economy indicators from Shandong Province for the period 2014–2023, this study filled the gap in previous research that predominantly focused on national-level or earlier data, whilst considering both the latest development trends and regional characteristics. Second, beyond traditional economic growth and scale effects, this research incorporated "green" elements into the high-quality development evaluation indicator system, systematically examining for the first time the synergistic improvement of resource utilisation efficiency and environmental friendliness in the textile industry's digital transformation. Third, based on entropy method-weighted dual system evaluation indicators, this study employed a coupling coordination model to quantify the interaction and coordination level between the two systems, filling the research gap in the application of such models in the textile industry field. Fourth, beyond empirical calculations, this study drew upon the "micro-meso-macro" analytical framework to deeply analyse how technological innovation, industrial integration, and policy guidance at different levels promoted the evolutionary path of coupling coordination. Fifth, combining Shandong Province's transformation and upgrading experience, this study proposed precise policy recommendations and pathway designs targeting the "lag" and "imbalance" issues in coupling coordination, demonstrating strong operability and promotional value. Sixth, this study proposed a "digital economy-textile industry green high-quality development" mutually reinforcing and complementary "strong engine" model, enriching the theoretical system of industrial transformation and upgrading and regional economic growth.

LITERATURE REVIEW

The connotation of digital economy

The digital economy has emerged as a transformative force in the modern world, reshaping industries and driving economic growth on a global scale [15, 16]. On one hand, the rapid development of the digitalised economy has been marked by the vigorous promotion of digital infrastructure construction, which includes critical components such as information and communication technology (ICT) and the industrial internet [17]. These advancements have not only generated new business models but also brought unprecedented opportunities to various industries, propelling the rapid progress of related sectors [18, 19]. For instance, the integration of advanced ICT solutions has enabled businesses to streamline their operations, enhance customer engagement, and develop innovative products and services that were previously unimaginable [20]. Similarly, the industrial internet has facilitated the interconnectivity of industrial systems, allowing for real-time data exchange and collaborative production processes that boost efficiency and productivity [21, 22].

On the other hand, the digital economy is inextricably linked to the quality of digital applications, which is prominently demonstrated in the breakthrough and integrated development of cutting-edge technologies such as blockchain, big data, and AI. These technologies have revolutionised the way data is managed, analysed, and utilised, thereby accelerating equipment access and system deployment [23]. Blockchain technology, with its decentralised and secure nature, has the potential to transform supply chain management, financial transactions, and digital identity verification, among other applications [24, 25]. Big data analytics enables organisations to extract valuable insights from vast amounts of information, informing decision-making processes and driving strategic business initiatives [26]. AI, with its ability to learn and adapt, has become an integral part of numerous sectors, from healthcare diagnostics to autonomous vehicles, significantly enhancing efficiency and effectiveness [27, 28].

Moreover, government investment in digital research and experimental funding has emerged as a key factor in bolstering the digital economy's research and development capabilities [29]. This support has been instrumental in facilitating the continuous release of the digital economy's potential, fostering innovation and driving technological advancements. For example, government-backed research initiatives have led to breakthroughs in quantum computing, which promises to revolutionise data processing and encryption [30, 31]. Additionally, funding for experimental projects has enabled startups and established companies alike to explore new digital frontiers, such as the development of smart cities and the Internet of Things (IoT), which have the potential to transform urban living and industrial operations [32–34].

This study delves into the connotation of the digital economy from an economic perspective, interpreting it as an economic form that achieves progress through the digitalisation of knowledge and information. By leveraging digital technologies, the digital economy guides the optimal allocation and regeneration of resources, ensuring that they are utilised as efficiently and productively as possible. This not only drives economic growth but also fosters social development by creating new job opportunities, enhancing educational outcomes, and improving public services. As the digital economy continues to evolve, it is poised to play an even more significant role in shaping the future of our global society, offering endless possibilities for innovation and progress.

The connotation of green advancement in the textile industry

Rapid development of the textile industry was conducive to enhancing the transformation of economic development patterns and establishing a modern economic system [35, 36]. At the macroscopic level, this referred to stable economic growth, balanced urban-rural development, green, coordinated sustainable development, and the sharing of development outcomes by the people. Therefore, the textile industry needed to implement the understanding of healthy, green, and sustainable development [37]. From an industrial perspective, development of the textile industry referred to a reasonable industrial structure, continuously optimised industrial layout, achievement of transformation and upgrading, and enhancement of sustainable development capabilities [38]. From the perspective of textile enterprises, high-quality development was influenced by factors such as first-class competitiveness, reliable quality, and brand influence [39]. Development of the textile industry needed to focus on intelligent manufacturing, accelerate the deep integration of the digital economy with the textile industry, promote the digitalisation and intelligentisation of textile industry development, and advance towards high-quality development [40].

The coupling relationship between digital economy and green development of textile industry

In recent years, international and domestic market layouts, commodity structures, and trade patterns have undergone profound adjustments, and these changes provided a window of opportunity for the formation of a new pattern characterised by domestic circulation as the main section and mutual improvement of domestic and international dual circulation [41]. As a pillar industry of the national economy, the textile industry had witnessed digital transformation become the core driving force for high-quality development within this developmental context, with the digital economy becoming a key element in technological innovation and transformation of the textile industry [42]. The higher the degree of digitalisation in the textile industry, the deeper the integration with the digital economy, and consequently, the stronger the coupling relationship between the two systems. Against the backdrop of the digital economy driving industrial transformation and upgrading, big data and cloud computing technologies highly integrated supply-side and demand-side data, reduced production energy consumption, and achieved efficient digital management of textile production, resulting in breakthroughs across three dimensions: cost, quality, and profit. The textile industry transformed from "manufacturing" to "intelligent manufacturing", with enhanced automation levels, further promoting digital transformation and technological innovation in the textile industry whilst improving competitive advantages [43]. This provided a platform for the development of four indicators: economic development, technological resources, green development, and innovation performance in the new era, consolidating the rapid development of the textile industry and thereby supporting the advancement of digital economy industrialisation processes, as illustrated in figure 1.

Analysis of digital economy application scenarios in Shandong textile enterprises

The year 2024 represented a year of particular significance in China's modernisation construction process,

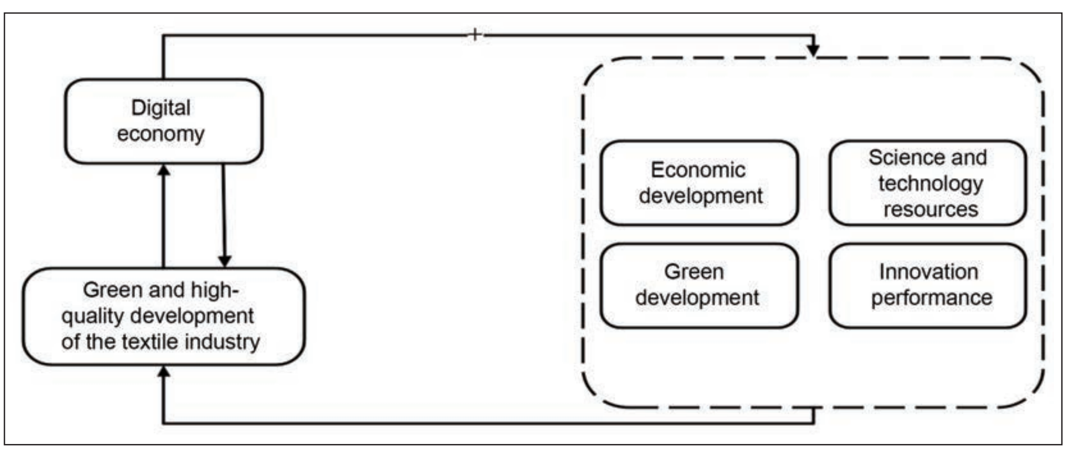

Fig. 1. The coupling relationship between digital economy and green high-quality development of textile industry

where “pandemic prevention and control” and “economic recovery”, “global cooperation” and “strategic competition”, and “human survival” and “sustainable development” were interwoven and overlapping, creating a complex environment. As an important light industry sector, the textile industry was not only closely related to people’s daily lives but also had extensive applications in industry, national defence, and medical and health sectors. The textile industry represented a labour-intensive industry, where a series of processes including textile design and development, production, and sales constituted factors that influenced the transformation and upgrading of textile enterprises. This study selected textile enterprises in Shandong Province with high levels of digitalisation and representativeness as examples to analyse the digital application scenarios in their design and development, production, and sales processes, as detailed in table 1.

In addition, we used the texts of the Shandong Provincial Government work reports from 2014 to 2023, employing word cloud diagrams to depict the development of the digital economy in Shandong Province (as shown in figure 2) and the development of the textile industry in Shandong Province (as shown in figure 3).

Figure 2 displayed the keywords “Economy”, “Blockchain”, “Infrastructure”, and “Digital data”, which signalled Shandong Province’s focus on digital infrastructure, blockchain technology, and big data as foundational pillars of its digital-economy agenda.

During the past five years the province accelerated investment in fifth-generation (5G) mobile networks, industrial internet, and data centres, thereby creating a robust underpinning for digital growth. National-level internet backbone nodes were commissioned in Jinan and Qingdao, markedly improving inter-provincial data-transfer speeds. Blockchain was designated a strategic priority: the Shandong Blockchain Research Institute initiated multiple technology-development projects and industry partnerships, fostering a trusted digital ecosystem across supply-chain management, government services, and finance.

Shandong also expanded access to public-sector data, established a provincial data-trading platform, and trialled data-asset valuation mechanisms, which deepened the use of digital information in agriculture, manufacturing, and services. As China’s largest industrial province, Shandong promoted widespread “cloud adoption, data activation, and intelligentisation” among factories, generating benchmark demonstrations in smart manufacturing, intelligent mining, and precision agriculture and enhancing the competitiveness of traditional sectors.

These initiatives raised total-factor productivity by integrating technological innovation with data-driven decision-making, facilitating a shift from resource-intensive to technology-intensive development. Digital technologies upgraded legacy industries and spawned new business formats: platform economy, shared manufacturing, and digital trade, thereby diversifying and upgrading the industrial structure.

By building advanced digital infrastructure and strengthening innovation capacity, Shandong assumed a leading role in the ecological protection and development of the Yellow River Basin and elevated its strategic position within China’s digital-economy landscape. Data, treated as a new factor of production, improved efficiency in finance, logistics, health care, and education through circulation and exchange, creating additional sources of economic growth.

Overall, the province used digital infrastructure as its foundation and blockchain, big-data analytics, and other emerging technologies as engines to achieve deep integration between the digital and physical economies. This process injected new momentum into Shandong’s economy and provided a replicable “Shandong model” for China’s wider digital transformation. Looking forward, further marketisation of data elements and refinement of digital governance systems are likely to establish Shandong as a major growth pole for high-quality national digital development.

Fig. 2. Digital economy word cloud

Figure 1 contained a set of fragmented terms implying flame-retardant cotton, Cocoon, Bast, Syntehti Fibre and Tenac, which collectively signalled Shandong Province’s move toward a broad-spectrum fibre portfolio spanning natural sericulture, bast fibres, high-tenacity synthetics and functionalised cellulosics.

Over the past decade Shandong consolidated its position as China’s largest bast-fibre processing base, utilising locally grown hemp and ramie to manufacture high-count yarns for technical textiles. The province simultaneously rejuvenated its centuries-old sericulture belt in the Yimeng mountainous region; annual cocoon output rose to 18,000 tonnes, thereby securing a domestic feedstock for premium silk apparel and medical sutures.

On the synthetic side, Sinopec Yanshan and Luxi Chemical commissioned polyester and nylon 6 chips plants with a combined capacity exceeding 1.5 Mt yr^{-1}. Drawing on these chips, downstream filament-spinners in Qingdao and Weifang introduced ultra-high-tenacity (≥8.0 cN $dtex^{-1}$) industrial yarns now embedded in tyre cord, soft-body armour and geogrids.

To satisfy stringent fire-safety standards, Shandong researchers developed flame-retardant cotton (FRC) using a phosphorus-nitrogen synergetic finish that withstands 50 wash cycles while maintaining limiting-oxygen index ≥ 28%. Pilot mills in Zibo produced 30 million metres of FRC sheeting in 2022, chiefly exported to European work-wear brands.

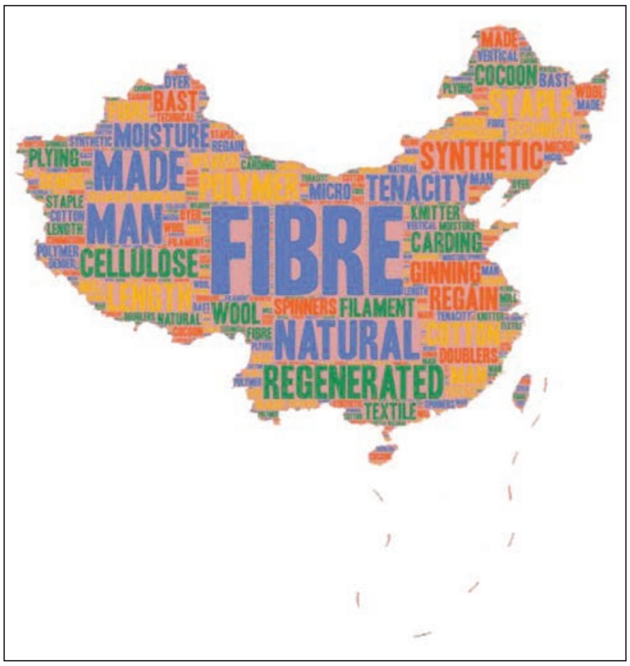

Fig. 3. Textile industry word cloud

Economic significance emerged on three fronts. First, value-added per tonne of fibre climbed from RMB 6 300 to RMB 11 800 between 2015 and 2023 as the share of technical and functional textiles rose above 42 % of provincial output. Second, the integrated bast-fibre → yarn → fabric chain created 47,000 rural jobs and lifted hemp growers' income by 18 % relative to cereal cropping. Third, substitution of imported aramid with locally engineered high-tenacity nylon and FRC saved an estimated USD 240 million in foreign-exchange outflows and strengthened Shandong's resilience against volatile commodity prices.

In sum, Shandong leveraged both its agricultural bast-fibre heritage and its petrochemical backbone to build a diversified, innovation-driven textile ecosystem. This trajectory not only raised regional value capture but also offered a replicable model for upgrading traditional fibre provinces into high-margin technical-textile hubs within China's broader supply-chain security strategy.

CONSTRUCTION OF EVALUATION INDICATOR SYSTEM FOR DIGITAL ECONOMY AND DEVELOPMENT OF TEXTILE INDUSTRY

Shandong digital economy evaluation indicator system

This study adhered to the principles of objectivity, operability, systematicity, and scientific rigour, and combined with the exposition of the connotation of digital economy, constructed a digital economy development evaluation indicator system for Shandong Province [44]. Three dimensions were selected to assess the quality of Shandong's digital economy advancement: digital infrastructure, digital network penetration, and digital research and development capabilities, as presented in table 1.

Table 1

SHANDONG DIGITAL ECONOMY DEVELOPMENT EVALUATION INDICATOR SYSTEM

Primary indicators	Secondary indicators	Weights
Digital infrastructure	ICT development index	0.1132
	Total post and telecommunications business	0.0348
	Fibre optic line long way	0.1178
	Percentage of informatized employees	0.0155
	Number of internet broadband access subscribers	0.1299
Quality of digital applications	Average e-commerce turnover of enterprises	0.0365
	Digital TV coverage rate	0.1333
	Internet penetration rate	0.0461
	Mobile phone subscribers at the end of the year	0.1454
Digital R&D capabilities	Contribution rate of scientific and technological progress	0.1155
	Transformation of scientific and technological achievements	0.1120
	Investment in scientific research and experimental funding	0.0554

Shandong textile industry development evaluation index system

Combined with the above analysis, four first-level indicators of scientific and technological resources, innovation performance, economic progress, and green development, a total of 14 second-level indicators, were used to build a Shandong textile industry development evaluation index system [45]. In addition to the annual emissions of sewage as a reverse indicator of the green development of the textile industry, the rest are positive indicators. Table 2 presents the detailed evaluation index system.

Data sources

This study selected data from Shandong Province covering 10 years from 2014 to 2023 as the foundational data for the research. The original data were sourced from the Statistical Yearbook of Shandong Province, Shandong Provincial Bureau of Statistics, Shandong Provincial People's Government, and the National Bureau of Statistics. To address missing indicator data for certain years, mean replacement interpolation methods were employed to complete the dataset.

Standardisation Processing

Due to the different dimensions and orders of magnitude among the selected indicator data, this study first conducted standardisation processing on the original indicator data before data analysis to eliminate the influences these differences might cause [46].
The standardisation processing formula for positive indicators was:

$$X'_{ij} = \frac{X_{ij} - m_j}{M_{ij} - m_j} \tag{1}$$

The formula for normalising the reverse indicator is:

$$X'_{ij} = \frac{M_{ij} - X_{ij}}{M_j - m_j} \tag{2}$$

In equation 1 and equation 2, i denotes the year, j denotes the indicator, and X_{ij} is the original data, which denotes the original value of the j^{th} indicator in the i^{th} year. X_{ij} is the standardised statistical value of the indicator, which denotes the standardised value of the j^{th} indicator in year i. M is the maximum value of X_{ij} and m is the minimum value of X_{ij}.
To make the data analysis more meaningful, this paper eliminates the zero and negative values, so that the standardised data are shifted as a whole, that is:

$$\chi'_{ij} = X'_{ij} + \alpha \tag{3}$$

To maximise the preservation of the original data by following the intrinsic laws of the original data, α is any real number, and to make α the smallest value closest to χ'_{ij}, $\alpha = 0.0001$ is taken.

Entropy value method to calculate weights

The entropy value method is one of the commonly used objective assignment methods to determine the level of dispersion of an indicator. To obtain accurate and objective evaluation results, this article adopts the entropy value method as the assignment method for evaluating the performance of digital economy development and the green development of the textile industry.
(1) Compute the proportionate part of the j^{th} indicator to the indicator in the i^{th} year, i.e. P_{ij}:

$$P_{ij} = \frac{\chi'_{ij}}{\sum_{i=1}^{n} \chi'_{ij}} \tag{4}$$

$\sum_{i=1}^{n} \chi'_{ij}$ denotes the sum of statistical values of all years of the j^{th} indicator after standardisation.
(2) Entropy value calculation: compute the entropy value e_j of the j^{th} indicator, that is:

$$e_j = -\frac{1}{Inn} \sum_{i=1} P_{ij}\, In(P_{ij}),\ 0 \le e_j \le 1 \tag{5}$$

Table 2

SHANDONG TEXTILE INDUSTRY GREEN HIGH-QUALITY DEVELOPMENT EVALUATION INDEX SYSTEM			
Primary indicators	**Secondary indicators**	**Attributes**	**Weights**
Science and technology resources	Textile engineers and technicians	+	0.0856
	Personnel with intermediate titles or above	+	0.0467
	Independent scientific research institutions	+	0.0555
	Land for public facilities	+	0.0389
	Private technology-based textile enterprises	+	0.0476
Innovation performance	Achievements through appraisal	+	0.0865
	Patent applications received	+	0.1111
Economic development	Capital return rate	+	0.0532
	Cloth production	+	0.0844
	Yarn production	+	0.0666
Green development	Green space	+	0.0567
	Total water supply	+	0.0162
	Water penetration rate	+	0.0878
	Sewage annual emissions	-	0.1632

(3) Compute the parameter of variation of the indicator g_i. The value of the coefficient of variation is directly proportional to the degree of the indicator in the comprehensive evaluation system, ie:

$$g_i = 1 - e_j \quad (6)$$

(4) Compute the weight of each indicator W_j , i.e:

$$W_j = \frac{g_j}{\sum_{j=1}^{m} g_j}, \ j = 1,2,3,\ldots,m \quad (7)$$

The results of the weight calculation are shown in table 1 and table 2.

(5) Calculate the comprehensive score of Shandong's digital economy and development of the textile industry, U_1 is the digital economy development index, and U_2 is the development index of the textile industry, that is:

$$U_n = \sum_{j=1}^{m} W_j P_{ij}, \ (n = 1, 2) \quad (8)$$

The results of the index calculation are shown in table 4.

Third, the digital economy and the textile industry green development coupling and coordination degree analysis

CONSTRUCTING THE COUPLING AND COORDINATION DEGREE MODEL

Combined with the relevant research, to determine the coupling degree of the digital economy and the textile industry green development, the formula, that is:

$$C = \sqrt{\frac{U_1 \times U_2}{(U_1 + U_2)^2}} \quad (9)$$

The larger the value of C, the stronger the coupling effect between the two systems and $0 \leq C \leq 1$.

The coupling degree model can only reflect the degree of mutual influence between the two systems of the digital economy and the high-quality development of the textile industry, and cannot reflect the level of the two systems. To accurately and objectively measure the level of coordinated development between the two systems, drawing on relevant research, the coupling coordination degree D of the digital economy and the development of the textile industry is calculated, that is:

$$D = \sqrt{C \times T} \quad (10)$$

$$T = \alpha U_1 + \beta U_2 , \ \alpha + \beta = 1 \quad (11)$$

D is the coupling coordination level of the digital economy and the development of the textile industry, and T is the extensive coordinated development index of the two systems of the digital economy and the development of the textile industry, reflecting the value of the contribution of the overall development level of the two to the degree of their coupling coordination, respectively. Both α and β are coefficients to be determined, according to the description of the coupling relationship between digital economy and textile industry in this paper, it is believed that the digital economy can promote the development of the textile industry, and the high-quality development of the textile industry will also promote the progress of the digital economy to a certain degree, and the importance of the two systems is equal, so it is given to $\alpha = \beta = 0.5$, and the results of the calculation are shown in table 5.

In order to objectively and effectively study the coupling development status between the digital economy and the development of the textile industry, with reference to the grades of the coupling coordination degree division in related literature, the coupling coordination degree judgment standard of this paper is presented in table 3.

COUPLING COORDINATION FINDINGS

Using the coupling degree coordination model, the results are calculated according to the formula and table 4 is obtained.

Figure 4 shows the coordinated relationship between the advancement of the digital economy and the green development of the textile industry. Table 4 clearly reflects the coupling degree, coupling coordination degree, and coordination levels between digital economy development and green development of the textile industry. Overall, from 2014 to 2023, the

Table 3

CRITERIA FOR JUDGING THE DEGREE OF COUPLING COORDINATION

Coupling harmonization	Coupling development stage	Coupling harmonisation level	Classification
0.00≤D≤0.10	Minimum coupling	Extreme dissonance	Type of dysregulation decline (Unacceptable interval)
0.10≤D≤0.20	Low level coupling	Severe dissonance	
0.20≤D≤0.30	Low level coupling	Moderate dissonance	
0.30≤D≤0.40	Antagonistic coupling	Mild dissonance	
0.40≤D≤0.50	Antagonistic coupling	Threatened dissonance	Intermediate transition type (Antagonistic interval)
0.50≤D≤0.60	Antagonistic coupling grinding phase	Barely coordinated	
0.60≤D≤0.70	Grinding coupling	Primary coordination	Coordination elevation type (Acceptable interval)
0.70≤D≤0.80	Grinding coupling	Intermediate coordination	
0.80≤D≤0.90	High level coupling	Good coordination	
0.90≤D≤1.00	Maximum coupling	Quality coordination	

Table 4

COUPLING COORDINATION LEVEL OF GREEN AND DEVELOPMENT OF DIGITAL ECONOMY AND TEXTILE INDUSTRY, 2014–2023						
Year	**Digital economy development index U1**	**Textile industry green quality development index U2**	**Coupling C**	**Degree of coupling coordination D**	**Harmonization level**	**Classification**
2014	0.123	0.078	0.067	0.076	Extreme coordination	Type of dysregulation decline (Unacceptable interval)
2015	0.119	0.122	0.111	0.145	Severe dissonance	
2016	0.368	0.248	0.321	0.205	Moderate dissonance	
2017	0.389	0.299	0.444	0.467	Endangered coordination	Intermediate transition type (Antagonistic interval)
2018	0.412	0.367	0.489	0.567	Barely coordinated	
2019	0.544	0.443	0.522	0.666	Primary coordination	Coordination elevation type (Acceptable interval)
2020	0.667	0.566	0.603	0.723	Intermediate coordination	
2021	0.778	0.670	0.777	0.799	Intermediate coordination	
2022	0.880	0.783	0.815	0.812	Good coordination	
2023	0.965	0.888	0.899	0.900	Quality coordination	

coupling degree between Shandong's digital economy and green development of the textile industry increased from 0.076 to 0.900, whilst the coupling coordination degree rose from 0.067 to 0.899, with both demonstrating upward trends. The coordination level evolved from extreme disorder to high-quality coordination, and the coupling development type transformed from a disordered decline type to a coordinated improvement type. During this period, Shandong's digital economy and development of the textile industry demonstrated rapid evolution towards a coordinated relationship with high growth potential, establishing a solid foundation for the high-quality development of Shandong's textile industry.

PATHWAYS FOR GREEN DEVELOPMENT OF SHANDONG TEXTILE INDUSTRY

Looking towards the future, a new positioning for the textile industry has emerged: a pillar industry for national economic development, a fundamental industry for addressing livelihood issues and beautifying life, and an advantageous industry for international cooperation. To enable Xuzhou's textile industry to seize new opportunities, pursue digital transformation, and achieve high-quality development, this study proposed the following development pathways.

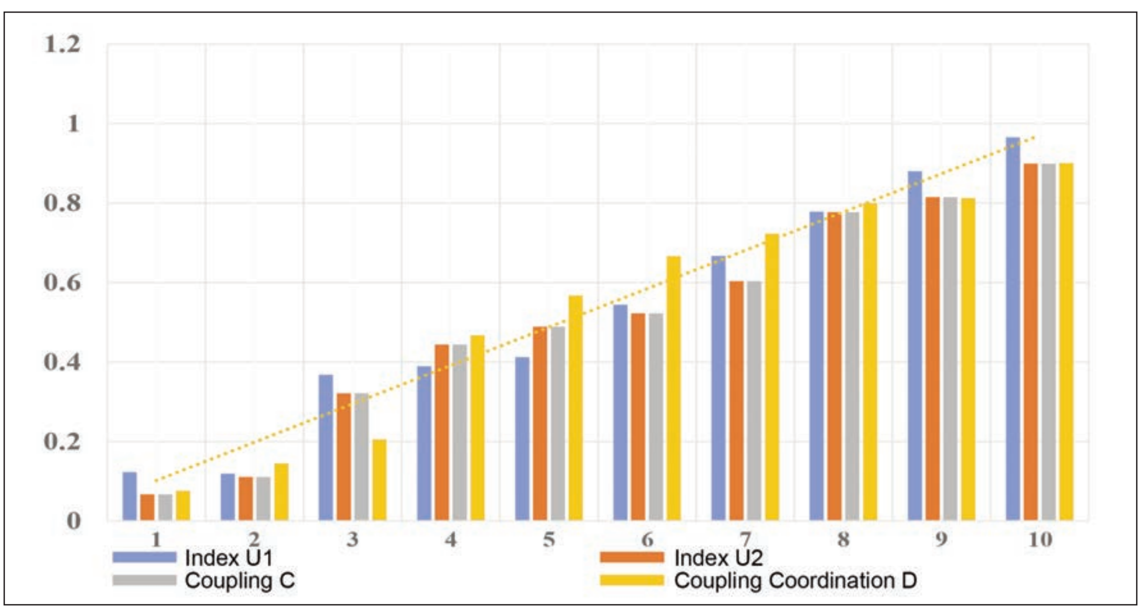

Fig. 4. The coupling degree coordination

Maintaining digital economy leadership and exploring new models for high-quality development

Through coupling coordination model analysis, it was evident that the coupling coordination level between the digital economy and textile industry had gradually improved from 2014 to 2023, reaching high-quality coordination. This demonstrated the important role of the digital economy in the development process of textile enterprises, suggesting that the leading position of the digital economy should be consistently maintained. Although the coordination degree between the digital economy and textile industry development had been high in recent years, with the digital economy demonstrating favourable development trends, compared to developed countries, there remained shortcomings in new materials, software, high-end equipment, and chips, which represented the key to promoting high-quality development of Xuzhou's textile industry. Xuzhou textile enterprises needed to centre on the digital economy and increase research and development and investment efforts in textile technology. The Utilization of digital technology in textile firms needed to be deepened, with emphasis on cultivating research and development personnel, conducting training on key core internet technology research, accelerating the digital development of manufacturing equipment in key fields, integrating with traditional production methods, and enabling digital technology to be deeply embedded in the textile industry. With promoting integrated development as the primary prerequisite, traditional conceptual constraints needed to be broken, and new models for high-quality development of the textile industry that aligned with digital development needed to be created, facilitating enterprises to form new economic growth points.

Accelerating digital transformation and creating a "strong engine" for high-quality development

Digital transformation had been the core driving force for the development of the textile industry. Therefore, textile enterprises should fully utilise digital economy advantages, gradually integrate digital economy into various departments of the textile industry, actively guide enterprise digital transformation, enable adaptation to new enterprise economic development models, consolidate the foundation for high-quality development, and provide substantial domestic demand support for China's digital technology development. High-technology, high-value-added products needed to be created to construct new patterns of enterprise development. Digital transformation needed to be emphasised, converting enterprises' comparative advantages into competitive advantages for market participation whilst improving comprehensive competitiveness. Addressing the current situation of outdated equipment and narrow research dimensions in textile enterprise application scenarios, the government should integrate resources and construct new textile industry research and development bases centred on digital technology, promote industrial clustering, and form production and trade centres. Support should be provided for enterprises to introduce advanced equipment, register trademarks, and improve brand concentration to create well-known brands, attract foreign investment, and gradually form a "strong engine" that drives development of the textile industry.

Implementing innovation-driven engineering and promoting scientific and technological achievement transformation

On one hand, textile enterprises needed to enhance independent innovation capabilities, strengthen the leading position of textile enterprises in technology demand and project selection, establish collaborative innovation chains with high-end research talent from universities, formulate talent development plans for textile enterprises and high-level research team cultivation plans, and create a research team with modern management levels. On the other hand, the government should incorporate digital technology innovation as one of the standards for performance evaluation, formulate incentive policies, stimulate the enthusiasm of digital talent for scientific and technological research and development, fully utilise regulation, support, and guidance functions for the textile market, strengthen cooperation with authoritative research institutions such as intermediary agencies and research institutions, and promote scientific and technological achievement transformation of textile enterprises and institutions through complementary advantages.

With respect to the new era of high-quality development, the digital economy has attracted significant attention and entered rapid development. Future textile industry supply chains would be more driven by the digital economy, with closer and more transparent cooperation. Shandong needed to firmly grasp this historical opportunity, maintain unwavering commitment to new development concepts, focus on textile industry transformation, concentrate on innovation-driven development, advance high-quality development, and create hundred-billion-level industrial clusters and world-class high-end textile new material bases.

RESEARCH LIMITATIONS AND FUTURE PROSPECTS

Research limitations

This article achieved certain outcomes in advancing research on the coupling coordination relationship between the digital economy and green development in the textile industry. However, several limitations remained:

This research focused solely on Shandong Province as the study subject. Although Shandong Province possessed certain representativeness in textile industry development, the universality and generalisability of the research conclusions required further verification. Significant differences existed in economic development levels, industrial structures, and policy environments across different regions, which could potentially influence the manifestation of coupling coordination relationships between the digital economy and textile industry.

Despite employing the entropy method for objective weighting, certain subjectivity remained in the indicator selection and system construction process. Particularly regarding indicator selection in the "green development" dimension, the complexity of environmental impacts in the textile industry may not have been comprehensively reflected, with key environmental indicators such as carbon emissions, water resource consumption, and waste treatment requiring further refinement.

Due to statistical data availability limitations, some key indicators potentially exhibited gaps or insufficient precision. Particularly against the backdrop of rapid digital economy development, traditional statistical systems may not have fully captured the genuine progress of digital transformation, with quantification of new business models such as the platform economy and sharing economy remaining challenging.

This research primarily focused on static calculation and trend analysis of coupling coordination degrees, with inadequate exploration of deep-level issues such as dynamic mechanisms, transmission pathways, and influencing factors of the mutual interaction between the digital economy and green development in the textile industry.

The study failed to adequately consider the influence of policy factors on coupling coordination development, with analysis of synergistic effects of digital economy policies, environmental policies, and industrial policies requiring strengthening.

Future prospects

Based on the aforementioned limitations, future research could be further deepened and expanded in the following directions:

(1) Expanding research scope to enhance conclusion universality

Future research could extend the scope to the national level or conduct cross-regional comparative studies. Through comparative analysis of differences in coupling coordination development between the digital economy and the textile industry across different regions, exploration of regional characteristics of influencing factors would provide theoretical support for formulating differentiated policies.

(2) Improving indicator systems to enhance measurement precision

Regarding indicator system construction, green development indicators should be further refined, incorporating more precise environmental indicators such as carbon footprint, water footprint, and recycling rates. Simultaneously, as the connotation of the digital economy continues to enrich, dynamic adjustment and optimisation of digital economy evaluation indicator systems would be necessary to better reflect actual digitalisation transformation levels.

(3) Deepening mechanism research to explore action pathways

Future research should focus more attention on the internal mechanisms of coupling and coordination between digital economy and green development in the textile industry, employing structural equation modelling, panel vector autoregressive models, and other methods to thoroughly analyse causal relationships, transmission pathways, and influence mechanisms between the two.

(4) Integrating policy analysis to assess policy effects

Policy factors should be incorporated into research frameworks, utilising quasi-natural experiments, difference-in-differences methods, and other approaches to evaluate the impact effects of relevant policies on coupling coordination development, providing empirical evidence for policy formulation and optimisation.

(5) Conducting international comparative research

Through comparative analysis with developed countries' experiences in textile industry digitalisation transformation and green development, advantages and deficiencies in China's digital economy and textile industry integration development could be identified, providing international experience for China's textile industry high-quality development.

(6) Establishing early warning mechanisms for dynamic monitoring

Based on coupling coordination degree models, early warning mechanisms should be constructed to establish dynamic monitoring systems for digital economy and textile industry green development, providing timely decision-making references and risk warnings for government departments and enterprises.

(7) Expanding research methods to enhance research depth

Future research could attempt to utilise emerging technological methods such as machine learning and big data analysis, combined with traditional econometric methods, to enhance research scientific rigour and precision. Simultaneously, qualitative research methods such as field investigations and case analyses could deepen understanding of coupling coordination development mechanisms.

In conclusion, research on the coupling coordination relationship between digital economy and green development in the textile industry possesses significant theoretical value and practical significance. Future research should overcome existing limitations, continuously improve research methods, expand research perspectives, and provide more robust theoretical support and practical guidance for promoting China's textile industry green high-quality development in the digital era.

REFERENCES

[1] Zhao, G., Zhai, X., Wu, Y., Ma, S., *Spatial and Temporal Evolution Patterns and Influencing Factors of Logistics Expansion in the Beijing-Tianjin-Hebei-Shanxi Region*, In: Promet Traffic & Transportation, 2025, 37, 6, 1525–1544

[2] Liu, H., Cong, R., Liu, L., Li, P., Ma, S., *The impact of digital transformation on innovation efficiency in construction enterprises under the dual carbon background*, In: Journal of Asian Architecture and Building Engineering, 2025, 1–18

[3] Li, Y., Yang, X., Ma, S., *The Efficiency Measurement and Spatial Spillover Effect of Green Technology Innovation in Chinese Industrial Enterprises*, In: Sustainability, 2025, 17, 7, 3162

[4] Shen, D., Zhao, X., Lyu, S., Liu, H., Zeng, H., Ma, S., *Qualification and construction enterprise innovation–quasi-natural experiments based on specialised, high-end and innovation-driven "small giant" enterprises*, In: Journal of Asian Architecture and Building Engineering, 2025, 1–19

[5] Li, Y., Cong, R., Zhang, K., Ma, S., Fu, C., *Four-way game analysis of transformation and upgrading of manufacturing enterprises relying on industrial internet platform under developers' participation*, In: Journal of Asian Architecture and Building Engineering, 2024, 1–22

[6] Wu, Y., Hou, L., Yuan, Y., Ma, S., Zeng, H., *Green credit policy's influence on construction firm ESG performance: a difference in differences estimation*, In: Journal of Asian Architecture and Building Engineering, 2025, 1–13

[7] Pan, W., Xie, T., Wang, Z., Ma, L., *Digital economy: An innovation driver for total factor productivity*, In: Journal of Business Research, 2022, 139, 303–311

[8] Shan, S., Li, Y., Su, J., Yang, Y., Wang, Y., Wang, Z., *Why Does the US Dominate the Digital Economy? A Strategic Analysis Based on the Policy–Coordination–Talent Framework and the Policy Implications for China*, In: Systems, 2025, 13, 5, 392

[9] Dilyard, J., Zhao, S., You, J.J., *Digital innovation and Industry 4.0 for global value chain resilience: Lessons learned and ways forward*, In: Thunderbird International Business Review, 2021, 63, 5, 577–584

[10] Ma, S., Zeng, H., Liu, H., Yan, H., *Impact of virtual community online reviews on the reputation of cross-border e-commerce platforms,* In: South African Journal of Business Management, 2025, 56, 1, a4984

[11] Si, H., Tian, Z., Guo, C., Zhang, J., *The driving effect of digital economy on green transformation of manufacturing*, In: Energy & Environment, 2024, 35, 5, 2636–2656

[12] Heping, G., Fuxiang, W., *Digital Economy Enables High-Quality Economic Development: Theoretical Mechanisms and Empirical Evidence*, In: Frontiers of Economics in China, 2022, 17, 4, 643

[13] Fromhold-Eisebith, M., Marschall, P., Peters, R., Thomes, P., *Torn between digitized future and context dependent past–how implementing 'Industry 4.0'production technologies could transform the German textile industry*, In: Technological Forecasting and Social Change, 2021, 166, 120620

[14] Tseng, M.L., Bui, T.D., Lim, M.K., Fujii, M., Mishra, U., *Assessing data-driven sustainable supply chain management indicators for the textile industry under industrial disruption and ambidexterity*, In: International Journal of Production Economics, 2022, 245, 108401

[15] Hua, Y., Tong, T., *Renewable energy integration in the Belt and Road Initiative: Government expenditure, green finance, and economic growth*, In: Renewable Energy, 2025, 123980

[16] Hu, J., Wang, D., Zeng, H., Ma, S., *From disclosure to decision: how climate risk shapes firms' human capital strategies in China*, In: Theoretical and Applied Climatology, 2025, 156, 556

[17] Xia, J., Ma, S., Wei, W., *Perceptions of economic policy uncertainty and digital transformation: Evidence from China*, In: South African Journal of Business Management, 2025, 56, 1, a4993

[18] Zhang, L., Ma, S., Hao, N., Li, W., Tang, W., *Ordering and financing strategies in electronic business platform financing with a loss averse retailer*, In: International Journal of Industrial Engineering Computations, 2025

[19] Ding, Y., Li, B., Ma, S., Yu, C., Zhao, X., *Digital transformation and wage distortion in R&D and innovation activities-Causal inference based on double machine learning*, In: International Review of Financial Analysis, 2025, 104541

[20] Ma, S., Benkraiem, R., Abedin, M.Z., Zeng, H., *Climate Anomalies and Corporate Environmental Governance: Empirical Evidence from ENSO Events*, In: Finance Research Letters, 2025, 107970

[21] Wu, Y., Wang, X., Xie, H., Ma, S., *How digital trade can reshape the trajectory of green and low-carbon development under the leadership of dual-control objectives*, In: Global NEST Journal, 2025

[22] Tian, Y., Hua, M., Li, W., Nike, J., *Energy poverty, digital economy, and financial deepening: A study of regional differences based on transportation geography*, In: International Journal of Hydrogen Energy, 2025, 131, 287–297

[23] Cheng, X., Fan, Z., Chen, M., Ma, S., *FDI Driving China's Green Economic Transformation: The "Bridge" Role of the Digital Economy*, In: Global NEST Journal, 2025

[24] Sun, D., Li, Y., *Carbon peaking pressure and corporate R&D investment*, In: Economics Letters, 2025, 251, 112328

[25] Ding, Y., Guo, J., Ji, Y., Guo, K., Ma, S., *The digital economy and city innovation convergence – an empirical research based on the innovation value chain theory*, In: Technological and Economic Development of Economy, 2025, 1–36

[26] Zhang, X., Li, G., Wu, R., Zeng, H., Ma, S., *Impact of Carbon Emissions, Green Energy, Artificial Intelligence and High-Tech Policy Uncertainty on China's Financial Market*, In: Finance Research Letters, 2025, 107599

[27] Wen, L., Xu, J., Zeng, H., Ma, S., *The impact of digital services trade in belt and road countries on China's construction green goods export efficiency: a time – varying stochastic frontier gravity model analysis*, In: Journal of Asian Architecture and Building Engineering, 2025, 1–24

[28] Sun, D., Luo, Q., *Green transition under carbon peak pressure: beyond greenwashing*, In: Applied Economics, 2026, 1–17
[29] Chen, L., Ying, J., He, S., Chen, X., *Multi-causal event extraction with domain-aware modular architecture for economic and strategic decision support*, In: Engineering Applications of Artificial Intelligence, 2026, 181, 115395
[30] Zou, F., Ma, S., Liu, H., Gao, T., Li, W., *Do Technological Innovation and Environmental Regulation Reduce Carbon Dioxide Emissions? Evidence from China*, In: Global NEST Journal, 2024, 26, 7
[31] Ma, S., Zeng, H., Abedin, M.Z., *The impact of the reforms in the Chinese equities exchange and quotations on innovation in cross-border e-commerce enterprises*, In: Asia Pacific Business Review, 2025, 1–41
[32] Feng, Y., Li, X., Hai, S., Ma, S., *Digital transformation and employees' unethical pro-self behaviours: Roles of uncertainty and job security*, In: South African Journal of Business Management, 2025, 56, 1, a5250
[33] Ma, S., Appolloni, A., *Can financial flexibility enhance corporate green innovation performance? Evidence from an ESG approach in China*, In: Journal of Environmental Management, 2025, 387, 125869
[34] Ding, Y., Guo, J., Ji, Y., Guo, K., Ma, S., *The digital economy and city innovation convergence – an empirical research based on the innovation value chain theory*, In: Technological and Economic Development of Economy, 2025, 1–36
[35] Ma, Q., Tariq, M., Mahmood, H., Khan, Z., *The nexus between digital economy and carbon dioxide emissions in China: The moderating role of investments in research and development*, In: Technology in Society, 2022, 68, 101910
[36] Wu, Q., Jin, Y., Ma, S., *Impact of dual pilot policies for low-carbon and innovative cities on the high-quality development of urban economies*, In: Global NEST Journal, 2024, 26, 9, 1–14
[37] Liang, Y., Dong, R., Wan, R., Ma, S., Huang, Y., Pan, D., *Perception of Economic Policy Uncertainty and Energy Consumption Intensity: Evidence from Construction Companies*, In: Energies, 2025, 18, 12, 3183
[38] Xia, W., Ruan, Z., Ma, S., Zhao, J., Yan, J., *Can the digital economy enhance carbon emission efficiency? Evidence from 269 cities in China*, In: International Review of Economics & Finance, 2024, 103815
[39] Ruan, Y., Wang, W., Abubakar, M., Ahmad, N., *Global economic resilience: Developing green growth strategies, renewable energy integration, and environmental economics for sustainability*, In: Renewable Energy, 2025, 251, 123341
[40] Zeng, H., Abedin, M.Z., Lucey, B., Ma, S., *Tail risk contagion and multiscale spillovers in the green finance index and large US technology stocks*, In: International Review of Financial Analysis, 2024, 103865
[41] Zhang, K., Li, Y., Ma, S., Fu, C., *Research on the Impact of Green Technology Innovation in the Manufacturing Industry on the High-Quality Development of the Manufacturing Industry Under "Dual Circulation"*, In: Polish Journal of Environmental Studies, 2025, 34, 4, 3919–3932
[42] Wen, L., Ma, S., Zhao, G., Liu, H., *The Impact of Environmental Regulation on the Regional Cross-Border E-Commerce Green Innovation: Based on System GMM and Threshold Effects Modeling*, In: Polish Journal of Environmental Studies, 2025, 34, 2
[43] Ma, S., Liu, H., Wang, C., Zeng, H., *Knowledge Structure and Hotspot Evolution of "Greenwashing": Based on Citespace and Text Analysis Perspectives*, In: Asia Pacific Economic and Management Review, 2025, 1, 2
[44] Ma, S., Wen, L., Yuan, Y., *Study on the coupled and coordinated development of tourism, urbanization and ecological environment in Shanxi Province*, In: Global NEST Journal, 2024, 26, 4
[45] Ma, S., Liu, H., Li, S., Lyu, S., Zeng, H., *Quantifying the Relative Contributions of Climate Change and Human Activities to Vegetation Recovery in Shandong Province of China*, In: Global NEST Journal, 2025, 27, 5
[46] Sun, D., Li, J., *Carbon peaking pressure and corporate earnings management*, In: International Review of Economics & Finance, 2025, 104503

Authors:

SHICHAO GAO[1], QIANKAI JIANG[2,3]

[1]College of Economics and Management, Central South University of Forestry and Technology, Changsha, China

[2]College of Business Administration, Capital University of Economics and Business, Beijing, China

[3]Pacific Property Insurance Co., Ltd, China

Corresponding author:

QIANKAI JIANG
e-mail: 17715667381@163.com

Biocomposite filaments reinforced with natural-origin fibres for specialised biomedical applications

DOI: 10.35530/IT.077.04.2025140

MARIA FELICIA DONDEA
EMILIA VISILEANU
FLORIN MICULESCU
AURA-CĂTĂLINA MOCANU
CIPRIAN PREDA
DANIELA MANOLE

ABSTRACT – REZUMAT

Biocomposite filaments reinforced with natural-origin fibres for specialised biomedical applications

In this study, biocomposite filaments based on alginic acid (sodium salt) reinforced with cotton fibres (length of 2 ± 0.5 mm) were developed. The polymeric matrix was prepared using alginic acid at a concentration of 1%, while cotton fibres were incorporated at concentrations of 0.5%, 1%, and 1.5%. The synthesis of biocomposite filaments was carried out using the wet spinning technique employing a mechanically actuated syringe, followed by crosslinking using a 1% calcium chloride solution.

The obtained filaments were initially characterised from morphological and chemical perspectives using scanning electron microscopy (SEM), energy-dispersive spectroscopy (EDS) and Fourier Transform Infrared Spectroscopy (FT-IR). The SEM results demonstrated that the obtained alginate filament has a dense, homogeneous structure with certain folds resulting from the wet-spinning process. Additionally, the reinforcement with cotton fibres forms a 3D network within the matrix and significantly modifies the porosity of the alginate filaments. Regarding the chemical composition of the filaments, the EDS analysis revealed that the predominant elements are carbon and oxygen, thus indicating the organic nature of both the alginate matrix and the reinforcing agent. FTIR analysis enabled the identification of the main functional groups corresponding to characteristic absorption bands from the fingerprint region of each precursor material, for all composite materials. Afterwards, the absorption capacity of all filaments, with/without cotton fibres, was tested in physiological serum. The results revealed statistically significant differences as a function of the cotton fibres incorporation ratio, highlighting the impact of composition on the hydrophilic behaviour of the filaments.

The development of composite filaments based on alginic acid is a crucial aspect in obtaining innovative hybrid materials characterised by low cost, biocompatibility, and biodegradability. These structures can be effectively implemented in various biomedical applications, including controlled and targeted drug delivery, soft tissue engineering, and the development of advanced dressings for wound treatment.

Keywords: *alginic acid, hybrid biomaterials, natural fibres reinforced, wound dressings.*

Filamente biocompozite ranforsate cu fibre de origine naturală pentru aplicații biomedicale avansate

În acest studiu au fost dezvoltate filamente biocompozite pe bază de alginat de sodiu, ranforsate cu fibre de bumbac cu lungimea de 2 ± 0,5 mm. Matricea polimerică a fost obținută dintr-o soluție de alginat de sodiu cu concentrația de 1%, iar fibrele de bumbac au fost adăugate în proporții de 0,5%, 1% și 1,5%. Filamentele au fost fabricate prin tehnica de filare umedă (wet spinning), utilizând o seringă acționată mecanic, după care au fost reticulate într-o soluție de clorură de calciu 1%.

Filamentele obținute au fost caracterizate inițial din punct de vedere morfologic și chimic prin microscopie electronică de baleiaj (SEM), spectroscopie de dispersie a energiei razelor X (EDS) și spectroscopie în infraroșu cu transformată Fourier (FT-IR). Imaginile SEM au evidențiat faptul că filamentul de alginat prezintă o structură compactă și relativ uniformă, cu anumite neregularități de suprafață generate în timpul procesului de filare. Totodată, introducerea fibrelor de bumbac a determinat formarea unei rețele tridimensionale în interiorul matricei polimerice și a influențat semnificativ gradul de porozitate al filamentelor.

Analiza EDS a arătat că principalele elemente prezente în compoziția filamentelor sunt carbonul și oxigenul, confirmând caracterul organic atât al matricei de alginat, cât și al fibrelor de bumbac utilizate ca material de ranforsare. Prin analiza FT-IR au fost identificate grupările funcționale caracteristice materialelor componente, evidențiindu-se prezența benzilor de absorbție specifice atât alginatului, cât și fibrelor de bumbac în structura biocompozitelor obținute.

În continuare, a fost evaluată capacitatea de absorbție a filamentelor în ser fiziologic. Rezultatele au evidențiat diferențe semnificative statistic între probe, în funcție de conținutul de fibre de bumbac, demonstrând că proporția materialului de ranforsare influențează comportamentul hidrofil și capacitatea de absorbție a filamentelor.

Dezvoltarea filamentelor compozite pe bază de acid alginic reprezintă un pas important în obținerea unor materiale hibride inovatoare, caracterizate prin costuri reduse, biocompatibilitate și biodegradabilitate. Datorită acestor caracteristici, ele pot fi utilizate în numeroase aplicații biomedicale, precum sistemele de eliberare controlată a medicamentelor, ingineria țesuturilor moi și realizarea de pansamente moderne pentru tratarea și regenerarea rănilor.

Cuvinte-cheie*: acid alginic, biomateriale hibride, materiale ranforsate cu fibre naturale, pansamente pentru vindecarea rănilor*

INTRODUCTION

The world of biomaterials, especially polymers, continues to have a significant impact on the field of biomedicine. The diversity of polymers and the different ways in which they can be used in scaffolds have developed considerably in recent years, offering active solutions to everyday problems. In the last decades, combinations of different scaffolds in a single solution have been investigated, showing great potential in wound healing and drug delivery systems, in particular in the fight against antibiotic-resistant pathogens.

The development of composite filaments based on biodegradable and biocompatible polymers has led to remarkable advances in regenerative therapies. These innovative materials are of great interest to both science and engineering, offering unmatched versatility and effectiveness across a wide range of biomedical applications (e.g., tissue engineering scaffolds for bone and cartilage regeneration, biodegradable sutures, controlled drug delivery systems, wound healing dressings, and nerve regeneration conduits) [1]. By harmoniously integrating with biological tissues and creating a favourable environment for cell proliferation and tissue regeneration, hydrogel-based therapies have demonstrated exceptional potential in addressing clinical challenges, particularly in wound healing [2]. Consequently, there is a growing demand for the development of next-generation dressings, patches, and bandages capable of effectively treating a wide spectrum of skin conditions, especially wounds and burns [3].

The reinforcement of pure alginate filaments with various fillers is widely recognised as an effective strategy for enhancing mechanical properties and liquid absorption capacity. A representative study in this area is that of Ahmad et al., who systematically investigated the incorporation of several types of fillers into alginate-based systems, including natural-based polymers (e.g., chitin, chitosan, cellulose, carrageenan, gelatin, and starch), synthetic polymers, carbon-based materials such as graphene oxide and carbon nanotubes, as well as inorganic fillers such as silver nanoparticles [4].

Recent literature reports the use of alginate as a polymeric matrix for the incorporation of various bioresorbable materials, functional composites, and smart hydrogels intended for biomedical applications; however, these approaches are often limited by drawbacks such as insufficient mechanical performance, tribological wear, or processing difficulties, thereby highlighting the innovative nature of the strategy investigated in the present study [5].

This study aims to develop sodium alginate filaments reinforced with natural cotton fibres, which could be successfully integrated into various biomedical applications, such as soft tissue engineering [6] or wound healing. These filaments are produced using the wet spinning technique, which involves extruding the polymer solution through a syringe and crosslinking it in a calcium chloride solution [7]. The quality of the process depends on several parameters, including the needle gauge, the length, density, and fineness of the cotton fibre, the actuation system of the syringe (manual or automated), and the ambient temperature [8]. Alginate, like starch [9], is a natural polysaccharide extracted from marine algae and is known for its gelling properties in the presence of calcium ions, forming three-dimensional hydrophilic networks (figure 1). The integration of natural fibres, such as cotton, into the alginate matrix can lead to enhanced mechanical properties of the biocomposite filaments [10]. Cotton, composed of 90–95% cellulose, has a fibrillar structure that promotes efficient interactions with the polymer matrix. Studies have shown that the addition of cotton fibres to alginate fibre structures can increase the Young's modulus up to 56.45 MPa, compared to 4.74 MPa for pure alginate fibres, highlighting a significant improvement in stiffness and mechanical strength [11].

Here, the integration of cotton fibres into the structure of alginate filaments is intended to increase the stiffness and tensile strength of the biocomposite materials, to provide superior structural stability, and to improve the overall material handling during final applications. The selection of this filler is based on the hypothesis that the specific properties of cotton (e.g., good mechanical strength, flexibility, biocompatibility, and excellent absorbency) can lead to the

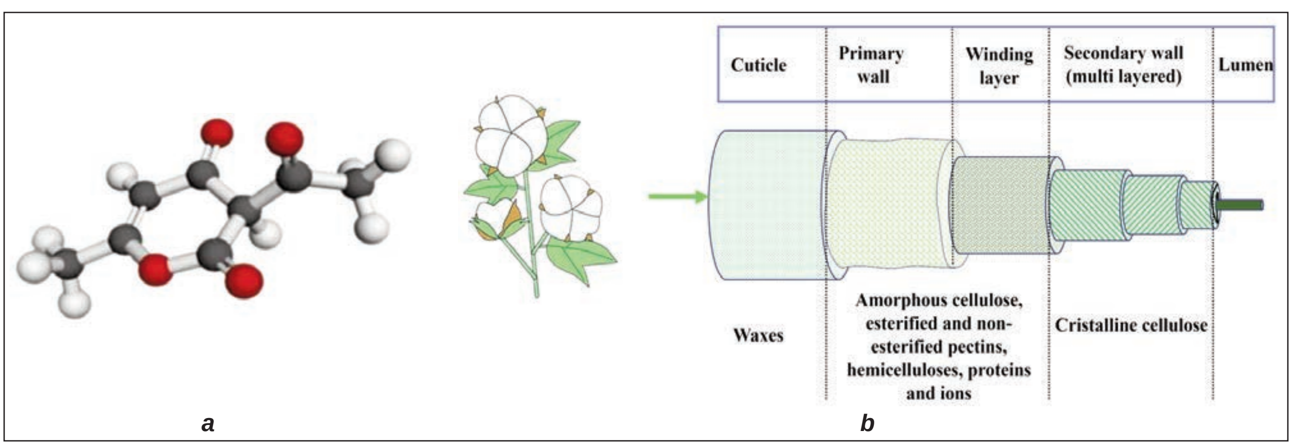

Fig. 1. Graphical representation of: *a* – alginate structure; *b* – structure of cotton fibre

development of biocompatible composite materials with superior performance compared to pure alginate [12].

MATERIALS AND METHODS

Synthesis of alginate-based biocomposite filaments reinforced with cotton fibres

In this experiment, two types of precursor materials were used: alginate powder (ALG) and cotton fibres (CTF), obtained by shredding cotton yarn. The cotton yarn spool was sourced from a textile company collaborating with the National Research & Development Institute for Textiles and Leather.

For the cotton fibres used in the biocomposite filaments, quality control measures were implemented to ensure batch-to-batch consistency. These included measuring fibre length and diameter to verify uniformity, inspecting for residual finishes or impurities that could affect filament formation, and monitoring moisture content to prevent degradation during storage. Such measures are essential for maintaining reproducible mechanical and structural properties of the resulting composite filaments.

Sodium alginate was supplied by Thermo Scientific, while the calcium chloride ($CaCl_2$) used for fibre crosslinking (density = 2.15 g/cm^3, M = 110.98 g/mol, granule size ≤ 7 mm, purity ≥ 93%) was purchased from Sigma-Aldrich.

Within the experiment, sodium alginate played the role of a precursor polymer, being water-soluble and allowing the formation of a viscous solution suitable for the wet-spinning process. Calcium chloride was used as a crosslinking agent in the coagulation bath, with Ca^{2+} ions interacting with the carboxyl groups of the alginate chains. Crosslinking occurs through an ion-exchange reaction, in which sodium ions are replaced by calcium ions, according to the "egg-box" mechanism, equation 1:

$$2NaC_6H_7O_6 + CaCl_2 \rightarrow Ca(C_6H_7O_6)_2 + 2NaCl \quad (1)$$

This reaction leads to the formation of a stable three-dimensional network, which instantaneously solidifies the extruded filament.

Table 1

SAMPLE CODIFICATION	
Sample code	**Sample description**
P0	CTF
P1	1%ALG
P2	1%ALG 0,5%CTF
P3	1%ALG 1%CTF
P4	1%ALG 1,5%CTF

To obtain both simple and composite filaments from sodium alginate, as well as filaments reinforced with cotton, the wet spinning technique was employed. A concentration of 1% ALG was used, while for the cotton-reinforced filaments, three different concentrations of cotton fibres were considered: 0.5% CTF, 1% CTF, and 1.5% CTF. Sodium alginate powder was dissolved in distilled water for 8 hours at a constant temperature of 30°C using a magnetic stirrer hotplate. The same procedure was followed for the preparation of biocomposite filaments reinforced with cotton fibres. The filaments were crosslinked in a 1% calcium chloride ($CaCl_2$) solution, in which they were immersed for 15 minutes. Afterwards, they were rinsed with distilled water and allowed to dehydrate at room temperature (figure 2).

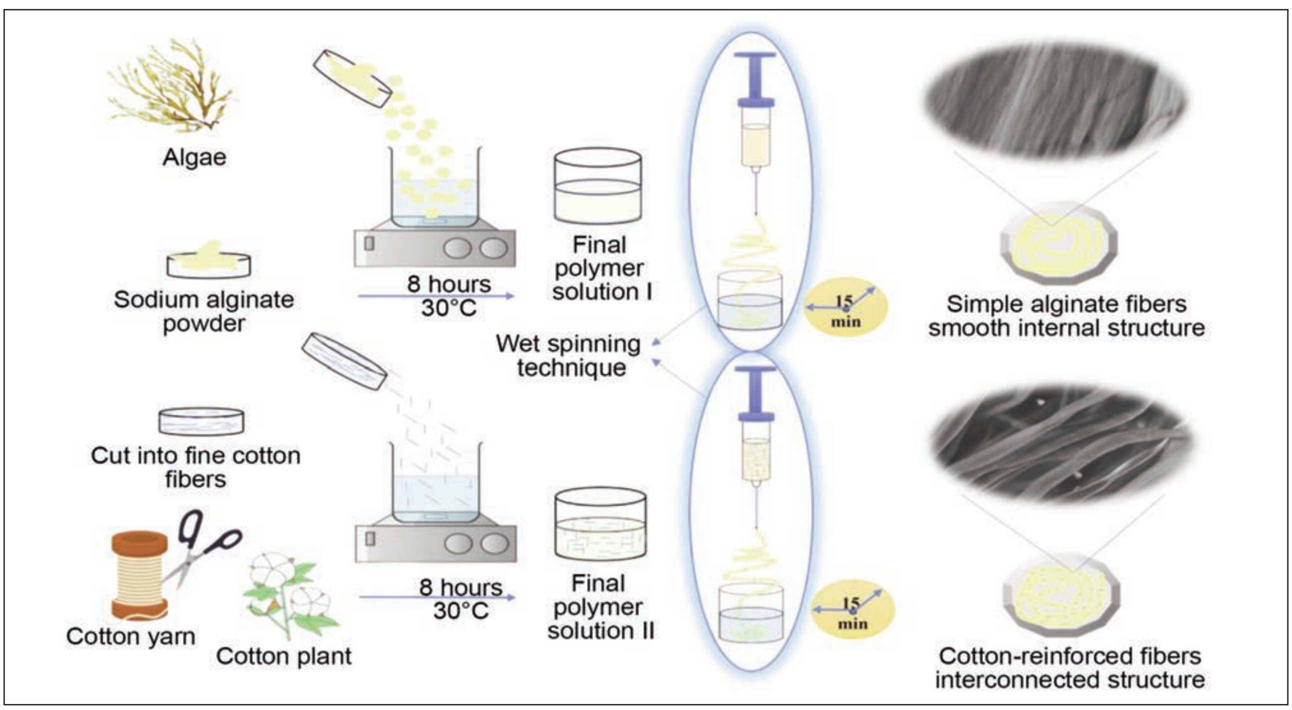

Fig. 2. Graphical representation of the process for obtaining simple alginate filaments and composite filaments reinforced with natural cotton fibres

The fibre spinning process was carried out by mechanically applying constant pressure to a syringe equipped with a 16G needle. For long-term preservation, it is recommended that the filaments be stored in distilled water, which should be replaced every 72 hours.

RESULTS AND DISCUSSIONS

Morphological characterisation by scanning electron microscopy (SEM)

The surface topography and morpho-compositional analysis of the alginate filaments and those reinforced with cotton fibres were performed by scanning electron microscopy (SEM) (Philips XL 30 ESEM TMP) coupled with energy-dispersive X-ray spectroscopy (EDS) (EDAX Sapphire spectrometer) [13].

SEM analysis for sample P1 showed that the sodium alginate biocomposite filaments revealed a smooth and uniform surface with no agglomerations or obvious pores. The fibre presents a linear and elongated structure, while the surface appears homogeneous and without significant roughness. This degree of smoothness is characteristic of pure alginate filaments. The absence of surface defects or fibril discontinuities suggests a stable spinning process with well-controlled parameters, leading to a continuous and structurally homogeneous filament [11]. Therefore, the observed morphology confirms the reliability and efficiency of the wet-spinning method employed.

With the addition of cotton fibres as a reinforcing agent, changes in fibre morphology and structure are observed. For sample P2, the surface is deeply textured, with folds and agglomerations. The cotton fibres are uniformly distributed inside and outside the long fibre, creating an interlocking system between the alginate matrix and the cotton fibres, which may contribute to increased resistance during final application. A non-uniformity in fibre distribution within the filament could lead to anisotropy of mechanical properties.

The surface of sample P3 is also rough, with visible fibres partially exposed, suggesting effective bonding and sufficient adhesion between the alginate matrix and the reinforcing agent.

The morphology of this fibre is in fact a combination of folds with a fibrous texture, which denotes that the internal structure is becoming more and more consolidated (figure 3).

Fibrillar continuity remains well preserved, however, and at this level of reinforcement, the P3 fibre shows no macroscopic discontinuities, i.e. no breaks or segregations of phases along the filament length are observed. The images suggest that most of the cotton fibres are firmly embedded in alginate, with the polymer matrix adhering around them, denoting a compatible interface (alginate is hydrophilic like cotton cellulose, facilitating hydrogen bond adhesion) [14].

In the case of sample P4, it is visible that the high content of cotton fibers that have penetrated the

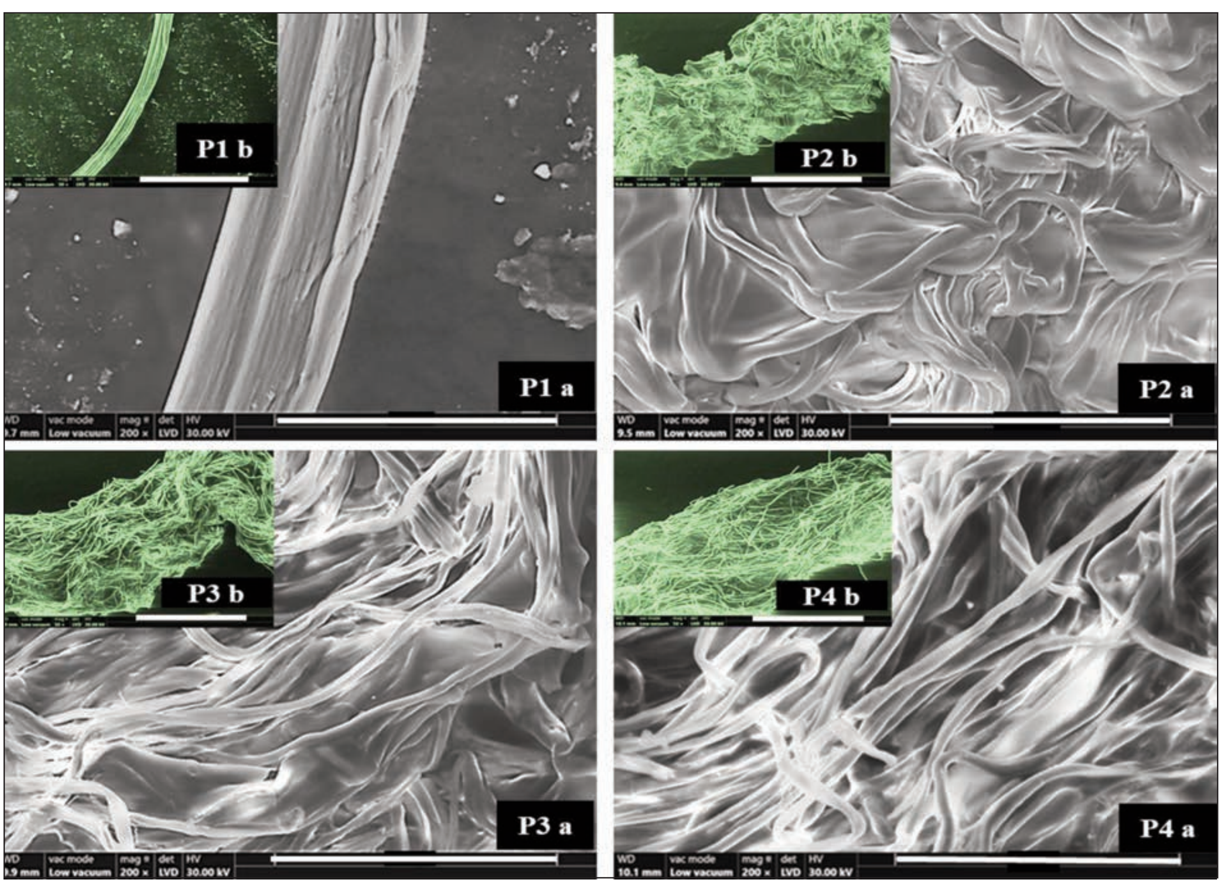

Fig. 3. Morphological evaluation of sodium alginate and composite fibres; scale bar: *a* – 300 μm; *b* – 1 mm

polymer matrix, forming a dense and pronounced network. The fibre surface is more uniform, unlike the other fibres, and has a less compact morphology. Despite the high amount of solid phase, the fibre retains its overall elongated shape, but with a higher porosity [15]. The CTF fibre dispersion in P4 is thus less uniform, although on a global scale cotton is still well dispersed; areas of higher cotton fibre density can be identified. These micro-agglomerations lead to the heterogeneous surface appearance and may indicate the existence of stress concentration points in the structure. In terms of fibrillar continuity, the P4 fibre remains overall continuous – no macroscopic fibre breaks or complete phase segregation are observed; the alginate forms a filament that binds the whole structure [16].

Determination of chemical composition by Energy Dispersive X-ray Spectroscopy (EDS)

The EDS spectrum shows that the predominant elements in P1 are carbon (C) and oxygen (O), derived from the organic matrix of alginate. This result is expected, since sodium alginate is a polymer rich in C and O (figure 4).

On the other hand, sodium (Na) appears in very small amounts, indicating that most of the initial Na^{+} from sodium alginate was removed or replaced by Ca^{2+} during fibre formation. The literature reports that pure sodium alginate has an atomic ratio of C:O:Na ≈ 6:6:1, according to its chemical formula. In the case of the obtained calcium alginate, Na decreases substantially, while Ca becomes the characteristic crosslinking element in the polymeric network [17–20]. Additionally, traces of chlorine (Cl) can be detected in P1, which may be residual, resulting from insufficient washing.

Carbon and oxygen are the dominant elements in the composition of all samples, being the primary constituents of polysaccharides (both alginate and the cellulose from cotton). In sample P1 (only 1% alginate hydrogel), EDS analysis indicates a predominance of C and O due to the organic backbone of alginate. With the addition of cellulose fibres (P2–P4), the carbon and oxygen signals remain high or even increase slightly in relative proportion.

Thus, as the fibre content increases from P1 to P4, carbon and oxygen remain the most abundant elements, highlighting the organic nature of all the composites. The qualitative trend shows either maintenance or a slight increase in their relative percentages, considering that the addition of cotton is a rich source of C and O.

Structural investigations by FT-IR analysis

The bonding architecture, structure and environment of functional groups present for both the precursors, namely sodium alginate and cotton fibres, as well as the alginate filaments reinforced with cotton fibres, were analysed by Fourier Transform Infra-Red (FTIR) spectroscopy in attenuated total reflectance (ATR)

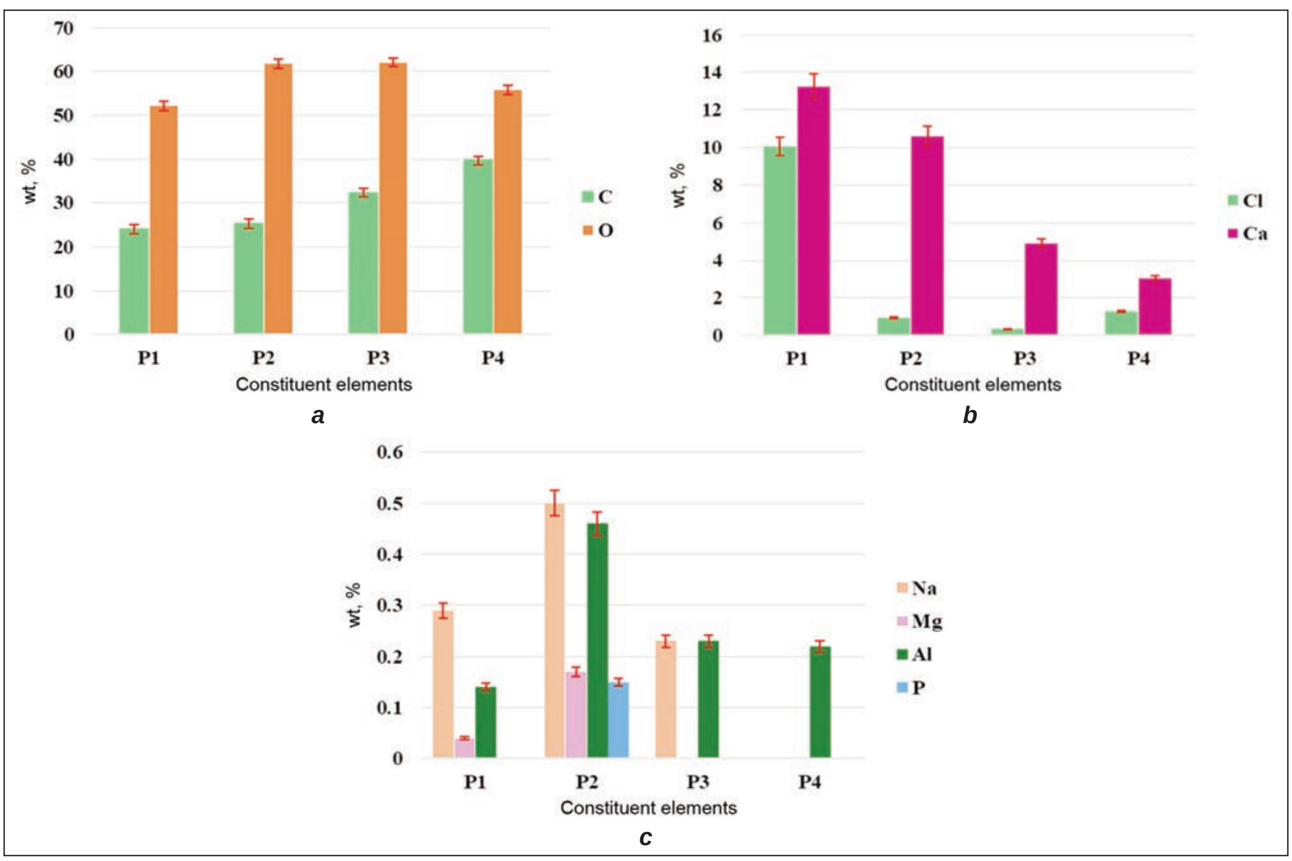

Fig. 4. The distribution of constituent elements for simple and composite ALG filaments:
a – distribution of the main elements C and O; *b* – distribution of the elements Ca and Cl;
c – distribution of the trace elements Na, Mg, Al and P

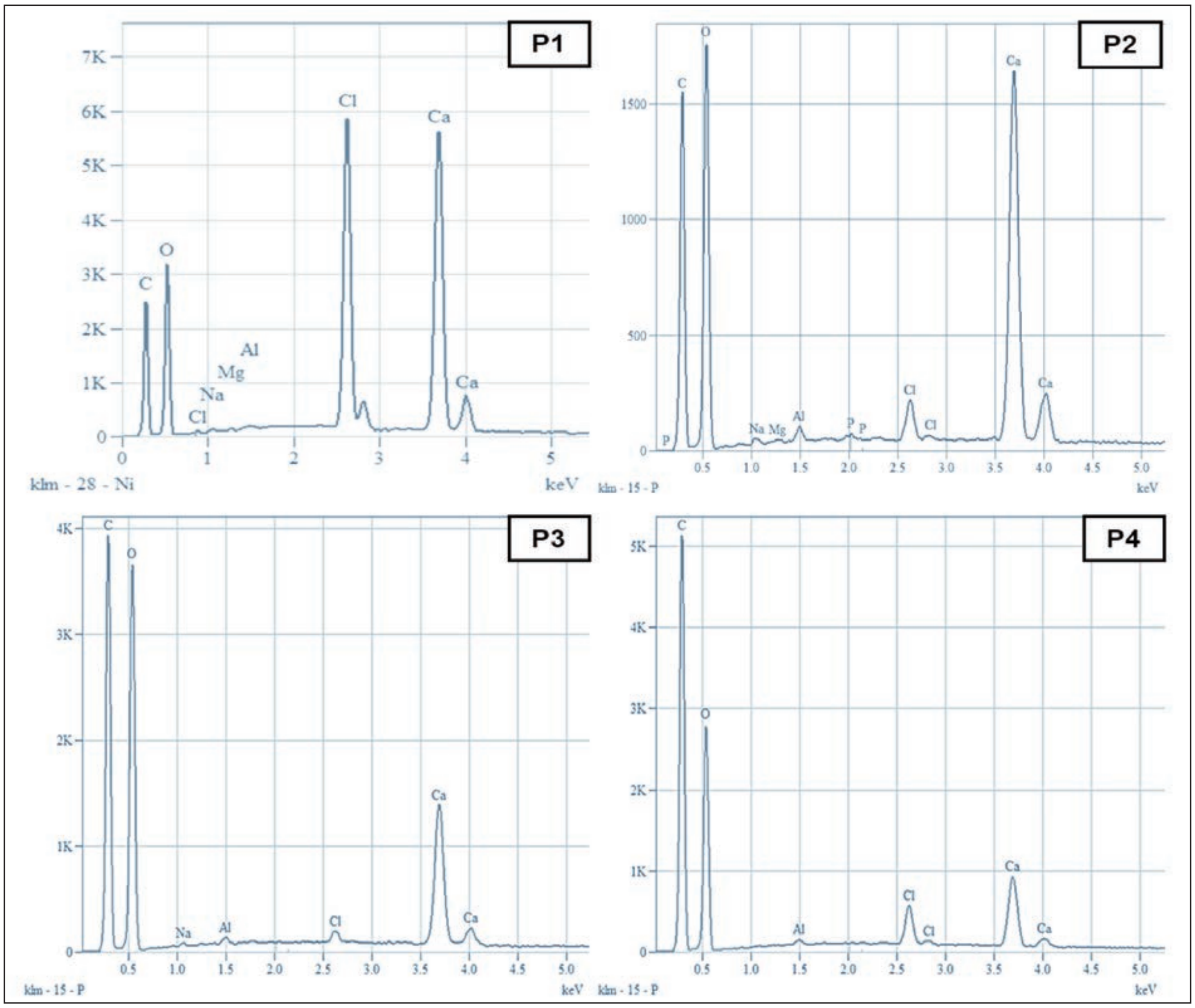

Fig. 5. The chemical composition of biocomposite filaments reinforced with natural cotton fibres

mode. The spectra were collected in the 4000 – 400 cm^{-1} wavenumber range. The IR fingerprints of all samples are presented in figure 6.

In the case of cotton fibres, a characteristic broad peak can be observed in the wavelength range of 3250–3500 cm^{-1}, corresponding to the –OH functional groups. Additionally, the absorption bands at 2900 cm^{-1} and 1630 cm^{-1} are associated with C–H stretching and –CO stretching vibrations, respectively. The peaks located at 1020 cm^{-1} and 1417 cm^{-1} were attributed to C–O stretching and C=C stretching vibrations, respectively. All these features confirm the highly cellulosic structure of cotton fibres.

For the pure alginate filament, a characteristic peak at approximately 1600 cm^{-1} was identified, which is attributed to the asymmetric stretching vibration of the COO^{-} group originating from the carboxylic acid salt. Another prominent peak appears around 3200 cm^{-1} and is assigned to the –OH group, arising from intermolecular hydrogen bonding. Two additional relevant peaks were observed at around 1030 cm^{-1} and 1100 cm^{-1}, corresponding to –CH stretching and –OH bending vibrations, respectively [11].

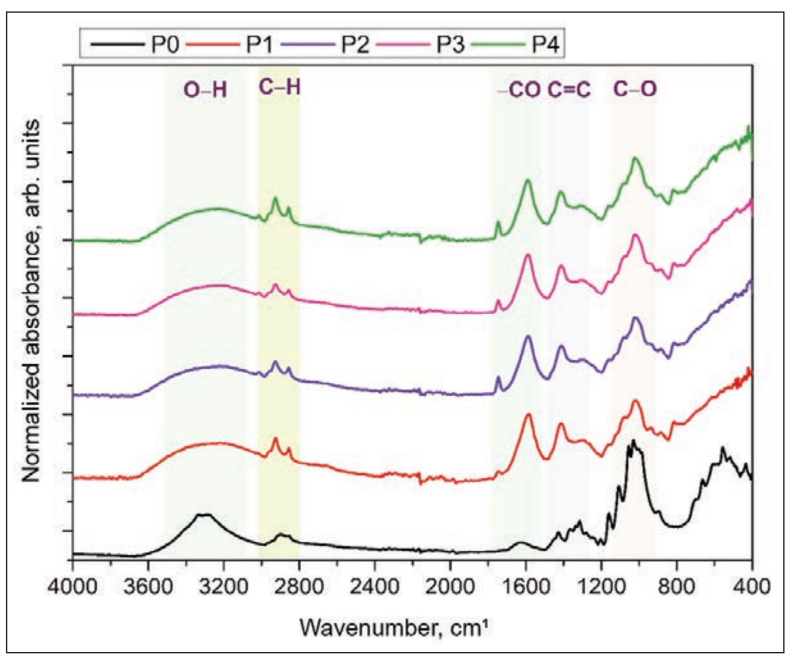

Fig. 6. Comparative FT-IR spectra of biocomposite filaments reinforced with natural cotton fibres

In the case of alginate filaments reinforced with cotton fibres, the FT-IR spectra confirmed a decrease in the intensity of the characteristic peaks near 3300 cm^{-1} and 2900 cm^{-1}, which can be attributed to the presence of cotton fibres within the alginate matrix. The formation of hydrogen bonds between the sodium alginate hydrogel and the cotton fibres, facilitated by hydroxyl and carbonyl functional groups, leads to a reduction in peak intensity as well as a shift in the corresponding spectral bands, as reported in other studies [12].

Absorption in liquids

Absorption was carried out in physiological serum (0.9% NaCl). The absorbance of physiological serum at the filament interface was investigated using the ASTM D570 standard. The sample was first dried in an oven for 4 h at 70°C, then weighed (M_i) on an analytical balance with a minimum division of 0.1 mg. Preconditioned samples were then placed in physiological saline for 24 hours at room temperature and pressure. After 24 hours, the samples were removed, blotted with filter paper to remove excess serum and then reweighed (M_f). After determination of the dry and wet mass of the fibres, the water absorption capacity was calculated using equation 2 [21]. The statistical analysis for the absorption capacity was performed using the one-way ANOVA test (post hoc Tukey's multiple comparisons test); the p values below 0.05 are considered to be statistically significant:

$$\text{Absorption of physiologic serum } \left(\frac{g}{g}\right) = \frac{M_f - M_i}{M_i} \times 100 \qquad (2)$$

High absorption capacity is the main characteristic of alginate filaments. One of the key aspects of scaffolds is their water content and their ability to retain water. Wound exudates must be absorbed in order to promote the healing process by controlling cellular dehydration and stimulating both angiogenesis and collagen synthesis. Proper moisture control accelerates the healing rate, reduces pain, and provides protection against wound infections. Wound exudates can separate tissue layers, leading to delayed healing. Therefore, absorption is a crucial property of alginate filaments used as scaffolds for various biomedical applications. Table 2 presents the values obtained from weighing the samples using the analytical balance, both before absorption (M_i) and after absorption (M_f).

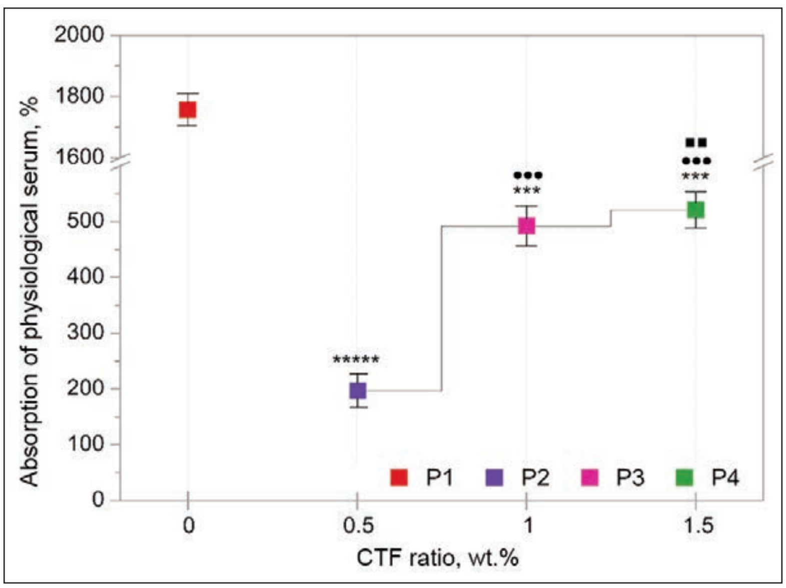

Fig. 7. Absorption of physiological serum of simple and biocomposite filaments after 24 hours of immersion. The ALG material was used as reference (P1) sample; data analysis was based on mean ± SD (n = 5; ***** p < 0.0001, *** p < 0.001 vs. P1; ●●● p < 0.001 vs. 1% ALG 0.5%CTF; ■■ p < 0.05 vs. 1%ALG 1%CTF)

Serum absorption decreases with increasing cotton concentration: the 1.5% CTF samples retrieved the lowest serum absorption, while the 1% CTF one the highest. On the other hand, the serum uptake of cotton-reinforced alginate filaments is statistically lower than that of pure alginate filaments. Overall, the decrease in absorbency was owed to the use of CTF reinforcement, a material known for its hydrophilic character and ability to absorb fluids [11].

CONCLUSIONS

The feasibility of developing alginate/cotton biocomposite materials and filaments through the proposed preparation mechanism was confirmed.

All composite filaments maintained a proper morphology, exposing good fibrillar continuity and demonstrating the viability of the wet-spinning process even in the presence of the disperse phase.

The alginate-cotton interface exhibited satisfactory adhesion, supported by the

Table 2

ABSORPTION OF PHYSIOLOGIC SERUM AFTER 24 H OF IMMERSION

Sample code	Sample description	M_i (g)	M_f (g)	Absorption of physiologic serum (%)
P1	1% ALG	0.005	0.094	1780
P2	1% ALG 0,5%CTF	0.0078	0.0231	196
P3	1%ALG 1%CTF	0.0081	0.0485	499
P4	1%ALG 1,5%CTF	0.0123	0.075	510

common hydrophilic nature of the two components, favourable for hydrogen bond formation. The EDS analysis revealed the consistent presence of calcium, carbon and oxygen in the matrix.

Further, the FT-IR analysis confirmed the successful incorporation of cotton fibres into the alginate matrix, as evidenced by the presence and modification of characteristic spectral bands. The observed changes in peak intensity and slight band shifts indicated the formation of intermolecular hydrogen bonds between alginate and cotton fibres, demonstrating good interfacial compatibility and structural stability of the composite filament.

Overall, the alginate filaments exhibited statistically high serum absorption, a key requirement for biomedical scaffolds. The addition of cotton fibres reduced the absorption capacity compared to pure alginate, with higher cotton content leading to lower uptake; however, the reinforced filaments still retain adequate absorbency suitable for wound-healing applications.

Thus, alginate/cotton biocomposite filaments are promising materials for areas such as wound care, medical textiles or applications with flame retardant requirements. However, for targeted applications in the biomedical field, future research directions are envisioned in terms of mechanical behaviour investigation, biocompatibility assessments, along with antimicrobial evaluations, which will lead to an optimised modulated composition of the composite materials.

REFERENCES

[1] Prasad, A., Datta, S., Kumar, A., Gupta, M., *Introduction to Next-Generation Materials for Biomedical Applications*, 2023, https://doi.org/10.1002/9781394166985.ch1

[2] Vig K. et al., Advances in skin regeneration using tissue engineering, In: MDPI AG., 2017, https://doi.org/10.3390/ijms18040789

[3] Zdiri, K., Cayla, A., Elamri, A., Erard, A., Salaun, F., *Alginate-Based Bio-Composites and Their Potential Applications*, In: MDPI, 2022, https://doi.org/10.3390/jfb13030117

[4] Ahmad Raus, R., Wan Nawawi, W.M.F., Nasaruddin, R.R., *Alginate and alginate composites for biomedical applications*, Shenyang Pharmaceutical University, 2021, https://doi.org/10.1016/j.ajps.2020.10.001

[5] Roquero, D.M., Katz, E., *Smart alginate hydrogels in biosensing, bioactuation and biocomputing: State-of-the-art and perspectives*, In: Sensors and Actuators Reports, 2022, 4, https://doi.org/10.1016/j.snr.2022.100095

[6] Earar, K., et al., *Effect of the Sterilization Procedures of Different Surgical Meshes for Abdominal Surgery*, In: Revista de Chimie, 2017

[7] de Azevedo, A.R.G., et al., *Natural fibers as an alternative to synthetic fibers in reinforcement of geopolymer matrices: A comparative review*, In: MDPI AG, 2021, https://doi.org/10.3390/polym13152493

[8] Olteanu, G., et al., *Advancements in Regenerative Hydrogels in Skin Wound Treatment: A Comprehensive Review*, In: Multidisciplinary Digital Publishing Institute (MDPI), 2024, https://doi.org/10.3390/ijms25073849

[9] Miculescu, F., et al., *Synthesis and Characterization of Jellified Composites from Bovine Bone-Derived Hydroxyapatite and Starch as Precursors for Robocasting*, In: ACS Omega, 2018, 3, 1, 1338–1349, https://doi.org/10.1021/acsomega.7b01855

[10] Var, C., Palamutcu, S., *Diverse Approaches in Wet-Spun Alginate Filament Production from the Textile Industry Perspective: From Process Optimization to Composite Filament Production*, In: Multidisciplinary Digital Publishing Institute (MDPI), 2024, https://doi.org/10.3390/polym16131817

[11] Azam, F., Ahmad, F., Ahmad, S., Zafar, M.S., Ulker, Z., *Preparation and Characterization of Alginate Hydrogel Fibers Reinforced by Cotton for Biomedical Applications*, In: Polymers (Basel), 2022, 14, 21, https://doi.org/10.3390/polym14214707

[12] Sharma, A., Verma, C., Mukhopadhyay, S., Gupta, A., Gupta, B., *Development of sodium alginate/glycerol/tannic acid coated cotton as antimicrobial system*, In: Int. J. Biol. Macromol., 2022, 216, 303–311, https://doi.org/10.1016/j.ijbiomac.2022.06.168

[13] Miculescu, F., et al., *Considerations and Influencing Parameters in EDS Microanalysis of Biogenic Hydroxyapatite*, In: J. Funct. Biomater., 2020, 11, 4, https://doi.org/10.3390/jfb11040082

[14] Arslan, A.A., et al., *Influence of wetting-drying curing system on the performance of fiber reinforced metakaolin-based geopolymer composites*, In: Constr. Build. Mater., 2019, 225, 909–926, https://doi.org/10.1016/j.conbuildmat.2019.07.235

[15] Mocanu, A.C., et al., *Internal and external surface features of newly developed porous ceramics with random interconnected 3D channels by a fibrous sacrificial porogen method*, In: Appl. Surf. Sci., 2019, 489, 226–238, https://doi.org/10.1016/j.apsusc.2019.05.354

[16] Li, J., Pan, K., Tian, H., Yin, L., *The Potential of Electrospinning/Electrospraying Technology in the Rational Design of Hydrogel Structures*, In: Wiley-VCH Verlag, 2020, https://doi.org/10.1002/mame.202000285

[17] Mocanu, A.C., et al., *Naturally-derived biphasic calcium phosphates through increased phosphorus-based reagent amounts for biomedical applications*, In: Materials, 2019, 12, 3, https://doi.org/10.3390/ma12030381

[18] Vellingri, V., Sundaram, J.S., Kunal, K., Madeshwaren, V., *Sustainable biomedical waste management in healthcare: exploring composting through Fuzzy DEMATEL-ANP analysis*, In: Industria Textila, 2025, 76, 5, 664–674, https://doi.org/10.35530/IT.076.05.202520

[19] Mihai, C., Grosu, C., Chirila, L., Olaru, S., Popescu, A., *Design and development of experimental models for textile structures integrated in wound dressings applied in curative therapy of inflammatory skin diseases, using specific*

instruments of descriptive statistics, In: Industria Textila, 2021, 72, 5, 579–584, http://doi.org/10.35530/IT.072.05.1848
[20] Iordache, M., Grosu-Bularda, A., Bordeanu-Diaconescu, E.-M., Frunza, A., Andrei, M.-C., Grama, S., Costache, R.-A., Neagu, T-.P., Lascar, I., Chiotoroiu, A.L., Chiotoroiu, S.M., Dondea, M.-F., *Therapeutic management of burns affecting major joints of the limbs and the role of medical textiles in enhancing the rehabilitation process: 1 year retrospective study*, In: Industria Textila, 2025, 76, 1, 131–143, https://doi.org/10.35530/IT.076.01.2023144
[21] ASTM International, *Test Method for Water Absorption of Plastics*, West Conshohocken, PA, 2010, https://doi.org/10.1520/D0570-98R10E01

Authors:

MARIA FELICIA DONDEA[1,2], EMILIA VISILEANU[1], FLORIN MICULESCU[2], AURA-CĂTĂLINA MOCANU[2], CIPRIAN PREDA[2], DANIELA MANOLE[2]

[1]National Research and Development Institute for Textiles and Leather,
16 Lucretiu Patrascanu Street, 030508 Bucharest, Romania
e-mail: e.visilenu@incdtp.ro

[2]National University of Science and Technology POLITEHNICA Bucharest, Department of Metallic Materials Science, Physical Metallurgy, 313 Splaiul Independenței, J Building, RO-060042, Bucharest, Romania
e-mail: f_miculescu@yahoo.com, mcn_aura@hotmail.com

Corresponding author:

FELICIA DONDEA
e-mail: felicia.dondea@incdtp.ro

Predicting ozone bleaching in denim fabrics with ensemble learning models

DOI: 10.35530/IT.077.04.2025125

YASIN TAŞTEKİN
GÖKTUĞ YÜCEER
EDA GÖZ
MEHMET YÜCEER

ABSTRACT – REZUMAT

Predicting ozone bleaching in denim fabrics with ensemble learning models

Ensemble learning models, particularly advanced methods such as LightGBM and CatBoost, were applied to predict and improve the ozone bleaching process of denim fabrics, an eco-friendly alternative to conventional chemical methods that reduces water and energy consumption. Complex interactions among variables, including indigo/cotton ratio, sulphur/cotton ratio, moisture content, pH, temperature, and processing time, hinder consistent bleaching results. Although machine learning has been increasingly used to model textile processes, research specifically focused on predicting and optimising ozone bleaching performance in denim fabrics remains limited. To address this gap, we developed predictive models using six techniques (Random Forest, AdaBoost, GBM, XGBoost, LightGBM, and CatBoost) to estimate ΔEcmc values. The dataset was split into training (80%) and testing (20%) subsets, and model parameters were optimised via GridSearch. LightGBM provided the best fit in terms of explained variance (R^2 = 0.9972) with low test error (RMSE = 0.4214), while CatBoost achieved the best test-set generalisation with the lowest error metrics (RMSE = 0.4168 and MAPE = 4.9138%). These results show that ensemble models effectively capture complex interactions in the bleaching process, thereby reducing trial and error. To enhance applicability, the CatBoost model was coupled with a Genetic Algorithm to identify optimal ozone bleaching conditions across four fabric types (CI, CS, CEI, CES), yielding input settings that minimised ΔEcmc and supporting a sustainable, data-driven production approach.

Keywords: *ozone bleaching, ensemble learning, optimisation, denim fabrics, machine learning, sustainability*

Preconizarea decolorării cauzate de ozon în țesăturile din denim cu ajutorul modelelor de învățare de tip ansamblu

Au fost aplicate modele de învățare de tip ansamblu, în special metode avansate precum LightGBM și CatBoost, pentru a preconiza și a îmbunătăți procesul de decolorare cu ozon a țesăturilor din denim, o alternativă ecologică la metodele chimice convenționale care reduce consumul de apă și energie. Interacțiunile complexe dintre variabile, inclusiv raportul indigo/bumbac, raportul sulf/bumbac, conținutul de umiditate, pH-ul, temperatura și timpul de procesare, împiedică obținerea unor rezultate consistente în ceea ce privește decolorarea. Deși învățarea automată a fost utilizată din ce în ce mai mult pentru modelarea proceselor textile, cercetările axate în mod specific pe preconizarea și optimizarea performanței decolorării cu ozon a țesăturilor din denim rămân limitate. Pentru a remedia această lacună, am dezvoltat modele predictive utilizând șase tehnici (Random Forest, AdaBoost, GBM, XGBoost, LightGBM și CatBoost) pentru a estima valorile ΔEcmc. Setul de date a fost împărțit în subansambluri de antrenare (80%) și de testare (20%), iar parametrii modelului au fost optimizați prin GridSearch. LightGBM a oferit cea mai bună potrivire în ceea ce privește varianța explicată (R^2 = 0,9972) cu o eroare de testare redusă (RMSE = 0,4214), în timp ce CatBoost a obținut cea mai bună generalizare pe setul de testare cu cele mai mici metrici de eroare (RMSE = 0,4168 și MAPE = 4,9138%). Aceste rezultate arată că modelele de tip ansamblu surprind în mod eficient interacțiunile complexe din procesul de albire, reducând astfel procesul de încercare și eroare. Pentru a spori aplicabilitatea, modelul CatBoost a fost combinat cu un algoritm genetic în vederea identificării condițiilor optime de albire cu ozon pentru patru tipuri de țesături (CI, CS, CEI, CES), generând setări de intrare care au redus la minimum valoarea ΔEcmc și susținând o abordare de producție sustenabilă, bazată pe date.

Cuvinte-cheie*: albirea cu ozon, învățarea de tip ansamblu, optimizare, țesături din denim, învățare automată, sustenabilitate*

INTRODUCTION

Ozone bleaching has become a sustainable, cost-effective alternative to conventional methods, reducing water, hazardous chemicals, and energy use while meeting industry sustainability demands. Its reactions proceed via direct oxidation (dominant in acidic media) and indirect/radical pathways catalysed under alkaline conditions [1, 2]. Ozone effectively degrades chromophores in synthetic and natural fibres, enabling colour fading [3–5], and substantially lowers water/chemical consumption versus traditional processes [6, 7]. Yet process outcomes remain sensitive to parameters such as ozone concentration, moisture content, pH, temperature, and exposure time, necessitating careful optimisation [8–9]. Recent finishing innovations target aesthetics and functionality, but conventional fading often incurs high resource use and toxic effluents [10]. By contrast, ozone is an eco-friendly oxidant that decomposes to O_2, can be applied in gas form, and markedly reduces water use [11–15]. Still, optimising colour fading depends on material properties and process settings (e.g., temperature, time) [16–18]. Consequently, researchers increasingly employ process modelling and machine learning (ML) [19–22]. Prior ML studies in textiles show promise with ANNs (fast learning) [23, 24], SVMs (good generalisation) [25], and Random Forests (variable-interaction insights) [26, 27], spanning applications from defect detection [28] to property prediction [29]; for ozone-related fading on cotton, ANN/SVM/RF have also been effective [30].

However, direct work on predicting and optimising ozone bleaching in denim via ensemble learning remains limited. This study addresses that gap by developing ensemble learning–based predictive models tailored to ozone bleaching conditions in denim fabrics and, further, by integrating a CatBoost model with a Genetic Algorithm to identify parameter sets that minimise ΔEcmc. In doing so, it tackles process variability and advances sustainable, data-driven bleaching practice for the textile industry.

MATERIALS AND METHODS

Fabric samples

For the experiments, samples were taken from four types of denim fabrics: CI fabric 100% cotton fabric dyed with indigo 448 g/m^2, CS fabric: 100% cotton fabric dyed with sulphur, 479 g/m^2, 3/1 Z, CEI fabric 98% cotton–2% elastane fabric dyed with indigo 399 g/m^2, 3/1 Z, and CES fabric: 98% cotton–2% elastane fabric dyed with sulphur, 325 g/m^2, 3/1 Z.

Equipment and devices

A range of specialised equipment and devices was employed to conduct experimental procedures. The Smartex Miracle Ozone Machine was used to generate ozone gas required for the bleaching treatments. At the same time, the Denim Ozone Generator enabled precise regulation and monitoring of ozone levels throughout the bleaching process. Fabric samples were spin-dried before or after bleaching using the YILMAK HG30 Spin Machine, and subsequently dried with the Tolkar Carina 405 Industrial Dryer. For sample preparation, the Vibral Gold Weighing Device was employed to obtain accurate fabric weights. The APERA PH800 pH Meter was used to determine the pH values of the fabric samples. Colour characteristics were assessed using the LABORTEKS X-Rite Ci7800 Spectrophotometer, which measured colour changes and differences, while the Laborteks James Heal Grey Scale was applied to evaluate the colour fastness properties of the fabrics.

Ozone bleaching

Ozone bleaching was conducted on four fabric samples: CI (100% cotton, indigo-dyed), CS (100% cotton, sulphur-dyed), CEI (98% cotton–2% elastane, indigo-dyed), and CES (98% cotton–2% elastane, sulphur-dyed). Different pH levels, temperatures, and moisture conditions were tested, with colour fading observed at varying durations. Ozone concentration was controlled and monitored using the Denim Ozone Generator, with ozone feeding set at 300 g/h. The temperature was adjusted using precision heating devices, and moisture was controlled through various spin-drying levels. The fabric colour was measured using a spectrophotometer, and fast tests were performed to assess dye retention and fabric strength after bleaching.

Experimental design

Selected denim fabrics were evaluated under five different moisture conditions: dry (0% moisture), fully spun (35% moisture), half spun (38% moisture), quarter spun (41% moisture), and no spun (69% moisture). Ozone bleaching experiments were conducted at specific combinations of pH (4, 5, 6, 7, 9), temperature (15°C, 25°C, 35°C, 45°C, 55°C), and ozonation time (ranging from 10 to 80 minutes). However, experimental intervals varied according to fabric types. For example, while some fabrics can be subjected to ozonation for up to 80 minutes, others have a time limit of 40 minutes due to material sensitivity and colour change behaviour. These differences were determined through preliminary experiments. Instead of a full factorial design, a partial factorial sampling strategy specific to the fabric type was adopted in the study, which is highly suitable for industrial use and experimentally applicable. Numerous treatment combinations were evaluated on four different fabric types, with each experimental condition repeated three times to generate reliable data sets. The resulting data were used in advanced modelling and optimisation studies.

Colour measurement

Colour changes were measured with the Ci7800 spectrophotometer in accordance with ASTM E3098 and CIE guidelines. The device, equipped with internal temperature and humidity sensors, recorded conditions during each reading to ensure comprehensive data documentation. Optional UV balancing was used to control fluorescence and optical brighteners, improving measurement reliability in textiles. Integration with NetProfiler and Colour iMatch/Colour iQC software ensured consistent calibration and quality control, while Pantone Digital Colour Libraries provided digital references without the need for physical samples. The $\Delta Ecmc$ formula measures perceptible colour difference more precisely than the basic CIE76 ΔE, as it incorporates weighting factors reflecting human visual sensitivity to lightness, chroma, and hue [31]. Equation (1) presents the $\Delta Ecmc$ formula:

$$\Delta Ecmc = \left(\frac{\Delta L^*}{l \cdot S_L}\right)^2 + \left(\frac{\Delta C^*}{c \cdot S_C}\right)^2 + \left(\frac{\Delta H^*}{S_H}\right)^2 \quad (1)$$

where ΔL^* is difference in lightness, ΔC^* – difference in chroma (colour saturation), ΔH^* – difference in hue (colour tone), S_L, S_C, S_H – weighting factors that account for the sensitivity of the human eye to lightness (L^*), chroma (C^*), and hue (H^*), l and c – user-defined parameters, often set as l = 2 (sensitive to lightness differences) and c = 1 (standard chroma differences), depending on the application.

The CMC model is widely adopted in textiles, paints, and printing because it aligns more closely with human perception, providing accurate evaluation of colour differences. In denim bleaching, predicting $\Delta Ecmc$ values is essential for fine-tuning process parameters (moisture, pH, temperature, time) to optimise bleaching while ensuring uniform batch-to-batch colour consistency.

Dataset

The dataset consisted of 415 experimental records with six inputs: indigo/cotton ratio, sulphur/cotton ratio, moisture (%), initial pH, temperature (°C), and processing time (min). Figure 1 illustrates their distributions using box–whisker plots, showing variability, scale, and outliers. This analysis supported preprocessing, confirming dataset suitability and guiding normalisation to ensure consistent feature scaling for model training and validation.

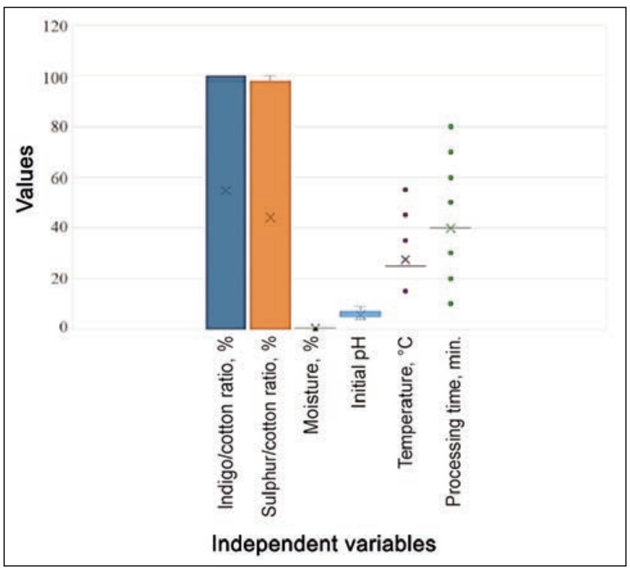

Fig. 1. Distribution of key input variables (indigo/cotton ratio, sulphur/cotton ratio, moisture content, pH, temperature, time) used in the machine learning models, providing insights into data variability and feature range

Data preprocessing

All inputs were z-score standardised (mean=0, SD=1) to avoid scale dominance across mixed units. The data were then split 80/20 into training and test sets for unbiased evaluation. Assumptions: stable environmental/equipment conditions (e.g., temperature, ozone concentration), uniform ozone output (300 g/h), and consistent fabric dyeing/thickness; automated spectrophotometer settings minimised measurement bias. Potential variability from fabric structure, residual chemicals, ambient humidity, and airflow may persist, slightly limiting generalizability beyond the tested conditions.

Hyperparameter optimisation and ensemble algorithms for ΔEcmc prediction

GridSearch was used to systematically explore predefined hyperparameter grids for each model and select configurations that maximised performance on the training/validation data. Six ensemble learners were then employed to capture nonlinear relationships among pH, temperature, moisture, and time: Random Forest Regression reduces variance via bagging and random subspaces [32]; AdaBoost iteratively reweights harder samples to build a strong learner from weak ones [33]; GBM fits residuals stage-wise to minimize a chosen loss [34]; XGBoost accelerates GBM with sparsity-aware learning and parallel block processing for large/sparse data [35]; LightGBM speeds training through histogram binning and high parallel efficiency [36]; and CatBoost uses oblivious trees with native categorical handling (e.g., indigo/cotton, sulphur/cotton ratios) and strong regularization [37]. Assumptions included accurate/consistent spectrophotometer $\Delta Ecmc$ readings and (for modelling convenience) independent inputs; limitations involved RF/GBM interpretability and potential overfitting on small/noisy data, finite GridSearch coverage of the hyperparameter space, and restricted generalizability beyond the studied fabric types and conditions.

Workflow overview

This study followed an integrated workflow to predict and optimise ΔEcmc values in the ozone bleaching of denim fabrics. The steps include data preprocessing, model training, performance evaluation, and optimisation using a Genetic Algorithm. The process begins with data collection and preprocessing, where fabric characteristics and relevant input variables, such as the indigo/cotton ratio, sulphur/cotton ratio, moisture content, pH, temperature, and treatment time, are organised and structured into a dataset. The dataset is then split into training and testing sets. In the model selection phase, ensemble learning algorithms including Random Forest, XGBoost, LightGBM, and CatBoost are implemented. To ensure optimal performance, hyperparameter tuning is carried out using GridSearch. Models are trained on the training set and evaluated using key performance metrics such as *RMSE*, *MAPE*, and R^2. Following model evaluation, the best-performing algorithm, CatBoost, is selected for integration with a Genetic Algorithm (GA). This GA-based optimisation identifies the ideal process conditions that minimise $\Delta Ecmc$ values for different fabric types. The integration of predictive modelling and heuristic optimisation ensures a robust, data-driven approach for enhancing the sustainability and efficiency of the ozone bleaching process.

Statistical evaluation of model performance

Model performance was evaluated using Root Mean Square Error (*RMSE*), Mean Absolute Percentage Error (*MAPE*), Mean Squared Error (*MSE*), and

Coefficient of Determination (R^2). All machine learning models were implemented using Python, with the corresponding code written in Jupyter Notebooks. Libraries such as Scikit-learn, XGBoost, LightGBM and CatBoost were utilised for model development, while data preprocessing and evaluation metrics were executed using Pandas and NumPy.

Optimisation Process with CatBoost-Based Genetic Algorithm

The ozone bleaching parameters were optimised using a Genetic Algorithm (GA) integrated with a CatBoost regression model [38]. The implementation was carried out in Python using the DEAP library [39], considering four continuous variables (moisture %, pH, temperature °C, time min). A population of 200 was evolved for 50 generations with tournament selection, blend crossover, and Gaussian mutation. The fitness function was the $\Delta Ecmc$ predicted by a pre-trained CatBoost model (inputs z-score standardised). To minimise $\Delta Ecmc$, individuals exceeding a set threshold were penalised, following a penalty-based constraint handling strategy [40]. Optimisation was performed per fabric type; the best individuals were ranked by fitness, and the optimal parameter sets were recorded for experimental validation.

RESULTS AND DISCUSSION

This study used ensemble learning to predict $\Delta Ecmc$ in ozone bleaching of denim, with inputs including indigo/cotton and sulphur/cotton ratios, moisture (%), initial pH, temperature (°C), and processing time (min). Six models, Random Forest, AdaBoost, GBM, XGBoost, LightGBM, and CatBoost, were applied to predict bleaching outcomes across different conditions. Hyperparameters (e.g., *n_estimators, learning_rate, max_depth*) were tuned via GridSearch, yielding model configurations tailored to the dataset and process characteristics.

Performance of machine learning algorithms in predicting ΔEcmc values

Six ensemble models (RF, AdaBoost, GBM, XGBoost, LightGBM, and CatBoost) were evaluated based on their ability to predict $\Delta Ecmc$ values. Performance was assessed using Root Mean Square Error (*RMSE*), Mean Absolute Percentage Error (*MAPE*), Mean Squared Error (*MSE*), and R^2. The results, summarised in table 1, show that LightGBM and CatBoost achieved the strongest performance, particularly in terms of generalisation accuracy on the test set.

LightGBM demonstrated strong overall performance, achieving the highest R^2 (0.9972) and low RMSE values (*RMSE_train* = 0.3620; *RMSE_test* = 0.4214), confirming its ability to reliably predict $\Delta Ecmc$ values across bleaching conditions (figure 2). These findings show that LightGBM effectively captured complex nonlinear patterns in ozone bleaching with strong generalisation ($R^2 > 0.995$), outperforming models such as ELM, SVR, and RF reported in [30].

CatBoost also performed strongly (figure 3), achieving the lowest test *RMSE* (0.4168) and lowest *MAPE* (4.9138%), confirming its superior generalisation capability with minimal preprocessing, consistent with [37]. Random Forest fit the training data well ($R^2 = 0.9969$) but showed a higher test *RMSE* (0.4995), suggesting slight overfitting, a limitation also noted in earlier textile studies [29]. AdaBoost delivered balanced results (*RMSE_train* = 0.3686; *RMSE_test* = 0.4303) with reliable generalisation, while GBM and XGBoost showed stable and similar outcomes, with XGBoost slightly ahead on the test set. Overall, LightGBM provided the best fit (highest R^2), whereas CatBoost achieved the best test set generalisation (lowest *RMSE* and *MAPE*). Both models effectively captured nonlinear dynamics and interactions between key variables such as moisture and pH. From a practical standpoint, ensemble models reduce trial and error in experiments and revealed that higher moisture levels and slightly acidic pH values yield better bleaching efficiency in shorter times. Their application supports sustainable process optimisation by lowering chemical and water use, improving control, and reducing environmental impact. These results align with sustainability goals in textile production and highlight the value of integrating AI into bleaching. One key finding was the strong influence of moisture and initial pH, consistent with earlier research. Conversely, RF's weaker test performance despite high training accuracy highlighted the advantage of boosting methods for complex

Table 1

COMPARISON OF MODEL PERFORMANCE ON TRAINING AND TEST SETS

Method/Statistical parameters	Training				Test			
	RMSE	MAPE (%)	MSE	R^2	RMSE	MAPE (%)	MSE	R^2
Random Forest	0.3764	5.2577	0.1417	0.9969	0.4995	5.5497	0.2495	0.9940
AdaBoost	0.3686	5.1546	0.1358	0.9971	0.4303	5.0415	0.1851	0.9955
GBM	0.3640	5.4451	0.1325	0.9971	0.4220	5.1061	0.1781	0.9957
XGBoost	0.3646	5.3991	0.1330	0.9971	0.4254	5.1497	0.1810	0.9956
LightGBM	0.3620	5.0849	0.1311	0.9972	0.4214	4.9570	0.1776	0.9957
CatBoost	0.3645	5.4349	0.1329	0.9971	0.4168	4.9138	0.1737	0.9958

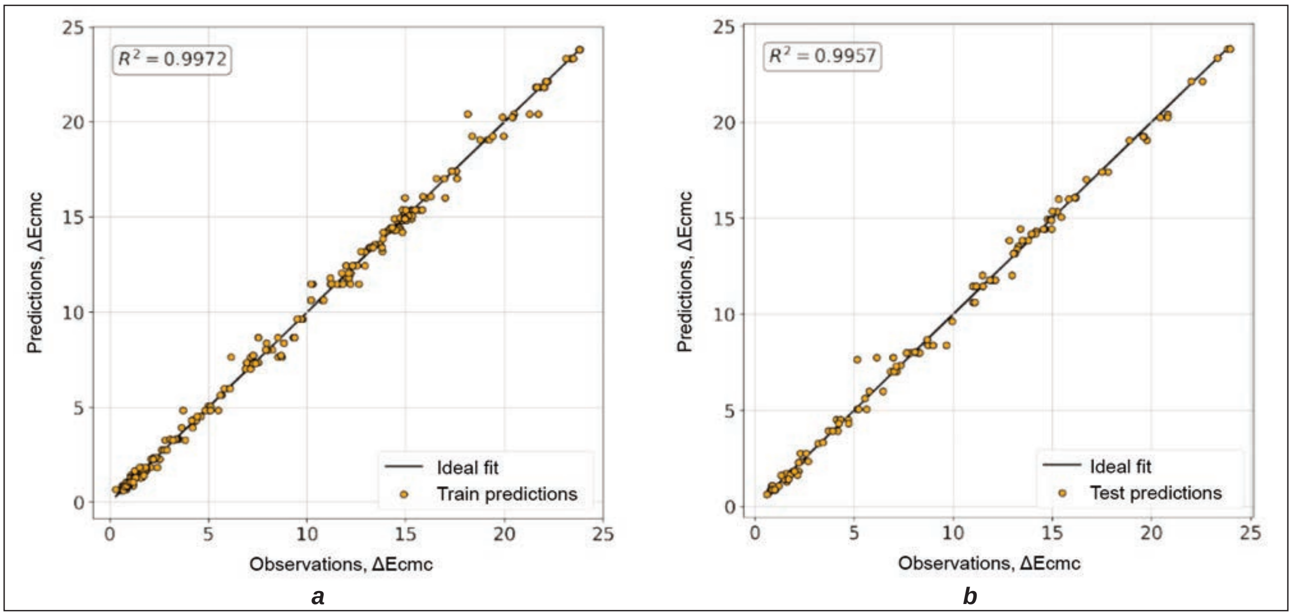

Fig. 2. Predicted vs. observed Δ*Ecmc* using LightGBM for:
a – training; *b* – test, showing strong correlation and low prediction error

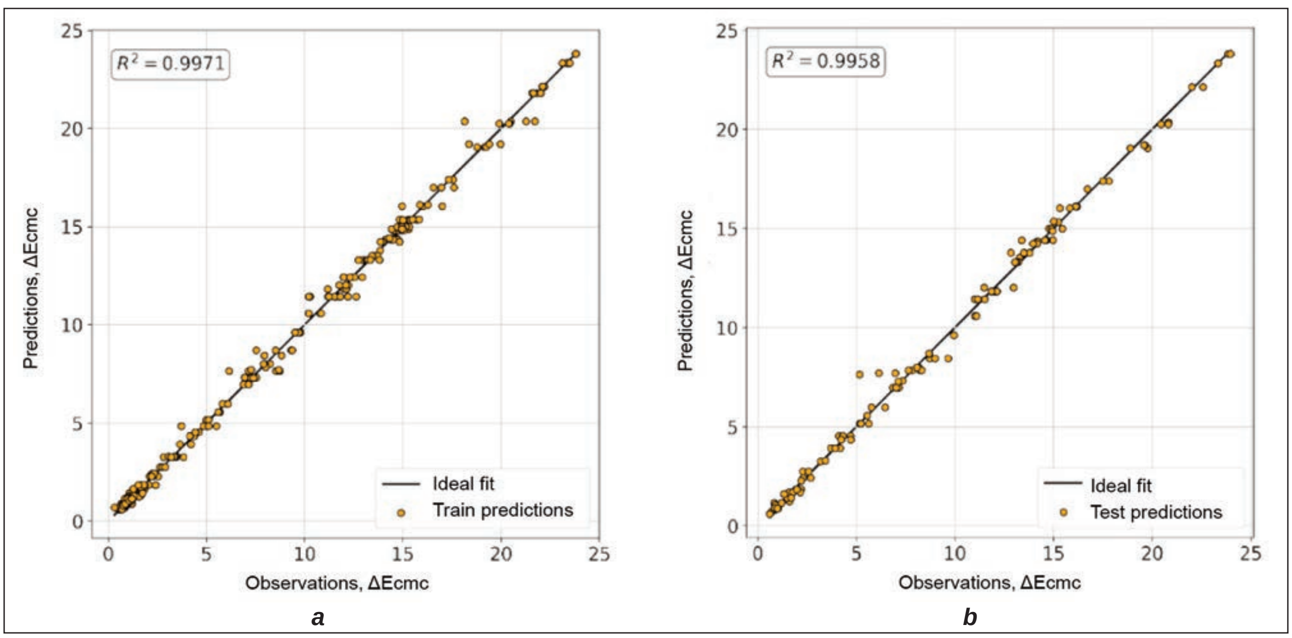

Fig. 3. Predicted vs. observed Δ*Ecmc* using CatBoost for:
a – training; *b* – test, indicating good agreement between predictions and observations

interactions. While promising, limitations (including the focus on specific denim types and controlled laboratory settings) may affect generalizability, pointing to the need for broader datasets and real-world trials in future work.

Optimisation of ozone bleaching conditions using CatBoost and Genetic Algorithm

CatBoost was chosen for GA because it delivered the best test set generalisation (lowest *RMSE* and *MAPE*), which is critical when evaluating new parameter combinations beyond the training data. A CatBoost regression model coupled with a Genetic Algorithm (GA) was used to minimise Δ*Ecmc* by optimising moisture (%), pH, temperature (°C), and time (min) for four denim types (CI, CS, CEI, CES). GA-generated parameter sets were scored by CatBoost, and the best candidates were validated experimentally. Predictions closely matched measurements (*MAPE* < 5%; CI 2.7219%, CEI 3.2063%, CS 4.3370%, CES 4.2410%), confirming the CatBoost–GA framework as a reliable, industry-ready approach for ozone bleaching optimisation.

CONCLUSIONS

Ensemble learning, particularly LightGBM and CatBoost, accurately predicted Δ*Ecmc* in ozone bleaching, with LightGBM achieving the highest R^2 (best fit) and CatBoost delivering the lowest test-set

RMSE and *MAPE* (best generalisation), outperforming alternatives across *RMSE*, *MAPE*, and R^2. Leveraging this predictive strength, the CatBoost–GA framework identified process settings (moisture, pH, temperature, time) that minimised $\Delta Ecmc$ for four fabric types, with experimental validation showing close agreement ($MAPE < 5\%$). These results demonstrate a practical, industry-ready pathway that reduces trial and error, improves process control, and lowers waste, costs, and environmental impact. In contexts where conventional bleaching is resource-intensive, ozone paired with machine learning offers a cleaner and more efficient option. Overall, the approach provides data-driven guidance for sustainable manufacturing. Future work should broaden fabric and dye coverage, include more diverse operating ranges, and deploy real-time, model-based control to enable dynamic decision-making at scale.

REFERENCES

[1] Gottschalk, C., Libra, J. A., Saupe, A., *Ozonation of water and wastewater: A practical guide to understanding ozone and its applications*, Wiley-VCH, 2010, https://doi.org/10.1002/9783527628926.

[2] Chu, W., Ma, C.W., Quantitative prediction of direct and indirect dye ozonation kinetics, In: *Water Research*, 2000, 34, 12, 3153–3160, https://doi.org/10.1016/S0043-1354(00)00043-9.

[3] Morali, E.K., Uzal, N., Yetis, U., *Ozonation pre and post–treatment of denim textile mill effluents: Effect of cleaner production measures,* In: Journal of Cleaner Production, 2016, 137, 1–9, https://doi.org/10.1016/j.jclepro.2016.07.059.

[4] Vandevivere, P.C., Bianchi, R., Verstraete, W., *Treatment and reuse of wastewater from the textile wet–processing industry: Review of emerging technologies*, In: Journal of Chemical Technology and Biotechnology, 1998, 72, 4, 289–302, https://doi.org/10.1002/(SICI)1097-4660(199808)72:4

[5] Kamppuri, T., Mahmood, S., *Finishing of denim fabrics with ozone in water*, In: Journal of Textile Engineering & Fashion Technology, 2019, 5, 2, 96–101, https://doi.org/10.15406/jteft.2019.05.00189.

[6] Wasinger, E., *Ozone decolorization of garments*, European Patent No. 0554648, 1998

[7] Ledakowicz, S., Solecka, M., Zylla, R., *Biodegradation, decolourization and detoxification of textile wastewater enhanced by advanced oxidation processes,* In: Journal of Biotechnology, 2001, 89, 2–3, 175–184, https://doi.org/10.1016/S0168-1656(01)00296-6.

[8] Ben Hmida, S., Ladhari, N., *Study of parameters affecting dry and wet ozone bleaching of denim fabric*, In: Ozone: Science & Engineering, 2016, 38, 3, 175–180, https://doi.org/10.1080/01919512.2015.1113380.

[9] Bahtiyari, M. I., Benli, H., *Ozone bleaching of cotton fabrics with the aid of ultrasonic humidifier*, In: Cellulose, 2016, 23, 4, 2715–2725, https://doi.org/10.1007/s10570-016-0978-y.

[10] Paul, R., Denim: Manufacture, finishing and applications, Elsevier Science, 2015

[11] Mao, Y.H., Guan, Y., Luo, D.H., Zheng, Q.K., Feng, X.N., Wang, X.X., *Investigation of a homogeneous activating ozonation method in the rinsing procedure of cotton fabric dyed with reactive dye*, In: Colouration Technology, 2011, 127, 4, 256–267, https://doi.org/10.1111/j.1478-4408.2011.00309.x.

[12] Eren, S., Gümüş, B., Eren, H.A., *Colour stripping of reactive-dyed cotton by ozone treatment*, In: Colouration Technology, 2016, 132, 6, 466–471, https://doi.org/10.1111/cote.12240

[13] Kan, C.W., Cheung, H.F., Chan, Q., *A study of plasma-induced ozone treatment on the colour fading of dyed cotton*, In: Journal of Cleaner Production, 2016, 112, 4, 3514–3524, https://doi.org/10.1016/j.jclepro.2015.10.100

[14] Kıcık, H., Eren, H.A., *Application of ozone gas for the stripping of fabric ink-jet-printed with reactive dyes*, In: Colouration Technology, 2017, 133, 6, 485–490, https://doi.org/10.1111/cote.12302

[15] Yigit, I., Eren, S., Eren, H.A., *Ozone utilization for discharge printing of reactive dyed cotton*, In: Colouration Technology, 2018, 134, 1, 13–23, https://doi.org/10.1111/cote.12306

[16] He, Z., Li, M., Zuo, D., Changhai, Y., *The effect of denim colour fading ozonation on yarns*, In: Ozone: Science & Engineering, 2018, 40, 5, 377–384, https://doi.org/10.1080/01919512.2018.1435259

[17] He, Z., Li, M., Zuo, D., Changhai, Y., *Colour fading of reactive-dyed cotton using UV-assisted ozonation*, In: Ozone: Science & Engineering, 2019, 41, 1, 60–68, https://doi.org/10.1080/01919512.2018.1483817

[18] He, Z., Li, M., Zuo, D., Xu, J., Changhai, Y., *Effects of colour fading ozonation on the colour yield of reactive-dyed cotton*, In: Dyes and Pigments, 2019b, 164, 417–427, https://doi.org/10.1016/j.dyepig.2019.01.006

[19] Wu, L., Yick, K. L., Ng, S. P., Yip, J., Kong, K.H., *Parametric design and process parameter optimization for bra cup molding via response surface methodology*, In: Expert Systems with Applications, 2012, 39, 1, 162–171, https://doi.org/10.1016/j.eswa.2011.07.003

[20] Balci, O., Oğulata, R.T., *Prediction of the changes on the CIELab values of fabric after chemical finishing using artificial neural network and linear regression models*, In: Fibers and Polymers, 2009, 10, 3, 384–393, https://doi.org/10.1007/s12221-009-0384-2

[21] Elemen, S., Akçakoca Kumbasar, E.P., Yapar, S., *Modeling the adsorption of textile dye on organoclay using an artificial neural network*, In: Dyes and Pigments, 2012, 95, 1, 102–111, https://doi.org/10.1016/j.dyepig.2012.03.001.

[22] Zervent Ünal, B., *The prediction of seam strength of denim fabrics with mathematical equations*, In: Journal of the Textile Institute, 2012, 103, 7, 744–751, https://doi.org/10.1080/00405000.2011.603509

[23] Sette, S., Van Langenhove, L., *An overview of soft computing in textiles*, In: Journal of the Textile Institute, 2003, 94, 1–2, 103–109, https://doi.org/10.1080/00405000308630598
[24] Suzuki, K. (Ed.), Artificial neural networks – industrial and control engineering applications, InTech, 2011, https://doi.org/10.5772/2041
[25] Vapnik, V.N., *The nature of statistical learning theory*, Springer, 1995, https://doi.org/10.1007/978-1-4757-2440-0
[26] Breiman, L., *Random forests*, In: Machine Learning, 2001, 45, 1, 5–32, https://doi.org/10.1023/A:1010933404324
[27] Liaw, A., Wiener, M., *Classification and regression by randomForest*, In: R News, 2002, 2, 3, 18–22, Available at: https://CRAN.R-project.org/doc/Rnews/ [Accessed on August 2025]
[28] Kwon, B.K., Won, J.S., Kang, D.J., *Fast defect detection for various types of surfaces using random forest with VOV features*, In: International Journal of Precision Engineering and Manufacturing, 2015, 16, 5, 965–970, https://doi.org/10.1007/s12541-015-0125-y.
[29] Venkatraman, V., Alsberg, B. K., *A quantitative structure-property relationship study of the photovoltaic performance of phenothiazine dyes,* In: Dyes and Pigments, 2015, 114, 69–77, https://doi.org/10.1016/j.dyepig.2014.10.026
[30] He, Z., Tran, K.P., Thomassey, S., Zeng, X., Xu, J., Changhai, Y., *Modeling colour fading ozonation of reactive-dyed cotton using the extreme learning machine, support vector regression, and random forest*, In: Textile Research Journal, 2020, 90, 7–8, 896–908, https://doi.org/10.1177/00405175198830
[31] Clarke, F.J.J., McDonald, R., Rigg, B., *Modification to the JPC79 Colour-Difference Formula*, In: Journal of the Society of Dyers and Colourists, 1984, 100, 4, 128–132, https://doi.org/10.1111/j.1478-4408.1984.tb00969.x
[32] Ganesh, N., Jain, P., Choudhury, A., Dutta, P., Kalita, K., Barsocchi, P., *Random forest regression-based machine learning model for accurate estimation of fluid flow in curved pipes*, In: Processes, 2021, 9, 11, 2095, https://doi.org/10.3390/pr9112095.
[33] Freund, Y., Schapire, R.E., *A decision-theoretic generalization of on-line learning and an application to boosting*, In: Journal of Computer and System Sciences, 1997, 55, 1, 119–139, https://doi.org/10.1006/jcss.1997.1504
[34] Belyadi, H., Haghighat, A., Machine learning guide for oil and gas using Python: A step-by-step breakdown with data, algorithms, codes, and applications, Gulf Professional Publishing, 2021, Available at: https://www.sciencedirect.com/book/9780128219294/machine-learning-guide-for-oil-and-gas-using-python [Accessed on August 2025]
[35] Mesut, B., Başkor, A., Aksu, N.B., *Role of artificial intelligence in quality profiling and optimization of drug products*, In: Philip, A., Shahiwala, A., Rashid, M., Faiyazuddin, M. (Eds.), A handbook of artificial intelligence in drug delivery, Academic Press, 2023, 35–54, https://doi.org/10.1016/B978-0-323-89925-3.00003-4
[36] Thongthammachart, T., Araki, S., Shimadera, H., Matsuo, T., Kondo, A., *Incorporating light gradient boosting machine to land use regression model for estimating NO2 and PM2.5 levels in Kansai region, Japan*, In: Environmental Modelling & Software, 2022, 155, 105447, https://doi.org/10.1016/j.envsoft.2022.105447
[37] Prokhorenkova, L., Gusev, G., Vorobev, A., Dorogush, A. V., Gulin, A., *Catboost: Unbiased boosting with categorical features*, In: Proceedings of the 32nd International Conference on Neural Information Processing Systems, 2018, 6639–6649
[38] Goldberg, D.E., Genetic Algorithms in Search, Optimization, and Machine Learning, Addison-Wesley, 1989
[39] Fortin, F.A., De Rainville, F.M., Gardner, M.A., Parizeau, M., Gagné, C., *DEAP: Evolutionary algorithms made easy*, In: Journal of Machine Learning Research, 2012, 13, Jul, 2171–2175
[40] Coello Coello, C.A., *Theoretical and numerical constraint-handling techniques used with evolutionary algorithms: A survey of the state of the art,* In: Computer Methods in Applied Mechanics and Engineering, 2002, 191, 11–12, 1245–1287, https://doi.org/10.1016/S0045-7825(01)00323-1

Authors:

YASIN TAŞTEKİN[1], GÖKTUĞ YÜCEER[2], EDA GÖZ[3], MEHMET YÜCEER[1]

[1]Inonu University, Faculty of Engineering, Chemical Engineering Department, 44280, Malatya, Türkiye

[2]Sakarya University Faculty of Computer and Information Sciences, Computer Engineering Department, 54050, Sakarya, Türkiye
e-mail: goktug.yuceer@ogr.sakarya.edu.tr

[3]Ankara University Faculty of Engineering, Chemical Engineering Department, Dögol Street, 06100, Ankara, Türkiye
e-mail: esemizer@eng.ankara.edu.tr

Corresponding author:

MEHMET YÜCEER
e-mail: mehmet.yuceer@inonu.edu.tr

Natural thermo-insulation panels made from local renewable resources: esparto grass (alfa) and kenaf fibres

DOI: 10.35530/IT.077.04.202437

YOSR BEN MLIK
RIADH ZOUARI
MOUNIR JAOUADI
RIM HOUIDI
CHAMA FAIDI
EMILIA VISILEANU

ABSTRACT – REZUMAT

Natural thermo-insulation panels made from local renewable resources: esparto grass (alfa) and kenaf fibres

This study aims to develop efficient, eco-friendly insulation panels made from abundant local resources from Tunisia. Nonwoven panels were manufactured from kenaf and alfa fibres at different densities, and their air permeability and thermal conductivity were evaluated. A fire-retardant treatment based on natural salt was applied to the fibres, and its influence on the flammability of the resulting nonwoven was assessed. These properties are essential for the use of panels in building thermo-insulation. The thermal conductivity of these panels varies from 0.034 to 0.41 W·m^{-1}·K^{-1}, and kenaf panels present lower thermo-conductivity than alfa panels. These values are comparable to those of polystyrene and rock wool fibre panels. The fire-retardant treatment, based on the use of natural salt, showed its efficiency by improving the behaviour of panels exposed to flame.

Keywords: *natural fibres, thermal insulation, kenaf, alfa, thermal conductivity, fire retardancy*

Panouri termoizolante naturale realizate din resurse regenerabile locale: fibre de iarbă esparto (alfa) și fibre de kenaf

Acest studiu își propune să dezvolte panouri de izolație eficiente și ecologice, realizate din resurse locale abundente din Tunisia. Au fost fabricate panouri nețesute din fibre de kenaf și alfa, la diferite densități, iar permeabilitatea lor la aer și conductivitatea termică au fost evaluate. Fibrelor li s-a aplicat un tratament ignifug pe bază de sare naturală, iar influența acestuia asupra inflamabilității materialelor nețesute rezultate a fost analizată. Aceste proprietăți sunt esențiale pentru utilizarea panourilor în termoizolația clădirilor. Conductivitatea termică a acestor panouri variază între 0,034 și 0,41 W·m^{-1}·K^{-1}, iar panourile din kenaf prezintă o conductivitate termică mai redusă decât cele din fibre alfa. Aceste valori sunt comparabile cu cele ale panourilor din polistiren și din fibre de vată minerală. Tratamentul ignifug, bazat pe utilizarea sării naturale, și-a demonstrat eficiența prin îmbunătățirea comportamentului panourilor expuse la flacără.

Cuvinte-cheie: *fibre naturale, izolație termică, kenaf, alfa, conductivitate termică, rezistență la foc (ignifugare)*

INTRODUCTION

Thermo-insulation panels are used in buildings to improve their energetic efficiency by reducing heat transfer. We find these materials in walls, roofs, and floors to minimise heat exchange with exterior volumes. They are thermal barriers that guarantee a comfortable indoor temperature by reducing heat gain in summer and heat loss in winter, in a way that reduces energy consumption. These panels are not only a thermal barrier but also present other general properties, such as moisture resistance, sound insulation, and fire resistance. These properties depend on the materials used and the manufacturing process [1].

Several materials and products are thermal insulators for building applications provided they are light in weight, easy to handle, durable, and resistant to moisture and environmental factors. The most common products are made from polystyrene, which is commercialised as a rigid board providing high thermo-insulation properties and good moisture resistance and used especially as basement walls, foundation slabs, and also in roofs and floors [1, 2].

Rigid foam boards from polyurethane have low thermal conductivity, and they are used as a thin panel in walls and roofs for thermo-insulation.

Glass fibres and mineral wool insulators are chosen for their excellent thermo-insulation, sound resistance, and fire resistance properties.

The choice of insulating products used in the building is determined by several factors such as thermal and sound insulation performance, fire resistance properties, the application area, and, in some cases, environmental considerations [3].

Nowadays, eco-friendly and sustainable materials such as natural fibres or recycled content insulation panels are used [4]. These materials reduce environmental impact and contribute to green building practices.

The development of insulation panels made from natural resources was a topic of interest for multiple researchers [5, 6]. These natural resources may be either raw materials, waste or recycled materials [7–9].

Ali et al. [10] suggest that Boards made of Agave and wheat straw fibres using corn starch as a binder have excellent thermal insulation properties (thermal conductivity equal to 0.043 $W \cdot m^{-1} \cdot K^{-1}$). However, they reported that the major problem faced is the moisture sensitivity of natural fibre. So other studies were focused on the impact of moisture content on the mechanical and physical properties of the insulation panel, and in this context, Korjenic et al. [11], who developed insulation products made of jute, flax, and hemp, have demonstrated that when using the correct combination of natural materials, properties will be comparable with those of conventional materials.

Our research work focused on the development of eco-friendly insulation panels made of local resources, alfa, and kenaf fibres, by evaluating their thermal conductivity in terms of the panel density, and then by improving their flame behaviour by biological treatment of the fibres based on natural salt.

MATERIALS AND METHODS

Natural fibres used in this study are local alfa and kenaf cultivated in an experimental field in Tunisia.

Stippa tenacissima, or esparto grass plant, also known as alfa, is a plant with a graceful tuft of green, linear leaves that are composed of several circular bundles. It is abundant in dry regions of North Africa, especially in Tunisia, Algeria, and Morocco. Alfa fibres are mostly used to produce paper, but recently they have been explored as reinforcement of green composites and other technical applications.

The kenaf or *Hemp Deccan,* belonging to the Malvaceae family, is an annual plant having a long stem that can reach 2 m to 4 m in length in five months. Kenaf fibres are extracted from the stem, and nowadays they attract the attention of researchers and industry thanks to their properties and performance, which compete with synthetic fibres in many technical applications such as automobile interior panels and eco-friendly products.

A combined process was used to extract kenaf and alfa fibres. For kenaf fibre, first fibres were separated from the stem mechanically using a horizontal opener, a Shirley, and then chemically treated to improve fibre separation.

For alfa fibre, chemical extraction was used to move noncellulosic materials, and then the Shirley was used to improve fibre individualisation.

Fibre treatment for fire retardancy

The flammability of cellulose fibres is the major disadvantage that prevents them from being

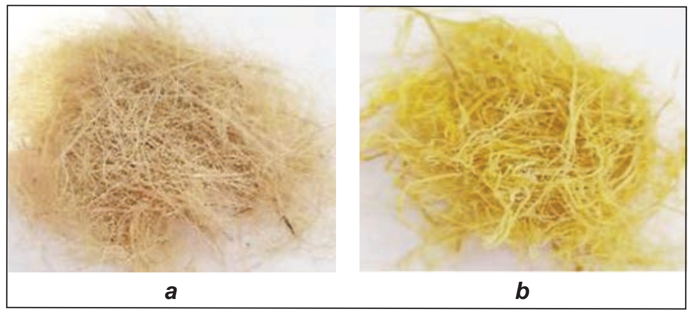

Fig. 1. Image of: *a* – Kenaf fibres; *b* – Alfa fibres

exploited in building thermo-insulation products. In our study, Salt (NaCl) was used to treat kenaf and alfa fibres to improve their fire retardancy performance. It's a non-permanent treatment used with materials that will not be exposed to water during their life cycle.

The fibres were soaked in a 35 g/l NaCl solution for 1 hour at room temperature and then drained and dried in a special oven, equipped with a ventilator and a thermostat, at 80°C for 4 hours. Table 1 presents the extraction process applied to kenaf and alfa.

Fibre characterization

The gravimetric method was used to determine the linear density of the fibres according to the standard NF G07-007. Also, 300 randomly selected fibres were examined to measure the diameter using an optical microscope according to standard NF G 07-004. Finally, the tensile test was carried out according to NF G07-002 to determine the mechanical properties of the fibres.

Development of the nonwoven panels

The "Airlaid machine" used to make nonwoven panels from kenaf and alfa is a lab-scale machine developed in the Textile Engineering Laboratory (National Patent Number: TN 2013/117) [12]. Panels are then thermally consolidated. So, two types of nonwovens were made by mixing kenaf and alfa fibres with 10 wt % of PLA fibres (polylactic acid). The fibrous mixtures, composed of either binding fibres mixed with alfa fibres or binding fibres with kenaf fibres, are well homogenised to make an air-laid nonwoven.

Structures are finally submitted to a temperature of 180°C for 60 s to ensure melting of the bonding polymer, then cooled to room temperature.

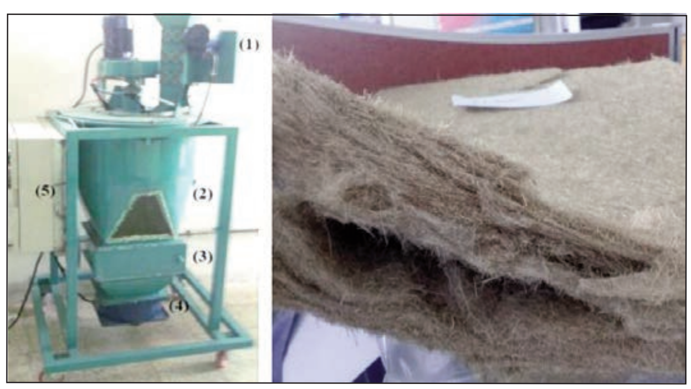

Fig. 2. Airlaid machine and Kenaf panel K1

Table 1

EXTRACTION PROCESS FOR BOTH ALFA AND KENAF FIBRES		
Phase	**Kenaf**	**Alfa**
1	Mechanical separation: Horizontal opener + Shirley analyser	Chemical extraction: NaOH concentration: 80 g/l Duration: 2 h Temperature: 80°C + Sodium hypochlorite NaClO: 100 ml/l Duration: 1 h Temperature: 70°C
2	Chemical extraction: NaOH concentration:120 g/l Duration: 2 h Temperature: 80°C	Finishing: Washing fibre with hot water Neutralised by 2 ml/l H_2O_2 Drying in a special oven at 80°C for 4 h
3	Finishing: Washing fibre with hot water Neutralised with 10 ml/L acetic acid Drying in a special oven at 80°C for 4 h	Mechanical separation: Shirley analyser
4	Fibre treatment for fire retardancy: NaCl concentration: 35g/l duration: 1 h Temperature: at room temperature (25°C) Finishing: Drying in a special oven at 80°C for 4 h	

Table 2

THE THERMOBINDER FIBRES "PLA" PROPERTIES				
Linear density (dtex)	**Length (mm)**	**Melting point (°C)**	**Tenacity (cN/tex)**	**Elongation (%)**
1.5	6	160	32 ± 2.5	55 ± 5

The properties of the thermobinder fibres are presented in table 2.

Nonwoven characterization

Some physical and thermal properties of nonwovens made, such as thickness, density, thermal conductivity, and air permeability, were investigated.
The nonwoven thickness was measured according to the standard ISO 5084 at different areas of each sample. The thickness was calculated as an average of the thickness measurements at five separate points with a Digmatic Thickness Meter ID-F 543-553. The samples were weighed using an electronic scale. The surface of each panel was 0.09 m^2, so nonwoven density was deduced using the following formula:

$$Density\ (\text{kgm}^{-3}) = \frac{m}{V} \qquad (1)$$

where m is the sample weight (kg), and V is the sample volume.
The air permeability was measured according to ISO 9237 (1995) using an air permeability tester at five positions on the sample surface selected randomly. All measurements were performed on the same side (face) of the sample.

Also, the thermal conductivity is measured according to French Standard NF EN 12667 using a hot/cold plate apparatus, which measures the difference in temperature between the two surfaces of the tested sample. The principle behind measuring thermal conductivity consists of passing a uniform, unidirectional, and constant thermal flow through a flat sample and measuring the temperature on both sides of the sample. Samples were dried in an oven at 70°C to remove all humidity until their mass variation was equal to zero. Then it was placed between the hot and cold plates of the apparatus, ensuring direct contact to avoid heat dissipation, and the thermal conductivity was measured in two cases: the first for cold and hot plate temperatures of 0°C to 20°C and the second for 10°C to 30°C.
The thermal conductivity k ($\text{Wm}^{-1}\text{k}^{-1}$) is described by Fourier's law (equation 2):

$$q\ (\text{wm}^{-2}) = -k \times A \times \frac{dT}{dx} \qquad (2)$$

where q is unidirectional heat flow (w·m^{-2}), A – cross-sectional area of the sample (m^2), dT/dx – the temperature gradient (k/m).
Finally, to evaluate the efficiency of flame-retardant treatment applied on fibre, the flame test was carried out. It is a qualitative and subjective test. The test is conducted according to the standard ISO 694. So, the sample is placed vertically on a sample holder exposed to a burner placed horizontally at 7 mm from the sample. The material is exposed to flame for 20 s. The results of the examination are a subjective description of the behaviour of the samples during and after exposure to the burner flame.

RESULTS AND DISCUSSION

The results of fibre characterisation are presented in table 3.

Table 3

KENAF AND ALFA FIBRES PROPERTIES				
Fibre type	**Diameter (μm)**	**Linear density (dTex)**	**Tenacity (cN/tex)**	**Elongation (%)**
Kenaf	103.96	17.32	10.32	2.40
Alfa	281.19	49.97	20.53	1.7

By examining the properties of alfa and kenaf fibres, it was concluded that alfa fibres are thicker, more resistant, more rigid, and more difficult to deform.

These fibres were used to make nonwovens with two different densities. Alfa samples are noted A1 and A2, and kenaf samples are noted K1 and K2. Results of the nonwoven characterisation are presented in table 4.

The samples present density and thickness comparable to those of most commercial insulating products already used in buildings. It can be concluded through the results of table 4 that the air permeability increases when the density of nonwovens is contrary to what is expected. Typically, a higher density of the nonwoven reduces its air permeability because there is less space between the fibres, so they prevent air from passing through the structure. But in this case, the fibres used are rigid and thick, leading to an increase in the fibres' interspace in a given volume.

The kenaf and alfa fibre nonwovens have the same range of thermal conductivity, which varies from 0.034 $W{\cdot}m^{-1}{\cdot}K^{-1}$ to 0.041 $W{\cdot}m^{-1}{\cdot}K^{-1}$ and which is similar to other commercialised insulation materials.

Table 5 presents the thermal conductivity of some commercial products compared to those of the studied samples. Through the values presented in the table, kenaf and alfa panels present better thermal conductivity than glass fibre panels and values similar to those of rock wool and polystyrene panels, which are the most commonly used in building.

Low thermal conductivity values lead to good insulation properties of both alfa and kenaf fibres, and this can be explained by the fact that these fibres present a porous microstructure [14] as presented in figure 3 for kenaf fibres and as reported in the work of Ayadi et al. [15] for alfa fibres. The fibre structure is porous (figure 3), allowing air to be stored and trapped in the fibre, which prevents heat transfer through the panel [13, 16, 17].

A flame test was carried out on a panel made of treated and untreated kenaf and alfa fibres. Results of this test are illustrated in figure 4 for samples made from kenaf fibres and figure 5 for those made from alfa fibres.

For untreated kenaf fibre, the sample begins to burn after 1 s of exposure and ignites after 10 s. The flame continues to spread slowly after the burner is removed. But for treated kenaf fibre, there is a superficial burn in the presence of a burner, and when it is removed, sparks appear and disappear in fractions of a second. By exploring the photos in figure 4, it can be seen that the flame impact on the panels has diminished, and the damaged area is smaller.

For untreated alfa fibre, the sample begins to burn after 1 s and ignites after 4.8 s. The flame continues to spread after the burner removal. For treated alfa fibres, there is a superficial burn in the presence of the burner, and the flame extinguishes simultaneously with burner removal. Figure 5 illustrates the damaged area for both untreated and treated alfa fibre panels. The damaged area in the treated fibre panel is smaller.

NaCl has the potential to be used as a fire extinguishing agent. It can form a thin layer of sodium chloride on the surface of the fibre. This layer acts as a physical barrier to the burning material, stopping the oxygen supply and extinguishing the fire [13].

Table 4

NONWOVEN PROPERTIES						
Sample	**Mi (g)**	**Ms (g)**	**Air permeability (mm/s)**	**Thickness (mm)**	**Density ($kg{\cdot}m^{-3}$)**	**k ($W{\cdot}m^{-1}{\cdot}K^{-1}$)**
A1	203.81	191.72	1116.69 ± 108.31	12.55 ± 2.16	180.43 ± 13.08	0.040
A2	234.73	222.26	453.80 ± 95.75	18.83 ± 0.22	138.07 ± 1.61	0.039
K1	206.18	194.65	546.81 ± 35.15	20.57 ± 0.25	111.32 ± 1.39	0.034
K2	65.42	61.71	1866.63 ± 268.27	8.04 ± 0.40	90.38 ± 4.56	0.041

Note: Mi: initial panel weight; Ms: panel weight after drying at 70°C.

Table 5

EXAMPLES OF THERMAL CONDUCTIVITY OF COMMERCIALISED PRODUCTS [13]					
	Kenaf	**Alfa**	**Glass fibre**	**Polystyrene**	**Rock wool**
k ($W{\cdot}m^{-1}{\cdot}k^{-1}$)	0.034 – 0.041	0.039 – 0.040	0.030 – 0.060	0.030 – 0.040	0.030 – 0.040

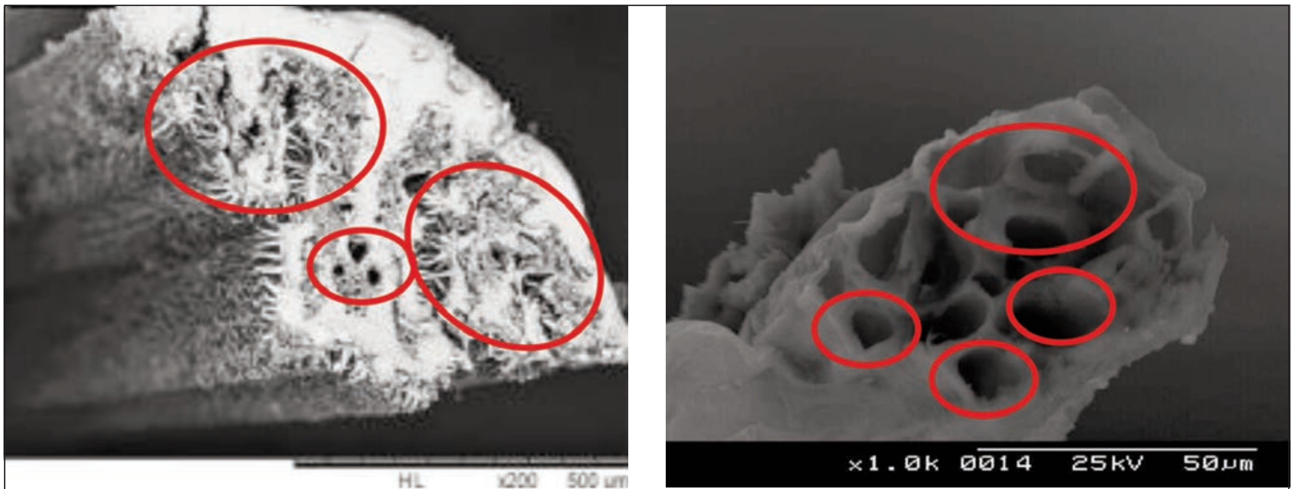

a *b*

Fig. 3. SEM image of: *a* – Alfa Fibre cross-section; *b* – Kenaf fibre cross-section

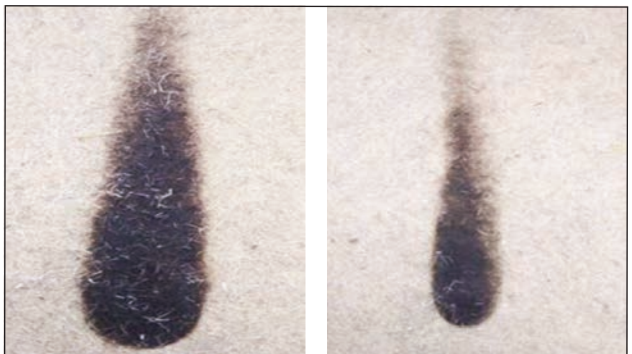

a *b*

Fig. 4. Image of Kenaf nonwoven panel after flame test: *a* – untreated fibre; *b* – treated fibre

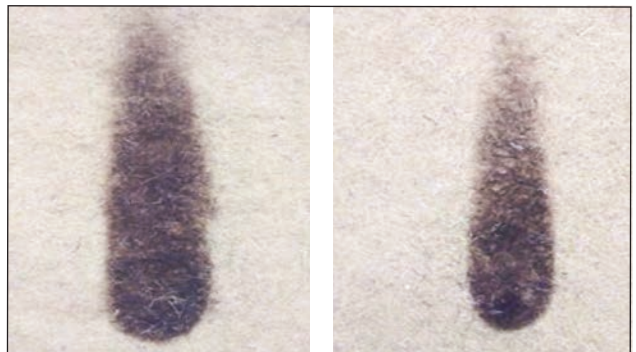

a *b*

Fig. 5. Image of alfa nonwoven panel after flame test: *a* – non-treated fibre; *b* – treated fibre

CONCLUSION

Eco-friendly nonwoven insulation panels were successfully produced from alfa and kenaf fibres. The results demonstrate that these biobased materials exhibit thermal properties comparable to conventional commercial insulation panels, especially in thermal conductivity values ranging from 0.034 $W \cdot m^{-1} \cdot K^{-1}$ to 0.041 $W \cdot m^{-1} \cdot K^{-1}$ for our panels and from 0.030 $W \cdot m^{-1} \cdot K^{-1}$ to 0.060 $W \cdot m^{-1} \cdot K^{-1}$ reported for commercialised products.

Among the developed nonwovens, kenaf-based panels displayed the most efficient thermo-insulation performance, highlighting the potential of this fibre in eco-friendly building.

Air permeability measurements highlighted the strong dependency on fibre.

Kenaf-based panels generally exhibit higher air permeability than alfa-based panels, indicating a more open and porous structure. This characteristic can enhance vapour transfer and breathability, which is beneficial in certain building applications.

Additionally, an ecological fire retardancy treatment applied to the fibres and based on the use of NaCl (salt) improved the behaviour of the panels when exposed to the flame, confirming its effectiveness as a simple and non-toxic enhancement method.

Overall, Kenaf and alfa natural fibres proved their competitive alternatives to the commercial insulation products from a thermal insulation performance standpoint.

Future work should focus on evaluating the effects of moisture absorption on the panels' mechanical and physical properties and ensuring long-term durability in real building conditions.

REFERENCES

[1] Abu-Jdayil, B., Mourad, A.H., Hittini, W., Hassan, M., Hameedi, S., T*raditional, state-of-the-art and renewable thermal building insulation materials: An overview*, In: Constr Build Mater, 2019, 214, 709–735, https://doi.org/10.1016/J.CONBUILDMAT.2019.04.102

[2] Ahmed, A., Qayoum, A., Mir, F.Q., *Investigation of the thermal behavior of the natural insulation materials for low temperature regions*, In: Journal of Building Engineering, 2019, 26, 100849, https://doi.org/10.1016/j.jobe.2019.100849
[3] Zhou, X., Zheng, F., Li, H., Lu, C., *An environment-friendly thermal insulation material from cotton stalk fibres*, In: Energy Build, 2010, 42, 7, 1070–1074, https://doi.org/10.1016/j.enbuild.2010.01.020
[4] Zach, J., Hroudová, J., Korjenic, A., *Environmentally efficient thermal and acoustic insulation based on natural and waste fibres*, In: Journal of Chemical Technology & Biotechnology, 2016, 91, 8, 2156–2161, https://doi.org/10.1002/JCTB.4940
[5] Erkmen, J., Yavuz, H.I., Kavci, E., Sari, M., *A new environmentally friendly insulating material designed from natural materials*, In: Constr Build Mater, 2020, 255, 119357, https://doi.org/10.1016/J.CONBUILDMAT.2020.119357
[6] Ajabli, H., Zoubir, A., Elotmani, R., Louzazni, M., Kandoussi, K., Daya, A., *Review on Eco-friendly insulation material used for indoor comfort in building*, In: *Renewable and Sustainable Energy Reviews*, 2023, 185, 113609, https://doi.org/10.1016/J.RSER.2023.113609
[7] Savic, A., Antonijevic, D., Jelic, I., Zakic, D., *Thermomechanical behavior of bio-fibre composite thermal insulation panels*, In: Energy Build, 2020, 229, 110511, https://doi.org/10.1016/j.enbuild.2020.110511
[8] Majumder, A., Canale, L., Mastino, C.C., Pacitto, A., Frattolillo, A., Dell'isola, M., *Thermal Characterization of Recycled Materials for Building Insulation*, In: Energies, 2021, 14, 12, 3564, https://doi.org/10.3390/EN14123564
[9] Hadded, A., Benltoufa, S., Fayala, F., Jemni, A., *Thermo physical characterization of recycled textile materials used for building insulating*, In: Journal of Building Engineering, 2016, 5, 34–40, https://doi.org/10.1016/J.JOBE.2015.10.007
[10] Ali, M., et al., *Thermal Analyses of Loose Agave, Wheat Straw Fibres and Agave/Wheat Straw as New Hybrid Thermal Insulating Materials for Buildings*, In: Journal of Natural Fibres, 2021, 18, 12, 2173–2188, https://doi.org/10.1080/15440478.2020.1724232
[11] Korjenic, A., Petránek, V., Zach, J., Hroudová, J., *Development and performance evaluation of natural thermal-insulation materials composed of renewable resources*, In: Energy Build, 2011, 43, 9, 2518–2523, https://doi.org/10.1016/J.ENBUILD.2011.06.012
[12] Ben Mlik, Y., Jaouadi, M., Jmali, M., Slah, M., *New lab-scale device for nonwoven production: optimization of setting parameters*, In: The Journal of The Textile Institute, 2016, 107, 12, 1636–1643, https://doi.org/10.1080/00405000.2015.1133015
[13] Loh, T.W., Nguyen, K.T., *Durability and fire resistance of compressed wheat-straw (Triticum aestivum) panels subjected to real-world aging environments*, In: Ind Crops Prod, 2023, 203, https://doi.org/10.1016/j.indcrop.2023.117141
[14] Cascone, S., Catania, F., Gagliano, A., Sciuto, G., *Energy performance and environmental and economic assessment of the platform frame system with compressed straw*, In: Energy Build, 2018, 166, 83–92, https://doi.org/10.1016/J.ENBUILD.2018.01.035
[15] Ayadi, M., et al., *Influence of Anatomy, Microstructure, and Composition of Natural Fibres on the Performance of Thermal Insulation Panels*, In: ACS Omega, 2023, 8, 51, 48673–48688, https://doi.org/10.1021/ACSOMEGA.3C02481
[16] Kanat, Z.E., *Modelling thermal resistance of woven fabrics in wet state*, In: Industria Textila, 2025, 76, 1, 3–10, https://doi.org/10.35530/IT.076.01.2024134
[17] Sarpkaya, Ç., Sabir, E.C., *Investigation of sound and thermal properties of basalt, aramid and carbon reinforcement layered composites*, In: Industria Textila, 2025, 76, 6, 883–890, https://doi.org/10.35530/IT.076.06.202522

Authors:

YOSR BEN MLIK[1], RIADH ZOUARI[1], MOUNIR JAOUADI[1], RIM HOUIDI[2], CHAMA FAIDI[2], EMILIA VISILEANU[3]

[1]Laboratory of Textile Engineering, University of Monastir, Tunisia

[2]The Higher Institute of Technological Studies ISETKh, Monastir, Tunisia

[3]National Research and Development Institute for Textiles and Leather, Bucharest, Romania

Corresponding author:

YOSR BEN MLIK
e-mail: yosrbenmlik@gmail.com

Examining factors influencing sustainable technology adoption among apparel manufacturers with supportive HR practices

DOI: 10.35530/IT.077.04.2025159

NUHA AWADH ALJUAID ABDULRAHMAN AWADH ALJUAID

ABSTRACT – REZUMAT

Examining factors influencing sustainable technology adoption among apparel manufacturers with supportive HR practices

This study examines the influence of supportive HR practices, knowledge of apparel technology, environmental issues, competitor pressure, customer pressure, and regulatory pressure on employee intention to adopt sustainable technology in apparel manufacturing. It also explores the moderating role of government support on the relationship between employee attitude and intention to adopt sustainable technology. Data were collected from employees in apparel manufacturing firms. Findings reveal that these factors explain 74.2% of the variance in employee attitude toward adopting sustainable technology. Additionally, government support and employee attitude account for 30.3% of the variance in employee intention to adopt such technology. Effect size f^2 analysis highlights supportive HR practices and knowledge of apparel technology as the most significant predictors of employee attitude. Practically, the study emphasises the importance of knowledge, competitor pressure, and government support in fostering employee confidence and adoption of sustainable technology. The framework is original and schematizes these influencing factors.

Keywords: *environmental issues, regulator pressure, competitor pressure, customer pressure, sustainable technology*

Examinarea factorilor care influențează adoptarea tehnologiei durabile în rândul producătorilor de îmbrăcăminte cu practici de resurse umane favorabile

Acest studiu examinează influența practicilor de resurse umane favorabile, a cunoștințelor privind tehnologia din industria de îmbrăcăminte, a problemelor de mediu, a presiunii concurențiale, a presiunii clienților și a presiunii normative asupra intenției angajaților de a adopta tehnologii durabile în producția de îmbrăcăminte. De asemenea, studiul explorează rolul moderator al sprijinului guvernamental asupra relației dintre atitudinea angajaților și intenția acestora de a adopta tehnologii durabile. Datele au fost colectate de la angajații unor firme din industria de îmbrăcăminte. Rezultatele arată că acești factori explică 74,2% din variația atitudinii angajaților față de adoptarea tehnologiilor durabile. În plus, sprijinul guvernamental și atitudinea angajaților reprezintă 30,3% din variația intenției angajaților de a adopta astfel de tehnologii. Analiza mărimii efectului f^2 evidențiază practicile de resurse umane favorabile și cunoștințele privind tehnologia confecțiilor ca fiind cei mai semnificativi predictori ai atitudinii angajaților. Din punct de vedere practic, studiul subliniază importanța cunoștințelor, a presiunii concurenței și a sprijinului guvernamental în consolidarea încrederii angajaților și în adoptarea tehnologiilor durabile. Cadrul conceptual este original și schematizează acești factori de influență.

Cuvinte-cheie: *probleme de mediu, presiunea autorităților de reglementare, presiunea concurenței, presiunea clienților, tehnologie durabilă*

INTRODUCTION

With the advent of the 4th industrial revolution organizations are using cutting-edge technology to bring innovation in the manufacturing process.

Nevertheless, less attention is paid to sustainable technology to promote green practices in the manufacturing process [1]. The apparel industry is considered the most polluted sector globally, producing vast amounts of waste and emitting hazardous gases [2]. Moreover, the clothing manufacturing process consumes excessive natural resources and generates waste disposal in the environment, causing air and water pollution [2, 3]. Due to rising concern about environmental pollution, the United Nations climate change body has introduced a framework, namely the Fashion Industry Charter for Climate Action (FICCA), with an objective to achieve zero emissions by 2025 [4]. Thus, apparel manufacturers are striving to find factors which conserve natural resources and reduce greenhouse gases. Nevertheless, sustainable technology is recognised as an emerging technology to reduce the carbon footprint in the clothing manufacturing process. Sustainable technology assists manufacturers in monitoring and controlling the manufacturing process through automation, resulting in efficient production with minimum waste [5]. Although sustainable technology reduces energy and material consumption and mitigates the carbon footprint in the manufacturing process, adoption of sustainable technologies among apparel manufacturers is still in its initial stages [6].

The apparel industry in Saudi Arabia is predicted to grow by 2.68% from the period of 2024 to 2028, with an attractive market volume of US$ 19.35 bn [7]. Nevertheless, there is less discussion on how clothing manufacturers could benefit through sustainable technology. Therefore, current research fills the research gap and develops a sustainable technology adoption model in the context of apparel manufacturing. The research model of this study comprises factors like supportive HR practices, knowledge of apparel technology, knowledge of environmental issues, competitor pressure, customer pressure and regulatory pressure and investigates industry willingness towards adoption of sustainable technology. The factors underpinning the research framework have a strong conceptual linkage with the adoption of sustainable technology. For instance, studies have revealed that supportive HR practices encourage employees to adopt sustainable technologies in manufacturing firms [8–10]. Similarly, prior studies have revealed that employees with adequate knowledge about apparel technology and environmental issues have shown more inclination toward adoption of sustainable technology in the apparel industry [1, 11, 12]. According to a previous study [12], deploying energy and material-saving technologies has created competitive pressure among apparel manufacturers. In addition to that, customer pressure and regulatory pressure have also pushed manufacturers to adopt sustainable and environmentally friendly technologies in apparel manufacturing [12, 13].

Consistent with the above arguments, this study has assumed that supportive HR practices, knowledge of apparel technology, knowledge of environmental issues, competitor pressure, customer pressure and regulatory pressure are key factors that could motivate employees to adopt sustainable technologies in the apparel manufacturing industry. More precisely, this study strives to investigate how supportive HR practices impact employee attitudes toward adopting sustainable technology in the apparel industry. How does knowledge about apparel technology and environmental issues impact employee attitude to adopt sustainable technology? Do competitor, customer and regulatory pressure impact employee attitudes toward adopting sustainable technology in the apparel industry? Aside from the above research objectives, this study adds a new dimension to the research framework and investigates the moderating effect of government support. This study seeks to investigate how government support moderates the relationship between employee attitudes and their behavioural intention to adopt sustainable technology. Although sustainable technology has been examined in the food industry and in marine renewable energy projects [14, 15], its impact in the apparel sector remains largely overlooked. Nevertheless, this study is unique as it develops a completely new sustainable model and directs employees that with sustainable technologies, they could reduce energy and material consumption, resulting in a positive contribution to the environment and society. The remainder of this research is followed by a literature review, questionnaire development, research methods, data analysis, discussion, research contributions to theory and practice, conclusion, research limitations and future research directions.

LITERATURE REVIEW

Supportive HR practices, knowledge and environment

The adoption of technology is a complex phenomenon, and therefore recruitment of technology-oriented personnel could play an important role in achieving organisational goals. Traditionally, the role of HR practices is to equip employees to deal with ongoing challenges through training and development programs. Nevertheless, supportive human resource practices ensure that employees and employers are both on the same page to achieve sustainable goals [16]. Therefore, and with the support of prior literature, it is assumed that supportive HR practices encourage employees to adopt sustainable technologies in the apparel manufacturing process [8–10, 17]. Aside from supportive HR practices, two other important factors, namely knowledge about apparel technology and environmental issues, have gained significant attention of academician and practitioners in sustainability literature. According to a previous study [11], manufacturing firms experiencing regulation regarding sustainability must have adequate knowledge about apparel technology.

Adequate knowledge about sustainable technology assists managers to understand the impact of technology in achieving the firm's sustainable goals. Literature has substantial support that employees with adequate knowledge of apparel technology have shown more inclination toward adoption of sustainable technology in the apparel industry [1, 11]. Similarly, knowledge about environmental issues enables employees to understand the adverse impact of apparel manufacturing on the environment. Prior studies have revealed that employees having knowledge about environmental issues tend to show more inclination towards adoption of sustainable technology [1, 12]. Nevertheless, a lack of knowledge about the impact of waste on environmental issues could reveal undesirable and disastrous outcomes [18]. Therefore, employees with higher knowledge of environmental issues will prefer to adopt sustainable technologies in the apparel manufacturing process [12, 18]. Therefore, the following hypotheses are assumed:

H1: Supportive HR practices are positively related to employee attitude toward adopting sustainable technology.

H2: Knowledge about apparel technology is positively related to employee attitude toward adopting sustainable technology.

H3: Knowledge about environmental issues is positively related to employee attitude toward adopting sustainable technology.

Competitor, customer and regulatory pressure

The proliferation of technology has led organisations to adopt the latest technology software to bring innovation in the manufacturing process. Among these technologies, sustainable technology has gained significant attention due to echo friendly nature. In addition to that, the Fashion Industry Charter for Climate Action (FICCA) has also encouraged manufacturers to adopt sustainable technology in the apparel manufacturing process. Sustainable technology improves the manufacturing process and ensures business continuity. Moreover, Hoque et al. [12] revealed that deploying energy- and material-saving technologies in the apparel manufacturing process provides a competitive edge to apparel manufacturers.

Sustainable technologies bring innovation and empower manufacturers to remain competitive in a volatile market. In line with the above argument, authors like Baah et al. [19] have stated that adoption of sustainable technology enhances competitive advantage by reducing energy and material consumption in the manufacturing process. Therefore, competitor pressure is considered a unique driving force that motivates manufacturers to adopt sustainable technology in the manufacturing process. Moreover, the literature has also revealed that customer and regulatory pressures are key antecedents of technology adoption. It is established that manufacturers' sustainable practices are largely dependent on customer expectations of how they respond to eco-friendly products. Studies have revealed that customers have refused to buy company products that degrade or are harmful to the environment [20, 21]. Therefore, customer pressure is considered a key factor that pushes manufacturers to adopt sustainable and environmentally friendly technologies in the apparel manufacturing process [12, 13]. Similarly, the importance of regulatory bodies cannot be ignored in the corporate world. Prior literature has revealed that manufacturing firms are facing local and global regulatory pressure to use sustainable technologies in building green products [22–24]. Therefore, regulatory pressure is considered another force that encourages employees to use sustainable and environmentally friendly technology. Thus, the following hypotheses are assumed:

H4: Competitor pressure is positively related to employee attitude toward adopting sustainable technology.

H5: Customer pressure is positively related to employee attitude toward adopting sustainable technology.

H6: Regulatory pressure is positively related to employee attitude toward adopting sustainable technology.

The moderating effect of government support

The adoption of sustainable technology could be increased through government support. According to a previous study [11], a green manufacturing process is not possible without government support. The role of government is not only to push manufacturers towards adoption of green technology but also to provide support through incentives and subsidies for green technology. There is mutual consensus among researchers that adoption of sustainable technology in the manufacturing process brings efficiency and boosts green production [11, 25–27]. Prior studies have revealed that government bodies could exert pressure on manufacturers to train employees, provide technical support and adequate infrastructure, which in turn encourages employees to adopt sustainable technology in apparel manufacturing [25–27]. Moreover, adoption of sustainable technology will assist apparel manufacturers to achieve United Nations sustainable goals, such as the Fashion Industry Charter for climate action. Nevertheless, without stakeholders like the government, this target could not be achieved. Thus, government support is considered a key determinant of employee attitude and intention to adopt sustainable technology [26]. Therefore, it is inferred that government support moderates the relationship between employee attitude and intention to adopt sustainable technology in the manufacturing process. Studies have also established that with the deployment of energy-saving technologies, apparel manufacturers could reduce the impact of CO_2 emissions [28, 29]. Therefore, the following hypotheses are assumed:

H7: Employee attitude is positively related to behavioural intention to adopt sustainable technology.

H8: Government support positively moderates the relationship between employee attitude and behavioural intention to adopt sustainable technology.

RESEARCH METHODS

Scale development

The research framework has outlined multiple latent factors that were measured with scale items. In quantitative kind of research, the literature has suggested either adopting or developing a completely new scale. Nevertheless, in this study, a scale exists, and therefore scale items are adopted. Supportive human resource practices are measured with scale items established by some researchers [16, 17, 30, 31]. Scale items for the latent factor knowledge about apparel technology were adapted from previous studies [2, 32]. Scale items for knowledge about environmental issues were adapted from Dickson [32] and Xie et al. [33]. Similarly, competitor pressure scale items were adapted from research work conducted by Shahadat et al. [27]. Scale items for the factor customer pressure were adapted from Lin and Ho [30]. Likewise, scale items for regulatory pressure were adapted from research work conducted by Ullah et al. [34]. Scale items for the factors attitude and intention to adopt sustainable technology were adapted from previous studies [16, 27, 35, 36]. Therefore, government support factors are measured with scale items adapted from Shahadat et al. [27] and Lin and Ho

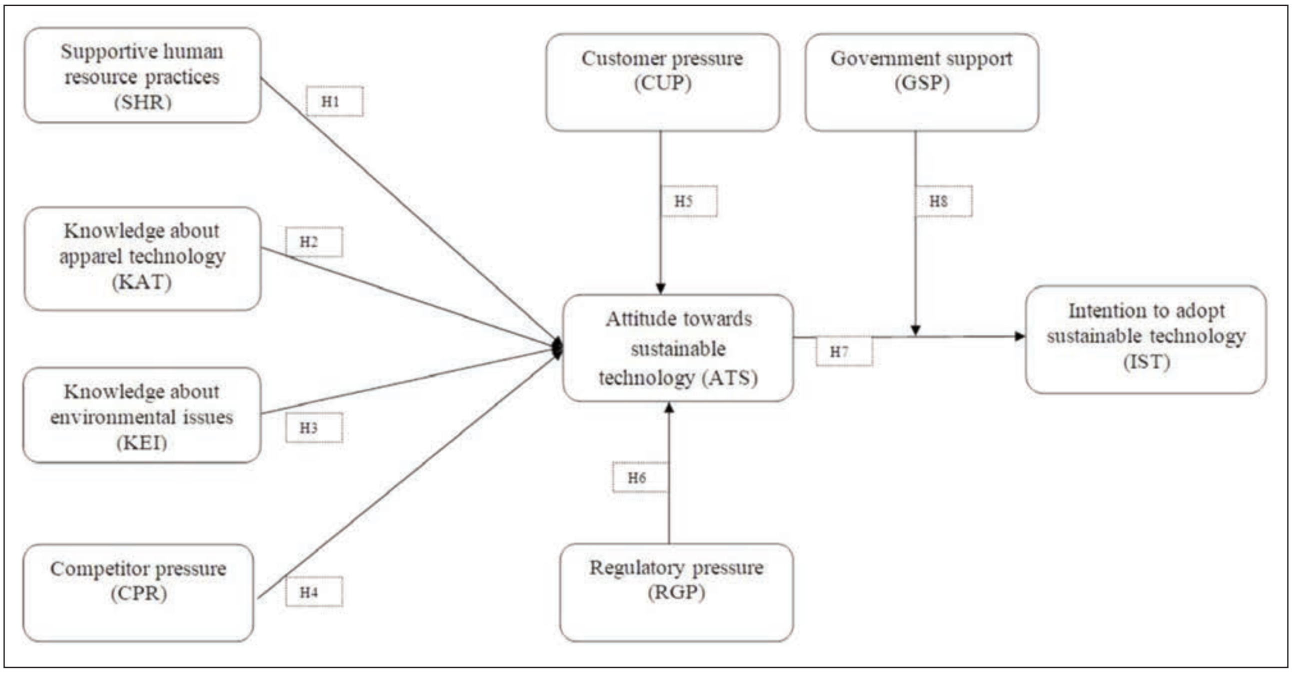

Fig. 1. Research model

[30]. These scale items were emerged into survey questionnaire. The survey questionnaire was evaluated by an expert panel that included three experts from academia and four senior managers from apparel manufacturers. Following the experts' opinion, contextual changes were made in scale items wherein the "technology adoption" phrase was changed to "sustainable technology adoption" to ensure clarity in scale items. Finally, these refined scale items were measured with a seven-point Likert scale ranging from 1 (Strongly disagree) to 7 (Strongly agree).

Sample size and data collection

The population of this study is employees working in apparel manufacturing firms. Consistent with research objectives, employees working in apparel manufacturing firms are considered the most relevant individuals to answer questions about sustainable technology adoption. Nonetheless, the sample size is selected following the criterion suggested by Rahi [37]. Rahi has postulated that for factor analysis, data must be ten times greater than scale items. Following that, in this study, 320 (32×10) responses are required for factor analysis. The data collection process was started in the first week of July 2024 and ended in the second week of August 2024. Respondents were approached physically and requested to fill out the survey questionnaire. Moreover, respondents were also briefed about sustainable technology in apparel manufacturing. Employees' participation in this study was completely voluntary, with a guarantee that personal information would not be disclosed. Data were collected through a purposive sampling approach that is consistent with prior studies [38, 39]. This approach is also relevant as respondents were selected from apparel manufacturing firms purposively with an aim that they would have better knowledge about sustainable technology adoption in the apparel manufacturing process. Therefore, 389 questionnaires were distributed among employees working in apparel manufacturing firms. After questionnaire distribution, several reminders were given to respondents through phone calls and by email. Nevertheless, only 335 responses were recovered and used for empirical investigation.

STATISTICAL ANALYSIS AND RESULTS

Descriptive analysis and common method bias

This study has analysed respondents' profiles using descriptive analysis. Data in this study have comprised 230 valid responses. Among 230 responses, 33% were found to be aged between 21 and 30 years. Therefore, 98 respondents were found in the age bracket of 31 to 40 years. Nevertheless, the remaining 55 respondents had revealed their age between 41 and 50 years. Similarly, respondents were asked about their experience in the apparel industry. Results indicate that 36 respondents were working in the apparel industry for the last 5 years. Therefore, 138 respondents were attached to the apparel industry for the last 10 years. Nonetheless, 56 respondents were found with a maximum experience of 15 years and onward. These findings have ensured that all cadre employees from junior level to senior management have participated in the research survey. Respondent's gender was asked, and results revealed that among 230 respondents, 203 were male and the remaining 27 were female employees. After analysing respondents profile common method bias issue is addressed with procedural and statistical remedies [37, 40]. Although literature has suggested multiple statistical analyses to address common method variance bias (CMVB), in this study, data are computed with Harman's single-factor analysis [16, 17]. According to Rahi [16] espouses that Harman's analysis has the potential to detect the CMVB issue and recommended threshold value, i.e. 40% of the first un-rotated factor. To compute Harman's test, data are analysed with SPSS software. Statistical results have revealed that the variance explained by the first un-rotated factor was only 13% and hence confirmed data validity. In the following section, factor analysis is conducted with a structural equation modelling approach.

Structural equation modelling

Structural equation modelling is considered the most reliable approach for multivariate analysis. Therefore, data are estimated with a structural equation modelling approach following a two-stage approach, namely measurement model assessment and structural model assessment. At the first step, factor reliability, discriminant validity and convergent validity are established. Therefore, hypotheses, effect size and coefficient of determination are examined in the second stage. At the first stage, factor loadings are achieved following the threshold value of 0.60 as recommended by Rahi [41]. Therefore, factor reliability is established following the threshold value of 0.70 in line with previous studies [41, 42]. Similarly, convergent validity is established with average variance extracted following the threshold value of AVE 0.50 as recommended by prior researchers [40, 41].

Findings of the measurement model are shown in table 1, depicting satisfactory convergent validity, indicator reliability and factor reliability.

After establishing factor reliability, discriminant validity of the factors is tested. At the first stage, discriminant

Table 1

MEASUREMENT MODEL ASSESSMENT

Scale items	Loadings	AVE	CR	α
ATS1: Sustainable technology-enabled apparel manufacturing is useful.	0.848	0.798	0.922	0.874
ATS2: Sustainable technology-based manufacturing process is beneficial.	0.917			
ATS3: Sustainable technology-driven manufacturing is attractive.	0.913			
CPR1: Adoption of sustainable technology is strategically necessary to compete in the market.	0.791	0.640	0.877	0.813
CPR2: Adoption of sustainable technology assists in achieving competitive advantages.	0.788			
CPR3: I am afraid that we will lose customers due to lack of sustainable technology in the manufacturing process.	0.829			
CPR4: Adoption of sustainable technology will enable us to compete in market place.	0.793			
CUP1: Our customers are concerned about environmental changes.	0.954	0.756	0.902	0.869
CUP2: Our customers feel that environmental safety must be considered during manufacturing.	0.841			
CUP3: Our customers feel that apparel manufacturers must use sustainable technology for environmental safety.	0.805			
GSP1: Government is giving support to apparel manufacturers to adopt sustainable technology in the manufacturing process.	0.796	0.699	0.874	0.784
GSP2: Government is providing technical assistance to manufacturers to adopt sustainable technology.	0.822			
GSP3: Government is providing subsidies on green technology to encourage manufacturers to adopt sustainable technology.	0.887			
IST1: Adoption of sustainable technology reduces carbon emissions in the environment.	0.954	0.848	0.943	0.910
IST2: Adoption of sustainable technology increases speed and reliability in the manufacturing process.	0.898			
IST3: Adoption of sustainable technology reduces carbon emissions in the environment.	0.909			
KAT1: This firm has adequate knowledge about sustainable technology.	0.879	0.835	0.938	0.901
KAT2: This firm can compete in the market through sustainable technology.	0.938			
KAT3: This firm can make environmentally friendly products with sustainable technology.	0.924			
KEI1: Manufacturing process is designed to reduce environmental impacts.	0.822	0.825	0.950	0.928
KEI2: Manufacturing firms are reachable for environmental audits.	0.961			
KEI3: Apparel manufacturers are adopting cleaner production methods.	0.940			

Table 1 (continuation)

Scale items	Loadings	AVE	CR	α
KEI4: Stakeholders are involved in planning and executing environmental practices.	0.904			
RGP1: Apparel manufacturers are being strictly monitored by regulators.	0.852	0.636	0.875	0.810
RGP2: Apparel manufacturers are bound to follow environmental regulations.	0.757			
RGP3: Apparel manufacturers could face penalties over noncompliance with environmental regulators.	0.793			
RGP4: Production standards in manufacturing firms have been strictly imposed by regulators.	0.786			
SHR1: Employees get equal opportunities to learn and use sustainable technology.	0.919	0.730	0.914	0.876
SHR2: This firm offers flexible training programs to improve employee skills.	0.835			
SHR3: Employees get quick technical support to solve problems.	0.937			
SHR4: Employees are encouraged to share knowledge.	0.706			

validity is established with the Fornell and Larcker method, and then results were compared with HTMT ratios and cross-loading values. In the Fornell and Larcker analysis, the very first value of the factor in the correlation table is considered the square root of average variance extracted.

Therefore, a study such as Rahi [37] suggests that the square root of the average variance extracted should be greater than its correlations with other constructs. Similarly, Fornell [43] has recommended that for satisfactory discriminant validity, the square root of average variance extracted should be higher in comparison to other factor values. Data were estimated, and results have shown that the first value of each factor is found higher, demonstrating that factors are discriminant. Table 2 demonstrates the results of the discriminant analysis and hence establishes the discriminant validity of the factors.

To ensure discriminant validity of the factors, the Heterotrait-Monotrait Ratio (HTMT) analysis is taken into consideration. There is debate in statistical literature that HTMT analysis is the most reliable analysis to compute discriminant validity of the factors [37, 44, 45]. Consequently, data were also confirmed with HTMT analysis. According to Rahi [37], a threshold value of 0.90 has been suggested, indicating that the associated estimates should fall below this limit. Nevertheless, results have disclosed that HTMT values are lower than the threshold value and hence confirmed the discriminant validity of the factors. Results of the discriminant validity are shown in table 3.

The cross-loading analysis is piloted to assess discriminant validity. In cross-loading analysis, factor loadings are compared with other factors' loadings following a pattern that each factor must have higher loadings in comparison to other factors [37, 46]. Nonetheless, results have disclosed that loadings are satisfactory and each factor loading is greater than other factors' loadings in cross-loading comparison. Table 4 depicts results of the cross-loading analysis.

Hypotheses analysis

Hypotheses are tested with a structural model. Structural model assessment reveals path coefficient values, p-values, and t-statistics that are further evaluated with threshold values to accept or reject hypotheses. Nevertheless, these values were

Table 2

DISCRIMINANT VALIDITY									
Factors	**ATS**	**CPR**	**CUP**	**GSP**	**IST**	**KAT**	**KEI**	**RGP**	**SHR**
ATS	0.893								
CPR	0.490	0.800							
CUP	0.130	0.079	0.869						
GSP	0.048	–0.004	0.143	0.836					
IST	0.530	0.340	0.129	0.112	0.921				
KAT	0.630	0.313	0.132	0.045	0.312	0.914			
KEI	0.536	0.231	0.054	–0.050	0.288	0.214	0.908		
RGP	0.082	0.051	0.009	–0.003	0.089	0.001	0.056	0.798	
SHR	0.703	0.355	0.113	0.078	0.425	0.349	0.417	0.189	0.854

Table 3

HETEROTRAIT MONOTRAIT RATIO METHOD									
Factors	**ATS**	**CPR**	**CUP**	**GSP**	**IST**	**KAT**	**KEI**	**RGP**	**SHR**
ATS									
CPR	0.582								
CUP	0.124	0.085							
GSP	0.059	0.065	0.157						
IST	0.580	0.396	0.125	0.133					
KAT	0.703	0.363	0.160	0.073	0.343				
KEI	0.590	0.266	0.074	0.061	0.304	0.234			
RGP	0.095	0.089	0.082	0.102	0.107	0.065	0.077		
SHR	0.761	0.395	0.096	0.101	0.468	0.368	0.450	0.220	

Table 4

CROSS LOADINGS									
Coding	**ATS**	**CPR**	**CUP**	**GSP**	**IST**	**KAT**	**KEI**	**RGP**	**SHR**
ATS1	0.848	0.422	0.064	0.021	0.366	0.470	0.454	0.012	0.487
ATS2	0.917	0.441	0.132	0.063	0.564	0.560	0.541	0.116	0.722
ATS3	0.913	0.452	0.143	0.038	0.468	0.645	0.436	0.077	0.645
CPR1	0.386	0.791	0.077	0.020	0.362	0.219	0.224	0.006	0.232
CPR2	0.376	0.788	0.041	0.017	0.289	0.202	0.202	0.017	0.187
CPR3	0.395	0.829	0.071	–0.052	0.259	0.281	0.157	0.042	0.304
CPR4	0.411	0.793	0.062	0.004	0.184	0.294	0.158	0.093	0.402
CUP1	0.159	0.081	0.954	0.153	0.143	0.119	0.049	–0.010	0.141
CUP2	0.067	0.063	0.841	0.084	0.069	0.146	0.037	0.022	0.042
CUP3	0.039	0.046	0.805	0.106	0.090	0.074	0.065	0.056	0.048
GSP1	0.011	–0.022	0.171	0.796	0.089	–0.023	–0.067	0.013	0.030
GSP2	0.078	0.025	0.082	0.822	0.086	0.067	–0.031	0.035	0.080
GSP3	0.033	–0.012	0.106	0.887	0.104	0.066	–0.030	–0.047	0.083
IST1	0.470	0.325	0.127	0.095	0.954	0.297	0.219	0.066	0.384
IST2	0.540	0.318	0.134	0.085	0.898	0.286	0.367	0.097	0.437
IST3	0.444	0.291	0.091	0.132	0.909	0.278	0.190	0.081	0.343
KAT1	0.602	0.295	0.039	0.051	0.316	0.879	0.189	–0.050	0.341
KAT2	0.572	0.297	0.144	0.035	0.262	0.938	0.214	–0.002	0.309
KAT3	0.549	0.264	0.184	0.037	0.275	0.924	0.182	0.060	0.304
KEI1	0.476	0.221	0.002	–0.045	0.176	0.204	0.822	0.034	0.287
KEI2	0.526	0.232	0.074	–0.067	0.309	0.197	0.961	0.057	0.439
KEI3	0.507	0.201	0.081	–0.009	0.303	0.184	0.940	0.059	0.397
KEI4	0.426	0.180	0.032	–0.064	0.250	0.192	0.904	0.052	0.385
RGP1	0.076	0.027	0.050	0.071	0.104	–0.001	0.058	0.852	0.153
RGP2	0.049	0.075	0.069	0.057	0.127	0.037	0.084	0.757	0.109
RGP3	0.062	0.032	–0.015	–0.080	0.051	–0.034	0.058	0.793	0.172
RGP4	0.069	0.041	–0.065	–0.057	0.015	0.008	–0.010	0.786	0.161
SHR1	0.618	0.323	0.105	0.115	0.402	0.264	0.369	0.197	0.919
SHR2	0.716	0.408	0.122	0.024	0.350	0.434	0.366	0.118	0.835
SHR3	0.617	0.259	0.091	0.079	0.398	0.279	0.419	0.206	0.937
SHR4	0.362	0.160	0.047	0.052	0.291	0.143	0.236	0.122	0.706

Table 5

HYPOTHESES TESTING						
Hypothesis	**Path**	***B***	**STDEV**	**t-statistics**	**Significance**	**Decision**
H1	SHR → ATS	0.410	0.058	7.033	0.000	Accepted
H2	KAT → ATS	0.380	0.059	6.492	0.000	Accepted
H3	KEI → ATS	0.245	0.041	6.031	0.000	Accepted
H4	CPR → ATS	0.170	0.036	4.662	0.000	Accepted
H5	CUP → ATS	0.008	0.044	0.173	0.431	Rejected
H6	RGP → ATS	-0.018	0.036	0.501	0.308	Rejected
H7	ATS → IST	0.527	0.063	8.401	0.000	Accepted

retrieved through the bootstrapping method as recommended by prior researchers [41–47]. Results of the hypothesis analysis have revealed that supportive human resource practices are positively related to employee attitude to adopt sustainable technology in manufacturing firms, followed by $\beta = 0.410$, STDEV = 0.058, t-statistics = 7.033, $p < 0.000$, and hence endorsing H1. Knowledge about apparel technology is positively related to employee attitude to adopt sustainable technology, followed by $\beta = 0.380$, STDEV = 0.059, t-statistics = 6.492, $p < 0.000$ and hence accepting H2. Similarly, knowledge about environmental issues has shown a positive impact in measuring employee attitude to adopt sustainable technology, followed by $\beta = 0.245$, STDEV = 0.041, t-statistics = 6.031, $p < 0.000$ and hence supporting H3.

Results have shown that competitor pressure is positively related to employee attitude to adopt sustainable technology, followed by $\beta = 0.170$, STDEV = 0.036, t-statistics = 4.662, $p < 0.000$, and hence establishing H4. Nevertheless, customer pressure has shown an insignificant impact in determining employee attitude to adopt sustainable technology, followed by $\beta = 0.008$, STDEV = 0.044, t-statistics = 0.173, $p > 0.05$, and hence rejecting H5. Moreover, the relationship between regulatory pressure and employee attitude to adopt sustainable technology is found insignificant, followed by $\beta = -0.018$, STDEV = 0.036, t-statistics = 0.501, $p > 0.05$, and hence rejecting H6. Nevertheless, employee intention to adopt is measured with employee attitude. Results have revealed a significant influence of employee attitude towards employee intention to adopt sustainable technology, followed by $\beta = 0.527$, STDEV = 0.063, t-statistics = 8.401, $p < 0.000$, and hence establishing H7. Results of the hypotheses are shown in table 5.

Importance performance analysis

The hypothesis analysis has revealed that factors such as supportive human resource practices, knowledge about apparel technology, knowledge about environmental issues and competitor pressure have shown a positive association towards employee intention to adopt sustainable technology.

Nevertheless, the collective view is yet to be examined through importance-performance index analysis. Following the guidelines provided by Rani [37], the outcome factor is selected before data computation. By selecting employee intention to adopt sustainable technology, data were estimated with importance-performance index analysis. Results have demonstrated that employee attitude is the most influential factor in measuring employee behavioural intention to adopt sustainable technology.

Nevertheless, in terms of factor importance, supportive human resource practices stand at the second stage in measuring employee behavioural intention to adopt sustainable technology. Therefore, knowledge about apparel technology is considered another important factor and stands at the third level in measuring employee behavioural intention to adopt sustainable technology. Similarly, knowledge about environmental issues has shown a medium level of importance in measuring employee behavioural intention to adopt sustainable technology. Moving further, factors like government support and has shown the least importance in measuring employee behavioural intention to adopt sustainable technology. However, customer pressure and regulatory pressure have shown no importance towards employee behavioural intention to adopt sustainable technology. Table 6 depicts IPMA values in terms of factor importance and performance.

Table 6

IPMA ANALYSIS		
Intention to adopt sustainable technology		
Factors	**Importance**	**Performance**
Employee attitude	0.527	61.466
Competitor pressure	0.089	71.445
Customer pressure	0.004	68.268
Government support	0.065	60.236
Knowledge of apparel technology	0.200	60.733
Knowledge of environmental issues	0.129	61.751
Regulatory pressure	–0.010	77.521
Supportive Human Resource practices	0.216	61.318

Effect size analysis f^2

The research model of this study has comprised factors such as supportive human resource practices, knowledge about apparel technology, knowledge about environmental issues, competitor pressure, customer pressure and regulatory pressure to investigate employee attitude towards adoption of sustainable technology. Nevertheless, the research model is considered complex due to multiple exogenous and endogenous factors. Furthermore, policymakers are struggling to find relevant factors so that they can achieve maximum goals with minimum resources. In this regard, effect size *f–squared* analysis is taken into consideration following threshold values of 0.02, 0.15 and 0.35 depicting small, medium and large effect size respectively. In addition to that, the factors' coefficient of determination is also computed to reveal the collective impact of exogenous factors in measuring endogenous factors. Results are given in table 7, comprising the coefficient of determination and effect size of factors.

Results indicate that altogether supportive human resource practices, knowledge about apparel technology, knowledge about environmental issues, competitor pressure, customer pressure and regulatory pressure have explained 74.2% variance in employee attitude towards adoption of sustainable technology. Therefore, government support and employee attitude have explained 30.3% variance in employee intention to adopt sustainable technology in apparel manufacturing. Next, this effect size analysis has disclosed that supportive HR practices and knowledge about apparel technology are the most influential factors in measuring employee attitude to adopt sustainable technology. Therefore, knowledge about environmental issues has shown a medium level of effect size in measuring employee attitude. Factors like competitor pressure have revealed a small effect. However, customer pressure and regulatory pressure have disclosed no effect and hence are considered insignificant factors.

Table 7

COEFFICIENT OF DETERMINATION R^2 AND EFFECT SIZE f^2		
Factors	**Results**	**Size**
Coefficient of determination R^2		
Attitude towards adoption of sustainable technology	74.2%	Substantial
Intention to adopt sustainable technology	30.3%	Substantial
Intention to adopt sustainable technology f^2		
Attitude towards adoption of sustainable technology	0.397	Substantial
Government support	0.006	Small
Attitude towards adoption of sustainable technology f^2		
Competitor pressure	0.092	Small
Customer pressure	0.000	No-effect
Knowledge about apparel technology	0.462	Substantial
Knowledge about environmental issues	0.189	Medium
Regulatory pressure	0.001	No-effect
Supportive Human Resource Practices	0.448	Substantial

Moderating analysis

The moderating effect of government support is tested between employee attitude and intention to adopt sustainable technology. Following the product indicator approach as suggested by Rahi [47], data were bootstrapped. Results revealed that government support positively moderates the relationship between employee attitude and intention to adopt sustainable technology, as indicated by β = 0.127, STDEV = 0.069, t-statistics = 1.834 significance at 0.033, also presented in Appendix 1. Moreover, simple slope analysis is conducted to ensure how the moderating effect strengthens the relationship. Therefore, result demonstrates that government support for GSP at + ISD shows an increasing trend and stands at the highest level when compared with GSP at – ISD. Therefore, simple slope analysis has endorsed H8 and confirmed that an increase in government support will boost employee attitude and intention to adopt sustainable technology. Figure 2 depicts the strength of the moderating relationship with positive and negative gradients.

DISCUSSION

In the past few decades, studies have widely focused on the usefulness of information technology in the apparel manufacturing process [48, 49].

Nevertheless, limited research exists on sustainable technology adoption by apparel manufacturers. Therefore, the current study adds knowledge to this emerging research field by examining the role of sustainable technology in the apparel manufacturing process. The apparel sector is considered a key sector in Saudi Arabia and significantly contributes to the Saudi economy. Nevertheless, the apparel industry is a source of water and air pollution and is considered the most polluted sector worldwide. Therefore, the current study aims to investigate factors that influence employee intention to adopt sustainable technology in the apparel industry, which in turn reduces the carbon footprint in the clothing manufacturing process. After detail literature review, this study has schematized that factors such as supportive HR practices, knowledge of apparel technology, knowledge of environmental issues, competitor pressure, customer pressure and regulatory pressure are key antecedents of employee intention to adopt sustainable technology in the manufacturing process.

Therefore, a conceptual linkage is established between exogenous and endogenous factors to investigate how these factors encourage employees to adopt sustainable technology in the apparel manufacturing process. Empirical investigation has

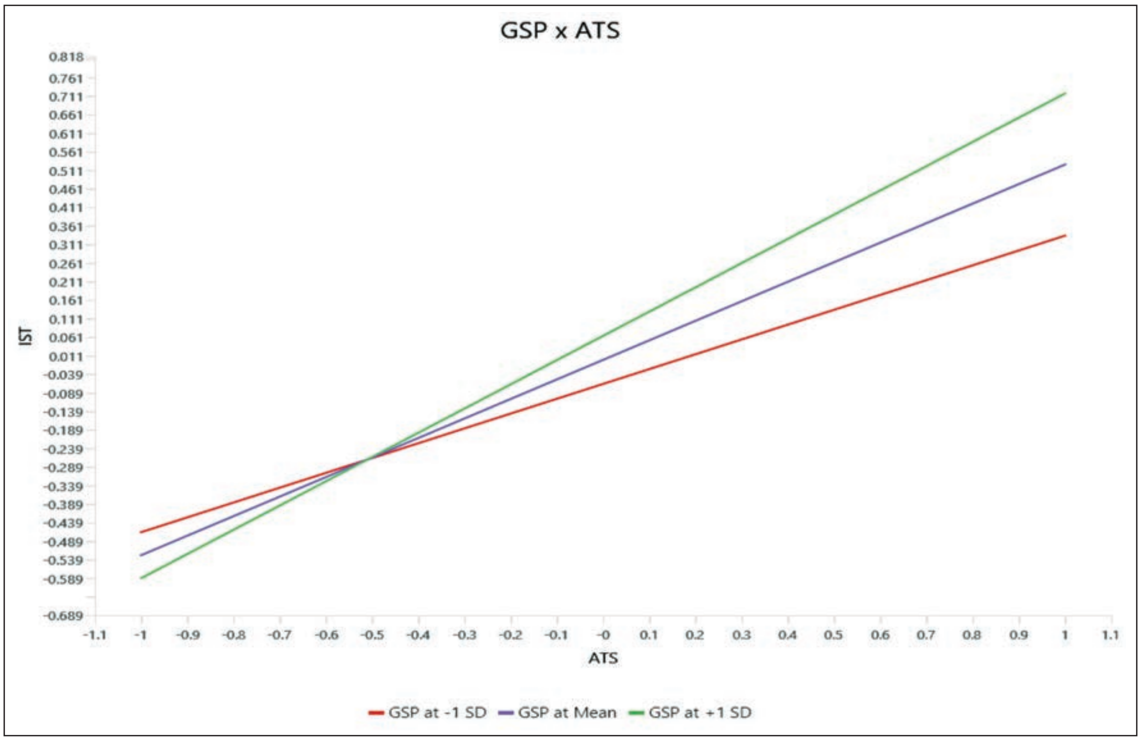

Fig. 2. Moderating trend with simple slope graph

revealed that supportive human resource practices are positively related to employee attitudes toward adopting sustainable technology in the manufacturing process and endorses arguments established by prior studies [8–10, 17]. Therefore, the first objective of this study is achieved with authentic findings that flexibility of human resource practices could encourage employees to adopt sustainable technology in the manufacturing process. The knowledge about apparel technology has also revealed a positive influence on employee attitude to adopt sustainable technology, in line with past studies [1, 11]. Likewise, knowledge about environmental issues has shown a positive impact in measuring employee attitude to adopt sustainable technology, consistent with past studies [1, 12]. These findings have established the second objective of this study with the recommendation that employees must know about apparel technology and environmental issues so that they put serious efforts in the deployment of sustainable technology in the apparel manufacturing process.

Empirical investigation has also disclosed that competitor pressure is positively related to employee attitude to adopt sustainable technology and is consistent with prior study [12]. Similarly, customer pressure and regulatory pressure were also conceptualised towards employee attitude to adopt sustainable technology in apparel manufacturing.

Nevertheless, contrary to the author's expectation bother customer pressure and regulatory pressure have shown insignificant impact in measuring employee attitude to adopt sustainable technology and hence reject arguments established by prior studies [22–24]. Therefore, the third objective of this study is achieved; following that, competitor pressure directly motivates employees and hence motivate to adopt sustainable technology in the manufacturing process. Nevertheless, employees are not concerned about regulatory pressure and customer pressure, and hence these factors have remained unsuccessful in creating an impact on employee attitude to adopt sustainable technology. Finally, the fourth objective of this study is achieved with empirical evidence that an increase in government support will boost employee attitude and employee intention to adopt sustainable technology in the apparel manufacturing process.

Theoretical contributions

The research framework of this study has schematized unique factors which influence employee attitude and intention to adopt sustainable technology in the apparel manufacturing process. For instance, this study has established that supportive human resource practices influence employee attitude to adopt sustainable technology and hence substantially contribute to the literature. Moreover, this study has summarised two core dimensions of knowledge, namely knowledge about apparel technology and knowledge about environmental issues and established the positive impact of these factors in determining employee attitude to adopt sustainable technology. Therefore, conceptualising these two unique dimensions of knowledge with relation to employee intention to adopt sustainable technology largely contributes to cognitive literature. Likewise, this study has also established that competitor pressure encourages employees to adopt sustainable technology in the apparel manufacturing process and hence enriches the literature. Nevertheless, this study has rejected claims established by past studies that regulatory pressure and customer pressure are key indicators that influence employee attitudes toward adopting sustainable technology in the manufacturing process. Therefore, the current study invites researchers to review the literature in the apparel manufacturing setting and compare findings with current research and acknowledge differences. Another unique theoretical contribution of this study is to conceptualise and test the government support factor as a moderator between employee attitude and intention to adopt sustainable technology. The research framework has explained 74.2% variance in employee attitude towards adoption of sustainable technology and hence ensured theoretical validity of the sustainable technology adoption model.

Research contributions to practice

The newly developed research model provides multiple solutions to apparel manufacturers to reduce the carbon footprint in the clothing manufacturing process using sustainable technology. Primarily, this study has revealed that supportive human resource practices bring ease in training and development programs, which in turn provide opportunities for employees to learn the usage of sustainable technology and improve the manufacturing process. Therefore, policymakers could enhance sustainable technology adoption among employees through supportive human resource practices. Similarly, this study has revealed that employees keeping knowledge about apparel technology and knowledge about environmental issues would be in a better position to adopt sustainable technology. Therefore, policymakers should launch an awareness campaign to improve employee knowledge about environmental issues and knowledge about apparel technology, which in turn positively impacts employee attitudes toward adopting sustainable technology. In a dynamic business environment, policymakers have shown consistent struggle to find the most relevant factors so that they can achieve maximum goals with minimum resources. In this regard, this study has provided a micro and macro view of the factors through IPMA analysis and effect size analysis. Specifically, effect size analysis has disclosed a substantial effect of supportive human resource practices and knowledge about apparel technology in measuring employee attitude to adopt sustainable technology.

Therefore, policymakers could achieve maximum targets by focusing on supportive human resource practices and employee knowledge about apparel technology. Nevertheless, IPMA analysis has revealed a broader perspective and suggested that supportive human resource practices, knowledge about apparel technology, knowledge about environmental issues, competitor pressure and government support are key factors that boost employee confidence and encourage employees to adopt sustainable technology in the apparel manufacturing process.

CONCLUSION

The apparel manufacturing process is consuming excessive natural resources and releasing hazardous gases into the environment. Moreover, the apparel industry is considered the most polluted sector worldwide. To address this issue, the current study has developed a research framework that comprises factors such as supportive HR practices, knowledge of apparel technology, knowledge of environmental issues, competitor pressure, customer pressure and regulatory pressure, and investigates employee intention to adopt sustainable technology in the apparel manufacturing process. Similarly, this study has examined the moderating impact of government support on the relationship between employee attitude and intention to adopt sustainable technology. The research model is empirically tested with data retrieved from employees working in apparel manufacturing firms. Findings unveiled that jointly supportive human resource practices, knowledge about apparel technology, knowledge about environmental issues, competitor pressure, customer pressure and regulatory pressure explained 74.2% variance in employee attitude to adopt sustainable technology. Therefore, government support and employee attitude have explained 30.3% variance in employee intention to adopt sustainable technology in the apparel manufacturing process. Nevertheless, effect size analysis has demonstrated that supportive HR practices and knowledge about apparel technology are the most influential factors in measuring employee attitude to adopt sustainable technology. Moving further, IPMA analysis has revealed a broader perspective of the underpinning factors and suggested that supportive human resource practices, knowledge about apparel technology, knowledge about environmental issues, competitor pressure and government support are key factors that boost employee confidence and encourage employees to adopt sustainable technology in the apparel manufacturing process. This study has schematized unique factors which influence employee attitude and intention to adopt sustainable technology in the apparel manufacturing process and contributes to the literature. Practically, this study has suggested that policymakers could enhance sustainable technology adoption among employees through supportive human resource practices. Moreover, this study has suggested that knowledge about apparel technology, knowledge about environmental issues, competitor pressure and government support are some other key antecedents that encourage employees to adopt sustainable technology in the apparel manufacturing process. Nevertheless, this study has also revealed that government support strengthens the relationship between employee attitude and employee intention to adopt sustainable technology. Concerning significance, this study is the first to establish a conceptual linkage between supportive human resource practices and employee intention to adopt sustainable technology. In addition, this study is vital as it focuses on the usage of sustainable technologies in the apparel manufacturing process, which in turn empowers a country to deal with societal and environmental challenges.

Limitations and future research directions

Despite several contributions, this study has some limitations and provides future research directions. For instance, the sustainable research model is developed and tested in Saudi Arabia, and therefore future researchers are suggested to conduct comparative research to reveal the differences.

Concerning the outlined factors, this study does not guarantee to include all factors that impact employee attitude toward adopting sustainable technology in the apparel manufacturing process. Therefore, the existing sustainable technology model could be extended with some other factors like awareness about apparel technology, green supplier and green innovativeness. The research model has direct and moderating hypotheses; however, mediating assumptions are lacking. Nevertheless, future researchers could add a mediating factor to enhance the strength of the research model. In this study, a single outcome factor is tested; however, future researchers are suggested to add other outcome factors in the research model, like sustainable purchase intention, environmental performance and organisational performance.

ACKNOWLEDGEMENT

This work was funded by the University of Jeddah, Jeddah, Saudi Arabia, under grant No. (UJ-24-DR-3049-1). Therefore, the authors thank the University of Jeddah for its technical and financial support.

REFERENCES

[1] Iqbal, M.A., Su, J., *Apparel professionals' perception of sustainability-related technology: a structural equation modelling approach*, In: Research Journal of Textile and Apparel, 2023, https://doi.org/10.1108/rjta-04-2023-0040

[2] Hoque, M.A., Rasiah, R., Furuoka, F., Kumar, S., *Critical determinants and firm performance of sustainable technology adoption in the apparel industry: the stakeholder approach*, In: Journal of Fashion Marketing and Management, 2023, 27, 1, 182–200

[3] Islam, M.M., Perry, P., Gill, S., *Mapping environmentally sustainable practices in textiles, apparel and fashion industries: a systematic literature review*, In: Journal of Fashion Marketing and Management, 2021, 25, 2, 331–353

[4] United Nations, *Climate Change. Fashion Industry Charter for Climate Action*, 2024, Available at: https://unfccc.int/climate-action/sectoral-engagement-for-climate-action/fashion-charter [Accessed on September 6, 2024]

[5] Jum'a, L., Zimon, D., Madzik, P., *Impact of big data technological and personal capabilities on sustainable performance on Jordanian manufacturing companies: the mediating role of innovation*, In: Journal of Enterprise Information Management, 2024, 37, 2, 329–354

[6] Hossain, M.T., Shahid, M.A., Limon, M.G.M., Hossain, I., Mahmud, N., *Techniques, applications, and challenges in textiles for a sustainable future*, In: Journal of Open Innovation: Technology, Market, and Complexity, 2024, 100230

[7] Statista, *Apparel – Saudi Arabia*, 2024, Available at: https://www.statista.com/outlook/cmo/apparel/saudi-arabia [Accessed on September 6, 2024]

[8] Allen, D.G., Shore, L.M., Griffeth, R.W., *The role of perceived organisational support and supportive human resource practices in the turnover process*, In: Journal of Management, 2003, 29, 1, 99–118

[9] Biswas, K., Boyle, B., Bhardwaj, S., *Impacts of supportive HR practices and organisational climate on attitudes of HR managers towards gender diversity – a mediated model approach*, In: Evidence-based HRM: a Global Forum for Empirical Scholarship, 2021, 9, 1, 18–33

[10] Mäkelä, L., Kinnunen, U., *International business travelers' psychological well-being: the role of supportive HR practices*, In: International Journal of Human Resource Management, 2018, 29, 7, 1285–1306

[11] Asadi, S., Nilashi, M., Samad, S., Rupani, P.F., Kamyab, H., Abdullah, R., *A proposed adoption model for green IT in manufacturing industries*, In: Journal of Cleaner Production, 2021, 297, 126629, https://doi.org/10.1016/j.jclepro.2021.126629

[12] Hoque, M.A., Rasiah, R., Furuoka, F., Kumar, S., *Linkages among automation, job displacement and reshoring: evidence from the Bangladeshi apparel industry*, In: Research Journal of Textile and Apparel, 2022, 26, 4, 515–531

[13] Zeng, S.X., Meng, X.H., Zeng, R.C., Tam, C.M., Tam, V.W.Y., Jin, T., *How environmental management driving forces affect environmental and economic performance of SMEs: a study in Northern China*, In: Journal of Cleaner Production, 2011, 19, 13, 1426–1437

[14] Cui, Y., Zhao, H., *Marine renewable energy project: environmental implication and sustainable technology*, In: Ocean & Coastal Management, 2023, 232, 106415

[15] Pandey, P.C., Pandey, M., *Highlighting the role of agriculture and geospatial technology in food security and sustainable development goals*, In: Sustainable Development, 2023, 31, 5, 3175–3195

[16] Rahi, S., *Fostering employee work engagement and sustainable employment during COVID-19 crisis*, In: Industrial and Commercial Training, 2023, 55, 3, 324–345

[17] Yamin, M.A., Almuteri, S.D., Bogari, K.J., Ashi, A.K., *The influence of SHRM and AI in determining supply chain agility and resilience*, In: Sustainability, 2024, 16, 7, 2688

[18] Iqbal, M.A., Su, J., *Apparel professionals' perception of sustainability-related technology: a structural equation modeling approach*, In: Research Journal of Textile and Apparel, 2023, 29, 1, 184–202

[19] Baah, C., Opoku-Agyeman, D., Acquah, I.S.K., Agyabeng-Mensah, Y., Afum, E., Faibil, D., Abdoulaye, F.A.M., *Stakeholder pressures, green practices, reputation and performance in SMEs*, In: Sustainable Production and Consumption, 2021, 27, 100–114, https://doi.org/10.1016/j.spc.2020.10.015

[20] Alyahya, M., Agag, G., Aliedan, M., Abdelmoety, Z.H., *Eco-innovation and customer boycott behaviour: a cross-cultural investigation*, In: Journal of Retailing and Consumer Services, 2023, 72, 103271

[21] Neureiter, A., Stubenvoll, M., Matthes, J., *Is it greenwashing? Environmental compensation claims and outcomes*, In: Journal of Advertising, 2024, 53, 4, 511–529
[22] Li, Z., Huang, Z., Su, Y., *New media environment, regulation and green innovation in China*, In: Energy Economics, 2023, 119, 106545, https://doi.org/10.1016/j.eneco.2023.106545
[23] Qiu, L., Hu, D., Wang, Y., *Green innovation under external pressures: environmental regulation and turbulence*, In: Business Strategy and the Environment, 2020, 29, 6, 2695–2714
[24] Song, M., Peng, L., Shang, Y., Zhao, X., *Green technology progress and productivity of resource-based enterprises*, In: Technological Forecasting and Social Change, 2022, 174, 121276
[25] Fu, Y., Kok, R.A., Dankbaar, B., Ligthart, P.E., van Riel, A.C., *Factors affecting sustainable process technology adoption: a systematic review*, In: Journal of Cleaner Production, 2018, 205, 226–251
[26] Guo, L., Zhang, Q., Wu, J., Gonzalez, E.D.S., *Evolutionary game of green technology strategies with subsidy*, In: Computers & Industrial Engineering, 2024, 189, 109918
[27] Shahadat, M.H., Nekmahmud, M., Ebrahimi, P., Fekete-Farkas, M., *Digital technology adoption in SMEs in emerging countries*, In: Global Business Review, 2023, https://doi.org/10.1177/09721509221137199
[28] Yang, R., Tang, W., Zhang, J., *Technology improvement strategy for green products under competition*, In: European Journal of Operational Research, 2021, 289, 2, 553–568
[29] Yu, H., Wang, J., Hou, J., Yu, B., Pan, Y., *Economic growth pressure and green technology innovation*, In: Journal of Environmental Management, 2023, 330, 117172
[30] Lin, C.-Y., Ho, Y.-H., *Determinants of green practice adoption for logistics companies in China*, In: Journal of Business Ethics, 2011, 98, 67–83
[31] Zhang, X., Ye, J., Wang, D., Tian, F., Fu, S., *Leadership mindsets, cultural norms and resilience: supportive HR practices as moderator*, In: Asia Pacific Business Review, 2023, 29, 1, 248–265
[32] Dickson, M.A., *Personal values and attitudes toward purchasing from responsible businesses*, In: Clothing and Textiles Research Journal, 2000, 18, 1, 19–30
[33] Xie, W., Zheng, D., Li, Z., Wang, Y., Wang, L., *Digital technology and industrial change in China*, In: Computers & Industrial Engineering, 2024, 187, 109825
[34] Ullah, S., Ahmad, T., Lyu, B., Sami, A., Kukreti, M., Yvaz, A., *Integrating stakeholders for green innovation performance*, In: International Journal of Innovation Science, 2024, 16, 4, 640–657
[35] Rahi, S., Abd Ghani, M., Ngah, A.H., *Internet banking adoption and technology acceptance*, In: Technology in Society, 2019, 58, 101120, https://doi.org/https://doi.org/10.1016/j.techsoc.2019.03.003
[36] Tan, K.S., Chong, S.C., Lin, B., Eze, U.C., *Internet-based ICT adoption in Malaysian SMEs*, In: Industrial Management & Data Systems, 2009, 109, 2, 224–244
[37] Rahi, S., *Research Design and Methods*, CreateSpace Publishing, 2018
[38] Alnaser, F., Rahi, S., Alghizzawi, M., Ngah, A.H., *Factors influencing citizen's intention to adopt e-health applications*, In: Global Knowledge, Memory and Communication, 2024, https://doi.org/10.1108/gkmc-07-2023-0242
[39] Yamin, M.A.Y., Abdalatif, O.A.A., *Consumer behaviour toward QR code mobile payments*, In: Humanities and Social Sciences Communications, 2024, 11, 1, 1–11
[40] Hair, J., Anderson, R., Black, B., Babin, B., *Multivariate Data Analysis*, Pearson Education, 2016
[41] Rahi, S., *Structural Equation Modeling Using SmartPLS*, CreateSpace Publishing, 2017. ISBN-13: 9781987550689
[42] Hair, F., Sarstedt, M., Hopkins, L., Kuppelwieser, V.G., *Partial least squares structural equation modeling (PLS-SEM): an emerging tool*, In: European Business Review, 2014, 26, 2, 106–121
[43] Fornell, C., *A National Customer Satisfaction Barometer: The Swedish Experience,* In: Journal of Marketing, 1992, 56, 6–21
[44] Gold, A.H., Malhotra, A., Segars, A.H., *Knowledge management: an organizational capabilities perspective*, In: Journal of Management Information Systems, 2001, 18, 1, 185–214
[45] Kline, R., *Principles and Practice of Structural Equation Modeling*, Guilford Press, New York, 2011
[46] Rahi, S., *Telemedicine application adoption during COVID-19*, In: Library Hi Tech, 2022, 40, 2, 394–420
[47] Rahi, S., *Research design and methods: systematic review*, In: International Journal of Economics & Management Sciences, 2017, 6, 2, 1–5
[48] Nayak, R., Singh, A., Padhye, R., et al., *RFID in textile and clothing manufacturing: technology and challenges*, In: Fashion and Textiles, 2015, 2, 9
[49] Varukolu, V., Park-Poaps, H., *Technology adoption by apparel manufacturers in India*, In: Journal of Fashion Marketing and Management, 2009, 13, 2, 201–214

Authors:

NUHA AWADH ALJUAID[1], ABDULRAHMAN AWADH ALJUAID[2]

[1]Department of Fashion Design, College of Design and Art, University of Jeddah, Jeddah, Saudi Arabia

[2]Department of Human Resources Management, College of Business, University of Jeddah, Jeddah, Saudi Arabia
e-mail: aaaljuaid@uj.edu.sa

Corresponding author:

NUHA AWADH ALJUAID
e-mail: naljuid8@uj.edu.sa

Modelling and simulation analysis of a direct-drive system for specific motion laws of the heald frame

DOI: 10.35530/IT.077.04.2025112

QINGYUAN GUO
TAO YANG
SIJIA FU
HONGBIN YU

ABSTRACT – REZUMAT

Modelling and simulation analysis of a direct-drive system for specific motion laws of the heald frame

This study presents a modelling and simulation analysis of a direct-drive system for the heald frame in looms, utilising an 11th-order polynomial to achieve smooth, continuous motion with C^3 continuity in displacement, velocity, and acceleration. A d-q axis mathematical model based on electromagnetic-mechanical coupling is established, and Clark-Park transformation enables decoupled control of flux and thrust. Simulations in MATLAB/Simulink under varying heald frame masses (2.5–10 kg) show linear increases in load force (±3.8 to ±15.2 N), q-axis current (±25 to ±90 mA), and electromagnetic thrust (±7.6 to ±30.3 N), with stable three-phase currents and rapid, overshoot-free response. Results validate the model's accuracy and the effectiveness of the control strategy, demonstrating excellent dynamic performance, load adaptability, and energy efficiency. The direct-drive system eliminates mechanical transmission losses, offering a foundation for high-precision, green weaving technology.

Keywords: *heald frame, direct-drive system, motion control, electromechanical coupling modelling, motion law, electromagnetic thrust*

Analiza modelării și simulării unui sistem cu acționare directă pentru legi specifice de mișcare ale ițelor

Prezentul studiu prezintă o analiză de modelare și simulare a unui sistem de acționare directă pentru mașinile de țesut cu ițe, utilizând un polinom de ordinul 11 pentru a obține o mișcare lină și continuă, cu continuitate de tip C^3 în ceea ce privește deplasarea, viteza și accelerația. Se elaborează un model matematic pe axele d-q bazat pe cuplajul electromagnetico-mecanic, iar transformarea Clark-Park permite controlul decuplat al fluxului și al forței de împingere. Simulările efectuate în MATLAB/Simulink pentru mase variabile ale ițelor (2,5–10 kg) arată creșteri liniare ale forței de sarcină (de la ±3,8 până la ±15,2 N), ale curentului pe axa q (de la ±25 la ±90 mA) și ale forței de împingere electromagnetică (de la ±7,6 la ±30,3 N), cu curenți trifazici stabili și un răspuns rapid, fără depășiri. Rezultatele validează acuratețea modelului și eficacitatea strategiei de control, demonstrând performanțe dinamice excelente, adaptabilitate la sarcină și eficiență energetică. Sistemul cu acționare directă elimină pierderile de transmisie mecanică, oferind o bază pentru o tehnologie de țesere ecologică și de înaltă precizie.

Cuvinte-cheie: *iță, sistem de acționare directă, controlul mișcării, modelare cuplaj electromecanic, legea mișcării, forță de împingere electromagnetică*

INTRODUCTION

In modern weaving technology, the Heald frame is the core actuating component responsible for the fabric's shedding motion, directly influencing loom efficiency, fabric quality, and equipment stability [1–3]. Traditional high-speed rotary electronic dobby (HRED) machines use conjugate cam-driven crank-rocker mechanisms to convert the main shaft's uniform rotation into variable-speed motion with intermittent pauses, accommodating different fabric structures [4, 5]. However, these mechanical transmission systems suffer from multiple stages, large inertia, slow response, and non-adjustable motion laws, limiting their suitability for high-speed, high-precision applications [6, 7].

Recent research has focused on structural optimisation, motion simulation, and dynamic modelling of dobby machines, laying the groundwork for drive system design [8, 9]. Despite these efforts, traditional mechanical structures remain constrained by inherent performance bottlenecks. With advances in linear drive technology, Permanent Magnet Linear Synchronous Motors (PMLSMs) have emerged as a promising alternative due to their high thrust density, fast response, and precise positioning [10–12]. Studies have explored structural design, electromagnetic optimisation, thrust ripple suppression, and advanced control strategies. For instance, Tan et al. reduced thrust ripple through pole pair optimisation [13], Huang et al. enhanced current control via dead-time compensation [14], Tan et al. improved positioning accuracy using disturbance observers [15], and Zeng et al. optimised motor structures via finite element analysis [16].

Compared to HRED systems, PMLSM-based direct-drive systems offer superior dynamic performance and flexibility. This study presents a mathematical model of a PMLSM direct-drive system tailored to the

Heald frame motion laws, addressing the complex electromechanical coupling characteristics and providing a foundation for advanced control and optimisation.

WORKING PRINCIPLE AND MATHEMATICAL MODEL OF THE DIRECT-DRIVE SYSTEM

Working principle

The heald frame direct-drive system is a novel linear drive system. Its core innovation lies in eliminating the conventional mechanical transmission devices commonly used in traditional looms, and instead adopting electromagnetic driving technology to directly drive the heald frame through electromagnetic thrust, achieving reciprocating vertical motion. This approach realises a highly integrated structural design. The structural diagram is shown in figure 1.

The system mainly consists of a stator winding (primary part), a permanent magnet mover (secondary part), a support and guidance mechanism, and mechanical structures directly connected to the heald frame. Unlike indirect drive systems that rely on intermediate components such as cams or linkages, which introduce backlash, wear, and friction, the direct-drive configuration ensures a one-to-one correspondence between electrical input and mechanical output, enhancing position fidelity and reducing parasitic power losses. The absence of lubricated joints lowers maintenance requirements and avoids contamination [17, 18]. Due to complex electromechanical coupling within the system, a comprehensive mathematical model integrating electromagnetic and mechanical dynamics is essential for developing high-performance control strategies and conducting system performance analysis.

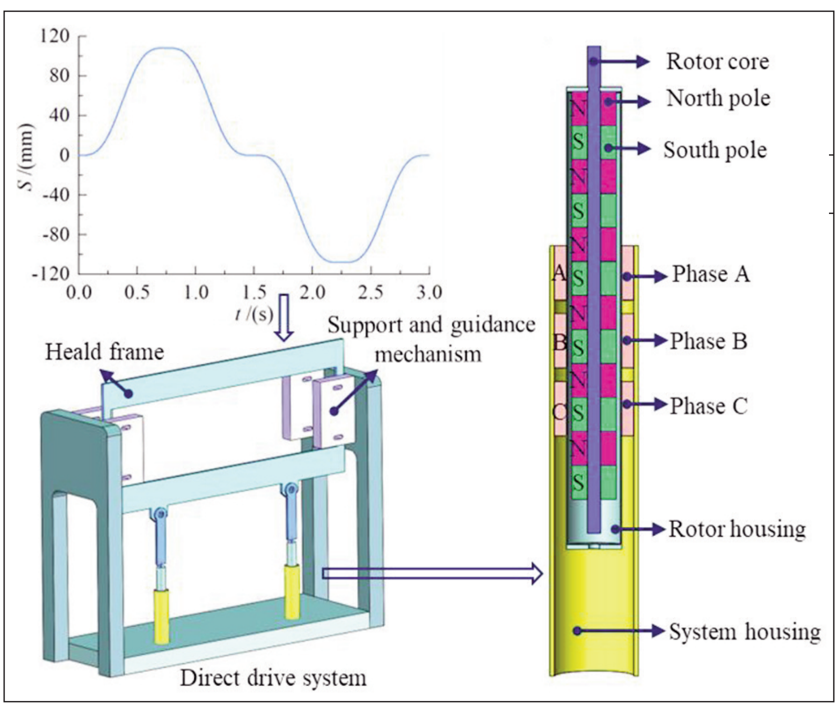

Fig. 1. Schematic diagram of the structure of the direct-drive heald frame system

Mathematical model

An 11th-order polynomial displacement function is designed for the heald frame to ensure smooth motion, continuous acceleration, and stable performance in high-speed weaving, meeting strict requirements for displacement, velocity, and jerk continuity:

$$S = h\begin{pmatrix} 336(\xi)^5 - 1890(\xi)^6 + 4740(\xi)^7 - 6615(\xi)^8 \\ +5320(\xi)^9 - 2310(\xi)^{10} + 420(\xi)^{11} \end{pmatrix} \quad (1)$$

where h is the heald frame lift, and ξ – the angular variable describing the heald frame motion position.

The total load force F_L experienced by the heald frame during motion can be expressed as:

$$F_L = F_e - Bv - ma \quad (2)$$

where m is the equivalent mass of the heald frame, B – the viscous friction coefficient, and a and v are the acceleration and velocity, respectively. The load force F_L reflects the sum of the inertial force and frictional force that must be overcome by the heald frame under different motion states, and serves as an important basis for the design of electromagnetic thrust.

The direct-drive heald frame system efficiently converts electrical energy into mechanical energy to drive the permanent magnet mover in linear reciprocating motion. The three-phase instantaneous power P_{abc}, which is related to the velocity v, reflects the process of electromagnetic thrust generation:

$$P_{abc} = e_a i_a + e_b i_b + e_c i_c =$$
$$= -\phi_f \omega_e \left[i_a \sin\theta_e + i_b \sin\left(\theta_e - \frac{2\pi}{3}\right) + i_c \sin\left(\theta_e + \frac{2\pi}{3}\right)\right]$$

where ϕ_f is the flux linkage produced by the permanent magnet, θ_e is the electrical angle, representing the electrical position of the mover relative to the stator, which affects the back EMF and thrust magnitude. ω_e is the electrical angular velocity.

According to the principle of energy conservation, the electromagnetic thrust F_e generated by the system can be derived from the relationship between instantaneous power and motion velocity. The specific expression is:

$$F_e = \frac{P_{abc}}{v} = \frac{\pi}{\tau_n}\phi_f \left[i_a \sin(-\theta_e) + \right. \quad (4)$$
$$\left. + i_b \sin\left(\theta_e - \frac{2\pi}{3}\right) + i_c \sin\left(\theta_e + \frac{2\pi}{3}\right)\right]$$

where τ_n is the pole pitch.

In order to achieve high-performance control of the direct-drive heald frame system, it is usually necessary to transform the three-phase stationary coordinate system (abc coordinate system) into a two-phase rotating coordinate system (d–q coordinate system), thereby achieving decoupled control of the magnetic field and thrust.

Clark transformation:

$$\begin{bmatrix} i_\alpha \\ i_\beta \end{bmatrix} = \sqrt{\frac{2}{3}} \begin{bmatrix} 1 & -\frac{1}{2} & \frac{1}{2} \\ 0 & \frac{\sqrt{3}}{2} & -\frac{\sqrt{3}}{2} \end{bmatrix} \begin{bmatrix} i_a \\ i_b \\ i_c \end{bmatrix} \tag{5}$$

Park transformation:

$$\begin{bmatrix} i_d \\ i_q \end{bmatrix} = \begin{bmatrix} \cos\theta_e & \sin\theta_e \\ -\sin\theta_e & \cos\theta_e \end{bmatrix} \begin{bmatrix} i_\alpha \\ i_\alpha \end{bmatrix} \tag{6}$$

where i_d and i_q are the d-axis and q-axis current, respectively.

Mathematical model in the d–q axis:

$$\begin{cases} u_d = R_s i_d + L_d \dfrac{di_d}{dt} - \omega_e L_q i_q \\ u_d = R_s i_q + L_q \dfrac{di_q}{dt} - \omega_e L_d i_d + \omega_e \phi_f \end{cases} \tag{7}$$

where R_s is the winding resistance, and L_d and L_q are the d-axis and q-axis inductances, respectively.

The corresponding electromagnetic thrust equation in the d–q coordinate system can be simplified as:

$$F_e = \frac{3\pi P_n}{2\tau_n} \phi_f i_q + (L_q - L_d) i_d i_q \tag{8}$$

where P_n is the number of pole pairs.

SIMULATION MODEL

To verify the applicability and effectiveness of the established electromagnetic thrust model and its decoupling control strategy in the direct-drive heald frame system, this study constructs a simulation model of the direct-drive system tailored to the specific motion law of the heald frame within the MATLAB/Simulink simulation environment. The model comprehensively integrates the d-q axis decoupling control strategy, three-phase voltage model, electromagnetic thrust model, and the mechanical dynamic model of the heald frame, forming a complete closed-loop control system [19, 20]. The structure of the simulation model is shown in figure 2.

The heald frame's motion profile, defined by preset displacement and acceleration curves, simulates high-speed weaving dynamics and influences system thrust requirements. Using parameters from table 1, a realistic simulation model was built. Considering structural symmetry, each heald frame is driven by two direct-drive systems. Total masses of 5 kg, 10 kg, 15 kg, and 20 kg correspond to 2.5 kg, 5 kg, 7.5 kg, and 10 kg per system, respectively. This setup evaluates dynamic response and control robustness under varying loads.

Table 1

SIMULATION PARAMETERS			
Parameter Name	**Symbol**	**Value**	**Unit**
Stator resistance	R_s	0.5	Ω
d-axis inductance	L_d	26.7	mH
q-axis inductance	L_q	26.7	mH
Flux linkage	ϕ_f	0.24	W_b
Pole pitch	τ_n	20	mm
Number of pole pairs	p_n	6	—
Viscous damping coefficient	B	0.2	$N{\cdot}s/m^2$

RESULTS AND DISCUSSION

Focusing on the modelling and simulation analysis of the direct-drive system tailored to the specific motion profile of the heald frame, this study presents a systematic study from multiple perspectives, including kinematic characteristics, load characteristics, current response, and electromagnetic thrust control.

Displacement, velocity, and acceleration analysis

In terms of kinematic characteristics, this study constructs the displacement function of the heald frame based on an 11th-order polynomial curve. The function was designed with full consideration of the smoothness and continuity requirements during the motion process. The displacement, velocity, and acceleration curves calculated using this polynomial function are shown in figure 3.

As illustrated in figure 3, the displacement profile follows a trapezoidal-like motion with rounded corners,

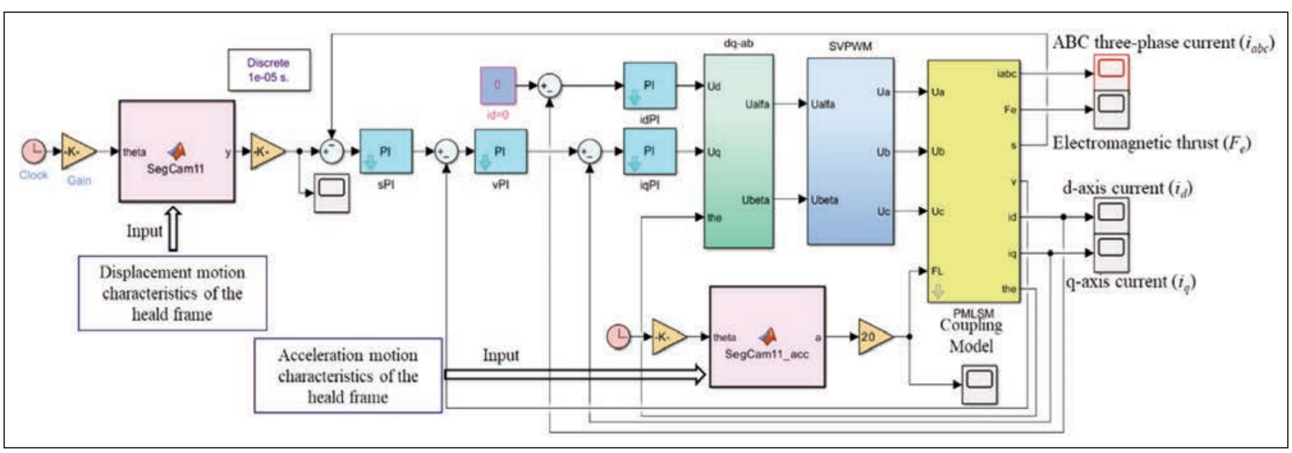

Fig. 2. Simulation modelling

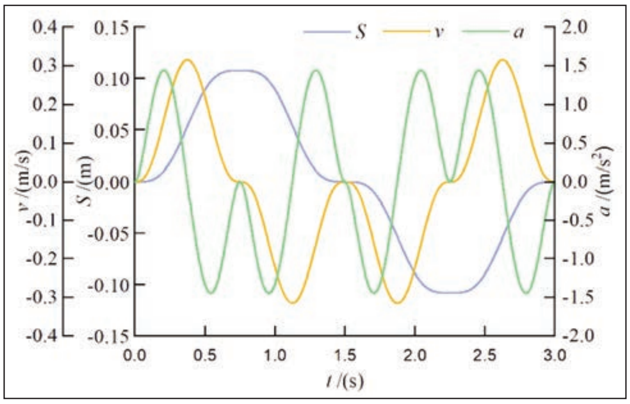

Fig. 3. Motion law of the heald frame

enabling rapid rise and fall while avoiding impulsive accelerations. The velocity curve is bell-shaped with zero initial and final values, satisfying the dwell requirements during the shedding process. Most importantly, the acceleration profile is continuous and differentiable, with no abrupt jumps, indicating C^2 continuity. Furthermore, the jerk remains bounded throughout the motion, achieving C^3 continuity; this is crucial for minimising excitation of structural resonances in the loom frame and preventing yarn breakage during high-frequency operation [21]. Compared to conventional fifth-order splines or modified sine profiles used in cam-based systems, the 11th-order polynomial offers greater tuning flexibility and superior dynamic performance.

Load analysis

In the modelling and simulation analysis of the direct-drive system tailored to the specific motion profile of the heald frame, load characteristics are one of the key indicators for evaluating system performance. By conducting simulation analysis on the acceleration of the heald frame under different mass conditions and combining this with the preset displacement trajectory, the variation of the load force experienced by the system during operation can be calculated, thereby obtaining the dynamic load response curve of the system, as shown in figure 4.

Figure 4 shows the load force curves under heald frame masses of 2.5 kg, 5 kg, 7.5 kg, and 10 kg,

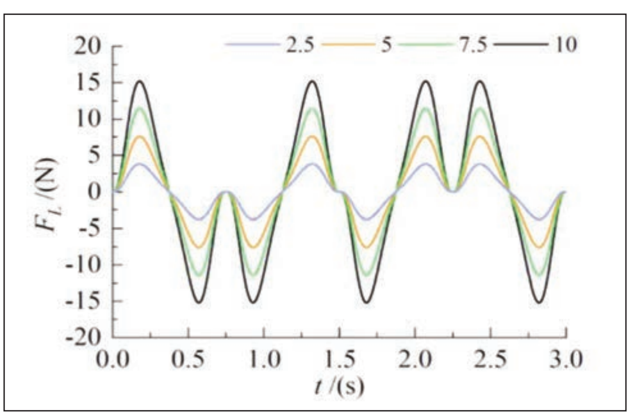

Fig. 4. Load variation law

exhibiting periodic fluctuations due to acceleration changes. The amplitude increases linearly with mass, reaching ±3.8 N, ±7.6 N, ±11.4 N, and ±15.2 N, respectively, verifying the theoretical model's accuracy. The observed linear scaling confirms Newtonian dynamics dominance; notably, $F_L/m \approx 1.52$ m/s^2 matches the peak acceleration from the motion profile, validating kinematic-force consistency and enabling feedforward control for improved precision.

Current response

Figure 5 presents the current responses. The d-axis current (figure 5, *a*) remains near zero with minimal fluctuation, indicating effective field-oriented control and decoupling between magnetic field and thrust. The q-axis current (figure 5, *b*) increases linearly with mass, peaking at ±25 mA, ±45 mA, ±70 mA, and ±90 mA, respectively, showing the system's ability to regulate thrust dynamically. These results confirm the control system's fast response and high accuracy, laying a foundation for electromagnetic thrust optimisation and improved system stability.

Further analysis of figure 5, *b* shows that the q-axis current increases linearly with the heald frame's effective mass. At 2.5 kg, 5 kg, 7.5 kg, and 10 kg, the peak q-axis current values are approximately ±25 mA, ±45 mA, ±70 mA, and ±90 mA, respectively, indicating real-time current regulation to control electromagnetic thrust and ensure accurate displacement tracking, demonstrating the system's fast dynamic response and strong robustness under varying loads. As shown in figure 5, *c–e*, the three-phase currents (A, B, C) also increase linearly with the load, rising from ±20 mA at 2.5 kg to ±90 mA at 10 kg, maintaining symmetry and stability during steady-state operation. The sinusoidal waveform and phase symmetry reflect proper synchronisation with rotor position estimation, suggesting low harmonic distortion and efficient utilisation of DC bus power. The near-zero d-axis current confirms successful implementation of field-weakening avoidance and maximum thrust per ampere control, thereby maximising thrust output per unit current. These results validate the effectiveness of the d-q axis decoupling control strategy, enabling independent regulation of magnetic flux and thrust, significantly improving dynamic response and energy efficiency, and supporting long-term system reliability.

Driving force analysis

In the modelling and simulation analysis of the direct-drive system tailored to the specific motion laws of the heald frame, electromagnetic thrust, being the core parameter of the system's output control force, has dynamic response characteristics that directly determine the motion control performance of the heald frame under different external load conditions. Figure 6 shows the dynamic response curves of electromagnetic thrust under different effective masses of the heald frame (2.5 kg, 5 kg, 7.5 kg, and 10 kg), reflecting the variation trend of thrust output during startup and steady-state operation, as well as the system's adaptability to changes in external loads.

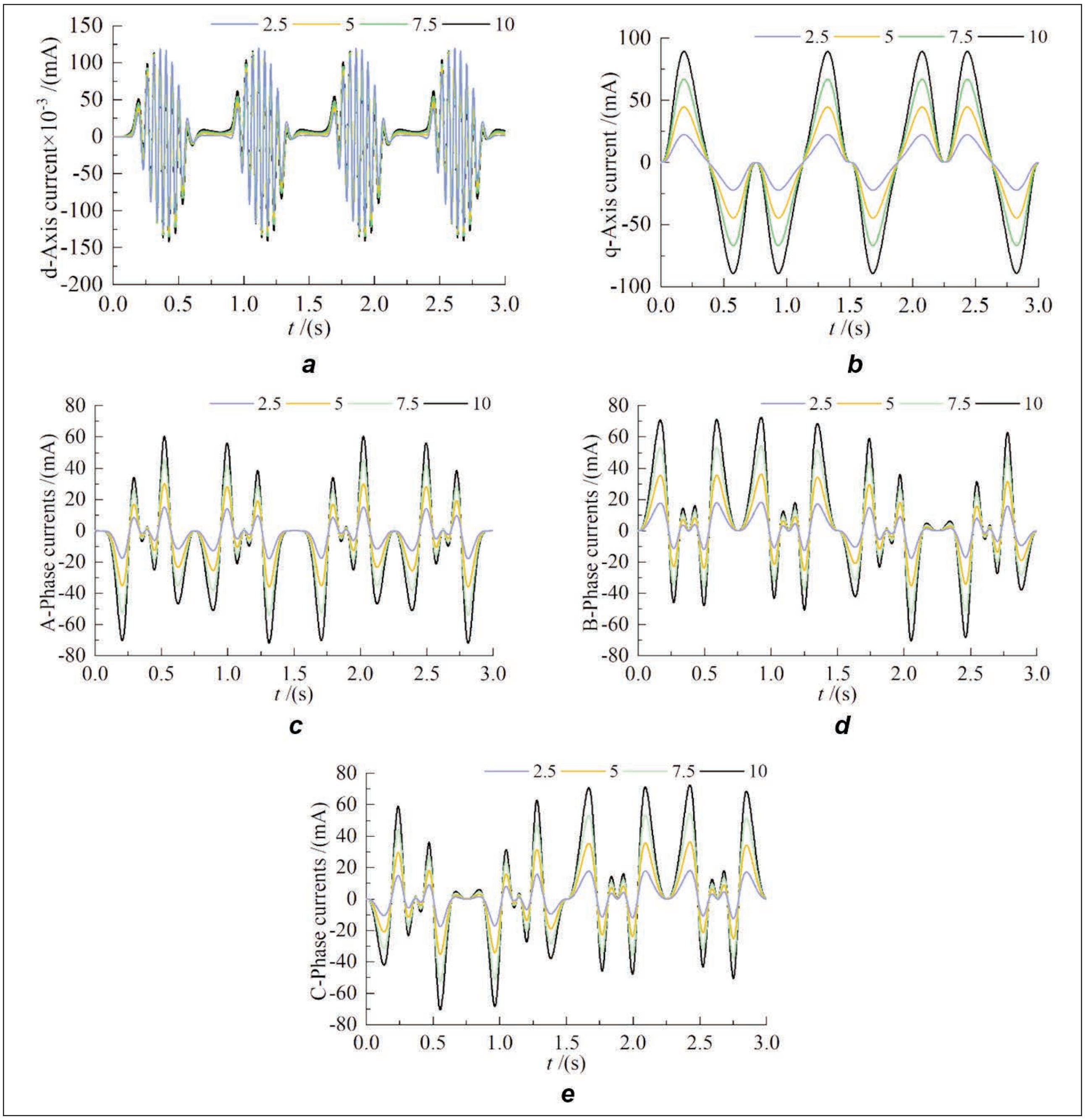

Fig. 5. Current results: *a* – d-Axis current; *b* – q-Axis current; *c* – Phase A current; *d* – Phase B current; *e* – Phase C current

As shown in figure 6, the electromagnetic thrust adaptively adjusts with load, increasing from ±7.6 N (2.5 kg) to ±30.3 N (10 kg), ensuring stable operation and precise displacement. The surplus thrust compensates for unmodeled disturbances like friction and misalignment, providing a safety margin for robust tracking. Although higher instantaneous power is required, the elimination of mechanical losses likely yields net energy savings. Thrust regulation correlates linearly with q-axis current, while near-zero d-axis current ensures effective decoupling, enhancing control efficiency and dynamic response.

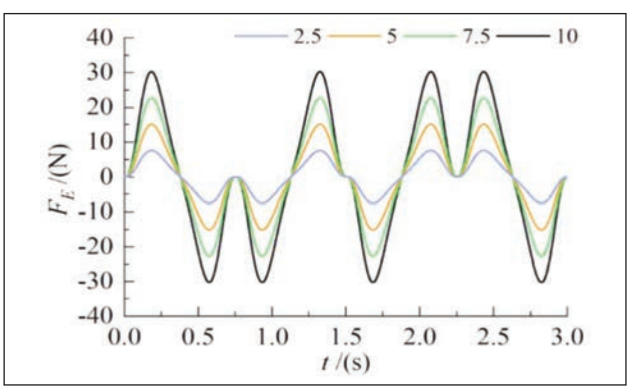

Fig. 6. Electromagnetic thrust results

CONCLUSIONS

This study focuses on modelling and simulating a direct-drive system for a loom heald frame using an 11th-order polynomial displacement function to ensure smooth motion profiles. A d-q axis mathematical model incorporating electromagnetic-mechanical coupling was established, and the Clark-Park transformation enabled decoupled control of flux linkage and thrust force. A closed-loop control system was simulated in MATLAB/Simulink under varying heald frame masses (2.5–10 kg) to evaluate dynamic performance. Results show fast response with no overshoot, stable and symmetrical three-phase currents, linear correlation between q-axis current and electromagnetic thrust, and near-zero d-axis current, confirming high control accuracy and system stability. The proposed direct-drive system demonstrates excellent dynamic performance and load adaptability. By eliminating mechanical transmission, it significantly reduces energy losses and maintenance requirements, extends service life, and lowers carbon emissions. Combined with high-efficiency electromagnetic actuation and the potential for regenerative braking in bidirectional operation, the system enhances energy recovery capability, aligning with the goals of green and intelligent manufacturing.

ACKNOLEDGEMENTS

The authors disclosed receipt of the following financial support for the research, authorship, and/or publication of this article: This research was financially supported by the Science and Technology Program of Tianjin Administration for Market Regulation (No. 2024-W43) and the National Key Research and Development Program (No. 2023YFC3081800). Thanks to partial support for this work from the Key Laboratory of Digital Twin Generic Technology in Special Equipment for State Market Regulation.

REFERENCES

[1] Jiang, J.B., Wei, C., Yu, Y.F., Sun, S.X., *Autonomous planning of discontinuous terrain-dependent crawling for space dobby robots,* In: Sensors, 2023, 23, 6, 3334, https://doi.org/10.3390/s23063334

[2] Kolčavová, B., Tunakova, V., Tunák, M., Jezik, K., *Influence of woven fabric construction parameters on electromagnetic shielding effectiveness: Part I – weave influence*, In: Textile Research Journal, 2022, 92, 21–22, 004051752211003, https://doi.org/10.1177/00405175221100390

[3] Wang, S., Yan, Z.J., Shen, F., Du, L.H., Li, G.L., Yang, Q., Hu, Q.H., *Novel aptasensor based on polyaniline functionalized carboxylated dobby carbon nanotubes and molybdenum disulfide for endotoxin detection,* In: Talanta, 2024, 276, 126256, https://doi.org/10.1016/j.talanta.2024.126256

[4] Yu, H.B., Yin, H.H., Peng, J.Q., Wang, L., *Comparison of the vibration response of a rotary dobby with cam-link and cam-slider modulators*, In: Autex Research Journal, 2021, 21, 4, 491–500, https://doi.org/10.2478/aut-2020-0037

[5] Qiu, H., Han, B., Huang, P.F., Zhang, H.W., *Structural design and dynamics optimization for heald frame made by carbon fiber reinforced composites*, In: Journal of Industrial Textiles, 2022, 52, 8, 252699082, https://doi.org/10.1177/15280837221130514

[6] Iftekhar, H., Umair, M., Hamdani, S.T.A., Imran, S.M., *Effect of hybrid weave patterns on the mechanical performance of woven fabrics*, In: Journal of Natural Fibers, 2022, 20, 1, 2145411, https://doi.org/10.1080/15440478.2022.2145411

[7] Li, L.Q., Fang, Y.F., Wang L., *Design of a family of multi-DOF drive systems for fewer limb parallel mechanisms*, In: Mechanism and Machine Theory, 2020, 148, 94–114, https://doi.org/10.1016/j.mechmachtheory.2020.103802

[8] Yoshida, T., *A method for approximating weave diagrams under heald frame constraint*, In: Textile Research Journal, 2023, 93, 15–16, 3527–3537, https://doi.org/10.1177/00405175221149684

[9] Sirkova, B.K., Mertova, I., *Prediction of warp and weft crimp in the construction of dobby woven fabrics, In:* Journal of the Textile Institute, 2020, 111, 10, 1401–1409, https://doi.org/10.1080/00405000.2019.1701967

[10] Hassan, M., Mostafa, A., Al-Oufy, A., El-Gholmy, S., *Numerical investigation of weaving machine heald shaft new design using composite material to improve its performance*, In: Autex Research Journal, 2024, 24, 01, 1–11, https://doi.org/10.1515/aut-2023-0026

[11] Cho, K., Kim, J., Choi, S.B., Oh, S., *A high-precision motion control based on a periodic adaptive disturbance observer in a PMLSM*, In: IEEE/ASME Transactions on Mechatronics, 2015, 20, 5, 2158–2171, https://doi.org/10.1109/TMECH.2014.2365996

[12] Ullah, N., Basit, A., Khan, F., Shah, Y.A., Khan, A., Waheed, O., *Design and optimization of complementary field excited linear flux switching machine with unequal primary tooth width and segmented secondary*, In: IEEE Access, 2019, 7, 106359–106371, https://doi.org/10.1109/ACCESS.2019.2932791

[13] Tan, Q., Wang, M.Y., Li, L.Y., Li, J.C., *Research on Non-integer pole number for segmental permanent magnet linear synchronous motor*, In: IEEE Transactions on Industrial Electronics, 2021, 68, 5, 4120–4130, https://doi.org/10.1109/TIE.2020.2985001

[14] Huang, X.Z., Yu, H.C., Zhou, B., Li, L.Y., Gerada, D., Gerada, C., *Detent-force minimization of double-sided permanent magnet linear synchronous motor by shifting one of the primary components*. In: IEEE Transactions on Industrial Electronics, 2020, 67, 1, 180–191, https://doi.org/10.1109/TIE.2019.2892704

[15] Tan, Z.X., Liu, L., Li, Y.J., He, F., Liu, B.Y., Yi, Z.X., *A Robust Model Predictive Current Control Strategy with Improved Adaptive Quantum Genetic Algorithm-Based Parameter Identification for PMSM*, In: IEEE Transactions on Energy Conversion, 2025, 1–11, https://doi.org/10.1109/TEC.2025.3596340

[16] Zeng, Z.Q., Lu, Q.F., *Investigation of novel partitioned-primary hybrid-excited flux-switching linear machines*, In: IEEE Transactions on Industrial Electronics, 2018, 65, 12, 9804–9813, https://doi.org/10.1109/TIE.2017.2786205

[17] Li, T., Sun, X.D., Lei, G., Guo, Y.G., Yang, Z.B., Zhu, J.G. *Finite-control-set model predictive control of permanent magnet synchronous motor Drive systems – an overview*, In: IEEE/CAA Journal of Automatica Sinica, 2022, 9, 12, 2087–2105, https://doi.org/10.1109/JAS.2022.105851

[18] Peng, J., Yao, M., *Overview of predictive control technology for permanent magnet synchronous motor systems*, In: Applied Sciences, 2023, 13, 10, 6255, https://doi.org/10.3390/app13106255

[19] Hazzab, A, Bousserhane, I.K., Zerbo, M., Sicard, P., *Real time implementation of fuzzy gain scheduling of PI controller for induction motor machine control*, In: Neural Processing Letters, 2006, 24, 3, 203–215, https://doi.org/10.1007/s11063-006-9018-5

[20] Sant, A.V., Rajagopal, K.R., Sheth, N.K., *Permanent magnet synchronous motor drive using hybrid PI speed controller with inherent and noninherent switching functions*, In: IEEE Transactions on Magnetics, 2011, 47, 10, 4088–4091, https://doi.org/10.1109/TMAG.2011.2159831

[21] Liao, C.S., Jeng, S.L., Chieng, W.H., *Electronic cam motion generation with special reference to constrained velocity, acceleration, and jerk*, In: ISA Transactions, 2004, 43, 3: 427–443, https://doi.org/10.1016/S0019-0578(07)60159-1

Authors:

QINGYUAN GUO[1,2], TAO YANG[3], SIJIA FU[4], HONGBIN YU[3]

[1]School of Electronics and Information Engineering, Tiangong University, Tianjin 300387, China
e-mail: 2320080144@tiangong.edu.cn

[2]Key Laboratory of Digital Twin Generic Technology in Special Equipment for State Market Regulation,
Tianjin Special Equipment Inspection Institute, Tianjin 300192, China

[3]School of Mechanical Engineering, Tiangong University, Tianjin 300387, China
e-mail: yangtao@tiangong.edu.cn

[4]Japan Electronics College, Tokyo 169-0073, Japan
e-mail: holymelon0000@163.com

Corresponding author:

HONGBIN YU
e-mail: yuhongbin@tiangong.edu.cn

Window dressing green: how performance aspiration gaps drive symbolic environmental management in the textile value chain

DOI: 10.35530/IT.077.04.2025149

GUOFU ZHANG
BIHAN XU
DING LI
HAN YAN

ABSTRACT – REZUMAT

Window dressing green: how performance aspiration gaps drive symbolic environmental management in the textile value chain

Addressing the recurring phenomenon of symbolic environmental management in which firms decouple environmental commitments from actual practice, this study analyses the impact of performance aspiration gaps on such strategic behaviours within the textile industry value chain. Based on a sample of listed companies in China's textile industry value chain from 2015 to 2023, we empirically test these relationships and find that performance aspiration gaps significantly induce symbolic environmental management in firms within the textile industry value chain. Specifically, firms are more likely to engage in high-profile disclosure without substantive implementation when facing performance shortfalls. Furthermore, this effect is time-dependent; the longer the performance aspiration gap, the more significant its impact on symbolic environmental management. Mechanism tests indicate that performance aspiration gaps drive this behaviour by exacerbating financing constraints and intensifying managerial myopia. Heterogeneity analysis further reveals that the inducement effect of performance aspiration gaps on symbolic environmental management is more pronounced in firms located in regions with lower marketisation levels and weaker environmental regulations, as well as in firms with poorer actual ESG performance. This study contributes to the literature by uncovering the internal micro-mechanisms of environmental decoupling under performance pressure.

Keywords: *textile industry value chain, symbolic environmental management, performance aspiration gap, behavioural theory of the firm, gap duration*

„Ecologie de fațadă”: cum decalajele dintre aspirațiile de performanță determină gestionarea simbolică a mediului în lanțul valoric al industriei textile

Abordând fenomenul recurent al managementului de mediu simbolic, în cadrul căruia întreprinderile disociază angajamentele de mediu de practicile efective, acest studiu analizează impactul decalajelor dintre aspirațiile de performanță și rezultatele reale asupra unor astfel de comportamente strategice în cadrul lanțului valoric al industriei textile. Pe baza unui eșantion de societăți cotate la bursă din lanțul valoric al industriei textile din China, pentru perioada 2015–2023, testăm empiric aceste relații și constatăm că decalajele dintre aspirațiile de performanță și rezultatele reale determină în mod semnificativ adoptarea unui management de mediu simbolic de către întreprinderile din lanțul valoric al industriei textile. Mai precis, firmele sunt mai predispuse să se angajeze în divulgări de mare vizibilitate, fără o implementare substanțială, atunci când se confruntă cu deficite de performanță. În plus, acest efect depinde de timp: cu cât durata decalajului dintre aspirațiile de performanță și rezultatele obținute este mai lungă, cu atât impactul său asupra managementului simbolic de mediu este mai semnificativ. Testele de mecanism indică faptul că decalajele dintre aspirațiile de performanță și rezultatele obținute determină acest comportament prin exacerbarea constrângerilor de finanțare și intensificarea miopiei manageriale. Analiza heterogenității relevă, de asemenea, că efectul de stimulare al decalajelor dintre aspirațiile de performanță și rezultatele obținute asupra managementului simbolic de mediu este mai pronunțat în cazul firmelor situate în regiuni cu niveluri mai scăzute de comercializare și reglementări de mediu mai slabe, precum și în cazul firmelor cu performanțe ESG efective mai slabe. Acest studiu contribuie la literatura de specialitate prin dezvăluirea micro-mecanismelor interne ale decuplării de mediu sub presiunea performanței.

Cuvinte-cheie*: lanțul valoric al industriei textile, managementul simbolic al mediului, decalajul dintre aspirațiile de performanță, teoria comportamentală a firmei, durata decalajului*

INTRODUCTION

As one of the pillar industries of the global economy, the textile and apparel industry occupies a prominent position in global value chains. According to World Trade Organisation statistics, global apparel exports totalled $576 billion in 2022. However, the industry's inherently complex supply chains, resource-intensive production models, and the proliferation of fast fashion business practices pose significant challenges to environmental and social sustainability [1]. Research by the United Nations Environment Programme indicates that the textile industry annually consumes approximately 93 billion cubic meters of water, accounting for 20% of global industrial water use (UNEP, 2018). Furthermore, the textile industry emits up to 1.2 billion tons of carbon dioxide equivalent annually, representing approximately 10% of total global greenhouse gas emissions [2]. This figure astonishingly exceeds the combined emissions of the aviation and shipping industries [2, 3]. These data underscore the formidable challenges confronting the textile industry within the global sustainable development agenda [4].

In response to increasingly stringent environmental regulations and stakeholder demands for sustainable development, a growing number of textile enterprises have begun publishing ESG reports and proclaiming environmental commitments. However, beneath these green declarations lies a troubling phenomenon of symbolic environmental management. A European Commission (2021) survey revealed that in screening online environmental claims, 53.3% contained vague, misleading, or unsubstantiated information, while 42% were identified as false or deceptive. The textile and fashion industry represents a particularly hard-hit sector for greenwashing practices. The Changing Markets Foundation (2021) report exposes the widespread tendency of fast fashion brands to exaggerate sustainability claims, employing vague terms such as "eco-friendly", "green" and "sustainable" without substantive supporting evidence. Such symbolic environmental management not only undermines market information efficiency and erodes investor confidence in ESG practices but also impedes the textile industry's transition toward genuinely sustainable business models [5] and may trigger spillover effects of greenwashing throughout supply chains [6,7]. Although institutional investors' ESG activism can improve corporate green supply chain management performance to some extent [8], the prevalence of greenwashing suggests that external pressure alone cannot fundamentally resolve this issue.

What internal driving forces, then, motivate firms to engage in symbolic environmental management? Behavioural theory of the firm provides an insightful explanatory framework [9]. Central to this theory is the notion that decision-makers' reference points are crucial in determining their course of action. At the organisational level, this reference point manifests as the firm's aspiration level, and decision-makers determine subsequent firm behaviour by assessing the gap between actual performance and aspirations (i.e., performance-aspiration gap). When a firm's actual performance falls short of aspirations (that is, when a performance-aspiration gap exists), its propensity for risk-taking becomes significantly activated. Existing research has confirmed that performance-aspiration gaps can trigger speculative motives, prompting firms to window-dress performance through financial irregularities such as earnings manipulation and related-party transactions [10–12]. However, performance pressure exhibits a dual effect. On one hand, moderate pressure may stimulate employee innovative thinking [13] and boundary-spanning behaviours [14]. On the other hand, excessive pressure may induce opportunistic conduct. This raises a critical research question: under the intense pressure of performance-aspiration gaps, do firms also resort to "strategic" ESG opportunism? Specifically, do they exaggerate or selectively conceal information in ESG disclosures?

There is broad consensus that even when experiencing poor performance, firms must signal their embrace of ESG principles to satisfy legitimacy requirements. Under performance pressure, textile enterprise management confronts a twofold dilemma. On one hand, they must meet stakeholder expectations through ESG information disclosure. On the other hand, they are constrained by the high costs of substantive environmental performance improvement. This dilemma may induce textile firms to adopt symbolic environmental management, exaggerating or selectively concealing information in ESG disclosures. Despite the prevalence of this problem in practice, systematic theoretical analysis and empirical testing remain lacking.

China's textile industry provides a uniquely valuable global research context for examining this issue. First, China is unquestionably the world's largest textile producer and exporter [15]. According to statistics, textile fibres produced by China's textile industry in 2022 accounted for over 50% of global output, while its textile and apparel exports consistently represent more than one-third of the global total. Second, China's textile industry is classified as a key heavily polluting sector. As early as 2008, it was listed by the former Ministry of Environmental Protection among 14 heavily polluting industries in the "Directory of Industry Classification Management for Environmental Protection Verification of Listed Companies". In 2022, the textile industry's chemical oxygen demand and ammonia nitrogen emissions totalled 56,251 tons, representing 16.4% of the national total and ranking first among all industries. This inherently polluting nature subjects the industry to immense environmental governance pressure. Finally, China's current environmental information disclosure regime (particularly the insufficiency of mandatory requirements and the lack of standardised disclosure protocols) further enhances the value of our research [16–18]. This institutional design objectively provides ample opportunities for regulatory arbitrage in symbolic environmental management [19]. On one hand, firms can selectively disclose favourable environmental information while downplaying or avoiding unfavourable information. On the other hand, the relative inadequacy of external audit and regulatory mechanisms means that information authenticity and completeness lack effective oversight, thereby lowering the potential costs of ESG information exaggeration.

Accordingly, we examine samples of Chinese A-share textile industry firms and their supply chain enterprises from 2015 to 2023 to empirically test the impact of performance-aspiration gaps on symbolic environmental management. Our main findings are as follows. Performance-aspiration gaps induce symbolic environmental management behaviour in textile firms. Moreover, the longer such gaps persist, the more pronounced their impact becomes. Further mediation analysis reveals that performance-aspiration gaps worsen financing constraints and intensify managerial myopia, thereby leading to exaggerated or concealed ESG disclosures. Additionally, heterogeneity analysis demonstrates that the effect of performance-aspiration gaps on symbolic environmental management is more pronounced in firms operating in less marketised regions, facing weaker environmental regulations, and exhibiting poorer actual ESG performance.

Our marginal contributions are primarily manifested in the following aspects.

First, we develop a novel theoretical framework grounded in behavioural theory of the firm to explain how performance-aspiration gaps trigger symbolic environmental management, addressing the limitation that existing research overly relies on agency theory or legitimacy theory while neglecting the role of internal performance pressure. The extant literature predominantly attributes greenwashing to external legitimacy demands or internal agency conflicts [20–22], yet research examining how internal performance pressure alters managerial risk preferences and thereby affects ESG information quality remains notably insufficient. We demonstrate that when firms experience performance-aspiration gaps, endogenous pressure inclines management toward symbolic and opportunistic ESG disclosure strategies rather than substantive ESG performance improvement. This contribution genuinely bridges the greenwashing literature with behavioural theory, advancing greenwashing research from an "external pressure response paradigm" toward an "internal pressure inducement paradigm" and providing a novel explanatory pathway for understanding the micro-level drivers of ESG information distortion.

Second, we demonstrate that performance-aspiration gaps exert not only triggering effects but also cumulative effects, contributing a temporal dynamics perspective to the application of behavioural theory of the firm in sustainability research. While existing literature has discussed how performance pressure may trigger short-term risk-taking behaviours [23, 24], systematic evidence on how such "temporal dynamics" influence non-financial information quality remains virtually absent. Our findings indicate that performance gaps generate both triggering effects (initiating symbolic environmental management strategies) and cumulative effects (amplifying such behaviour over time). This finding not only addresses the gap in behavioural theory of the firm regarding temporal considerations but also reveals that symbolic environmental management is not merely a short-term response. Instead, it may evolve into a sustained strategic information management pattern under prolonged performance pressure. This offers important insights for understanding how emerging market firms develop "institutionalised greenwashing" phenomena within chronically high-pressure operating environments.

Third, we identify the internal mechanisms through which performance-aspiration gaps lead to symbolic environmental management and reveal its heterogeneity across different institutional contexts, further advancing the micro-mechanistic and contextualised development of greenwashing research. Empirical analysis demonstrates that performance-aspiration gaps induce opportunistic ESG information behaviour through two channels: intensifying financing constraints and strengthening managerial myopia. Regarding financing constraints, performance pressure may prompt firms to allocate limited resources toward short-term financial assets rather than long-term environmental investments. Concerning managerial myopia, performance pressure incentivises management to prioritise cultivating a green image over advancing substantive innovation. While authentic ESG disclosure can promote corporate green innovation [25], firms under performance pressure tend to favour symbolic strategies. This not only deepens theoretical understanding of greenwashing drivers but also engages with research on financing and managerial pressures [26].

Fourth, this study elucidates the moderating roles of institutional environment and firm resource endowments in shaping ESG behaviour, providing contextualised evidence for understanding ESG governance in emerging markets. Heterogeneity analysis reveals that the inducing effect of performance-aspiration gaps on symbolic environmental management is more pronounced in contexts characterised by lower marketisation, weaker environmental regulation, and poorer actual firm ESG performance. This finding carries important theoretical implications. First, it supports institutional theory's proposition that "institutional voids induce opportunism" [27], demonstrating that absent formal institutional constraints, performance pressure more readily transforms into opportunistic disclosure behaviour. Second, it resonates with the resource-based view's "legitimacy deficit" hypothesis [28], suggesting that firms with inferior actual ESG performance face greater legitimacy pressures and thus are more inclined to compensate through exaggerated disclosures. Finally, this study furnishes empirical evidence for understanding institutionalised variations in ESG behaviour across emerging markets, responds to calls for research on "context dependency" [29], and provides theoretical grounding for optimising ESG governance pathways in emerging market contexts.

THEORETICAL ANALYSIS AND RESEARCH HYPOTHESES

Behavioural theory of the firm posits that absolute performance indicators fail to provide clear evaluation benchmarks for boundedly rational managers [9]. Consequently, decision-makers typically establish an aspiration level and assess firm status by comparing actual performance against this benchmark, thereby simplifying the decision-making process. Specifically, when actual performance exceeds the aspiration level, the firm operates in a relatively comfortable state, and management tends to maintain the status quo while avoiding unnecessary risks. Conversely, when actual performance falls below the aspiration level (i.e., when a performance-aspiration gap exists), this negative deviation activates management's problemistic search mechanism, prompting more risk-taking response strategies to close the performance gap. Performance pressure, as a salient manifestation of performance-aspiration gaps, may both stimulate employees' boundary-spanning behaviours [14] and induce strategic firm responses. Existing research demonstrates that performance-aspiration gaps significantly alter firms' risk-taking preferences and strategic choices. In the financial domain, firms experiencing performance difficulties are more prone to engage in financial opportunism such as earnings manipulation and related-party transactions [10, 11]. However, as financial regulation becomes increasingly stringent and auditing technology advances, opportunities for manipulating financial information have gradually narrowed, prompting firms to redirect opportunistic behaviour toward the relatively weakly regulated non-financial information domain. Compared with financial information, non-financial information lacks unified disclosure standards, proves difficult to verify, and exhibits higher information asymmetry, thereby affording firms greater latitude for strategic manipulation [30]. Based on a cost-benefit analytical framework, we argue that symbolic environmental management represents a rational choice for textile firms experiencing performance-aspiration gaps.

First, from a benefit perspective, symbolic environmental management by textile firms manifests primarily through two mechanisms: legitimacy maintenance and green marketing. Environmental performance has become a critical component of organisational legitimacy, particularly salient in the textile industry. When performance deteriorates, firms face scrutiny from investors, regulators, and the public, threatening their social legitimacy [20]. In this context, some firms selectively disclose environmental information to cultivate the impression that "performance decline stems from environmental investment", thereby attributing operational difficulties to environmental responsibility fulfilment and mitigating stakeholders' negative evaluations of managerial competence [31].

Additionally, symbolic environmental management serves as a vital tool for implementing green marketing strategies in textile firms. With growing global consumer environmental consciousness and downstream brand emphasis on supply chain environmental performance, ESG performance has increasingly become a key determinant of textile product competitiveness. However, genuine environmental performance improvement often necessitates substantial sustainability transformation investments, imposing considerable burdens on firms facing performance pressures. Under these circumstances, cultivating a green image through ambiguous labels such as "sustainable" and "eco-friendly fabrics" becomes a low-cost, high-efficiency short-term response strategy [32]. Even with limited substantive environmental practices, such strategic positioning may enhance product competitiveness and short-term sales in green consumer markets. Therefore, firms experiencing performance-aspiration gaps possess stronger incentives to intensify green marketing rhetoric and pursue performance improvement through exaggerated ESG disclosures.

Second, from a cost perspective, the low-cost nature of symbolic environmental management constitutes an important inducement for textile firms. On one hand, firms in performance difficulty often confront resource constraints that preclude substantial sustainability transformation expenditures. Substantive environmental improvement in the textile industry typically involves capital-intensive investments including production equipment upgrades, clean technology adoption, and wastewater treatment facility construction. According to United Nations Environment Programme research, textile industry green transformation demands considerable capital investment, yet firms experiencing performance-aspiration gaps typically allocate limited funds toward maintaining operations and short-term profitability. In contrast, strategic disclosure featuring ESG-oriented messaging entails lower costs with potentially higher returns. Consequently, when substantive ESG implementation proves challenging, strategic ESG communication becomes a pragmatic choice for firms experiencing performance-aspiration gaps [32].

On the other hand, firms in performance difficulty bear relatively lower reputational sanction costs. Reputation theory suggests that corporate reputation, as an intangible asset, derives value from stakeholder trust and recognition. Firms experiencing performance difficulties typically already possess diminished reputational standing. Even if symbolic environmental management is exposed, such firms incur lower marginal reputational losses compared with firms enjoying both strong reputation and performance. This "reputational floor effect" reduces the expected costs of opportunistic behaviour. More importantly, as performance-aspiration gaps widen, the marginal reputational costs from negative events progressively decline. This decreasing marginal cost structure incentivises firms to adopt increasingly opportunistic approaches, thereby intensifying symbolic environmental management [33].

Based on the foregoing analysis, we propose:

H1: Ceteris paribus, performance-aspiration gaps increase symbolic environmental management in textile firms.

Performance-aspiration gaps, as a multifaceted concept, exhibit multiple dimensions. Beyond the intensity dimension reflecting the magnitude by which current performance falls short of expectations, scholars should also examine the temporal dimension of persistence. Most existing research focuses on the intensity of performance-aspiration gaps, yet in practice, the persistence of performance difficulties equally influences firm behavioural decisions [10, 11].

Performance-aspiration gap persistence refers to situations where firm performance consecutively falls below aspiration levels across multiple operating periods [34]. Incorporating this temporal dimension proves critical for understanding firm behaviour. When confronting isolated performance-aspiration gaps, firms are more likely to employ external attribution, ascribing substandard performance to uncontrollable external factors such as economic fluctuations, natural disasters, or policy changes, thereby assuaging stakeholder concerns about operational deficiencies. Such external attribution typically garners understanding and tolerance in the short term, preserving organisational reputation and stakeholder trust.

However, when firms repeatedly and persistently experience performance-aspiration gaps, the effectiveness of external attribution significantly diminishes. Attribution theory suggests that when phenomena persist over time, observers become more inclined to attribute them to internal stable factors rather than external temporary circumstances [35].

Consequently, persistent performance-aspiration gaps reduce the credibility of external attribution, with stakeholders more likely attributing poor performance to insufficient operational capabilities, strategic missteps, or managerial deficiencies [34]. For textile firms, this persistent underperformance proves especially problematic. The textile industry operates within an environment characterised by intense competition, low profit margins, and excess capacity, subjecting the sector to substantial operational pressures. In this context, prolonged poor performance is perceived as a credible signal of competitive weakness, eroding investor and downstream brand confidence in sustainable operational capability and consequently affecting financing access and order acquisition.

To mitigate trust crises triggered by persistent performance difficulties, textile firms become more likely to engage in symbolic environmental management. The rationale for this behaviour involves creating an illusory green image to redirect external attention, mitigate negative perceptions of operational deficiencies, and obscure stakeholder assessments. Specifically, when firms persistently fail to meet performance expectations, managerial pressure stems not only from performance itself but also from doubts regarding long-term organisational viability. Under these circumstances, firms attempt to construct a narrative framework suggesting that “despite poor short-term financial performance, the firm retains competitiveness in long-term sustainable development” by amplifying positive ESG disclosures and exaggerating environmental investments and achievements [30]. This narrative can partially offset negative expectations from sustained poor performance and maintain stakeholder confidence [31].

Moreover, from an environmental strategy implementation perspective, remaining persistently in performance-aspiration gap states often precipitates resource scarcity, as firms face mounting pressures in capital raising and resource allocation [34]. Textile firms typically exhibit high energy consumption and emissions in spinning, dyeing, and printing processes, while environmental transformation requires substantial capital investment. When firms persistently experience performance-aspiration gaps, resource constraints intensify further. On one hand, sustained poor performance weakens internal financing capacity, as reduced operating cash flows limit internal fund deployment [36]. On the other hand, persistent performance difficulties deteriorate external financing conditions, with declining credit ratings and rising financing costs further constraining available resources. Under these circumstances, firms typically prioritise limited funds toward maintaining operations and short-term profitability, while adopting a “low investment, high disclosure” approach to environmental governance. This strategic choice manifests as cultivating superficial green images at minimal cost rather than pursuing substantive environmental performance improvements. As performance-aspiration gap duration extends, this resource constraint effect accumulates, correspondingly strengthening firms’ motivation and intensity for implementing symbolic environmental management.

More critically, performance-aspiration gap persistence also triggers systematic changes in managerial cognition and behavioural patterns. Behavioural theory suggests that sustained poor performance leads management to develop more pessimistic self-efficacy perceptions, diminishing confidence in reversing difficulties through substantive reform [37]. In this psychological state, management becomes more inclined toward short-term, superficial responses rather than substantive transformations requiring long-term investment with delayed returns. Symbolic environmental management exemplifies this short-term response strategy. Through strategic information disclosure, firms can rapidly obtain external green recognition without substantive environmental investment, alleviating anxiety and scrutiny from performance pressures.

Based on the foregoing analysis, we propose:

H2: Ceteris paribus, the longer the duration of performance-aspiration gaps, the more pronounced their impact on symbolic environmental management in textile firms.

The theoretical framework appears in figure 1.

RESEARCH DESIGN

Data sources and sample selection

We select listed companies in China’s A-share textile value chain from 2015 to 2023 as our initial sample. Regarding industry classification, following existing research [38, 39], we adopt the “Guidelines for Industry Classification of Listed Companies” revised by the China Securities Regulatory Commission in

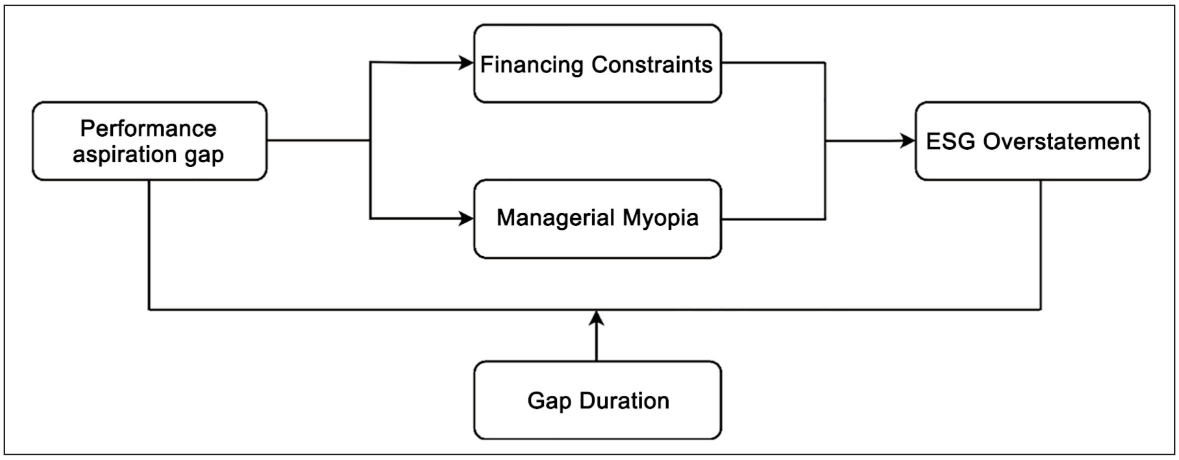

Fig. 1. Theoretical framework

2012. We select six industry categories integral to the textile value chain: C17 (Textile Industry), C18 (Textile, Apparel and Accessories), C19 (Leather, Fur, Feather and Related Products and Footwear), C26 (Chemical Raw Materials and Chemical Products Manufacturing), C28 (Chemical Fibre Manufacturing), and C29 (Rubber and Plastic Products).

This industry scope encompasses key segments of the textile value chain, including upstream raw material supply (chemical fibres and raw materials), midstream production and manufacturing (textiles and apparel), and downstream auxiliary materials (leather and plastic products), thereby comprehensively capturing ESG practice patterns across the industry. The data used in this study are primarily sourced from the China Stock Market & Accounting Research (CSMAR) database and hand-collected from firms' annual reports and CSR reports. Our sample selection process adheres to rigorous data quality standards. We exclude firm-year observations in which the company is designated as ST or *ST in that year, and winsorize all continuous variables at the 1st and 99th percentiles to mitigate the influence of outliers. After the above screening, the final sample comprises 3715 valid firm–year observations.

Variable definition

Symbolic Environmental Management (ESG_gap)

Symbolic environmental management mainly manifests as enterprises shaping a green image through a relatively high level of environmental information disclosure, but their actual environmental governance investment is relatively insufficient. Based on this, we use the difference between enterprise environmental information disclosure intensity and substantive environmental investment intensity to measure the degree of enterprise symbolic environmental management. Among these, enterprise environmental information disclosure intensity is measured by taking the natural logarithm of the frequency of occurrence of environment-related words in annual reports or social responsibility reports plus 1, and enterprise substantive environmental investment intensity is measured by the ratio of the amount of environmental investment to operating revenue. To eliminate scale differences, this paper standardises the two separately and constructs the following indicator:

$$ESG\_gap_{i,t} = \frac{ENV\_DIS_{i,t} - \overline{ENV\_DIS}}{\sigma_{DIS}} - \frac{ENV\_INV_{i,t} - \overline{ENV\_INV}}{\sigma_{INV}} \quad (1)$$

where $ENV\_DIS_{i,t}$ represents the environmental information disclosure intensity of enterprise *i* in year *t*, $ENV\_INV_{i,t}$ is the substantive environmental investment intensity of enterprise *i* in year *t*, $\overline{ENV\_DIS}$ and $\overline{ENV\_INV}$ represent the sample means of environmental information disclosure intensity and environmental investment intensity, respectively, and represents the corresponding sample standard deviation. The larger the value, the higher the enterprise's level of environmental information disclosure relative to actual environmental investment, that is, the enterprise is more likely to have "overstating" symbolic environmental management behaviour.

Performance-Aspiration Gap (Per_gap)

According to behavioural theory of the firm, firms establish expected performance levels with reference to both historical and industry average performance, then assess whether performance-aspiration gaps exist by comparing actual performance against these aspirations. We therefore employ formula 2:

$$Per\_gap_{i,t} = \begin{cases} |P_{i,t} - A_{i,t}|, & \text{if } P_{i,t} < A_{i,t} \\ 0 & \text{others} \end{cases} \quad (2)$$

where $P_{i,t}$ represents actual firm performance measured by return on assets (ROA), and $A_{i,t}$ represents expected performance calculated as a linear combination of historical and industry performance, as shown in formula 3:

$$A_{i,t} = \alpha_1 HA_{i,t} + \alpha_2 SA_{i,t} \quad (3)$$

Here, $HA_{i,t}$ denotes historical aspiration, fitted from the firm's actual performance (ROA) over the prior three years and representing the performance level the firm should achieve under normal operating conditions. $SA_{i,t}$ represents social aspiration, measured as the average performance of all firms in the focal firm's industry excluding the focal firm itself. The parameter α_1 denotes the weight assigned to historical aspiration; we report results using $\alpha_1 = 0.5$.

For performance-aspiration gap persistence (Cons), following existing research (Zhao & Xiao, 2024), we measure persistence as the number of consecutive periods during which performance-aspiration gaps occur. Specifically, *Cons* equals 1 when performance-aspiration gaps persist for two or more consecutive periods and 0 otherwise.

Control variables

To mitigate omitted variable bias, we control for factors that may influence symbolic environmental management intensity, including firm size (Size), firm age (Age), profitability (Profit), cash flow level (Cash), growth opportunities (Growth), leverage (Lev), ownership concentration (Balance), CEO-chairman duality (Dual), executive ownership (Share), executive overseas experience (Overseas), board size (Board), board independence (Indep), and board gender diversity (Female).

Model design

We estimate model 4 to examine the impact of performance-aspiration gaps on symbolic environmental management:

$$ESG\_gap_{i,t} = \alpha_0 + \alpha_1 Per\_gap_{i,t} + \alpha_i Controls_{i,t} + Year + Firm + \varepsilon_{i,t} \quad (4)$$

In model 4, subscripts *i* and *t* denote firm and year, respectively. $Controls_{i,t}$ denotes a vector of control variables, including firm financial characteristics and corporate governance variables. To account for unobservable heterogeneity, we include firm and year fixed effects, with standard errors clustered at the firm level. The term $\varepsilon_{i,t}$ represents the idiosyncratic error term.

EMPIRICAL RESULTS

Benchmark regression

Figure 2 reports baseline regression results examining the impact of performance-aspiration gaps on symbolic environmental management. Panel A controls only for firm and year fixed effects. The coefficient on *Per_gap* is 0.133 and statistically significant at the 5% level, indicating that performance-aspiration gaps significantly increase symbolic environmental management intensity.

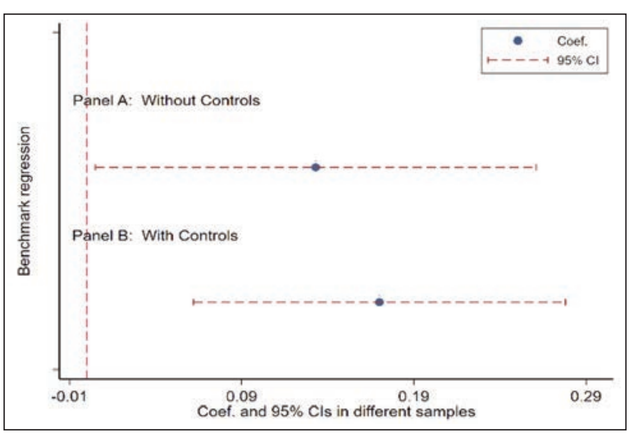

Fig. 2. Benchmark regression

Panel B incorporates all control variables. The coefficient on *Per_gap* rises to 0.170 and achieves significance at the 1% level, demonstrating enhanced statistical significance. This finding aligns with behavioural theory's core prediction: when actual performance falls below aspirations, managerial performance pressure activates problemistic search mechanisms, prompting risk-taking responses. Collectively, these results support H1.

Sub-sample regression

We partition the sample based on performance-aspiration gap persistence and re-estimate model 4 for each subsample. Figure 3 shows that in the high-persistence subsample (*Cons* = 1), the coefficient on *Per_gap* is positive and significant at the 1% level, whereas in the low-persistence subsample (*Cons* = 0), the coefficient is positive but insignificant. These results indicate that longer-lasting performance-aspiration gaps exert stronger effects on symbolic environmental management, thereby supporting H2.

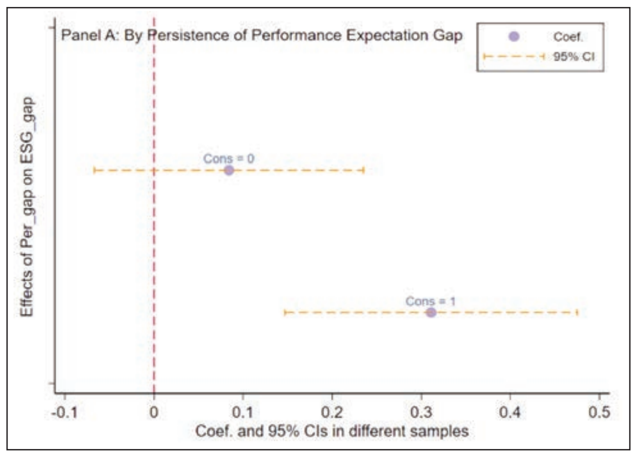

Fig. 3. Subsample regression results

Robustness tests

PSM and EBM

To mitigate potential bias from systematic differences across firms, we partition the sample into treatment (firms with performance-aspiration gaps) and control (firms without performance-aspiration gaps) groups and employ propensity score matching (PSM) with nearest-neighbour (1:1) matching. Figure 4 demonstrates that after propensity score matching, differences in control variables between treatment and control groups substantially diminish. Because PSM entails some sample loss, we further implement entropy balancing matching (EBM) as an alternative matching procedure. Results remain robust across both approaches. As shown in figure 5, the coefficient on *Per_gap* is positive and statistically significant in both specifications.

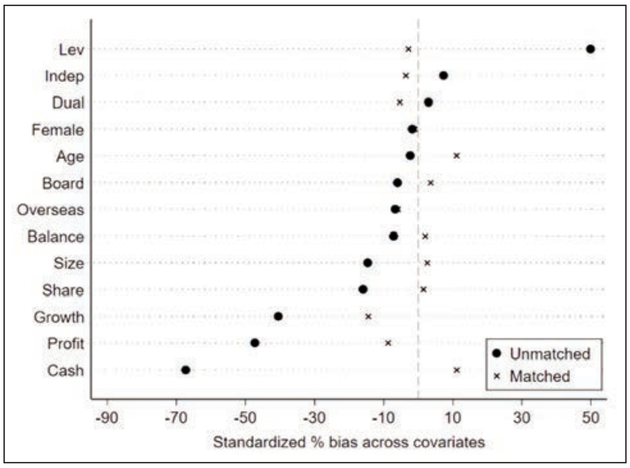

Fig. 4. Covariate balance diagnostics

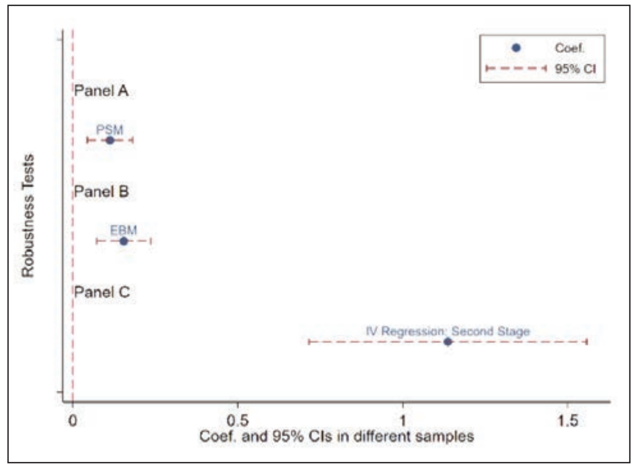

Fig. 5. Robustness tests

Instrumental variables

We construct an instrumental variable based on adjusted satellite nighttime luminosity data. To exploit temporal variation, we use the provincial-level average growth rate in nighttime light intensity as an instrument (IV) for performance-aspiration gaps. This variable satisfies the relevance condition: nighttime luminosity objectively reflects regional economic activity and development. Rising nighttime light intensity typically indicates improving local economic conditions, expanding market demand, and enhanced resource mobility, which collectively improve firm operating environments. Favourable macroeconomic conditions alleviate performance pressure and reduce the likelihood of persistent underperformance, thereby correlating with performance-aspiration gaps. This instrument also plausibly satisfies the exclusion restriction. Variation in nighttime luminosity primarily reflects regional-level macroeconomic fluctuations, infrastructure development, and policy interventions, which are unlikely to directly affect firm-level symbolic environmental management decisions.

We implement instrumental variable regression through the following two-stage specification [40]:

$$Per\_gap_{i,t} = \alpha_0 + \alpha_1 IV_{i,t} + \alpha_i Controls_{i,t} + Year + Firm + \varepsilon_{i,t} \quad (5)$$

$$ESG\_gap_{i,t} = \alpha_0 + \alpha_1 M\_Per\_gap_{i,t} + \alpha_i Controls_{i,t} + Year + Firm + \varepsilon_{i,t} \quad (6)$$

where $M\_Per\_gap_{i,t}$ denotes the first-stage predicted value, and other variables follow model 4. As shown in figure 5, the main findings remain robust.

Alternative measurement of performance aspiration gap

We employ two alternative measures. First, we measure performance-aspiration gaps (*Per_gap*1) as the shortfall when actual performance falls below analyst forecasts (winsorized at zero). Second, we vary the aspiration weighting by setting α_1 = 0.6 (*Per_gap*2). As shown in figure 6, the main conclusions remain unchanged.

Adding fixed effects

To account for unobservable regional characteristics, we augment the baseline specification with province fixed effects, controlling for cross-provincial variation in institutional environment and economic development. As shown in figure 6, the main results remain robust.

Alternative model specification

To further verify robustness, we alter the standard error clustering approach. Because our sample comprises exclusively textile firms, we cluster standard errors at the province rather than the firm level to address potential within-province correlation. As shown in figure 6, the main findings remain unchanged.

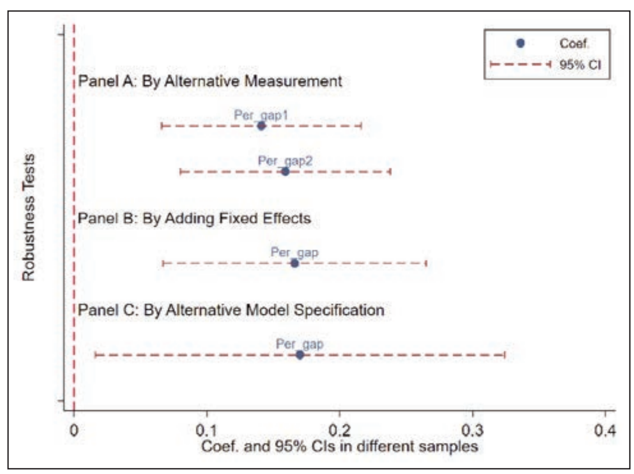

Fig. 6. Robustness tests

Double machine learning

Although baseline regressions reveal the relationship between performance-aspiration gaps and symbolic environmental management, linear models may suffer from misspecification bias. Linear specifications may fail to capture nonlinear relationships and interaction effects among variables. Moreover, high-dimensional controls may induce the curse of dimensionality and multicollinearity, compromising estimation precision and robustness. We therefore employ double/debiased machine learning [41]. Specifically, we implement a partially linear model using random forests with 1:4 and 1:7 cross-fitting splits, controlling for year and firm fixed effects and including both linear and quadratic control terms. The results show that the coefficients are all positive and statistically significant at the 1% level. Due to space limitations, the robustness results are available upon request.

FURTHER ANALYSIS

Mechanism tests

Based on our theoretical framework, performance-aspiration gaps may induce symbolic environmental management through two mechanisms.

First, resource constraints: underperformance deteriorates firm financial conditions [36] and intensifies financing constraints, forcing firms to trade off high-cost substantive environmental investment against low-cost symbolic disclosure [42], thereby favouring symbolic environmental management strategies. Second, cognitive biases: performance pressure strengthens managerial short-termism, prompting managers to prioritise green image cultivation over substantive innovation [23]. To test these mechanisms, we examine financing constraints and managerial myopia as mediating pathways.

We employ a two-stage mediation approach. First, we estimate the effect of performance-aspiration gaps on mediating variables (M). Second, we estimate the effect of fitted mediator values ($\hat{M}$) on symbolic environmental management. This approach follows the two-equation system:

$$M_{i,t} = \alpha_0 + \alpha_1 Per\_gap_{i,t} + \alpha_i Controls_{i,t} + \\ + Year + Firm + \varepsilon_{i,t} \qquad (7)$$

$$ESG\_gap_{i,t} = \alpha_0 + \alpha_1 \hat{M}_{i,t} + \alpha_i Controls_{i,t} + \\ + Year + Firm + \varepsilon_{i,t} \qquad (8)$$

where M denotes mediating variables, specifically two mediators: financing constraints (FC), measured using the absolute value of the SA index [43], where higher values indicate tighter constraints, and managerial myopia (Short), measured as short-term investment scaled by lagged total assets, where higher values indicate greater myopia.

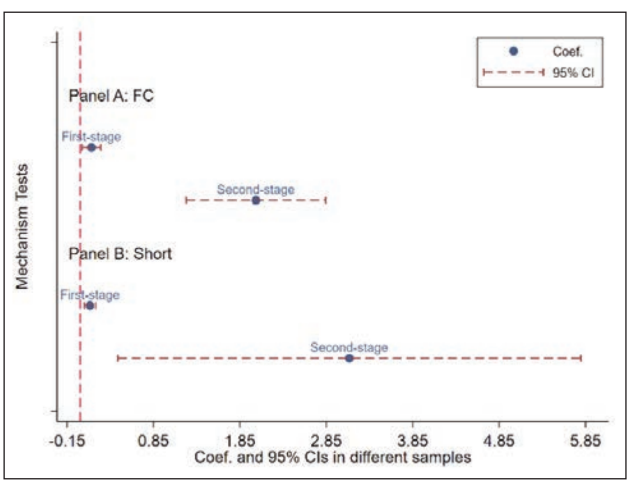

Fig. 7. Mechanism tests

Figure 7 shows that first-stage results indicate performance-aspiration gaps positively and significantly correlate with both financing constraints (coefficient = 0.131) and managerial myopia (coefficient = 0.114), confirming that performance-aspiration gaps intensify financing constraints and strengthen managerial short-termism. Second-stage results show that fitted values of both mediators positively and significantly affect symbolic environmental management intensity. Regarding financing constraints, performance-aspiration gaps create resource pressures, forcing firms to prioritise liquid asset accumulation and crowding out substantive environmental investment, thereby amplifying symbolic environmental management. Regarding managerial myopia, performance pressure induces short-term orientation, prompting managers to favour strategies yielding quick performance gains. Because green image cultivation delivers faster results than substantive innovation, myopic managers favour symbolic approaches.

Heterogeneity analysis

The effect of performance-aspiration gaps on symbolic environmental management varies across contexts. Organisational embeddedness theory [44] and institutional theory [45] posit that firm behaviour is shaped by both external institutional environments and internal resource endowments. In the textile industry, an environmentally sensitive, high-risk sector, significant variation in institutional environments and ESG foundations across firms may generate heterogeneity in opportunistic responses [46]. To identify context-dependent effects, we examine whether marketisation level, regulatory stringency, and firm ESG performance moderate the effect of performance-aspiration gaps on symbolic environmental management.

Marketisation

Marketisation reflects institutional quality and competitive intensity. In environmentally sensitive industries like textiles, marketisation constrains firms' conversion of performance pressure into opportunistic ESG disclosure. In highly marketised regions, stronger legal institutions and enforcement increase detection probability and sanction costs for opportunistic behaviour [47]. Additionally, intense market competition and mature stakeholder networks (including institutional investors, analysts, and media) create multilayered monitoring of high-emission, resource-intensive firms [48]. These forces encourage textile firms to address performance gaps through substantive improvements rather than information manipulation. Conversely, in weakly marketised regions, institutional voids enable opportunistic behaviour [27], and firms exploit information asymmetries to cultivate green images.

We measure provincial marketisation using the China Marketisation Index, which encompasses five dimensions: government-market relations, private sector development, factor market development, intermediary organisation development, and legal environment. We partition the sample at the median marketisation level.

Panel A of figure 8 shows that performance-aspiration gap coefficients are insignificant in highly marketised regions but positive and significant in weakly marketised regions. This indicates that in institutionally weaker regions, textile firms resort to symbolic environmental management when facing performance pressure. This finding aligns with institutional theory: firms in institutional voids adopt symbolic strategies to secure legitimacy.

Environmental regulation

The textile industry is characterised by high pollution and energy intensity, rendering firms' ESG disclosure particularly sensitive to environmental regulation. Regulatory stringency, as a key institutional constraint, enhances disclosure credibility by establishing stricter compliance standards and monitoring [49]. In stringently regulated regions, stricter emission standards and monitoring increase detection probability for misreporting [50]. Additionally, green finance instruments like green credit facilitate financing for substantive environmental investment [51], alleviating financing constraints. Environmental regulation both directly constrains emissions and indirectly enhances environmental performance by inducing green innovation [52, 53]. Stringent regulation also promotes digital transformation, which catalyses green innovation [54], creating a regulation-innovation-performance virtuous cycle. Conversely, lax regulation enables opportunism, prompting firms to resort to symbolic disclosure to address legitimacy pressures [55].

We measure regulatory stringency using keyword frequency in provincial government work reports, specifically counting mentions of "environmental protection", "pollution control", "energy conservation and emission reduction" and "green development". Higher frequency indicates stronger regulatory commitment. We partition the sample at the median.

Panel B of figure 8 shows that performance-aspiration gap coefficients are positive and significant in weakly regulated regions but insignificant in stringently regulated regions. This indicates that in lax regulatory environments, textile firms favour low-cost symbolic environmental management to deflect pressure over costly substantive investments. This result aligns with the Porter Hypothesis [56]: moderate environmental regulation induces substantive innovation, whereas regulatory laxity enables opportunism.

ESG performance

Within the textile industry, variation in ESG foundations shapes behavioural responses to performance-aspiration gaps. The resource-based view [28] and impression management theory [57] suggest that firms with weak ESG foundations face larger legitimacy deficits and resort to opportunistic disclosure to cultivate green images and deflect pressure [33]. ESG laggards typically lack robust environmental management systems and adequate environmental resources, face higher marginal costs of substantive improvement, and thus favour impression management over genuine improvement [58]. Financial constraints further push these firms toward liquid asset accumulation over environmental investment [59], amplifying symbolic management incentives. Conversely, ESG leaders possess robust environmental management systems and stakeholder communication mechanisms. Their valuable reputation capital makes them cautious about disclosure. They prioritise reputation preservation and avoid risking long-term reputation for short-term gains [60].

We measure ESG foundations using Bloomberg ESG performance scores and partition the sample at the median.

Panel C of figure 8 shows that coefficients on performance-aspiration gaps are positive and significant among ESG laggards but insignificant among ESG leaders. These results support the legitimacy deficit hypothesis: ESG laggards inflate disclosure to compensate for legitimacy deficits when facing performance pressure, whereas ESG leaders prioritise reputation preservation over opportunistic tactics.

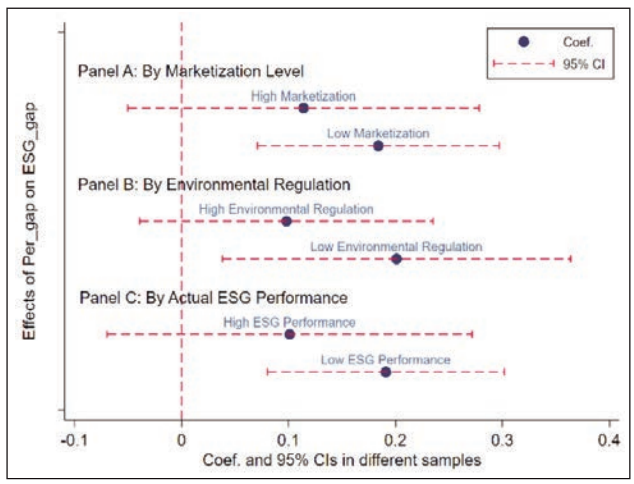

Fig. 8. Heterogeneity analysis results

CONCLUSION AND DISCUSSION

With the advancement of the global sustainable development concept, enterprise ESG information disclosure has increasingly become an important basis for stakeholders to evaluate their environmental responsibility. However, the significant divergence between enterprise ESG information disclosure and actual performance has become a key problem hindering the effective operation of the ESG system. Based on the behavioural theory of the firm, this study systematically analyses the influence mechanism of the performance-aspiration gap on enterprise symbolic environmental management, and conducts empirical testing using Chinese textile industry listed companies from 2015 to 2023 as a sample.

The results show that the performance-aspiration gap significantly induces textile enterprise symbolic environmental management behaviour, and this effect strengthens with the extension of performance pressure duration. Mechanism testing shows that the performance-aspiration gap leads to symbolic environmental management behaviour through two pathways: deteriorating enterprise financing constraints and intensifying managerial myopia. Heterogeneity analysis further reveals that in contexts of lower marketisation degree, weaker environmental regulation intensity, and poorer ESG actual performance, the inducing effect of the performance-aspiration gap on enterprise symbolic environmental management is more significant.

Theoretical contributions

The theoretical contributions of this study are manifested in the following four aspects.

First, it expands the application of behavioural theory of the firm in the ESG disclosure field, revealing the mechanism by which the performance-aspiration gap as an endogenous micro-motivation triggers greenwashing behaviour. Existing research mostly focuses on formal institutional pressure or external market supervision on greenwashing behaviour [33], while paying less attention to how internal operational pressure triggers opportunistic disclosure. This study introduces the concept of performance-aspiration gap from behavioural theory of the firm, constructs a theoretical framework with internal operational pressure as the core driving force, explaining how it acts as an endogenous micro-motivation to trigger management's adoption of symbolic environmental management behaviour. This compensates for the over-reliance on external theories in existing research, reveals the endogenous micro-motivation of ESG information distortion, and promotes the transformation of greenwashing research from an external pressure response paradigm to an internal pressure inducement paradigm.

Second, it reveals the temporal dynamics of the performance-aspiration gap's influence on ESG behaviour, adding a persistence dimension consideration to behavioural theory of the firm. Traditional behavioural theory of the firm assumes that organisational responses to performance gaps are immediate and short-term [9], while this study, by introducing the concept of performance-aspiration gap persistence, finds that performance gaps have both a short-term triggering effect and a long-term cumulative amplification effect on symbolic strategies. This finding not only expands the temporal dimension of behavioural theory of the firm but also reveals the possible path for symbolic environmental management behaviour to evolve into an institutionalised strategic pattern under long-term pressure, providing a new theoretical perspective for understanding strategic evolution under sustained pressure.

Third, it deepens the understanding of greenwashing driving mechanisms, identifying that the performance-aspiration gap influences symbolic environmental management behaviour through two complementary pathways: financing constraints and managerial myopia. The financing constraint mechanism embodies how resource scarcity changes the enterprise's trade-off between substantive environmental investment and symbolic information disclosure [42]. The managerial myopia mechanism reveals how performance pressure, by affecting management's time preferences, prompts them to prioritise strategic disclosure with short-term effects over long-term substantive improvement. This dual-mechanism framework echoes agency theory's assertions about resource allocation [61], providing a micro-foundation for understanding how performance pressure reshapes enterprise ESG strategies from the outside in.

Fourth, it reveals the moderating role of institutional environment and enterprise resource endowment in shaping ESG behaviour, providing contextualised evidence for understanding ESG governance in emerging markets. The heterogeneity analysis of this study finds that the effect of the performance-aspiration gap shows significant differences under different institutional environments and enterprise foundations. In contexts with weaker institutional environments or poorer enterprise foundations, performance pressure is more easily converted into opportunistic behaviour. This finding supports institutional theory's assertion about institutional voids inducing opportunism [27] and echoes the resource-based view's hypothesis about legitimacy deficit [28]. This study provides empirical evidence for understanding how institutional environment and enterprise resources jointly shape ESG behaviour, and also provides a theoretical basis for optimising ESG governance paths in the emerging market context.

Practical implications

Based on the above research findings, this study provides important practical implications for different market participants to address symbolic environmental management behaviour and improve ESG information quality.

First, regarding enterprise-level governance optimisation. Regarding performance-aspiration gap and managerial myopia issues, textile enterprises should abandon assessment models oriented toward short-term financial indicators and extend executive performance evaluation cycles to match the recovery cycle of green technology investment. More importantly, it is essential to establish a direct linkage mechanism between executive compensation and quantifiable, substantive ESG performance indicators, rather than focusing only on disclosure ratings or report quality. Specifically, enterprises can incorporate substantive environmental performance indicators such as carbon emission intensity, energy consumption efficiency, and wastewater treatment compliance rate into the executive performance assessment system, and assign sufficient weight to these indicators. Through institutional design, guide management to shift resource allocation toward long-term, substantive green innovation and operational improvement, fundamentally suppressing opportunistic behaviour. In addition, enterprises should establish independent ESG supervisory committees to conduct internal review of the authenticity of ESG information disclosure, ensuring that disclosure content matches actual actions.

Second, regarding the path to institutional environment improvement. Given that contexts with low marketisation degree and weak environmental regulation amplify greenwashing effects, regulatory agencies should formulate mandatory, differentiated environmental information disclosure and audit standards for the high-pollution characteristics of the textile industry. First, establish a unified environmental information disclosure framework, clarifying disclosure content, format, and verification requirements, reducing the space for strategic disclosure by enterprises. Second, strengthen third-party audit mechanisms, requiring textile enterprises to hire independent agencies to conduct substantive audits of ESG reports, especially on-site verification of key indicators such as energy consumption and pollution emissions. Third, increase the punishment for false disclosure, imposing multiple sanctions such as economic penalties, credit downgrading, and financing restrictions on enterprises verified to have symbolic environmental management behaviour. At the same time, financial institutions should use actual improvement data of enterprise environmental performance as the core approval basis when providing green credit and bond support, rather than relying on symbolic information. Through a mechanism of rewarding the excellent and punishing the poor, provide preferential financing for enterprises conducting clean production technology transformation and possessing genuine emission reduction results, effectively alleviating their financing constraints during the transition period, and increasing the cost of false disclosure for enterprises.

Third, regarding coping strategies for long-term pressure. To solve the cumulative effect caused by long-term pressure and the transformation difficulties of enterprises with poor actual performance, governments and industry associations should concentrate resources to support the research and development and promotion of key green technologies, prompting enterprises to fundamentally solve pollution problems. First, establish special funds to support clean production technology, circular economy models, and green supply chain management innovation in the textile industry, reducing the technological threshold and financial pressure of enterprise green transformation. Second, promote industry-university-research cooperation, facilitating universities, research institutions, and enterprises to jointly tackle key technologies such as energy conservation and emission reduction, wastewater treatment, and recycling, accelerating the transformation of technological achievements. Third, establish a transparent supply chain ESG information sharing platform, and promote independent third-party agencies to verify and certify enterprise environmental performance data. This comprehensive transparency and external supervision can effectively identify and constrain those enterprises that have long relied on symbolic information management, transforming sustainable development requirements into norms jointly observed by the industry. In addition, industry associations should formulate ESG best practice guidelines for the textile industry, promoting overall industry ESG level improvement through benchmark enterprise demonstrations, experience sharing, and peer pressure.

Research limitations and prospects

Although this study has achieved certain theoretical and practical contributions, it still has the following limitations, providing directions for future research.

First, regarding the limitations of sample selection. The sample of this study is concentrated on textile supply chain enterprises, which is beneficial for in-depth analysis of industry characteristics and control of industry heterogeneity, but may have certain limitations in the universality of conclusions. As a typical high-pollution, high-energy-consumption industry, the textile industry's ESG pressure and disclosure motivation may differ from other industries. Future research can extend to other industries, especially those with different ESG pressures, to test the external validity of this study's core mechanisms. Cross-industry comparative research will help identify industry boundary conditions for the influence of the performance-aspiration gap on ESG behaviour, deepening the understanding of greenwashing motivations in different industry contexts.

Second, regarding the expansion of the research context. This study focuses on the Chinese context, and China's unique institutional environment may influence research results, thereby limiting the direct universality of conclusions. It is crucial to test the findings of this study in different institutional and organisational contexts. Future research should conduct cross-country comparative research in countries with differences in institutional pressure intensity, marketisation degree, etc., to test the validity and universality of this study's core mechanisms in different contexts. This will help deeply explore the possible substitution or complementary relationships between performance-aspiration gap and formal environmental regulation and market mechanisms in different countries, thereby more comprehensively understanding the impact of performance pressure on ESG behaviour in a global context.

REFERENCES

[1] Liu, H., Yan, H., Zeng, H., Hu, T., Ma, S., T*angled Knowledge: Mapping Research Hotspots and Emerging Frontiers in Textile Technology through Bibliometric Analysis*, In: AUTEX Res. J., 2026, 26, 20250063

[2] Leal Filho, W., Perry, P., Heim, H., Dinis, M.A.P., Moda, H., Ebhuoma, E., Paço, A., *An Overview of the Contribution of the Textiles Sector to Climate Change*, In: Front. Environ. Sci., 2022, 10, 973102
[3] Boström, M., Micheletti, M., *Introducing the Sustainability Challenge of Textiles and Clothing*, In: J. Consum. Policy, 2016, 39, 367–375
[4] Wang, C., Song, J., Nunes, L.M., Zhao, H., Wang, P., Liang, Z., Arp, H.P.H., Li, G., Xing, B., *Global Microplastic Fiber Pollution from Domestic Laundry*, In: J. Hazard. Mater., 2024, 477, 135290
[5] Yuan, M., Hu, X., Zeng, L., *How Corporate Governance Shapes the Relationship between Internal Control and Information Disclosure*, In: J. Compr. Bus. Adm. Res., 2025
[6] Xiang, Y., Liu, Y., *Global Sustainable Supply Chain Governance, Effectiveness of Social Responsibility, and Performance in Emergent Markets: An Exploratory Multiple Case Study*, In: Rev. Adm. Empresas, 2025, 65, 6, e2024-0587
[7] Hu, T., Zhao, L., Huang, Y., Yan, H., Chen, X., *The Dark Side of Retail Investors' Green Activism: Evidence from Corporate Greenwashing*, In: Int. J. Bank Mark., 2026, 44, 6, 1191–1221
[8] Wu, B., Ren, K., Fu, Y., He, D., Pan, M., *Institutional Investor ESG Activism and Green Supply Chain Management Performance: Exploring Contingent Roles of Technological Interdependences in Different Digital Intelligence Contexts*, In: Technol. Forecasting Social Change, 2024, 209, 123789
[9] Greve, H.R., *Investment and the Behavioural Theory of the Firm: Evidence from Shipbuilding*, In: Ind. Corp. Change, 2003, 12, 1051–1076
[10] Yu, W., Minniti, M., Nason, R., *Underperformance Duration and Innovative Search: Evidence from the High-tech Manufacturing Industry*, In: Strateg. Manag. J., 2019, 40, 836–861
[11] Zhong, X., Ren, L., Song, T., *To Cheat When Continuously Missing Aspirations: Does CEO Experience Matter?*, In: Asia Pac. J. Manag., 2023, 40, 815–845
[12] Zhong, Y., Yan, H., Xia, Z., *Who Is Lifting the Green Veil? Climate Physical Risks and Supply Chain Spillovers of Corporate Carbon Greenwashing*, In: Technol. Soc., 2026, 85, 103203
[13] Li, J., Liao, Y., Wang, W., Han, X., Cheng, Z., Sun, G., *Is Stress Always Bad? The Role of Job Stress in Producing Innovative Ideas*, In: Knowl. Manag. Res. Pract., 2025, 23, 77–88
[14] Zhang, H.M., Liu, J.Y., Chen, J.W., *The Double-Edged Sword Effect of Performance Pressure on Employee Boundary-Spanning Behaviour*, In: J. Chin. Hum. Resour. Manag., 2024, 15, 3, 86–103
[15] Wang, Y., Jung, S., *The Aftermath of Greenwashing in the Fashion Industry: Chinese Consumer Responses to Different Types of Greenwashing*, In: Asia Pac. J. Mark. Logist., 2025, 37, 9, 2669–2685
[16] Yan, H., Li, Y., Zhong, Y., Xia, Z., *Will the 'Government-Court Coordination' of Corporate Bankruptcy Disposal Improve ESG Performance? Evidence from China*, In: Appl. Econ. Lett., 2025, 32, 20, 2998–3002
[17] Li, D., Yan, H., Ma, S., *ESG Performance Drivers and Corporate Growth: A Life-Cycle-Based fsQCA–PSM Study of China's Construction and Manufacturing Enterprises*, In: J. Asian Archit. Build. Eng., 2026, 25, 4, 3637–3654
[18] Zhou, C., Richardson-Barlow, C., *Climate Promotion Tournaments and Collaborative Governance: Central-Local Dynamics in China's Carbon Neutrality Policy Implementation*, In: J. Environ. Plann. Policy Manage., 2026, 1–18
[19] Yan, H., Yao, X., Li, Y., Xiong, Z., *Capital Market Liberalization and Corporate ESG Rating Divergence: A Quasi-Natural Experiment Based on the Trading System of SSHC*, In: Appl. Econ., 2025, 57, 60, 11107–11121
[20] Laufer, W.S., *Social Accountability and Corporate Greenwashing,* In: J. Bus. Ethics, 2003, 43, 253–261
[21] Robertson, J.L., Montgomery, A.W., Ozbilir, T., *Employees' Response to Corporate Greenwashing*, In: Bus. Strategy Environ., 2023, 32, 4015–4027
[22] Xu, T., Sun, Y., He, W., *Government Digitalization and Corporate Greenwashing*, In: J. Cleaner Prod., 2024, 452, 142015
[23] Martin, G.P., Wiseman, R.M., Gomez-Mejia, L.R., *Going Short-Term or Long-Term? CEO Stock Options and Temporal Orientation in the Presence of Slack*, In: Strateg. Manag. J., 2016, 37, 2463–2480
[24] Bai, C., Yao, D., Xue, Q., *Does Artificial Intelligence Suppress Firms' Greenwashing Behaviour? Evidence from Robot Adoption in China*, In: Energy Econ., 2025, 142, 108168
[25] Xu, C., Yao, X., Yan, H., Li, Y., *Does ESG Disclosure Improve Green Innovation Performance of New Energy Enterprises? Evidence from China*, In: Pol. J. Environ. Stud., 2025, 34, 4859–4868
[26] Deng, X., Kang, J., Low, B.S., *Corporate Social Responsibility and Stakeholder Value Maximization: Evidence from Mergers*, In: J. Financ. Econ., 2013, 110, 87–109
[27] Khanna, T., Palepu, K.G., *Winning in Emerging Markets: A Road Map for Strategy and Execution*, Harvard Business Press, 2010
[28] Barney, J., *Firm Resources and Sustained Competitive Advantage*, In: J. Manag., 1991, 17, 99–120
[29] Hahn, R., Lülfs, R., *Legitimizing Negative Aspects in GRI-Oriented Sustainability Reporting: A Qualitative Analysis of Corporate Disclosure Strategies*, In: J. Bus. Ethics, 2014, 123, 401–420
[30] Delmas, M.A., Burbano, V.C., *The Drivers of Greenwashing*, In: Calif. Manage. Rev., 2011, 54, 64–87
[31] Dowell, G., Hart, S., Yeung, B., *Do Corporate Global Environmental Standards Create or Destroy Market Value?,* In: Manage. Sci., 2000, 46, 1059–1074
[32] Ruiz-Blanco, S., Romero, S., Fernandez-Feijoo, B., *Green, Blue or Black, but Washing–What Company Characteristics Determine Greenwashing?*, In: Environ. Dev. Sustainability, 2022, 24, 4024–4045
[33] Lyon, T.P., Maxwell, J.W., *Greenwash: Corporate Environmental Disclosure under Threat of Audit*, In: J. Econ. Manag. Strategy, 2011, 20, 3–41
[34] Zhao, A.T., Xiao, S., *A Matter of Time: The Influence of Underperformance Duration on Corporate Misconduct*, In: Corp. Gov.: Int. Rev., 2024, 32, 2, 228–248
[35] Weiner, B., *An Attributional Theory of Achievement Motivation and Emotion*, In: Psychol. Rev., 1985, 92, 548–573

[36] Campello, M., Graham, J.R., Harvey, C.R., *The Real Effects of Financial Constraints: Evidence from a Financial Crisis*, In: J. Financ. Econ., 2010, 97, 470–487

[37] Audia, P.G., Greve, H.R., *Less Likely to Fail: Low Performance, Firm Size, and Factory Expansion in the Shipbuilding Industry,* In: Manage. Sci., 2006, 52, 83–94

[38] Ma, S., Li, D., Yan, H., *Entangled Value: Actor–Network Configurations and ESG Pathways in China's Textile Value Chain*, In: J. Text. Inst., 2025, 1–13

[39] Li, D., Yan, H., Zhang, S., *Weaving the Green Thread: Configurational Drivers of Sustainable Transformation in the Textile Industry*, In: Ind. Text., 2026, 77, 1, 68–82

[40] Li, D., Yan, H., Ma, S., *Trust in the Digital Age: How Cybersecurity Governance Willingness Shapes Trade Credit–Evidence from Supplier Credit Decisions*, In: J. Bus. Econ. Manag., 2026, 27, 323–343

[41] Chernozhukov, V., Chetverikov, D., Demirer, M., Duflo, E., Hansen, C., Newey, W., Robins, J., *Double/Debiased Machine Learning for Treatment and Structural Parameters*, In: The Econometrics Journal, 2018, 21, C1–C68

[42] Graham, J.R., Harvey, C.R., Rajgopal, S., *The Economic Implications of Corporate Financial Reporting*, In: J. Account. Econ., 2005, 40, 3–73

[43] Hadlock, C.J., Pierce, J.R., *New Evidence on Measuring Financial Constraints: Moving beyond the KZ Index,* In: Rev. Financ. Stud., 2010, 23, 1909–1940

[44] Granovetter, M., *Economic Action and Social Structure: The Problem of Embeddedness*, In: Am. J. Sociol., 1985, 91, 481–510,

[45] Scott, W.R., *Institutions and Organizations*, Sage, Thousand Oaks, CA, 1995

[46] Oliver, C., *Strategic Responses to Institutional Processes*, In: Acad. Manage. Rev., 1991, 16, 1, 145–179

[47] La Porta, R., Lopez-de-Silanes, F., Shleifer, A., Vishny, R.W., *Law and Finance*, In: J. Polit. Econ., 1998, 106, 1113–1155

[48] Dyck, A., Volchkova, N., Zingales, L., *The Corporate Governance Role of the Media: Evidence from Russia,* In: J. Financ., 2008, 63, 1093–1135

[49] Christmann, P., Taylor, G., *Globalization and the Environment: Determinants of Firm Self-Regulation in China*, In: J. Int. Bus. Stud., 2001, 32, 439–458

[50] Guo, J., Zhao, X., *Exploring the Nexus between Technological Innovation, Environmental Regulation, Human Capital, and Low-Carbon Economy*, In: J. Compr. Bus. Adm. Res., 2025

[51] Jiang, S., Yuan, X., *Does Green Credit Promote Real Economic Development? Dual Empirical Evidence of Scale and Efficiency*, In: PLOS ONE, 2025, 20, 8, e0326961

[52] Zhang, X., Li, D., Yan, H., Ma, S., *Does Air Pollution Affect the Green Innovation of Industrial Enterprises? Insights from Urban Sewage Control Policies in China*, In: Glob. NEST J., 2025, 27, 6, 1–14

[53] Yan, H., Li, D., Cao, P., *Beyond the Single Thread: How Organisational, Technological, and Environmental Factors Jointly Shape Green Patent Persistence in Textile Firms*, In: Ind. Text., 2026, 77, 1, 115–127

[54] Ma, J., Shang, Y., Liu, L., *Green Image, Digital Transformation, and Corporate Green Innovation*, In: Int. Rev. Financ. Anal., 2025, 106, 104518

[55] Berrone, P., Fosfuri, A., Gelabert, L., Gomez-Mejia, L.R., *Necessity as the Mother of 'Green' Inventions: Institutional Pressures and Environmental Innovations*, In: Strateg. Manag. J., 2013, 34, 891–909

[56] Porter, M.E., Linde, C. van der, *Toward a New Conception of the Environment-Competitiveness Relationship*, In: J. Econ. Perspect., 1995, 9, 97–118

[57] Bolino, M.C., Kacmar, K.M., Turnley, W.H., Gilstrap, J.B., *A Multi-Level Review of Impression Management Motives and Behaviours*, In: J. Manag., 2008, 34, 1080–1109

[58] Malinis, A., Tan, T.A., *The Impact of Perceived Environmental, Social, and Governance (ESG) on Employee Retention in the IT-BPM Sector in Cebu City*, In: J. Compr. Bus. Adm. Res., 2025, 2, 2, 114–123

[59] Peng, Y., Zhang, Q., Yan, H., Lei, X., Ma, S., *Short-Term Relief or Long-Term Risk? The Impact of Financial Asset Allocation on Corporate Risk in China's Construction and Manufacturing Firms*, In: J. Asian Archit. Build. Eng., 2025, 1–14

[60] Fombrun, C., Shanley, M., *What's in a Name? Reputation Building and Corporate Strategy*, In: Acad. Manage. J., 1990, 33, 233–258

[61] Jensen, M.C., Meckling, W.H., *Theory of the Firm: Managerial Behavior, Agency Costs and Ownership Structure*, In: J. Financ. Econ., 1976, 3, 4, 305–360

Authors:

GUOFU ZHANG[1], BIHAN XU[1], DING LI[1], HAN YAN[2]

[1]School of Economic and Management, Heilongjiang Bayi Agricultural University, Heilongjiang, China

[2]School of Business, Nankai University, Tianjin, China

Corresponding author:

GUOFU ZHANG
e-mail: zhangguofu@byau.edu.cn

A statistical model for predicting bursting strength of plain knitted fabrics from various fancy yarns

DOI: 10.35530/IT.077.04.202614

ZEHRA EVRİM KANAT NİLGÜN ÖZDİL

ABSTRACT – REZUMAT

A statistical model for predicting bursting strength of plain knitted fabrics from various fancy yarns

Fancy yarns contain certain planned irregularities in their structure in terms of colour and/or texture. The realisation by designers that these structural irregularities can create surface effects and achieve unique looks has led to an increase in research on fancy yarns. By incorporating these yarns, the surface characteristics of fabrics can be altered, resulting in improvements in softness and permeability. However, in addition to these aesthetic elements, the mechanical properties of products made from these yarns are also important. These irregularities in the yarn structure affect the physical properties of the yarn and, consequently, the fabrics made from it. The physical properties of the fabrics are also very important in terms of user satisfaction. This study investigated the prediction of bursting strength of knitted fabrics made from fancy yarns, which affect the properties of the fabrics produced. The research was carried out on plain knitted fabrics produced with four different fancy yarns: boucle, looped, knotted, and slub. The breaking strength and elongation at break of the fancy yarn type, as well as the fabric weight, thickness, elasticity, and stitch density properties, which affect bursting strength, were tested. Regression analysis of bursting strength was performed, and the adjusted R^2 value of the resulting model was found to be 0.997.

Keywords: *boucle yarns, looped yarns, knotted yarns, slub yarns, bursting strength, dummy variables*

Un model statistic pentru estimarea rezistenței la rupere a tricoturilor glat realizate din diverse fire fantezie

Firele fantezie prezintă anumite neregularități intenționate în structura lor, în ceea ce privește culoarea și/sau textura. Conștientizarea de către designeri a faptului că aceste neregularități structurale pot crea efecte de suprafață și pot conferi un aspect unic a condus la o intensificare a cercetărilor în domeniul firelor fantezie. Prin încorporarea acestor fire, caracteristicile de suprafață ale materialelor textile pot fi modificate, ceea ce duce la îmbunătățirea emolierii și a permeabilității. Cu toate acestea, pe lângă aceste elemente estetice, proprietățile mecanice ale produselor realizate din aceste fire sunt, de asemenea, importante. Aceste neregularități din structura firului afectează proprietățile fizice ale firului și, în consecință, materialele textile realizate din acesta. Proprietățile fizice ale materialelor textile sunt, de asemenea, foarte importante din punct de vedere al satisfacției utilizatorilor. Prezentul studiu a investigat predicția rezistenței la rupere a tricoturilor realizate din fire fantezie, care influențează proprietățile materialelor textile produse. Cercetarea a fost efectuată pe tricoturi glat, realizate cu patru tipuri diferite de fire fantezie: bouclé, buclate, cu noduri și cu nopeuri. Au fost testate rezistența la rupere și alungirea la rupere ale tipului de fir fantezie, precum și proprietățile tricotului, precum masa, grosimea, elasticitatea și desimea, care influențează rezistența la rupere. S-a efectuat o analiză de regresie a rezistenței la rupere, iar valoarea R^2 ajustată a modelului rezultat a fost de 0,997.

Cuvinte-cheie*: fire bouclé, fire buclate, fire cu noduri, fire cu nopeuri, rezistență la rupere, variabile fictive*

INTRODUCTION

Fancy yarns are formed by intentionally introducing irregularities into the structure of flat yarns. The use of fancy yarns also enables the economical production of original designs with high aesthetic and decorative appeal. However, while these irregularities enhance the visual appearance of fabrics, they also lead to variations in the physical properties of the yarns and the resulting fabrics. Adequate strength is one of the most critical parameters defining the performance of textile products.

A typical fancy yarn consists of three components: the *core* or *main* yarn, the *effect* material, and a *binder* that holds the structure together [1]. Among these, the main yarn has the greatest impact on the overall strength of the fancy yarn, while the effect material primarily contributes to aesthetic characteristics [2]. The structure of fancy yarns is shown in figure 1.

Due to their aesthetic advantages, fancy yarns are widely used in both woven and knitted fabrics, with increasing popularity in fields such as outerwear, upholstery, knitwear, and home decoration [4–6]. According to a market analysis by Data Insights Market, the global fancy yarn sector – valued at an estimated $4.21 billion in 2025 – is expected to grow at a CAGR of 4.3% from 2025 to 2033 [7].

The literature includes several studies examining how yarn production parameters influence the properties of fabrics made from different types of fancy yarns. Nergis and Candan found that the most critical parameter affecting the bursting strength of plain

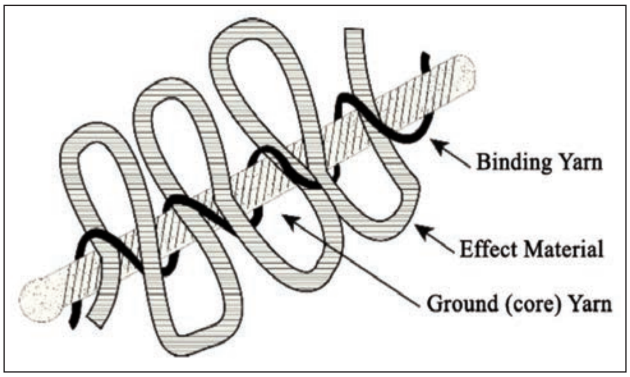

Fig. 1. The basic structure of fancy yarns [3]

knitted fabrics made from chenille yarns was the property of the component yarns [8]. In another study, Nergis reported that no clear relationship was found between bursting strength and the presence of elastane in chenille yarn in knitted fabrics produced from elastane chenille yarns [9]. Additionally, Turay et al. investigated knitted fabrics made from 100% wool and 100% acrylic bouclé yarns, reporting that acrylic fabrics exhibited higher bursting strength values [10]. The results of the study by Atef et al. showed that 1×1 rib fabrics have higher burst strength than plain knit and 3×1 rib fabrics. Furthermore, fabrics produced from yarns with a higher polyester content had higher burst strength compared to those with a higher cotton content [11]. Özdil and Kanat used four different types of fancy yarns produced from wool, PAC and wool/PAC blends as raw materials in their study examining the bursting strength of fabrics woven from fancy yarns. The study found that the effect of the raw material was statistically insignificant, while the effect of the yarn type was found to be significant [3].

Some studies have investigated the effect of fabric parameters knitted with conventional yarns on bursting strength. These studies indicate that yarn tenacity, elongation, fabric mass, stitch density, fabric thickness, and extension properties have an effect on bursting strength [12–13]. In addition, the bursting strength of knitted fabrics has been extensively studied using both regression-based and intelligent modelling approaches due to its strong dependence on structural and material parameters. Ghosh investigated plain knitted fabrics and showed that stitch length and density, fabric thickness, tightness factor, fabric weight (GSM), and porosity significantly affect bursting strength, with regression and ANOVA results revealing a particularly strong correlation between GSM and bursting strength ($R^2 \approx 0.94$) [14]. Islam et al. used multiple regression and ANOVA analyses to demonstrate that stitch length, yarn count, and tightness factor have significant effects, whereas GSM and fabric thickness exhibit relatively weaker influence [15]. Overall, regression-based studies confirm that structural parameters such as stitch density, loop length, and yarn fineness play dominant roles in bursting behaviour. In parallel, intelligent modelling approaches improve prediction accuracy for nonlinear relationships: Ertuğrul and Uçar showed that ANN and ANFIS outperform conventional regression models [16], and Jamshaid et al. reported superior accuracy of ANFIS over response surface regression [17].

As can be seen from the literature cited above, previous studies have focused on estimating the bursting strength of fabrics knitted from conventional yarns. Unlike other studies, this study used fabrics knitted from fancy yarns and the effect of fancy yarn type on the prediction of bursting strength of knitted fabrics was investigated in detail. Variance analyses and regression analyses were carried out using SPSS. This research, which was unstudied previously, aims to identify the fancy yarn and fabric parameters that are important in predicting fabric bursting strength.

MATERIALS AND METHODS

In this study, plain knitted fabrics were obtained from four different fancy yarn types: bouclé, loop, knotted, and slub yarns; 100% wool, 50% wool 50% PAC and 100% PAC yarns in Nm 12 count, and the effect of yarn type on the bursting strength of these fabrics was investigated in detail. Plain knitted fabrics were produced on an E7 knitting machine by using the NSSC122 model SHIMA SEIKI.

Yarn types featuring periodically thickened sections along their length are referred to as slub yarns. Bouclé yarn is classified as a compound yarn and is produced by combining a twisted core yarn with an effect yarn (or roving), resulting in characteristic wavy surface protrusions. In this structure, the effect yarn forms small loops by being twisted in the opposite direction and at a higher speed than both the core and the binder yarns [11, 18]. Knotted yarn is characterised by the presence of knots occurring at either regular or irregular intervals along its length. Loop yarn, on the other hand, consists of a base yarn around which an overfed effect yarn is wrapped, generating circular loop-like projections on the surface [2]. The properties of the yarns used in this study are summarised in table 1, and visual representations of the yarns and fabrics are given in figure 2.

Table 1

YARNS USED IN THE STUDY

Material	Yarn type			
%100 Wool	Bouclé yarn	Loop yarn	Knotted yarn	Slub yarn
%50 Wool/%50 PAC				
%100 PAC				

Yarn and fabric properties affecting the bursting strength of fabrics, as mentioned in the literature, were investigated. Tests were carried out on conditioned fabrics at 20±2°C; 65±4% Rh. All the tests applied to yarns and fabrics and their standards were given in table 2.

Table 2

YARNS AND FABRIC TESTS STANDARDS	
Test	**Test Standard**
Yarn breaking strength	ISO 2062
Elongation at break	ISO 2062
Fabric weight	EN 12127
Fabric thickness	ISO 5084
Stitch density	EN 14971
Elasticity	ISO 20932-1
Bursting strength	ISO 13938-2

RESULTS AND DISCUSSION

The means of the results of all tests applied to the yarn and fabric are given in the table 3. Among all types of yarn, the lowest weight value is seen in fabrics from loop yarn, and the highest weight value is seen in fabrics from slub yarn. In fabrics knitted at the same density, the loops on the yarn cause a more open fabric structure. Fabrics from slub yarns, on the other hand, have a less open structure, resulting in higher weight values.

As can be seen from the table, excluding boucle yarns, the lowest yarn strength was observed in woollen yarns and the highest yarn strength in PAC yarns. This can be explained by the higher fibre strength of PAC.

As shown in figure 3, the bursting strength of the fabric increases with increasing yarn strength, and the bursting strength of slub yarn and the fabric produced from this yarn are much higher than those of others. The lowest bursting strength was observed in fabrics produced from boucle yarn. In slub yarns, the presence of thicker regions positively affects the strength

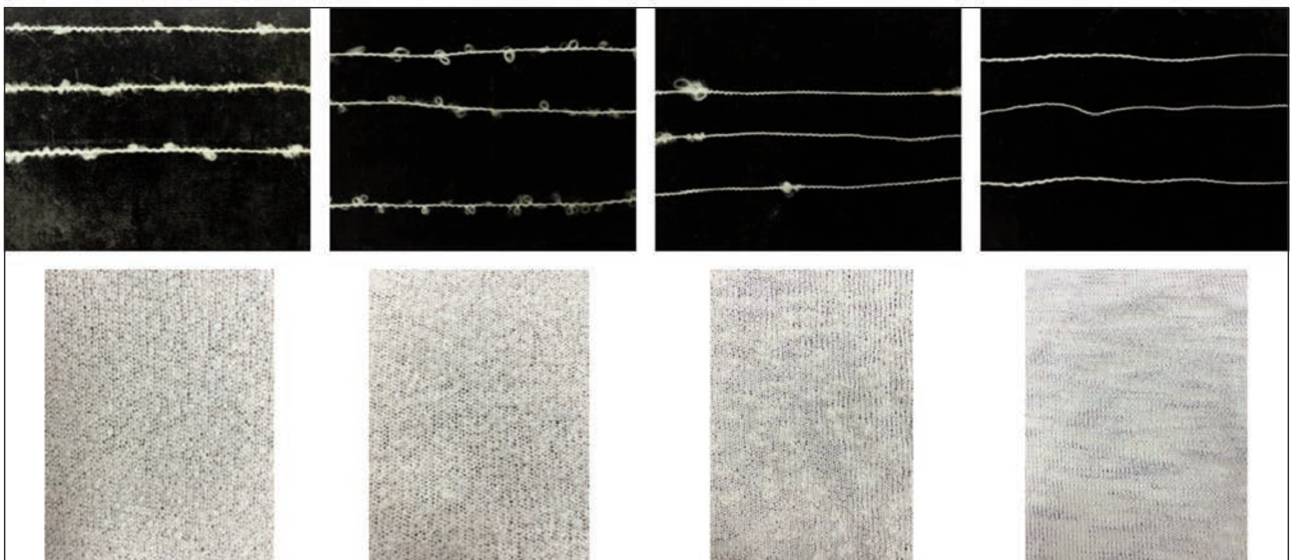

Fig. 2. Images of yarn types and fabrics knitted with these yarns [3]:
a – bouclé yarn; *b* – loop yarn; *c* – knotted yarn; *d* – slub yarn

Table 3

MEAN VALUES OF TEST RESULTS								
Yarn type	**Material**	**Yarn strength (N)**	**Yarn elongation (mm)**	**Mass per unit area (g/m^2)**	**Fabric thickness (mm)**	**Stitch density (stitch number/cm^2)**	**Fabric elasticity (%)**	**Bursting strength (kPa)**
Boucle	Wool	7.81	123.41	184.13	2.05	20.83	128	150.50
Boucle	Wool/ PAC	9.88	120.71	176.40	1.70	28.44	133	184.87
Boucle	PAC	8.40	79.22	166.30	1.40	26.00	103	152.73
Loop	Wool	9.44	154.56	156.16	1.87	25.83	118	170.36
Loop	Wool/ PAC	9.49	137.99	170.76	1.80	30.00	98	175.24
Loop	PAC	9.64	127.00	153.48	1.57	25.83	100	173.72
Knotted	Wool	10.94	108.16	247.04	1.91	36.94	112	218.43
Knotted	Wool/ PAC	11.61	91.26	243.52	1.87	33.33	93	219.58
Knotted	PAC	11.67	75.81	220.92	1.55	30.22	75	248.20
Slub	Wool	13.76	91.08	322.06	1.59	35.00	90	281.24
Slub	Wool/ PAC	18.00	97.98	330.56	1.50	42.00	80	345.06
Slub	PAC	20.64	86.08	263.84	1.31	35.00	75	354.82

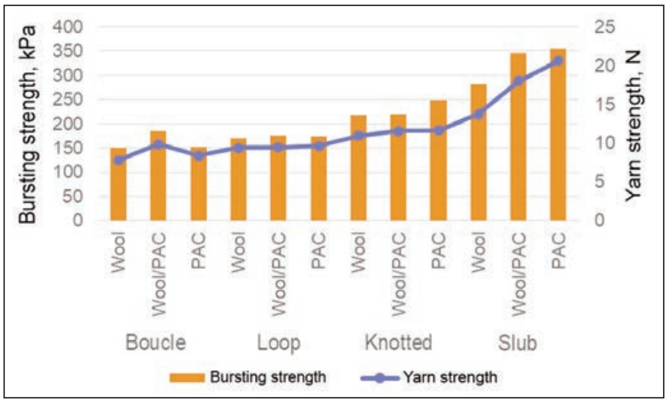

Fig. 3. Bursting strength and yarn strength of fabrics according to yarn type

Therefore, the effect of yarn types on the bursting strength of the fabric was investigated using one-way analysis of variance (ANOVA). According to the ANOVA test results given in table 4, the differences between the groups were found to be significant at $\alpha = 0.05$, and the differences between the groups were determined using post-hoc tests.

Since the Levene test result showed that the variance between the groups was different, multiple comparison tests were determined according to Tamhane. The multiple comparisons test results and the subsets of yarn type according to bursting strength values are shown in the tables 5 and 6, respectively.

Table 4

VARIANCE ANALYSES OF BURSTING STRENGTH					
Type	**Sum of squares**	**df**	**Mean square**	**F**	**Sig**
Between groups	230580.395	3	76860.132	147.057	0.000*
Within groups	24564.829	47	522.656		
Total	255145.224	50			

Note: * Statistically significant according to $\alpha = 0.05$.

Table 5

MULTIPLE COMPARISONS ACCORDING TO TAMHANE						
Yarn type (I)	**Yarn type (J)**	**Mean difference (I-J)**	**Std. Error**	**Sig.**	**95% Confidence interval**	
					Lower Bound	**Upper Bound**
Boucle	Loop	–10.40533	6.33945	0.584	–31.7621	10.9514
	Knotted	–66.13333*	7.97804	0.000	–89.9015	–42.3652
	Slub	–164.34000*	11.14432	0.000	–196.5804	–132.0991
Loop	Boucle	10.40533	6.33945	0.584	–10.9514	31.7621
	Knotted	–55.72800*	5.22951	0.000	–71.9874	–39.4686
	Slub	–153.93467*	9.37521	0.000	–182.4081	–125.4612
Knotted	Boucle	66.13333*	7.97804	0.000	42.3652	89.9015
	Loop	55.72800*	5.22951	0.000	39.4686	71.9874
	Slub	–98.20667*	10.55249	0.000	–128.8156	–67.5978
Slub	Boucle	164.34000*	11.14432	0.000	132.0991	196.5809
	Loop	153.93467*	9.37521	0.000	125.4612	182.4081
	Knotted	98.20667*	10.55249	0.000	67.5978	128.8156

Note: * The mean difference is significant at the 0.05 level.

value of the yarn and, consequently, the fabric. Another reason why fabrics from slub yarns have the highest bursting strength values is their high density and mass per unit area. In boucle and loop yarns, the effect yarn does not contribute to the strength value because it is not in the same direction as the main yarn structure.

Variance analyses

When the bursting strength values are statistically analysed, the skewness and kurtosis values are found to be 0.735 and –0.845, respectively. Since these values are within the range of +/– 1.5, it is stated that the data set shows a normal distribution according to the literature.

Table 6

SUBSETS OF YARN TYPE ACCORDING TO BURSTING STRENGTH			
Yarn type	**Subset for α=0.05**		
	1	**2**	**3**
Boucle	162.7000		
Loop	173.1053		
Knotted		228.8333	
Slub			327.0400

Linear regression

Additionally, multiple linear regression analysis was performed to determine the relationship between yarn and fabric properties and bursting strength. The parameters affecting bursting strength (BS), such as yarn breaking strength (YS) and elongation (YE), fabric weight (FW), fabric thickness (FT) and elasticity (FE), and stitch density (SD), were evaluated. Since the effect of raw material on bursting strength was not found to be significant in the previous study, it was not included as a parameter [3]. Furthermore, considering the statistically significant effect of yarn type on bursting strength, yarn type was also included as an independent variable in the regression analysis. Since yarn type is a nominal variable, it was converted into a dummy variable for the analysis. Knotted yarn was defined as the reference variable. The dummy variables were defined in table 7.

Table 7

TRANSFORMATION OF DUMMY VARIABLES			
Yarn type	**D1**	**D2**	**D3**
Boucle	1	0	0
Loop	0	1	0
Knotted	0	0	0
Slub	0	0	1

The regression model with dummy variables is given below (equation 1):

$$Y = a_0 + a_1 D_1 + a_2 D_2 + a_3 D_3 + b_1 X_1 + + b_2 X_2 + \cdots + b_k X_k + \varepsilon \quad (1)$$

Here, Y represents the dependent variable, and X's represent the independent variables. D_1, D_2, and D_3 represent dummy variables, and when the yarn type is boucle, $D_1 = 1$ and D_2, $D_3 = 0$; when it is loop, $D_2 = 1$ and D_1, $D_3 = 0$; when it is slub, $D_3 = 1$ and D_1, $D_2 = 0$; and when it is knotted, D_1, D_2, $D_3 = 0$.

Before the analysis, the skewness and kurtosis tests were used to verify that all variables showed a normal distribution, and the linear relationship between the dependent and independent variables was checked using graphs (figure 4). Means, standard deviations and Skewness and Kurtosis values of independent variables were given in table 8.

When table 8 is examined, it is seen that all Skewness and Kurtosis values are between ±1.5. Therefore, the normality test is satisfied. In addition, when figure 4 is examined, it is seen that the relationship between all independent variables and the dependent variable, bursting strength, is linear.

Yarn strength, elongation, fabric weight, fabric thickness, elasticity, and stitch density, along with dummy variables, were selected as independent variables in regression analysis. Pearson correlation coefficients of variables were given in table 9.

Examining the table, we see high ($R > 0.70$) and moderate ($0.3 < R < 0.7$) correlations between the independent and dependent variables. A positive correlation was observed between bursting strength and yarn strength, while a negative correlation was found between bursting strength and other variables

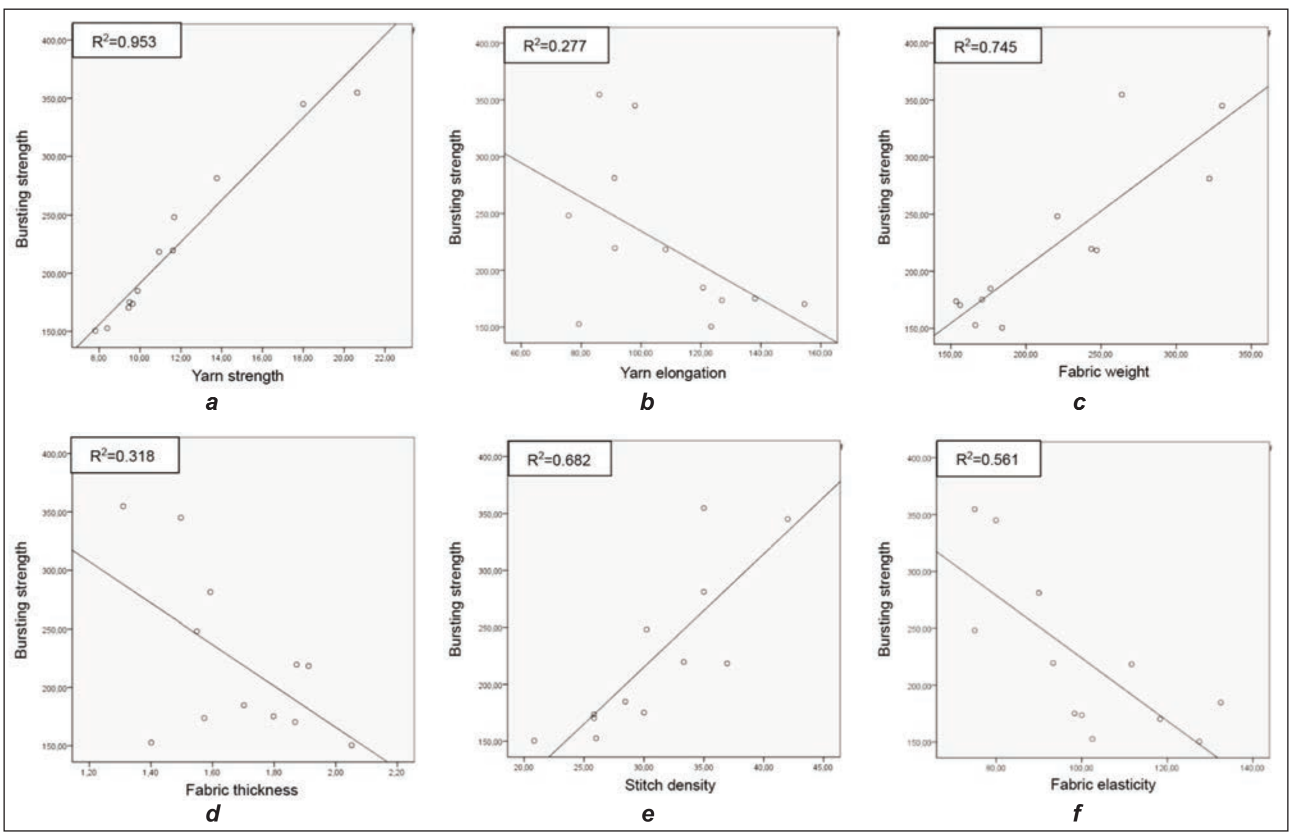

Fig. 4. Relationship between dependent and independent variables: *a* – Yarn strength; *b* – Fabric thickness; *c* – Fabric weight; *d* – Stitch density; *e* – Fabric elasticity; *f* – Yarn elongation

Table 8

DESCRIPTIVE STATISTICS AND SKEWNESS AND KURTOSIS VALUES OF INDEPENDENT VARIABLES				
Variable	**Mean**	**Standard Deviation**	**Skewness**	**Kurtosis**
YS	11.7743	3.90698	1.470	1.485
YE	107.7703	24.93194	0.471	–0.796
FW	219.5978	62.40707	0.730	–0.702
FT	1.6773	0.22634	0.013	–0.955
SD	30.7870	5.90164	0.242	–0.202
FE	100.3472	19.27492	0.275	–0.900

Table 9

PEARSON CORRELATIONS COEFFICIENTS OF VARIABLES										
Pearson correlation	**BS**	**YS**	**YE**	**FW**	**FT**	**SD**	**FE**	**D_1**	**D_2**	**D_3**
BS	1.000	0.976	–0.526	0.863	–0.564	0.826	–0.749	–0.511	–0.423	0.884
YS	0.976	1.000	–0.457	0.769	–0.602	0.765	–0.712	–0.475	–0.347	0.879
YE	–0.526	–0.457	1.000	–.0554	0.592	–0.428	0.644	0.000	0.776	–0.388
FW	0.863	0.769	–.0554	1.000	–0.287	0.859	–0.591	–0.425	–0.575	0.830
FT	–0.564	–0.602	0.592	–0.287	1.000	–0.333	0.666	0.109	0.184	–0.561
SD	0.826	0.765	–0.428	0.859	–0.333	1.000	–0.603	–0.582	–0.364	0.669
FE	–0.749	–0.712	0.644	–0.591	0.666	–0.603	1.000	0.641	0.163	–0.584
D_1	–0.511	–0.475	0.000	–0.425	0.109	–0.582	0.641	1.000	–0.333	–0.333
D_2	–0.423	–0.347	0.776	–0.575	0.184	–0.364	0.163	–0.333	1.000	–0.333
D_3	0.884	0.879	–0.388	0.830	–0.561	0.669	–0.584	–0.333	–0.333	1.000

(except dummies). Furthermore, the correlation between yarn strength and elasticity and bursting strength was quite strong ($R > 0.70$), while the correlation between elongation and fabric thickness and bursting strength was moderate ($0.3 \leq R \leq 0.70$). However, a correlation coefficient greater than $r > 0.80$ between the independent variables indicates multicollinearity. To avoid the multicollinearity problem observed between fabric weight and stitch density, stitch density was removed from the regression equation.

The regression analysis was repeated, and when the coefficients of the resulting model were examined, it was found that the effect of fabric weight was insignificant at the 95% confidence interval ($p = 0.754$); therefore, this variable was also excluded from the analysis.

In the new regression analysis, it is observed that the errors of the estimates show a normal distribution (figure 5, *a*). Furthermore, when examining figure 5, *b*, it is seen that the values are homogeneously distributed across the graph, thus ensuring homoscedasticity.

The Durbin-Watson test was used to check whether the errors were independent of each other. According to the literature, a Durbin-Watson test result in the range of 1 and 3 indicates that the errors are not autocorrelated. Since the value here is 2.275, it is seen that the model satisfies this condition (table 10).

Table 10 also shows that the adjusted R-squared value of the model is quite high. The relationship between the dependent and independent variables in this model is very strong. The independent variables in the model explain 99.7% of the variation in the dependent variable. Table 11 below shows the significance level of the model. The model is significant with $p = 0.000 < 0.05$. In other words, the independent variables in the model have a significant effect on the dependent variable.

Table 10

MODEL SUMMARY				
R	**R Square**	**Adjusted R Square**	**Std. Error of the Estimate**	**Durbin-Watson**
0.999	0.999	0.997	3.92973	2.275

Table 11

VARIANCE ANALYSES OF THE MODEL					
Model	**Sum of Squares**	**df**	**Mean Square**	**F**	**Sig**
Regression	55401.448	7	7914.493	512.505	0.000
Residual	61.771	4	15.443		
Total	55463.220	11			

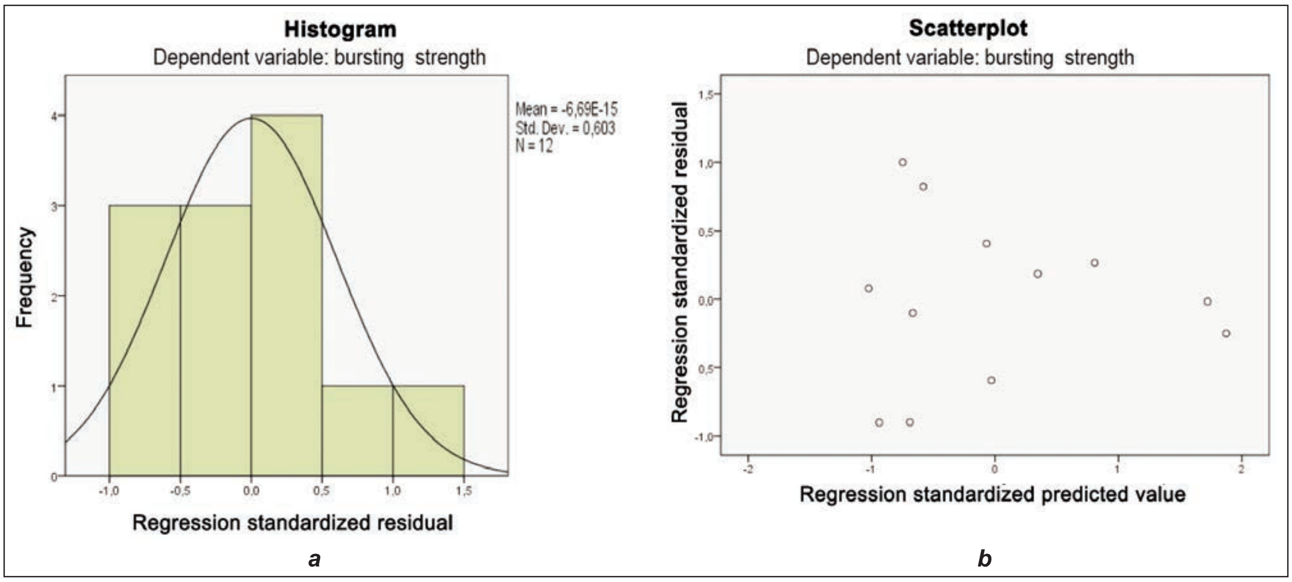

Fig. 5. Residual plots of model: *a* – Histogram; *b* – Residuals vs. Predicted Value

Since there are four categories for yarn type and the dataset is limited, the VIF values were checked in a model with only numerical data, after removing dummy variables, to evaluate the level of multi-collinearity [19]. The fact that these values are 1 < VIF < 5 indicates that there is no multicollinearity problem (table 12).

Table 13 shows the regression coefficients. Examination of the table reveals that all independent variables in the model significantly affect the dependent variable (Sig. $p < 0.05$). The regression equations for predicting bursting strength (BS) of the fabric for each yarn type are given below.

Table 12

VIF VALUES OF DEPENDENT VARIABLES		
Model	**Collinearity statistics**	
	Tolerance	**VIF**
YS	0.461	2.171
YE	0.534	1.871
FT	0.478	2.094
FE	0.341	2.935

Regression equation for knotted fabrics is (D_1, D_2, D_3 = 0) (equation 2):

$$BS = 307.803 + 4.393 * YS + 2.560 * YE - 109.489 * FT - 1.814 * FE \quad (2)$$

Regression equation for boucle fabrics is (D_1 = 1; D_2, D_3 = 0) (equation 3):

$$BS = (307.803 - 51.826) + 4.393 * YS + 2.560 * YE - 109.489 * FT - 1.814 * FE \quad (3)$$

Regression equation for loop fabrics is (D_2 = 1; D_1, D_3 = 0) (equation 4):

$$BS = (307.803 - 151.789) + 4.393 * YS + 2.560 * YE - 109.489 * FT - 1.814 * FE \quad (4)$$

Regression equation for slub fabrics is (D_3 = 1; D_1, D_2 = 0) (equation 5):

$$BS = (307.803 + 16.495) + 4.393 * YS + 2.560 * YE - 109.489 * FT - 1.814 * FE \quad (5)$$

In the obtained equations, yarn strength and elongation, fabric thickness and elasticity were found to be effective factors. Yarn strength and yarn elongation have a positive effect on bursting strength, while fabric thickness and fabric elasticity have a negative effect.

Table 13

COEFFICIENTS OF THE MODEL					
Model	**Unstandardized coefficients**		**Standardized coefficients**	**t**	**Sig.**
	B	**Std. Error**	**Beta**		
(Constant)	307.803	34.729		8.863	0.001
YS	4.393	1.352	0.242	3.248	0.031
YE	2.560	0.383	0.899	6.685	0.003
FT	–109.489	19.203	–0.349	–5.702	0.005
FE	–1.814	0.299	–0.492	–6.059	0.004
D1	–51.826	7.054	–0.330	–7.347	0.002
D2	–151.789	18.315	–0.967	–8.288	0.001
D3	16.495	5.823	0.105	2.833	0.047

CONCLUSION

This study investigated the bursting strength of plain knitted fabrics made from different types of fancy yarns and presented a statistical model on this subject. The effect of yarn type on bursting strength was found to be statistically significant.

Yarn strength and elongation, fabric thickness and elasticity parameters were tested, and regression analysis was performed using these parameters along with yarn type as a variable. Since yarn type is a nominal variable, the analysis was performed using dummy variables. Statistical prerequisites for the independent variables used in the regression equation were checked, and the model was revised accordingly. The regression equations for predicting the bursting strength of the fabric for each yarn type were presented.

In conclusion, it was shown that yarn type, yarn strength and elongation, fabric thickness and elasticity explain 99.7% of the bursting strength of plain knitted fabric produced from fancy yarn.

ACKNOWLEDGEMENTS

We would like to thank Textile Engineers Elif Nur Yılmaz, Nazlı Barlas and Özge Taşdemir for their contributions to the testing of this study.

REFERENCES

[1] Petrulytė, S., *Fancy Yarns: Efforts to Methodise, Problems, and New Suggestions*, In: Materials Science, 2004, 10, 1, 85– 88
[2] Özgen Keleş, B., *Fantezi İplikler ve Üretim Yöntemleri*, İksad Yayınevi, Ankara, 2021
[3] Özdil, N., Kanat, Z.E., *Fantazi iplik türünün örme kumaş mukavemetine etkisi,* In: Karadeniz 17th International Conference on Applied Sciences, 2024, Rize, Türkiye, 625–633
[4] Petrulytė, S., *Influence of Technological Parameters on the Periodical Effects of Fancy Yarns,* In: Fibres & Textiles in Eastern Europe, 2008, 16, 3, 68, 25– 29
[5] Ragaišienė, A., Kumpikaitė, E., *Investigation of End-use Properties of Woven Fabrics with Synthetics Fancy Yarns,* In: Materials Science, 2010, 16, 4, 337– 340
[6] Alshukur, M., Fotheringham, A., Gong, H., *The Influence of Component Stiffness on the Structure of Multithread Fancy Boucle´ Yarn*, In: Journal of Industrial Textiles, 2020, 49, 7, 889–905, https://doi.org/10.1177/ 152808371880136
[7] Dimarket, *Fancy Yarn Market's Role in Emerging Tech: Insights and Projections 2025–2033,* Available at: https://www.datainsightsmarket.com/reports/fancy-yarn-1356648# [Accessed on December 17, 2025]
[8] Nergis, B., Candan, C., *Properties of Plain Knitted Fabrics from Chenille Yarns,* In: Textile Research Journal, 2003, 73, 12, 1052–1056, https://doi.org/10.1177/004051750307301 20
[9] Nergis, B.U., *Performance of Chenille Yarns with Elastane,* In: Fibres & Textiles in Eastern Europe, 2006,14, 3, 45–47
[10] Turay, A., Özçelik, G., Süpüren, G., Özdil, N., *Bukleli İpliklerden Örülmüş Kumaşların Fiziksel Özellikleri,* In: Uluslararası Ulusal Meslek Yüksekokulları Sempozyumu, 2009, Konya, Türkiye, 321–331
[11] Atef, R., Elbealy, R., Badr, A.A., Elkhalek, R.A., *Performance of Knitted Fabrics Produced from Fancy Yarns with Different Slub/Meter and Blend Ratio*, In: Journal of Textile Science and Engineering, 2018, 8: 378, https://doi.org/10.4172/2165-8064.1000378
[12] Degirmenci, Z., Çelik, N., *Relation between Extension and Bursting Strength Properties of the Denim Viewed Knitted Fabrics Produced by Cellulosic Fibers,* In: Fibres & Textiles in Eastern Europe, 2016, 24, 1, 115, 101–106
[13] Uyanık, S., *The bursting strength properties of knitted fabrics containing recycled polyester fiber,* In: The Journal of the Textile Institute, 2021, 112, 12, 1998–2003, https://doi.org/10.1080/00405000.2020.1862490
[14] Ghosh, K., *An Investigation of Bursting Strength on Single Jersey Weft Knitted Fabrics,* In: IOSR Journal of Polymer and Textile Engineering, 2022, 9, 5, 9–20, https://doi.org/10.9790/019X-09050920
[15] Islam, A., Hossain, M.B., Haq, E., Shravan, A.S., Rahman, A., *Factors Influencing Bursting Strength of Single Jersey Knitted Fabrics*, In: European Scientific Journal, 2022, 18, 36, 68, https://doi.org/10.19044/esj.2022.v18n36p68
[16] Ertugrul, S., Ucar, N., *Predicting Bursting Strength of Cotton Plain Knitted Fabrics Using Intelligent Techniques*, In: Textile Research Journal, 2000, 70, 10, 845–851, https://doi.org/10.1177/004051750007001 0
[17] Jamshaid, H., Hussain, T., Malik, Z.A., *Comparison of regression and adaptive neuro-fuzzy models for predicting the bursting strength of plain knitted fabrics*, In: Fibers and Polymers, 2013,14, 1203–1207, https://doi.org/10.1007/ s12221-013-1203-3
[18] Gong, R.H., Wright, R.M., *Fancy yarns. Their manufacture and application*, Woodhead Publishing Limited, Cambridge, UK, 2002
[19] Murray, L., Nguyen, H., Lee, Y., Remmenga, M.D., Smith, D.W., *Variance inflation factors in regression models with dummy variables,* In: Conference on Applied Statistics in Agriculture, 2012, https://doi.org/10.4148/2475-7772.1034

Authors:

ZEHRA EVRİM KANAT[1], NİLGÜN ÖZDİL[2]

[1]Textile and Fashion Design Department, Faculty of Fine Arts, Canakkale Onsekiz Mart University,17100, Canakkale, Türkiye

[2]Textile Engineering Department, Faculty of Engineering, Ege University, 35100, İzmir, Türkiye
e-mail: nilgun.ozdil@ege.edu.tr

Corresponding author:

ZEHRA EVRİM KANAT
e-mail: zehraevrim.kanat@comu.edu.tr

Concentrate to compete: the role of equity concentration in textile and garment firms' global market responsiveness

DOI: 10.35530/IT.077.04.2025144

XIAOHUI YUAN KUN BAO

ABSTRACT – REZUMAT

Concentrate to compete: the role of equity concentration in textile and garment firms' global market responsiveness

As a key sector in China with a large global industrial system and a significant export share, the textile and garment industry faces competition in both high- and low-end markets amid global industrial chain restructuring, making internationalisation both imperative and challenging. This study examines how equity concentration affects the internationalisation of firms in the industry, focusing on the mediating mechanism of internal control optimisation. Results show that equity concentration effectively facilitates firms' internationalisation by enhancing internal control and boosting management efficiency, while excessively dispersed equity impedes this process: owing to delayed decision-making, reduced operational efficiency, and sluggish responses to the dynamic international market. We verify that equity concentration promotes firms' internationalisation, and this effect is achieved through improved internal control. The findings underscore the critical role of equity concentration and internal control in driving textile and garment firms' internationalisation.

Keywords: *equity concentration, internationalisation, internal control, textile industry, garment industry*

Concentrare pentru a face față concurenței: rolul concentrării capitalului propriu în capacitatea de adaptare la piața globală a întreprinderilor din sectorul de textile-îmbrăcăminte

Fiind un sector cheie în China, cu un sistem industrial global extins și o cotă semnificativă de export, industria textilă și de îmbrăcăminte se confruntă cu o concurență dublă pe piață, atât la segmentul de vârf, cât și la cel de bază, pe fondul restructurării lanțului industrial global, ceea ce face ca internaționalizarea să fie atât imperativă, cât și plină de provocări. Prezentul studiu analizează modul în care concentrarea capitalului propriu influențează internaționalizarea întreprinderilor din acest sector, punând accentul pe mecanismul de mediere reprezentat de optimizarea controlului intern. Rezultatele arată că un grad ridicat de concentrare a capitalului propriu facilitează în mod eficient internaționalizarea firmelor prin îmbunătățirea controlului intern și sporirea eficienței managementului, în timp ce o dispersie excesivă a capitalului propriu împiedică acest proces din cauza întârzierilor în luarea deciziilor, a eficienței operaționale reduse și a reacțiilor lente la dinamica pieței internaționale. Confirmăm că un grad ridicat de concentrare a capitalului propriu promovează internaționalizarea firmelor, iar acest efect este obținut prin îmbunătățirea controlului intern. Concluziile subliniază rolul esențial al concentrării capitalului propriu și al controlului intern în stimularea internaționalizării firmelor din industria textilă și de îmbrăcăminte.

Cuvinte-cheie*: concentrarea capitalului propriu, internaționalizare, control intern, industria textilă, industria de îmbrăcăminte*

INTRODUCTION

The textile and garment industry is a vital pillar of both national economic growth and social development. China has established the world's largest and most comprehensive textile industrial system, accounting for over 50% of global fibre processing and more than one-third of global textile and clothing exports. The industry plays a "ballast stone" role in stabilising China's economy and occupies a central position in the global textile supply chain. With deepening economic globalisation, internationalisation has become an inevitable trend for textile and garment firms. Expanding overseas allows firms to diversify markets, reach broader consumer bases, and mitigate dependence on single markets. By optimising global resource allocation, firms can exploit regional differences in factor costs, thereby lowering production costs and enhancing competitiveness [1–5]. Internationalisation also facilitates access to advanced technologies, managerial expertise, and innovative practices, which in turn improves technological capability and operational efficiency. Through cooperation with foreign enterprises and cross-border mergers and acquisitions, some Chinese firms have successfully introduced cutting-edge technologies and management systems, promoting product upgrading and reinforcing their global presence.

However, the accelerated restructuring of global industrial and supply chains presents new challenges. Developed economies dominate in high-performance fibre materials, functional textiles, and advanced textile equipment, while developing countries expand rapidly in labour-intensive, low-cost end products. Consequently, Chinese textile and garment firms face dual competitive pressures from both the high-end and low-end segments. To sustain competitiveness, they must enhance innovation capacity, optimise supply chain management, and pursue lean, efficient operations. In high-end markets, firms need to increase R&D investment and overcome technological bottlenecks to enhance product value. In low-end markets, they must retain cost advantages while ensuring quality through efficiency-oriented management and strategic resource allocation.

Equity concentration is widely recognised as a mechanism to improve management efficiency and decision-making quality [1]. Since the main decision-making power is concentrated in a few shareholders, firms can make decisions quickly when facing major decisions. This reduces internal differences and the cumbersomeness of decision-making procedures, allowing them to seize market opportunities promptly and respond quickly to market changes. When market demand changes suddenly, firms with concentrated equity can quickly adjust production plans and change product strategies. They can seize market opportunities before competitors are still in the decision-making discussion stage. Controlling shareholders often have clear long-term plans and strategic directions for the development of the firm. They are not easily disturbed by short-term market fluctuations and the interest demands of other shareholders. They can firmly promote the firm to move forward along the established strategic path, maintaining the stability and consistency of the firm's strategy. This stability helps firms continuously invest resources in technological R&D, brand building and market expansion, laying a solid foundation for their long-term development. For example, in some textile firms with a long-term internationalisation strategy, controlling shareholders can continue to invest funds in building overseas production bases and expanding marketing channels without being affected by short-term profit fluctuations, gradually realising the firm's international layout.

Then, how does equity concentration affect the internationalisation strategies of Chinese A-share textile and garment firms? Can it effectively boost a firm's overseas business income? What channels does equity concentration use to push a firm toward internationalisation? And what role do these channels play in the internationalisation of textile and garment firms? In today's policy context and market environment, what should textile and garment firms optimise to achieve better internationalisation? This paper studies these issues. It aims to offer theoretical support and practical guidance for the internationalisation of textile and garment firms in China and other developing countries. This support and guidance help boost their international competitiveness and ability to develop sustainably.

Studying the link between equity concentration and internationalisation helps firms adjust their equity structure properly. It also helps them improve corporate governance and raise decision-making efficiency. This lets them better handle the complex, changing international market environment. At the same time, it gives the government valuable references. These references help in making relevant industrial policies. They also guide the healthy development of textile and garment firms. By analysing in depth how equity concentration affects a firm's internationalisation mechanism, we can offer targeted suggestions. These suggestions help firms with technological innovation, market expansion, and supply chain optimisation. In turn, this helps them stand out in global textile industry competition.

LITERATURE REVIEW AND HYPOTHESIS DEVELOPMENT

Equity concentration and internationalisation

Ownership structure stands as a core element of corporate governance. It forms the base of governance systems. It also has far-reaching impacts on three key areas of firms: decision-making mechanisms, operational efficiency, and strategic development. Equity concentration is a key form of ownership structure. It happens when a small number of major shareholders hold a large share of a firm's stocks. With this high shareholding, these major shareholders gain significant control over the firm's operational decisions.

For Chinese A-share textile firms, equity concentration brings clear advantages. When equity is concentrated among a few major shareholders, the decision-making process becomes more streamlined. Major shareholders act based on their own interests and long-term development plans. This lets them respond quickly to market changes. They can create and carry out decisions without the inefficiencies and delays that come with dispersed ownership [1]. This streamlining is vital in the fast-paced textile industry, where slow decisions can mean lost opportunities.

To understand how equity concentration affects a firm's internationalisation plans, two key theories offer clear explanations: agency theory and resource dependence theory (figure 1).

From the angle of agency theory, a concentrated ownership structure cuts down agency costs significantly. It does this by reducing the gap in information between shareholders and management. Major shareholders have control advantages. They use these advantages to monitor managerial behaviour more effectively. This monitoring helps make sure strategic decisions are consistent. It also boosts the efficiency of putting these decisions into action. In turn, this provides a solid organisational guarantee for the firm's internationalisation efforts [6–15]. This effect is even more obvious in the textile industry. The textile industry has unique traits. It requires firms to react fast to changes in international market demand. A concentrated ownership structure helps shorten the chain of decision-making. It also improves how well resources are allocated across borders. For example, take emerging markets like India. In these markets, higher ownership concentration links to greater international diversification. So that the higher ownership concentration can come from either domestic or foreign investors. Major shareholders here have stronger reasons to seek long-term growth. They do this by expanding the firm's reach across the globe [7]. This shows that equity concentration can drive firms to look beyond their home markets.

From the perspective of resource dependence theory, equity concentration strengthens a firm's control over key resources. This control lays a material foundation for internationalisation. The textile industry is labour-intensive. Its internationalisation relies heavily on the ability to integrate resources. These resources include supply chain management, technological R&D, and brand building. Concentrated ownership gives major shareholders the power to inject resources into the firm. This injection enhances the firm's competitive advantages in the global value chain [8]. Research on family firms further supports this idea. It shows that concentrated ownership lets firms use unique social capital. It also lets them keep a long-term focus. These two factors help firms get past resource limits in international markets [2]. For textile firms, having access to more resources and a long-term view is key to succeeding in foreign markets.

Hypothesis 1: Equity concentration promotes the internationalisation of the textile and garment firms.

The mediating role of internal control

Internal control is of great importance to a firm's operations. It includes a range of self-regulatory methods, steps, and actions. These elements serve multiple purposes. They help the firm reach its operational goals. They protect the firm's assets. They make sure accounting information is reliable. They enforce operational policies. And they boost the efficiency and effectiveness of the firm's work. A strong internal control system works well [16]. It reduces operational risks. It increases efficiency. And it makes financial information more authentic and trustworthy.

For Chinese listed firms, the effectiveness of internal control has a strong positive link to the quality of corporate governance. This includes ownership concentration. Major shareholders have stronger motives to set up sound control mechanisms. They do this to protect their own interests [16]. So, equity concentration and strong internal control often go hand in hand.

Internal control is essential for the internationalisation of Chinese A-share textile firms. When a firm operates internationally, it faces many challenges. These include complex and changing market environments. They also include different legal and regulatory systems across regions. Cultural conflicts add another layer of difficulty. All these factors bring risks to the firm. Effective internal control can deal with these risks. It uses risk assessment mechanisms to spot potential risks early. Then, it develops strategies to respond to these risks. This reduces the level of risk during the internationalisation process [14].

From the resource-based view, internal control is an organisational capability. It improves operational efficiency in two key ways. First, it standardises internal processes. Second, it integrates internal and external resources. This capability helps firms adapt to changes in international markets. It also enhances their competitiveness. There is empirical evidence to back this up. Studies on Chinese manufacturing firms show that better internal control helps reduce the "liabilities of foreignness." This term refers to the extra costs and risks firms face when operating in foreign markets. This effect is especially strong for firms with higher governance quality [17, 18]. For textile firms looking to go global, this means strong internal control can make their international journey smoother.

Equity concentration plays a key role in enhancing a firm's internal control quality [6]. Major shareholders have two main goals: preserving their wealth and making it grow. These goals give them strong incentives to monitor management. They want to make sure the firm's operations align with their interests. So, they take active steps. They help set up and improve internal control systems. They also bolster supervision over financial and operational processes. When major shareholders hold a large number of shares, they invest more resources in monitoring. They keep an eye on key areas like procurement, production, and sales. This monitoring prevents managerial opportunism. Managerial opportunism refers to situations where managers act in their own interest instead of the firm's. By stopping this, major shareholders ensure the firm's operations are compliant and effective [15].

This finding matches other research results. Studies show that ownership concentration reduces weaknesses in internal control. It does this by increasing the intensity of monitoring. This is especially true in emerging economies. In these economies, external governance mechanisms, such as strong regulatory bodies or active stock markets, are less developed [7]. So, internal control becomes even more critical, and equity concentration helps strengthen it.

When we look at Chinese textile firms specifically, institutional factors further support the mediating role of internal control. Institutional transitions are taking place in China. During this period, firms with concentrated ownership prefer to develop high-quality internal control systems. They do this to meet the demands of international markets. These systems help them overcome institutional barriers in cross-border operations [18]. This creates a clear path: equity concentration improves internal control. Then, better internal control makes internationalisation easier. It does this by reducing risks and improving how resources are allocated.

Hypothesis 2: The textile and garment firms improve internal control quality through equity concentration, thereby facilitating their internationalisation.

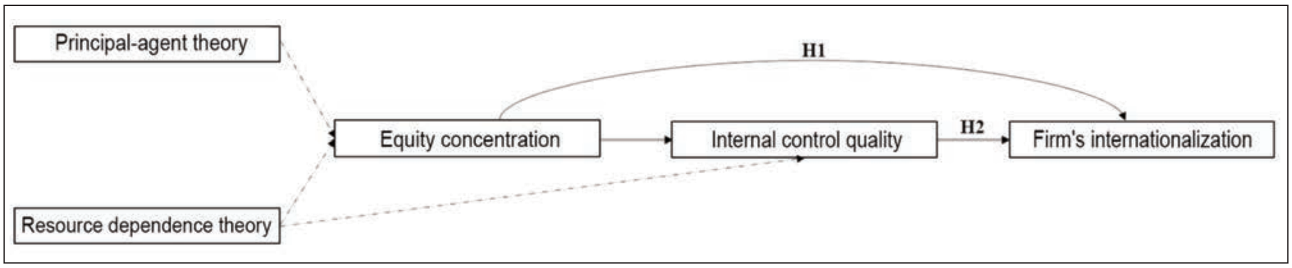

Fig. 1. Research frame

RESEARCH METHODOLOGY

Sample selection and data sources

The basic information and financial characteristics of the textile and garment firms come from the CSMAR database and the Wind database. To ensure the sample is valid, we screen data as follows: (1) Remove ST, *ST, and PT firms with abnormal operations. (2) Exclude firms that have been listed for less than a year, delisted, or suspended. (3) Exclude enterprises that issue B shares or H shares at the same time. (4) Exclude enterprises whose place of registration is not in China. (5) Eliminate enterprises with obvious deficiencies in financial characteristics data. After the above processing, 1290 observations of 157 firms are finally obtained for analysis. Table 1 shows the descriptive statistics for these variables.

Variable

Explanatory variable

We measure the equity concentration using the total shareholding ratio of the firm's top three shareholders, and mark it as Shrcr2. The higher the value of Shrcr2, the more concentrated the equity of the firm.

Explained variable

We measure a firm's internationalisation using the logarithm of its overseas business income, which reflects the scale and intensity of a firm's engagement in foreign markets. This indicator captures both the breadth and depth of international operations through actual revenue generated abroad, making it one of the most widely adopted measures of internationalisation in prior studies [9, 10, 13]. This indicator shows how much a firm participates in specific overseas markets. A higher value means the firm has more experience in international business.

Compared with alternative indicators such as the number of markets or the entry mode, overseas business income provides a more direct and continuous measure of firms' international performance. It reflects not only the presence but also the effectiveness of firms' operations in overseas markets. Revenue-based measures also account for differences in firm size and market strategies, allowing for cross-firm comparability within the same industry.

Mediating variable

We use the internal control index from the DIB database to measure the internal control quality of listed firms. IC stands for this index. A higher IC value means better internal control quality of the firm.

Control variables

To minimise estimation bias from omitted variables, this study includes several firm-level controls that may affect the degree of internationalisation. These variables capture key firm characteristics, which are commonly identified in prior research as determinants of firms' global expansion.

(1) Firm listing age (ListAge). Measured as the natural logarithm of the current year minus the firm's listing year, firm age reflects organisational experience and market stability. Older firms tend to possess stronger governance structures and accumulated capabilities, facilitating more effective international expansion.

(2) Firm size (FixedAss). Calculated as the natural logarithm of the net value of fixed assets at year-end, firm size captures financial strength and operational scale. Larger firms have greater capacity to absorb

Table 1

VARIABLES DESCRIPTIVE STATISTICS

Variable	Observations	Mean	St. Dev	Min	Max
lninc	1290	12.413	9.588	0	24.711
Shrcr2	1290	0.477	0.157	0.129	0.947
ListAge	1290	2.162	0.830	0	3.434
FixedAss	1290	20.397	1.438	15.113	26.127
ROA	1290	0.029	0.063	–0.578	0.218
Lev	1290	0.426	0.192	0.047	0.925
WW_index	1290	–1.005	0.181	–5.993	–0.779
In_tur	1290	0.091	0.742	0.002	21.861
OverseasBack	1290	0.566	0.983	0	6.000

internationalisation costs and manage complex global supply chains [9].
(3) Firm profitability (ROA), which is return on assets. Defined as net profit divided by total assets, profitability indicates a firm's internal capital availability and managerial efficiency. More profitable firms are better positioned to finance overseas investments and sustain longer payback periods in international projects [4].
(4) Firm leverage ratio (Lev). Measured by the ratio of total liabilities to total assets, leverage represents financial risk and debt burden. Higher leverage often constrains firms' flexibility to engage in risky foreign ventures due to stricter debt covenants and limited borrowing capacity.
(5) Firm financing constraints (WW_index). Constructed using the Whited and Wu [17] approach, this index reflects a firm's external financing difficulties. Firms facing fewer financial constraints can allocate more resources to R&D, marketing, and foreign market development [11].
(6) Firm inventory turnover (In_tur). Calculated as the ratio of cost of sales to average inventory, this variable proxies for operational efficiency and supply chain capability. Higher turnover indicates effective logistics and inventory management, which are essential for maintaining responsiveness in international markets [19].
(7) Number of directors with overseas backgrounds (OverseasBack). Measured as the number of executives or directors with overseas education or work experience, this variable captures international managerial expertise. Directors with global experience bring cross-cultural understanding and networks that enhance the firm's ability to identify and exploit foreign market opportunities.

Mathematical modelling

Benchmark model

We want to evaluate how equity concentration affects the internationalisation of textile and garment firms. So, we have developed a fixed-effect panel econometric model. This model is based on the theoretical analysis and research hypotheses from the previous section.

$$Ininc_{it} = \beta_0 + \beta_1 Shrcr2_{it} + \sum control_{it} + \delta_{it} + e_{it} \quad (1)$$

In the econometric model (1), the subscripts *i* and *t* stand for a textile and garment firm *i* and a year *t*, respectively. $Shrcr2_{it}$ shows the equity concentration of the sample firm in year *t*. $Ininc_{it}$ stands for the internationalisation of the firm in year *t*. $\sum control_{it}$ are the control variables, which may affect $Ininc_{it}$. δ_{it} is the time fixed effect, and e_{it} is the residual term. β_0 denotes the constants, and coefficient β_1 measures how equity concentration affects the firm's internationalisation.

Mediating effect model

We use a firm's internal control as a mediating variable. This helps us further explore how equity concentration affects a firm's internationalisation through specific paths. We use the mediation effect model from Baron and Kenny [3]. With this model, we create recursive equations 2 and 3. In these equations, M_{it} is the mediating variable: a firm's internal control. Also, δ_{it} and e_{it} have the same meanings as in Model 1. A mediating effect exists in two cases. First, the coefficient η of $Shrcr2_{it}$ in Model 2 must be significant. Second, the coefficient γ of the mediator in Model 3 must be significant.

$$M_{it} = \eta_0 + \eta_1 Shrcr2_{it} + \sum control_{it} + \delta_{it} + e_{it} \quad (2)$$

$$Ininc_{it} = \gamma_0 + \gamma_1 Shrcr2_{it} + \gamma_2 M_{it} + \sum control_{it} + \delta_{it} + e_{it} \quad (3)$$

MAIN ANALYSES

Empirical result

We present the regression results in table 2. Column (1) shows a univariate regression with no control variables. The coefficient estimate for Shrcr2 is positive and significant. Column (2) includes other control variables. The coefficient for Shrcr2 here is 8.783. In both columns (1) and (2), the benchmark regressions show that the coefficient for Shrcr2 is significantly positive at the 5% level. This means that higher equity concentration significantly promotes a firm's internationalisation. Thus, hypothesis 1 is supported.

Endogeneity test

The empirical results show that equity concentration is positively related to firms' internationalisation. But there may be another reason. Firms with higher overseas income are more willing and able to increase their equity concentration. This creates a reverse causality problem. We can reduce this reverse causality by using lagged explanatory variables. Lagged equity concentration is less likely to be affected by current internationalisation. Then we use one-period lagged equity concentration as the explanatory variable and re-run the regression. Columns (3) and (4) of table 2 show these re-run results. And they confirm that the conclusions remain robust.

Mechanism analysis

This study aims to examine how textile and garment firms improve their internal control quality through equity concentration, and how this helps their internationalisation. We test the mediating effect using a stepwise method. The results are in columns (1) and (2) of table 3. Column (1) shows the regression results. Here, the dependent variable is the internal control index. The coefficient for Shrcr2 is significantly positive. This means that a higher Shrcr2 value means the firm has better internal control quality. Column (2) shows the regression results after we add the mediating variable to the model. The coefficient for IC is significantly positive at the 10% significance level. The coefficient for Shrcr2 is significantly positive at the 5% significance level. What's more, the estimated coefficient for Shrcr2 in table 3, column (2) is smaller than that in table 2, column (2). This suggests that equity concentration can effectively improve internal control quality. In turn, this helps boost the firm's internationalisation. Therefore, hypothesis 2 is supported.

Table 2

EMPIRICAL RESULT AND ENDOGENEITY TEST				
VARIABLE	**(1)**	**(2)**	**(3)**	**(4)**
Shrcr2	8.072** (4.020)	8.783** (4.307)		
L.Shrcr2			8.343* (4.275)	8.346* (4.624)
ListAge		0.705 (0.921)		0.394 (1.291)
FixedAss		0.691 (0.455)		0.501 (0.485)
ROA		7.462** (3.730)		4.458 (4.182)
Lev		5.016** (2.395)		3.782 (2.582)
WW_index		3.104* (1.714)		–0.939 (2.497)
In_tur		–0.305 (0.255)		–0.324 (0.287)
OverseasBack		0.376 (0.336)		0.450 (0.310)
Constant	8.564*** (1.917)	–6.816 (8.953)	9.130*** (2.055)	–4.961 (10.299)
Firm FE & Year FE	Yes	Yes	Yes	Yes
Observations	1290	1290	1118	1118
Firms	157	157	157	157
R^2	0.739	0.749	0.769	0.774

Note: Robust standard errors in parentheses are clustered at the firm level. * p<0.1, ** p<0.05, *** p<0.01. All of the above are the same; omitted.

Placebo test

To check if the study's empirical results come from equity concentration rather than other factors [12], we create a random value for equity concentration (RanShrcr2). We use this value to run placebo tests. If equity concentration truly affects lninc, the random version of equity concentration will not affect a firm's internationalisation. We also create a random value for internal control quality (RanIC). This helps us run placebo tests for the mediating effect. These regression results are in table 3. In column (1) of table 3, the coefficient for random equity concentration is not significantly different from zero. This differs from the results in column (2) of table 2. It means our empirical results pass the placebo test. Similarly, columns (4) and (5) of table 3 show that our mechanism analysis results also pass the placebo test.

Other robustness checks

We need to test whether empirical results might differ based on how we define explanatory and dependent variables. We replace the equity concentration indicator with two measures. One is the sum of the shareholding ratio of the firm's top 1 shareholder (Shrcr1). The other is the sum of the shareholding ratios of the firm's top 5 shareholders (Shrcr5). The results are in table 4, columns (1) and (2). They show that our empirical results pass the placebo test.

We also redefine a firm's internationalisation. Now it depends on whether the sample firm has overseas business income. If it does, deep_yes scores 1; otherwise, it scores 0. The results are in table 4, columns (3) and (4). They confirm that our empirical results pass the placebo test. Since deep_yes is a dummy variable, we further change the regression model to xttobit. The results are in table 4, columns (5) and (6). They again show the empirical results pass the placebo test.

In addition, the sample may have a serious left-bias problem. The interpreted variable has a minimum value of 0. So we change the model's estimation method. We use the Poisson pseudo-maximum likelihood estimation (ppmlhdfe) for fixed-effect panels. We then re-run the regression. The results are in table 4, columns (7) and (8). These results show that

Table 3

MECHANISM ANALYSIS AND PLACEBO TEST					
VARIABLE	**(1)**	**(2)**	**(3)**	**(4)**	**(5)**
	IC	**lninc**	**lninc**	**RanIC**	**lninc**
Shrcr2	3.238*** (0.680)	8.231** (4.014)		–0.177 (0.654)	8.781** (4.308)
RanShrcr2			1.238 (0.775)		
IC		0.189* (0.106)			
RanIC					–0.010 (0.073)
Controls	Yes	Yes	Yes	Yes	Yes
Constant	Yes	Yes	Yes	Yes	Yes
Firm FE & Year FE	Yes	Yes	Yes	Yes	Yes
Observations	1290	1290	1290	1290	1290
Firms	157	157	157	157	157
R^2	0.757	0.740	0.746	0.167	0.749

Table 4

OTHER ROBUSTNESS CHECKS										
VARIABLE	Replace Shrcr2		Replace lninc		Replace lninc, xttobit		ppmlhdfe		Province	City
	lninc	lninc	deep_yes	deep_yes	deep_yes	deep_yes	lninc	lninc	lninc	lninc
	(1)	(2)	(3)	(4)	(5)	(6)	(7)	(8)	(9)	(10)
Shrcr1	7.344* (4.297)									
Shrcr3		8.015* (4.443)								
Shrcr2			0.342* (0.182)	0.431** (0.192)	0.516*** (0.145)	0.562*** (0.164)	0.778** (0.356)	0.789** (0.368)	8.783** (3.674)	8.783** (3.716)
Controls	Yes	Yes	No	Yes	No	Yes	No	Yes	Yes	Yes
Constant	Yes	Yes	Yes	Yes	Yes	Yes	Yes	Yes	Yes	Yes
Firm FE & Year FE	Yes	Yes	Yes	Yes	Yes	Yes	Yes	Yes	Yes	Yes
Observations	1290	1290	1290	1290	1290	1290	1056	1056	1290	1290
Firms	157	157	157	157	157	157	121	121	157	157
Pseudo R^2 or R^2	0.748	0.749	0.746	0.753	/	/	0.320	0.328	0.749	0.749

the findings in table 2, column (2), pass the placebo test.

Finally, the textile and garment industry often has an agglomeration effect. This may cause empirical results to miss regional-level variables. To address this, we conduct robustness tests by clustering at the provincial and city levels. The results are in table 4, columns (9) and (10). These results confirm that the findings in table 2, column (2), pass the placebo test.

FURTHER DISCUSSION: PRACTICAL INSIGHTS AND GLOBAL RELEVANCE

For textile and garment firms striving to enhance international competitiveness, two core strategies stand out. Firstly, optimise equity structure for moderate concentration. Excessively scattered ownership hampers decision speed and efficiency, leaving firms ill-equipped to adapt to global market shifts. Firms can issue private placements to investors who align with their development vision and possess strong financial backing, boosting major shareholders' stakes and control. They can also bring in strategic investors that offer industry experience, market resources and advanced management beyond capital. Firms must prioritise business compatibility to foster industrial chain synergy and clarify rights and obligations via articles of association to prevent power abuse and ensure strategic contributions. Secondly, build a comprehensive internal control system covering all operations, including overseas subsidiaries, which face higher risks from legal and cultural differences. Focus on cross-border capital flows and supply chain management. Monitor exchange rate fluctuations and financial policy changes using financial derivatives to mitigate currency risks. Establish long-term supplier partnerships and adopt intelligent management systems to track raw material deliveries, identify delays early and adjust production plans promptly.

Governments play a key supportive role. Promote equity incentives with tax benefits to align the interests of major shareholders, management, and minority investors. Enforce clear rules on incentive targets, methods, and exercise conditions to protect minority shareholders. Develop industry-specific internal control guidelines covering finance, risk management, and internal audit that are accessible to small and medium-sized firms. Conduct regular evaluations rewarding strong implementation and requiring timely fixes for flaws. Expand export credit insurance by lowering premiums, broadening coverage, and increasing compensation ratios. Provide tiered overseas investment subsidies with higher support for high-value R&D projects to encourage value-added activities.

Globally, the findings offer valuable guidance for developing countries facing similar competitive pressures and resource constraints. Adopting equity concentration and supply chain practices can help their firms improve market responsiveness. Chinese firms with robust internal control enhance global supply chain stability, supporting reliable sourcing and aligning with ethical production trends. The strategies foster South-South cooperation through job creation and technology transfer in host nations. They also facilitate North-South collaboration by enabling developing country firms to produce higher quality goods for high-end market partnerships. Balancing R&D investments and internal control efficiency helps firms navigate industrial chain restructuring, reducing intense competition and promoting a more balanced global textile industry.

CONCLUSION AND AVENUES FOR FUTURE WORK

This research investigates the influence of equity concentration on the internationalisation of Chinese A-share textile and garment firms, with a specific focus on the mediating role of internal control optimisation. Using firm-level panel data and multiple robustness checks, the study finds that moderate equity concentration effectively promotes firms' internationalisation. Theoretically, this study integrates ownership structure, internal control, and internationalisation into a unified mechanism-based framework, extending agency and resource-dependence theories to the labour-intensive, supply-chain-complex textile and garment sector, and providing governance-driven explanations for emerging-market multinationals. Empirically, it offers industry-specific evidence that governance configurations can partially substitute for technology or brand advantages in facilitating global expansion. Practically, this study suggests that firms should rationalise their equity structure to preclude excessive dispersion while safeguarding effective oversight, and establish a high-quality internal control system tailored to overseas operational needs.

Although this study provides important insights into how equity concentration and internal control influence the internationalisation of textile and garment firms, several limitations should be acknowledged, offering directions for future research. First, the empirical analysis focuses solely on Chinese A-share textile and garment firms. This industrial and regional concentration may constrain the generalizability of the findings. Future studies could conduct cross-country comparative analyses to verify whether the observed relationships hold in other emerging economies or developed markets, thereby enriching the external validity of this framework. Second, this paper focuses solely on identifying internal control as the key mediating mechanism. Future research might develop multiple-mediator or moderated mediation models to explore such alternative pathways, thereby offering a more comprehensive insight into the underlying process.

ACKNOWLEDGEMENT

This work is supported by the National Social Science Fund of China under Grant no. 22CJL019.

REFERENCES

[1] Arregle, J.L., Chirico, F., Kano, L., Kundu, S.K., Majocchi, A., Schulze, W.S., Family firm internationalisation: past research and an agenda for the future, In: Journal of International Business Studies, 2021, 52, 1159-1198

[2] Arregle, J.L., Duran, P., Hitt, M.A., van Essen, M., *Why is family firms' internationalization unique? A meta-analysis*, In: Entrepreneurship Theory and Practice, 2017, 41, 5, 801–831

[3] Baron, R.M., Kenny, D.A., *The moderator-mediator variable distinction in social psychological research: Conceptual, strategic, and statistical considerations*, In: Journal of Personality and Social Psychology, 1986, 51, 1173–1182

[4] Bausch, A., Krist, M., *The effect of context-related moderators on the internationalization-performance relationship: Evidence from meta-analysis*, In: Management International Review, 2007, 47, 3, 319–347

[5] Ettalibi, N., Arunachalam, M., Nguyen, T., ur Rehman, K., *The influence of institutional void and socio-cultural factors on the internationalization of emerging multinationals*, In: Research in International Business and Finance, 2025, 73, 102605

[6] Fama, E.F., Jensen, M.C., *Separation of ownership and control*, In: The Journal of Law and Economics, 1983, 26, 2, 301–325

[7] Gaur, A., Delios, A., *International Diversification of Emerging Market Firms: The Role of Ownership Structure and Group Affiliation*, In: Management International Review, 2015, 55, 235–253

[8] Grosfeld, I., *Ownership concentration and firm performance: evidence from an emerging market*, In: William Davidson Institute Working Papers, 2006

[9] Kirca, A.H., Hult, G.T.M., Roth, K., Cavusgil, S.T., Perryy, M.Z., Akdeniz, M.B., Deligonul, S., Mena, J.A., Pollitte, W.A., Hoppner, J.J., Miller, J.C., *Firm-specific assets, multinationality, and financial performance: A meta-analytic review and theoretical integration*, In: Academy of Management Journal, 2011, 54, 1, 47–72

[10] Lu, J.W., Beamish, P.W., *International diversification and firm performance: The S-curve hypothesis*, In: Academy of Management Journal, 2004, 47, 4, 598–609

[11] Manova, K., *Credit constraints, heterogeneous firms, and international trade*, In: Review of Economic Studies, 2013, 80, 2, 711–744

[12] Shao, Y., Zheng, M., Xu, X., Ji, X., *Does ESG performance have an impact on firm value? Evidence from the Chinese textile and garment industry*, In: Industria Textila, 2025, 76, 2, 249–256, https://doi.org/10.35530/IT.076.02.2023126

[13] Sullivan, D., *Measuring the degree of internationalization of a firm*, In: Journal of International Business Studies, 1994, 25, 2, 325–342

[14] Wang, C., Meng, L., Li, L., Zhao, Z., *Board of directors' internationalization, internal control quality, and corporate litigation risk,* In: Finance Research Letters, 2025, 76, 106994

[15] Wang, J., Wang, H., Wang, D., *Equity concentration and investment efficiency of energy companies in China: Evidence based on the shock of deregulation of QFIIs*, In: Energy Economics, 2021, 93, 105032

[16] Wang, Q., Xue, X., Yang, D., Lee, C.K., *Internal control system and mechanism of Chinese listed companies: an empirical study*, In: Enterprise Information Systems, 2021, 15, 1, 105–130

[17] Whited, T.M., Wu, G., *Financial Constraints Risk*, In: The Review of Financial Studies, 2006, 2, 531–559

[18] Xiao, S.S., Jeong, I., Moon, J.J., Chung, C.C., Chung, J., *Internationalization and performance of firms in China: Moderating effects of governance structure and the degree of centralized control*, In: Journal of International Management, 2013, 19, 2, 118–137

[19] Zhou, K.Z., Gao, G.Y., Zhao, H., *State ownership and firm innovation in China: An integrated view of institutional and efficiency logics*, In: Administrative Science Quarterly, 2017, 64, 2, 375–404

Authors:

XIAOHUI YUAN[1], KUN BAO[2]

[1]Capital University of Economics and Business, School of Economics, China
e-mail: 12024030008@cueb.edu.cn

[2]University of International Business and Economics, School of International Trade and Economics, China

Corresponding author:

KUN BAO
e-mail: 202100180030@uibe.edu.cn

Development and fitting evaluation of a new method for preparing women's pants patterns by using direct body measurements

DOI: 10.35530/IT.077.04.2025132

EMİNE UTKUN AKTENER

ABSTRACT – REZUMAT

Development and fitting evaluation of a new method for preparing women's pants patterns by using direct body measurements

Clothing is an integral part of human life. Clothing fit is one of the important, critical, complex, and dynamic factors considered by users to evaluate the garment quality and to make purchasing decisions. Therefore, one of the most important stages in garment manufacturing is the accurate preparation of the garment pattern. This study aims to examine a system proposed as an alternative to the most commonly used pattern-making methods globally, introduce it to industry, and contribute to its development. The patterns are prepared based on individual body measurements. In this study, women's basic pants were examined in practice. The fit of the clothing patterns made in this study was analysed using CLO 3D software. First, virtual avatars were created to simulate the wearers of the pants; then, these avatars were made to perform not only static poses but also 5 different dynamic movements (walking, running, sitting, climbing stairs, and kneeling) in order to evaluate the patterns. The results of the study indicate that this pattern system is brief, practical, and easily comprehensible by everyone, and also yields successful outcomes in terms of clothing fit.

Keywords: *clothing fitting, pattern design, women's pants, virtual try-on, dynamic fit*

Elaborarea și evaluarea adecvării unei noi metode de realizare a tiparelor pentru pantaloni de damă pe baza măsurătorilor directe ale corpului

Îmbrăcămintea reprezintă o parte integrantă a vieții umane. Corespondența îmbrăcămintei este unul dintre factorii importanți, critici, complecși și dinamici luați în considerare de utilizatori pentru a evalua calitatea articolului vestimentar și pentru a lua decizii de cumpărare. Prin urmare, una dintre cele mai importante etape în procesul de fabricație a articolelor vestimentare este proiectarea precisă a tiparului. Prezentul studiu își propune să examineze un sistem propus ca alternativă la metodele de realizare a tiparelor cele mai utilizate la nivel global, cu scopul de a le introduce în industrie și de a contribui la dezvoltarea acesteia. Tiparele sunt proiectate pe baza măsurătorilor corporale individuale. În cadrul acestui studiu, au fost analizați în practică pantalonii clasici pentru femei. Corespondența tiparelor realizate în cadrul acestui studiu a fost analizată cu ajutorul software-ului CLO 3D. Mai întâi, au fost create avatare virtuale pentru a simula purtătorii pantalonilor; apoi, aceste avatare au fost programate să execute nu doar poziții statice, ci și 5 mișcări dinamice diferite (mers, alergare, așezare, urcarea scărilor și îngenunchere) pentru a evalua tiparele. Rezultatele studiului indică faptul că acest sistem de tipare este concis, practic și ușor de înțeles de către oricine, oferind totodată rezultate în ceea ce privește corespondența articolelor vestimentare.

Cuvinte-cheie: *corespondența articolelor vestimentare, proiectarea tiparelor, pantaloni de damă, probare virtuală, ajustare dinamică*

INTRODUCTION

Importance of clothing fit

Clothing is an integral part of human life. Clothing comfort is when a person is anatomically, physically and/or mechanically, and psychologically in harmony with the material [1–3].

There is a mutual interaction amongst the human body, microclimate, and garment. While people cannot modify the characteristics of their environment and bodily features, garments are the only factor they can modify [4].

The garment's ability to adapt to body movements, to allow for free motion, to avoid restricting mobility, to be lightweight, to be fashionable, to appeal to the wearer's five senses for a feeling of comfort, and to enhance self-confidence through social approval refer to the characteristics of clothing fit.

Research on this topic is significant in terms of improving the living standards of humans.

Clothing fit is one of the important, critical, complex, and dynamic factors considered by users to evaluate the garment quality and to make purchasing decisions [5–16].

In order to meet consumers' demand for clothing fit, manufacturers and researchers are working with different garment patterns, different body types, and different size tables.

Importance of pattern design

In the light of the literature, it is understood that the concept of clothing fit is not only critical to clothing comfort but also multidimensional and complex. One of these dimensions is the pattern-making stage.

People expect to move freely within a garment. Even though all comfort parameters related to the garment are fulfilled, if the size of the garment is not fit for purpose, either freedom of movement will be restricted, or seam ruptures will occur due to the person's body movements. In other words, these forces that emerge with movements and impact the garment can become intense enough to tear it, depending on the type of motion and the cut of the garment. These issues, which are usually observed in pants, frequently occur in shirts, blouses, jackets, skirts, and dresses as well [17].

Achieving ergonomic compatibility and freedom of movement in the garment is possible by thoroughly understanding the human body, considering the garment's intended use, and being aware of the properties of the materials used [18].

In order to make patterns based on body size, body measurements are needed. Each pattern-making system has its own measurement techniques. The success of a system depends on how well the measurement technique is comprehended and practised. The German Müller & Sohn, the British Metric, the German Contec, and the American Basic Blocks Pattern-Making systems, which are empirical methods consisting of a set of drawing rules, are the most widely used systems for making basic garment patterns from scratch. Many measurements in these pattern-making systems are obtained through either various calculation methods and formulas or empirical constants directly. In some cases, since what these constants represent is not exactly known, the pattern-making process is acted out by rote. And sometimes, people preparing the patterns may fail to apply the formulas correctly [19].

Tama and Öndoğan, in their study utilising 4 different pattern-making systems to prepare basic skirt patterns with identical body measurements for different body types and conducting fitting evaluation, suggested that existing pattern-making systems were not sufficient for all body types [20]. Unal and Utkun examined how women's body types impact the pattern-making process, and studied different basic body patterns tailored to different female bodies [21]. Chrimes et al. identified a gap in the literature regarding subjective fit, and suggested that comprehensive surveys were needed to better understand consumers' thoughts on fit. In addition, they emphasised that women's body type had a significant impact on clothing fit, and suggested that body types needed to be taken into consideration when designing commercial collections [22].

In the literature, there are several studies that propose different pattern-making methods considering the issues in the existing pattern-making systems.

Cho et al. modified the conventional draping system and developed a personalised pattern-making system that could be used with 3D modelling techniques. When they compared the skirts, the patterns of which were prepared by their system to those prepared by conventional methods, they saw that approximately 80% of the users preferred the skirts made by the newly developed system [23].

Mete developed a new form-fitting basic pattern-making technique for women's upper body based directly on body measurements, and tested these patterns in terms of clothing fit. It was observed that the newly developed system (EFES) was able to provide full compatibility with the whole body, and applied to any body type or size during the pattern-making process [19].

Song and Ashdown split women into 3 different categories based on their lower body shapes by using a method they developed. Then, they examined the shortcomings of the Basic Blocks Pattern-Making system and modified the standard basic pants patterns prepared with this system (standard customisation method) by considering different body shapes and postures (body-shape-driven customisation method). It was observed that the pants patterns prepared based on body shapes yielded better clothing fit outcomes compared to standard patterns [24].

Similarly, in their study, Kılıç et al. developed a new pattern method (AnMePa) for women by using the measurements obtained through an anthropometric measurement system. They evaluated the fitting of the basic pants patterns through a 3D clothing system and fuzzy logic method. It was observed that the patterns made with this newly developed system yielded better clothing fit outcomes than those made with other pattern-making methods [25].

Jin and Gu aimed to achieve the automatic generation of individualised prototype patterns by combining 3D body clouds and 2D measurement techniques. This method aims to overcome the formulas used in other pattern-making methods and to consider different body types during the pattern-making process. The authors stated that in subsequent studies, they intended to simplify and streamline this method [26].

However, when these studies are reviewed, it is observed that these newly developed methods are not yet practical and therefore have not been widely popular within the industry. Furthermore, it is noted that a single garment category is exemplified in these studies, and studies on other garment categories are still ongoing.

3D clothing fitting evaluation

Conventionally, the evaluation of a garment's clothing fit is conducted through wear trials. These wear trials may involve feedback from subjects wearing the garment as well as expert opinions. However, this evaluation method is costly, time-consuming, inflexible, and also unsuitable for online (remote) shopping. In recent years, 3D garment computer-aided design (CAD) systems have been used to simulate the clothing experience. Software such as CLO 3D, OptiTex, and Browzwear are the virtual fitting solutions that are in use within the industry [27]. These solutions also facilitate communication among designers, patternmakers, and technical designers [28].

In the literature, there are studies on the applicability and success of 3D virtual systems for evaluating clothing fitting.

Song and Ashdown examined the validity of 3D virtual fitting systems for pants by both conducting wear trials and using 3D virtual try-on systems. The results of the study indicate that the overall accuracy of virtual fitting technology is moderately good for use, especially for pants with good fit, but not to the extent that apparel professionals could fully use it as a visual fit analysis tool [28].

Wu and Liu used the CLO 3D modelling system in their study aiming to improve clothing fit, and their findings yielded successful outcomes regarding the CLO 3D system when compared to subjective evaluations [29].

Mohamed et al. analysed the clothing fit of jacket patterns designed for obese women by using both real and 3D virtual methods (CLO 3D), and suggested that there was no difference between the two methods [30].

Teyeme et al. analysed a form-fitting T-shirt designed for cyclists by using the CLO 3D system. They evaluated a series of local fit levels and pressure at certain critical contact areas of the body with a tight-fitting shirt. At the end of the study, they stated that the variety of elastic fabrics available in the CLO 3D system's library was limited, that physical manufacturing was still necessary for deciding on a final prototype garment, and that CLO 3D significantly accelerated the progress in the early stages of the garment development process [31].

Kim and Baytar investigated the accuracy and applicability of virtual systems under dynamic human body conditions by using the CLO 3D software. In their study, 6 female participants performed 4 different athletic movements, and the participants' bodies were scanned in 3D. The data were evaluated in both real and virtual environments. As a result, the study revealed the advantages and disadvantages of 3D virtual fit technology, pointing out that the system remained limited in dynamic environments and identifying the areas that required improvement [32].

In this study, one different pattern-making systems developed by Saime Sezal were examined [33]. A pattern-making system based on body measurements was described. In this study, women's basic pants were examined in practice. While the proposed pattern system can be applied to non-stretch woven fabrics, it can also be applied to stretch fabrics. However, in such cases, it is required to reduce the width or length measurements of the pattern in line with the direction and degree of fabric stretch.

MATERIAL AND METHOD

Material

In the pattern-making system based directly on body measurements, only the waist and hip circumferences taken from the body are sufficient; other measurements vary depending on the design features of the pants. The waist circumference should be measured at the narrowest part of the waist by using a measuring tape, while the hip circumference should be measured at the widest part of the hips.

Within the scope of the study, first, a basic pants pattern of size 38 was prepared and graded across the sizes 36 and 40. Thereafter, to demonstrate how the proposed system performs in the model, a new modelling was conducted on the basic pants pattern of size 38, which was also graded across the sizes 36 and 40. The size table for both the basic size and modelled pants is given in table 1, while their technical drawings are given in figures 1 and 2.

The fabric used in the CLO 3D system for the study is a 100% cotton woven non-stretch fabric with a weight of 192 g/m^2, and a thickness of 0.38 mm.

Table 1

SIZE TABLE FOR WOMEN'S PANTS			
Measurement values (cm)	**Size 36**	**Size 38**	**Size 40**
Waist circumference	74	78	82
Hip circumference	93	97	101
Knee circumference of pants (measured 38 cm below the inseam)*	41	42	43
Hem circumference of pants*	37	38	39
Side length of pants*	103.5	104	104.5
Fly length*	13	14	14
Fly width*	3.5	3.5	3.5
Waistband height*	4	4	4
Side height of the front panel*	3	3	3
Front centre height of the front panel*	6	6	6
Side height of the back panel*	3	3	3
Front centre height of the back panel*	7	7	7

Note: *The measurements provided for the pants vary depending on the model.

Methodology

When compared to the well-known pattern systems, the pattern-making system developed within the scope of the study displays some distinctive properties as follows.

1. The descriptive language of the process steps is concise, in order, and clear.
2. The process steps are sequenced and associative.
3. The process steps are straightforward.
4. It is easy to keep the process steps in mind.
5. They require scarcely any mathematical formulas and calculations.
6. It is possible to perform measurement verification and validation.
7. Both length and width measurements can be drawn together during the pattern-making process.

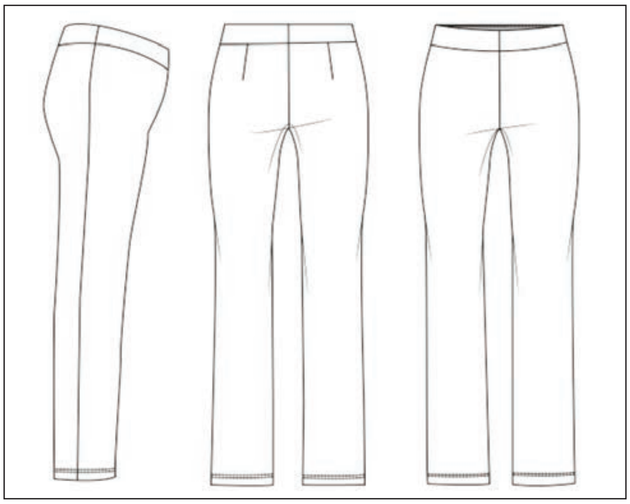

Fig. 1. Technical drawing of the basic size pants

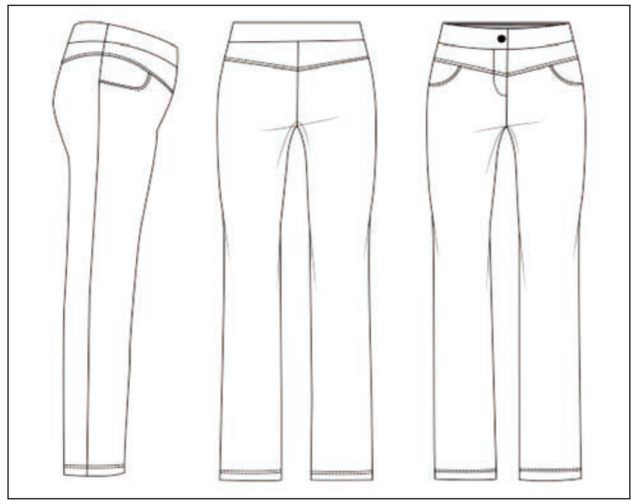

Fig. 2. Technical drawing of the modelled pants

8. The system, designed with the ergonomics of the body in mind, enables easy adjustment of modifications (e.g. dart lengths, etc.) by preventing unwanted looseness in the garment.
9. For lower body garments (skirts and trousers), the difference between the waist and hip measurements is not used for dart distribution, but instead, dart allowances are directly incorporated into the waist measurement.
10. A drawing method has been suggested within the system to prevent deformation (whiskering) that may occur while drafting the front crotch of the pants (figure 3). According to this method, the part between points F and L is divided into four equal parts and marked. Point E is connected to the first part of (F-L)/4, then the midpoint of this line is found and connected to the second part of (F-L)/4. The process continues in this way by preparing the front crotch curve of the pants from point E towards point L. This technique eliminates the need for bisector measurements while drafting the crotch, and prevents deformation.

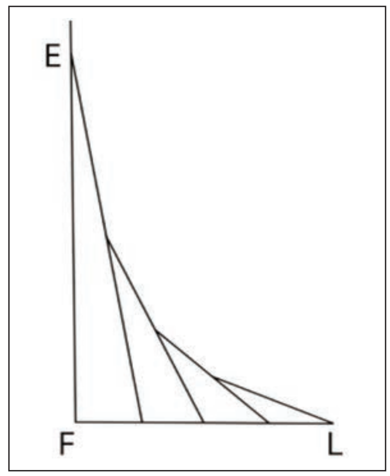

Fig. 3. The method developed for drawing a smooth crotch curve

Process steps

All process steps of front and back pants on pants patterns are given in table 2 and 3.

Table 2

FRONT PANTS DRAWING PROCESS STEPS	
Step no.	**Step description**
1	Draw a straight vertical line.
2	Mark from point A to B equal to the pants' side length.
3	Mark from point A to C equal to the crotch depth (hip circumference/4).
	Note: In this system, for high-rise pants, the crotch depth can be up to (hip circumference/4 + 1, 2, or 3 cm). For low-rise pants, the crotch depth can be up to (hip circumference/4 – 1, 2, or 3 cm). For pants with a lower rise, low-rise modelling should be conducted after preparing the basic pants pattern.
4	From point C, go up 8 cm (constant value) and find point D.
5	Draw horizontal lines from the marked points A, B, C, and D.
6	On the horizontal line from point D, mark (hip circumference/4 – 1) cm. Find point E; the line between D and E is the hip line.
7	Draw a perpendicular line from point E that intersects the horizontal lines coming from points A and C. Find points F and H.
8	From point H, mark 1 cm to the left. Find point I.

Table 2 (continuation)

Step no.	Step description
9	From point I toward point A, mark (waist circumference/4). If a dart is included in the pattern, add the dart width to (waist circumference/4). Find point J.
10	From point J, move 1 cm upwards and find point K.
11	Connect points I and K with a curved line (curving downward).
12	Connect points K and D with a front side curve.
13	From point F, mark (hip circumference/20) cm to the right and find point L.
14	The part between points I, E, and L forms the front crotch.
15	Mark the midpoint between points D and B, and find point M. Draw a horizontal line from M to construct the knee line.
16	Mark the midpoint between points C and L, and find point N.
17	From point N, draw vertical lines upward and downward to find point O on the knee line and point P on the hemline.
18	On the right and left sides of point O, mark (knee circumference/4 – 1 cm). Find points R and S. (42 cm / 4 = 10.5 cm; 10.5 cm – 1 = 9.5 cm)
19	On the right and left sides of point P, mark (hem circumference/4 – 1 cm). Find points T and U. (38 cm / 4 = 9.5 cm; 9.5 cm – 1 = 8.5 cm)
20	Connect R to T and S to U with straight lines.
21	Connect points C to R and L to S with straight auxiliary lines, and find the midpoints of these lines. From the midpoints, move inward by 0.5 cm to shape the calf area with a curve, and draw two lines opposite each other.

Table 3

BACK PANTS DRAWING PROCESS STEPS	
Step no.	**Step description**
1	The back pants pattern is drawn directly over the front pants pattern.
2	The horizontal lines D-E, C-L, R-S, and T-U, as well as the vertical line N-P, which are used for the front pattern, are also applicable to the back pattern.
3	For the difference between the front and back pants, add 2.5 cm (constant value) outward from points C and L, and find points C1 and L1.
4	For the difference between the front and back pants, add 2 cm (constant value) outward from points R and S, and find points R1 and S1.
5	For the difference between the front and back pants, add 2 cm (constant value) outward from points T and U, and find points T1 and U1.
6	Connect points R1 to T1 and S1 to U1 with straight lines.
7	Connect points C1 to R1 and L1 to S1 with straight auxiliary lines, and find the midpoints of these lines. From the midpoints, move inward by 0.5 cm to shape the calf area with a curve, and draw parallel lines.
8	From point L1, move downward by 0.5 cm (room for flexibility), and find point L2.
9	From point E, mark 1cm to the left. Find point V.
10	From point V, mark (hip circumference/4 + 1) cm to the left. Find point Y.
11	Connect points Y and C1 with a straight line.
12	Move inward by 4cm from point I, and find point Z.
13	Connect points V and Z with a straight line, while moving upward by 4cm from point Z along the same line without shifting the ruler. Find point W.
14	Connect points V and L2 with a curved line.
15	From point K, draw a horizontal auxiliary line to the left.
16	Starting at point W, estimate the length on the auxiliary line (waist circumference/4 + dart width), and find point Q.
17	Connect points Q and Y with a straight line.
	Note: The length between points D and K, which defines the sideline of the front pants, is measured. This length is compared to the length between points Q and Y on the back pants. If a discrepancy is observed due to curvature differences, the deficiency is compensated by moving point Q upward accordingly.
18	Find the midpoint of the distance between points V and Y, and from this point, draw a vertical line upward toward the waistline. On this line, draw the back dart by using a dart length (12 cm) downward from the waist, and a dart width (3 cm) sideways.

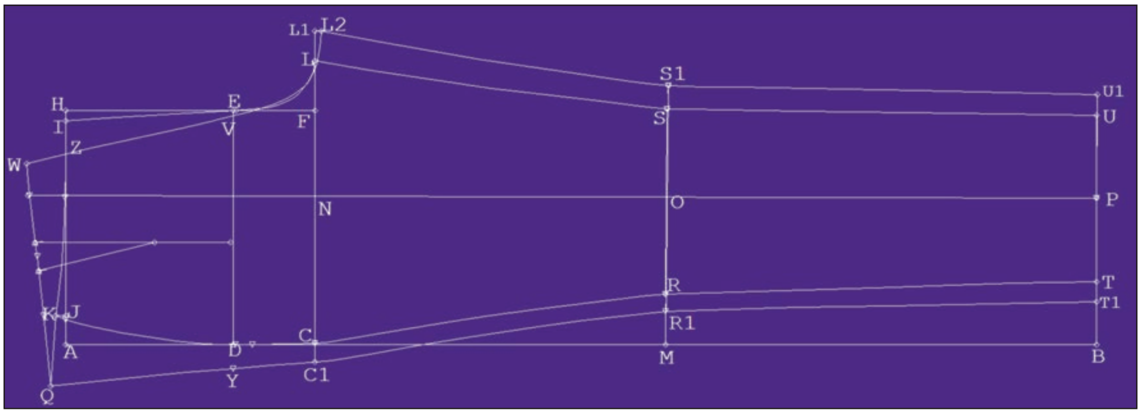

Fig. 4. Front and back women's basic pants patterns

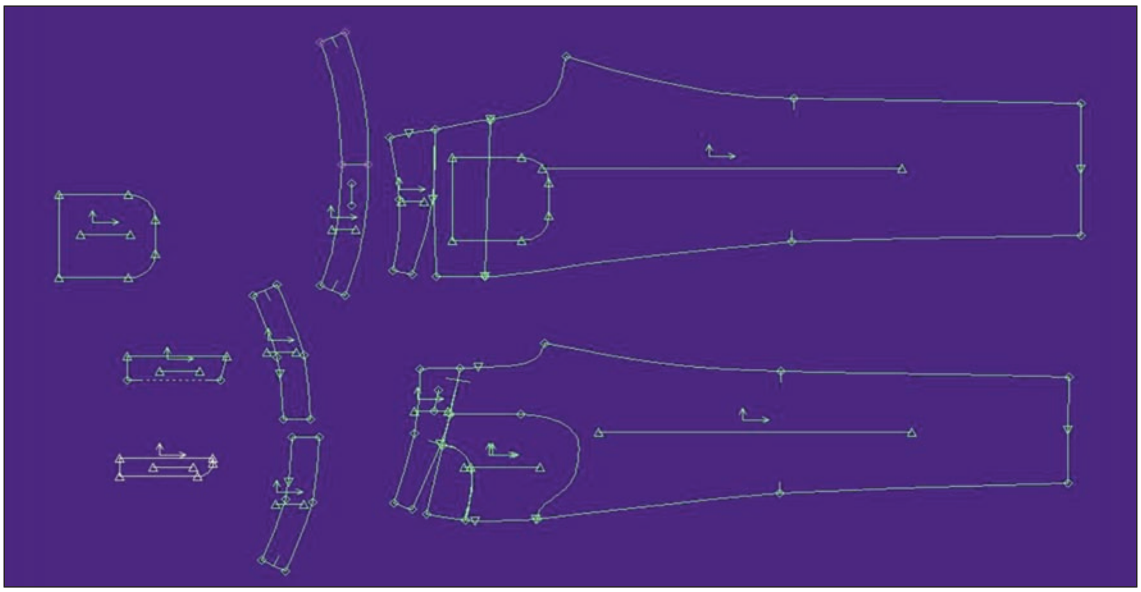

Fig. 5. Pattern pieces of the modelled pants

All points used for the process steps of front and back pants drawing are illustrated on pants patterns in figure 4. The pattern pieces of the modelled pants are given in figure 5.

3D fitting evaluation

The software CLO 3D is applied to measure digital clothing pressures. This software permits the creation of virtual, close-to-life garment visualisation with cutting-edge simulation technologies [34]. The clothing fitting of the patterns made within this study was analysed by using CLO 3D software, version 2024.2.284. First, virtual avatars were created to simulate the wearers of the pants; then, these avatars were made to perform not only static poses but also 5 different dynamic movements (walking, running, sitting, climbing stairs, and kneeling) in order to evaluate the patterns.

RESULTS AND DISCUSSION

Pressure and stress maps of the pants were obtained using the CLO 3D software. The pressure map helps to visually analyse the comfort levels in areas where the fabric comes into contact with the body. It typically illustrates the areas with minimal pressure (i.e. loose-fitting parts) and highlights the room for movement. A stress map, on the other hand, illustrates the amount of tension and pressure exerted by the fabric on the body using a colour-coded map. Areas with higher stress (tension) generally appear in brighter or red-toned hues. Using both maps in conjunction serves as a helpful method for optimising both the technical fit and user experience in garment design. The scales used for evaluating the stress and pressure maps are shown in figure 6. In table 4, what the colours in the scales represent based on the evaluation range is explained.

Table 4

COLOURS ACCORDING TO ASSESSMENT RANGE [19]

Assessment range	Colours
Very tight	Red
Tight	Red - Orange
Well	Yellow - Green
Large	Light blue - Yellow
Very large	White

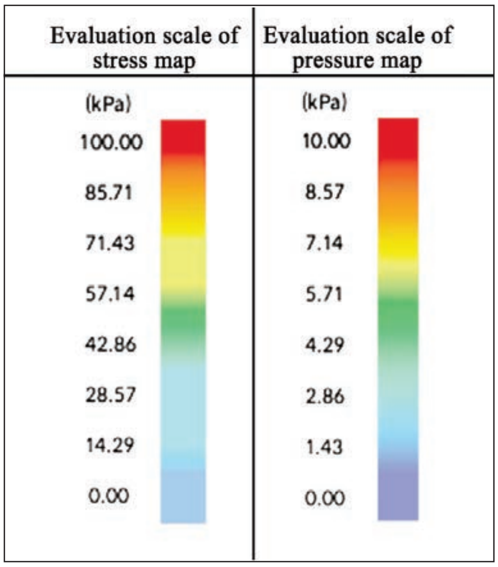

Fig. 6. Evaluation scales of stress and pressure maps

For both the basic and modelled pants of sizes 36, 38, and 40, the stress and pressure maps were prepared separately for standing, walking, sitting, stair climbing, and kneeling positions. The numerical values obtained from the stress and pressure maps are separately given in tables 5, 6, 7, and 8.

Upon analysing the maps of the pants, it is observed that each position yields unique values, which internally vary. It is observed that the values mostly fall within the yellow, green, blue, and white colour intervals, and remain within technically acceptable tolerance ranges. Moreover, it has been determined that the data given in the respective tables exhibit internal consistency and stability. This confirms both the accuracy of the patterns and the reliability of the grading process.

Due to space limitations, the images of stress maps and pressure maps, as well as the overall visuals of the positions used for the sample basic pants pattern of size 38, are given in figures 7, 8, 9, 10, 11, and 12.

Table 5

DIGITAL CLOTHING STRESS VALUES OF BASIC PANTS (kPa)

Position	Standing			Walking			Running			Sitting			Stair-climbing			Kneeling		
Size	36	38	40	36	38	40	36	38	40	36	38	40	36	38	40	36	38	40
Waist	30.56	32.85	39.4	22.46	28.12	36.09	47.05	49.55	53.41	72.25	85.08	95.33	22.05	41.89	50.69	22.52	40.55	49.93
Hip	10.62	12.85	17.55	15.82	20.64	20.72	23.52	20.93	19.91	25.86	28.91	30.99	39.25	42.62	43.5	15.68	19.4	20.14
Thigh	18.06	19.88	20.68	26.21	29.48	30.37	32.24	39.36	41.33	31.22	38.05	39.39	20.41	19.67	18.92	10.64	13.04	14.47
Knee	1.2	1.58	1.92	9.24	10.37	10.59	14.26	19.95	21.9	39.47	43.69	49.17	21.87	19.17	16.82	61.82	63.86	64.64
Calf	1.96	2.25	3.66	4.85	5.87	6.19	5.1	5.88	6.2	20.5	10.96	9.01	0.67	0.69	0.7	0.76	1.15	1.43
Ankle	0.03	0.46	0.5	0.85	0.51	0.14	0.23	0.41	0.66	0.49	0.59	0.76	0.07	0.14	0.17	4.17	4.77	4.96

Table 6

DIGITAL CLOTHING PRESSURE VALUES OF BASIC PANTS (kPa)

Position	Standing			Walking			Running			Sitting			Stair-climbing			Kneeling		
Size	36	38	40	36	38	40	36	38	40	36	38	40	36	38	40	36	38	40
Waist	0.13	0.15	0.16	0.06	0.08	0.16	0.2	0.18	0.13	0.3	0.37	0.4	0.12	0.28	0.2	0.02	0.9	0.1
Hip	0.02	0.04	0.06	0.02	0.07	0.09	0.57	0.52	0.41	0.51	0.49	0.46	0.44	0.53	0.59	0	0	0.03
Thigh	0.24	0.26	0.29	0.22	0.29	0.39	1.19	1.8	2.19	1.21	1.35	2.52	0.5	1.01	1.04	0.02	0.02	0.02
Knee	0	0	0	0.15	0.1	0.08	0.4	0.41	0.43	1.02	0.97	0.93	0.55	0.49	0.47	1.25	1.26	1.29
Calf	0.04	0.05	0.6	0.05	0.04	0.02	0.05	0.11	0.18	0.1	0.16	0.18	0.05	0.07	0.09	0.01	0	0
Ankle	0	0	0	0	0	0	0	0	0	0	0	0	0	0	0	0	0	0

Table 7

DIGITAL CLOTHING STRESS VALUES OF MODEL-APPLIED PANTS (kPa)

Position	Standing			Walking			Running			Sitting			Stair-climbing			Kneeling		
Size	36	38	40	36	38	40	36	38	40	36	38	40	36	38	40	36	38	40
Waist	29.19	31.87	32.01	52.19	54.26	55.31	49.43	50.59	52.41	44.21	38.54	44.89	66.59	58.69	59.65	9.01	15.29	30.7
Hip	10.68	15.21	19.36	4.68	10.86	18.01	50.68	54.35	55.46	3.88	4.06	5.11	2.94	2.89	2.93	3.45	11.08	16.2
Thigh	24.37	25.38	31.65	8.19	15.37	20.42	107.65	123.84	122.07	12.75	17.43	29.65	73.84	94.14	98.36	11.54	21.36	24.23
Knee	0.2	0.53	0.32	4.3	5.74	5.87	32.95	32.27	18.56	11.38	12.54	13.75	50.32	46.46	42.98	5.28	30.07	50.65
Calf	3.56	3.57	4.65	0.36	1.14	1.23	10.29	9.93	9.72	1.8	1.79	2.5	13.8	10.09	8.54	2.03	2.23	1.58
Ankle	4.5	3.53	2.84	0.25	0.23	0.24	0.31	0.34	0.52	0.05	0.09	0.11	0.67	0.22	0.18	3.55	4.3	6.54

Table 8

DIGITAL CLOTHING PRESSURE VALUES OF MODEL-APPLIED PANTS (kPa)																		
Position	**Standing**			**Walking**			**Running**			**Sitting**			**Stair-climbing**			**Kneeling**		
Size	**36**	**38**	**40**	**36**	**38**	**40**	**36**	**38**	**40**	**36**	**38**	**40**	**36**	**38**	**40**	**36**	**38**	**40**
Waist	0.2	0.17	0.11	0.18	0.19	0.23	0.6	0.66	0.35	0.2	0.23	0.21	0.01	0.25	0.3	0.29	0.22	0.21
Hip	0.06	0.06	0.07	0.1	0.12	0.17	0.82	0.81	0.77	0.13	0.13	0.11	0.28	0.17	0.16	0.15	0.33	0.34
Thigh	0.21	0.34	0.35	0.17	0.2	0.5	2.5	2.3	1.52	0.62	0.54	0.37	1.15	1.8	2.26	0.58	0.3	0.37
Knee	0	0	0	0.1	0.09	0.12	0.79	0.75	0.73	0.31	0.31	0.3	1.35	0.53	0.4	0.38	1.3	2.61
Calf	0.5	0.04	0.03	0	0	0	0.07	0.05	0.04	0.01	0.01	0.01	0.16	0.24	0.3	0.34	0.06	0.08
Ankle	0	0	0	0	0	0	0	0	0	0	0	0	0.02	0	0	0.05	0.1	0.16

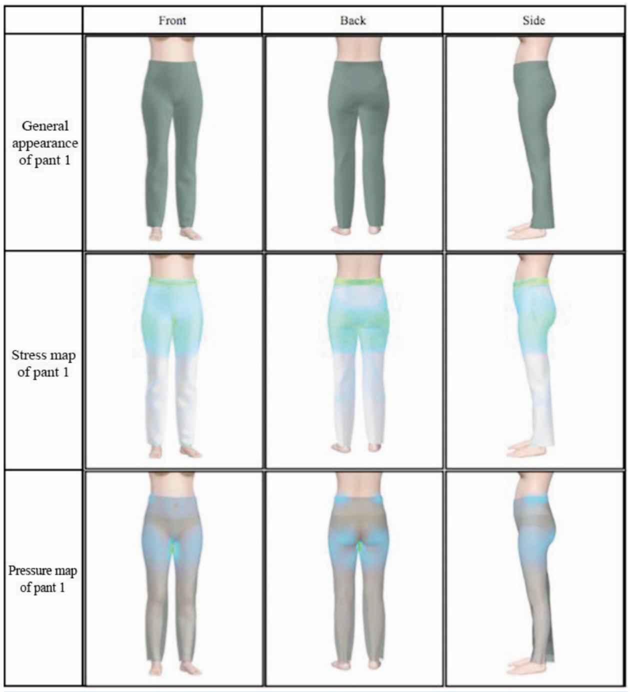

Fig. 7. Fit evaluation in standing position

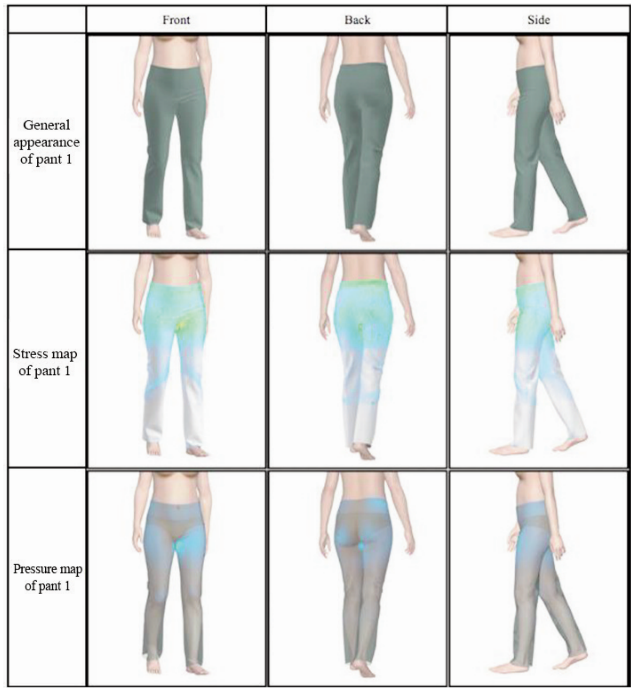

Fig. 8. Fit evaluation in walking position

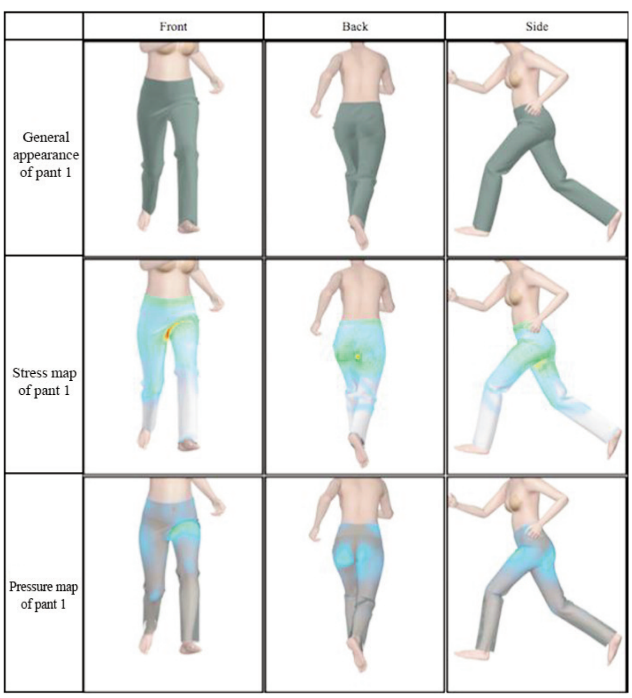

Fig. 9. Fit evaluation in running position

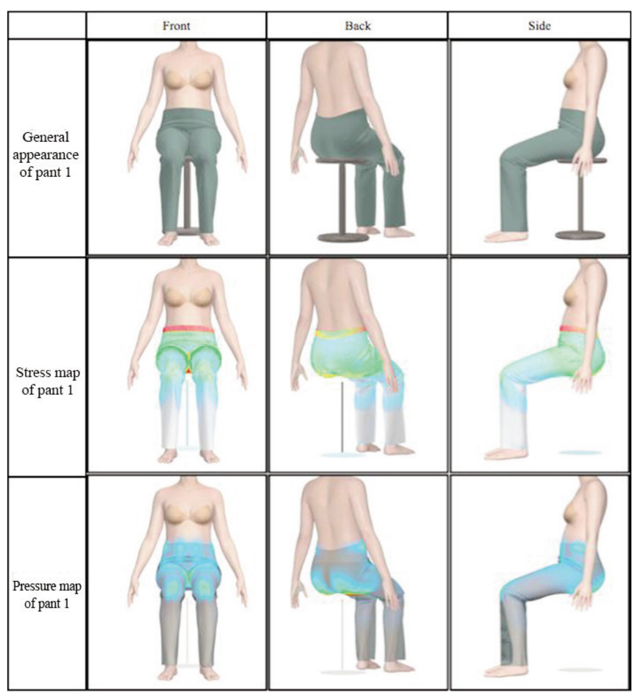

Fig. 10. Fit evaluation in sitting position

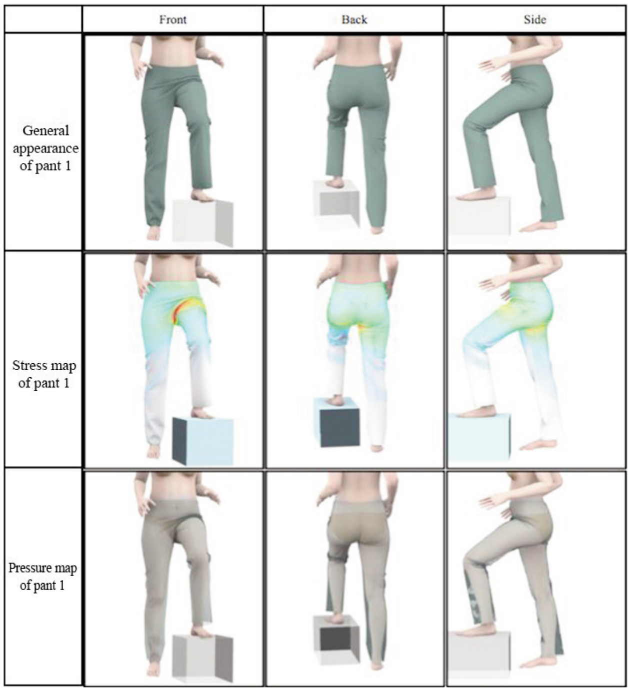

Fig. 11. Fit evaluation in stair-climbing position

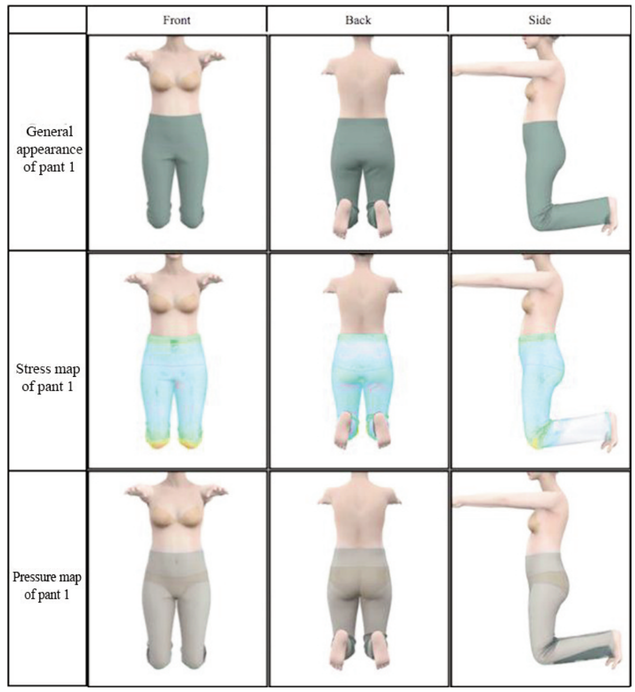

Fig. 12. Fit evaluation in kneeling position

CONCLUSION

As described in the literature review, one of the most important manufacturing stages in the clothing industry is the accurate preparation of the garment pattern. Each faulty pattern prolongs the sample manufacturing cycle and therefore results in losses in time, labour, and cost. It is essential to minimise this sample manufacturing cycle. Both 2D and 3D pattern-making systems are used to reduce this time frame. However, the skills, experience, and familiarity of the users with the pattern-making systems are also crucial. This study aims to contribute to the industry by proposing a simplified and practical system.

When the pressure and stress maps of the pants made with the pattern-making system proposed within the study are examined, it is clearly observed that the pants adapt well to the body and allow for body movement comfort. The system described is also practical and easy to learn, as it does not require complex formulas or calculations during the pattern-making phase; from this perspective, it is evident that the system meets the objectives of the study.

In addition, the following future research topics are proposed.

- While the clothing fit evaluation of the patterns made within this study was conducted by using the CLO 3D system, future studies may include wear trials with human subjects.
- The developed system may also be adapted for other garment categories.

ACKNOWLEDGEMENTS

This study was supported by the Scientific Research Coordination Unit of Pamukkale University under the project number 2025İAP001.

REFERENCES

[1] Sweeney, M. M., Branson, D. H., *Sensorial comfort, part I: A psychophysical method for assessing moisture sensation in clothing*, In: Textile Research Journal, 1990, 60, 7, 371–377

[2] Li, Y., *The science of clothing comfort, The Textile Institute Publications*, In: Textile Progress, Manchester, 2001, 31, ½

[3] Liao, X., Hu, J., Li, Y., Li, Q., Wu, X., *A review on fabric smoothness-roughness sensation studies*, In: Journal of Fiber Bioengineering & Informatics, 2011, 4, 2, 105–114

[4] Utkun, E., *The effects of different model and sewing features on clothing comfort*, Unpublished Doctoral Dissertation, Institute of Natural and Applied Science (Textile Engineering), Ege University, İzmir, Turkey, 2007, 187

[5] LaBat, K.L., DeLong, M.R., *Body cathexis and satisfaction with fit of apparel*, In: Clothing and Textiles Research Journal, 1990, 8, 2, 43–48

[6] Feather, B.L., Ford, S., Herr, D.G., *Female collegiate basketball players' perceptions about their bodies, garment fit and uniform design preferences*, In: Clothing and Textiles Research Journal, 1996, 14, 1, 22–29

[7] Anderson, L.J., Brannon, E.L., Ulrich, P.V., Presley, A.B., Woronka, D., Grasso, M., Gray, S., *Understanding fitting preferences of female consumers: Development an expert system to enhance accurate sizing selection*, In: National Textile Center Annual Report: November, 2000, I98–A08

[8] Hsu, H.-J., Burns, L.D., *Clothing evaluative criteria: A cross-national comparison of Taiwanese and United States consumers*, In: Clothing and Textiles Research Journal, 2002, 20, 4, 246–252

[9] Alexander, M., Jo Connell, L., Beth Presley, A., *Clothing fit preferences of young female adult consumers*, In: International Journal of Clothing Science and Technology, 2005, 17, 1, 52-64
[10] Kinley, T.R., *Fit and shopping preferences by clothing benefits sought*, In: Journal of Fashion Marketing and Management, 2010, 14, 3, 397–411
[11] Song, H.K., Ashdown, S.P., *An exploratory study of the validity of visual fit assessment from three-dimensional scans*, In: Clothing and Textiles Research Journal, 2010, 28, 4, 263–278
[12] Shan, Y., Huang, G., Qian, X., *Research overview on apparel fit*, In: Soft Computing in Information Communication Technology, 2012, 2, 39–44
[13] Rieke, S.E., Fowler, D.C., Chang, H.J., Velikova, N., *Exploration of factors influencing body image satisfaction and purchase intent: Millennial females,* In: Journal of Fashion Marketing and Management, 2016, 20, 2, 208–229
[14] Shin, E., Damhorst, M.L., *How young consumers think about clothing fit?*, In: International Journal of Fashion Design, Technology and Education, 2018, 11, 3, 352–361
[15] Makhanya, B.P., Mabuza, D.C., *Body cathexis and fit preferences of young South African women of different body shapes and ethnicity*, In: International Journal of Fashion Design, Technology and Education, 2020, 13, 2, 173–180
[16] Liu, K., Wu, H., Zhu, C., Wang, J., Zeng, X., Tao, X., Bruniaux, P., *An evaluation of garment fit to improve customer body fit of fashion design clothing*, In: The International Journal of Advanced Manufacturing Technology, 2022, 120, 3, 2685–2699
[17] Bozkurt, B., *Effect of body movements on clothing feature*s, Unpublished Doctoral Dissertation, Institute of Natural and Applied Science (Textile Engineering), Ege University, İzmir, Turkey, 1995, 158
[18] Vural, T., Çivitci, Ş., Ağaç, S., *Ergonomic approach to clothing design*, In: National Ergonomics Congress, Dokuz Eylül University, İzmir, Turkey, 25–26 October 2001, 201–209
[19] Tama, D., Öndoğan, Z., *Fitting evaluation of pattern making systems according to female body shapes*, In: Fibres & Textiles in Eastern Europe, 2014, 22, 4, 106, 107–111
[20] Ünal, N., Utkun, E., *Impacts of female body shapes on patternmaking*. In: Industria Textila, 2018, 69, 6, 519-523, http://doi.org/10.35530/IT.069.06.1222
[21] Chrimes, C., Boardman, R., McCormick, H., Vignali, G., I*nvestigating the impact of body shape on garment fit*, In: Journal of Fashion Marketing and Management, 2023, 27, 5, 741–759
[22] Cho, Y., Komatsu, T., Inui, S., Takatera, M., Shimizu, Y., Park, H., I*ndividual pattern making using computerized draping method for clothing*, In: Textile Research Journal, 2006, 76, 8, 646–654
[23] Mete, F., *The development of a new women's bodice pattern making technique that provides satisfactory fit, based on direct body measurements*, In: Dokuz Eylül University Faculty of Engineering Journal of Science and Engineering, 2001, 3, 2, 69–82
[24] Song, H.K., Ashdown, S.P., *Development of automated custom-made pants driven by body shape*, In: Clothing and Textiles Research Journal, 2012, 30, 4, 315–329
[25] Kılıç, A.Ş., Ünal, C., Öndogan, Z., *AnMePa: development of a new method for preparing trousers pattern by using the antropometric measurement system*, In: International Journal of Clothing Science and Technology, 2024, 36, 2, 367–382
[26] Jin, S., Gu, B., *An integrated 3D point cloud and 2D image-based approach for generating individualized female prototype pattern*, In: International Journal of Industrial Ergonomics, 2025, 107, 103748, 1–13
[27] Hu, P., Ho, E.SL., Aslam, N., Komura, T., Shum, H.PH., *A new method to evaluate the dynamic air gap thickness and garment sliding of virtual clothes during walking*, In: Textile Research Journal, 2019, 89, 19–20, 4148–4161
[28] Song, H.K., Ashdown, S.P., *Investigation of the validity of 3-D virtual fitting for pants*, In: Clothing and Textiles Research Journal, 2015, 33, 4, 314–330
[29] Wu, R., Liu, Z., *Research on improving garment fit through CLO 3D Modeling*, International Seminar on Computer Science and Engineering Technology (SCSET), Indianapolis, USA, January 2022, 204–207
[30] Mohamed, S.M., El-Newashy, R., Bekhet, E.Z., Mohamed, D., *Efficiency of 3D simulation software usage to fit the jacket pattern for obese women*, In: Journal of Textiles, Coloration and Polymer Science, 2023, 20, 1, 1–9
[31] Teyeme, Y., Malengier, B., Tesfaye, T., Vasile, S., Van Langenhove, L., *Fit and pressure comfort evaluation on a virtual prototype of a tight-fit cycling shirt*, In: AUTEX Research Journal, 2023, 23, 2, 153–163
[32] Kim, Y., Baytar, F., A*ccuracy and feasibility of 3D virtual dynamic fit technology*, In: International Journal of Clothing Science and Technology, 2024, 36, 3, 499–515
[33] Sezal, S., *Modelistlik (Kalıp) Kitabı*, Publisher: Egeus Yayınları, 2023, 320
[34] Clo3D, Available at: https://www.clo3d.com/en/clo/features [Accessed on June 1st, 2025]

Author:

EMİNE UTKUN AKTENER

Pamukkale University, Buldan Vocational School, Program of Fashion Design, 20400, Denizli, Türkiye

Corresponding author:

EMİNE UTKUN AKTENER
e-mail: eutkun@pau.edu.tr
ORCID NO: 0000-0002-6550-4168

Mechanical performance of woven fabrics made from virgin, semi-recycled, and fully recycled cotton/polyester yarns after natural weathering

DOI: 10.35530/IT.077.04.20263

ELIF YILMAZ

ABSTRACT – REZUMAT

Mechanical performance of woven fabrics made from virgin, semi-recycled, and fully recycled cotton/polyester yarns after natural weathering

Global warming and environmental pollution, which are the main problems of today's daily life, make the issue of sustainability increasingly important. Increasing UV radiation and climate change driven by global warming significantly affect the performance and lifespan of textile products, especially for outdoor use. In addition, sustainability research in the textile sector is increasingly focusing on the recycling of pre- and post-consumer textile waste and the use of fibres recycled from these wastes in yarn and fabric production. However, more scientific data is needed to determine the long-term resistance of textile products produced from recycled materials to environmental conditions. In this context, revealing the effects of natural weathering on the mechanical properties of textile fabrics by comparing them with fabrics produced from virgin fibres is very important in terms of both correct material selection and optimum product life. This study investigated and compared the mechanical performance of outdoor upholstery fabrics made from fully and semi-recycled cotton/polyester blended yarns, as well as virgin cotton/polyester blended yarns, which were exposed to natural weathering for three months in summer and three months in autumn. The results showed that virgin fabrics maintain their mechanical properties more effectively under natural weathering conditions, while semi-recycled fabrics exhibit acceptable mechanical performance comparable to virgin fabrics. These findings highlight their strong potential as a promising sustainable alternative for outdoor textile applications.

Keywords: *recycled cotton, recycled polyester, virgin and recycled blended yarns, woven upholstery fabric, tensile strength, natural weathering*

Caracteristicile mecanice ale țesăturilor realizate din fire din bumbac/poliester virgine, parțial și complet reciclate, după expunerea la intemperii naturale

Încălzirea globală și poluarea mediului, care reprezintă principalele probleme ale vieții cotidiene de astăzi, fac ca tema sustenabilității să capete o importanță din ce în ce mai mare. Creșterea radiației UV și schimbările climatice cauzate de încălzirea globală afectează în mod semnificativ performanța și durata de viață a produselor textile, în special a celor destinate utilizării în exterior. În plus, cercetarea în domeniul sustenabilității din sectorul textil se concentrează din ce în ce mai mult pe reciclarea deșeurilor textile pre- și post-consum și pe utilizarea fibrelor reciclate din aceste deșeuri în producția de fire și țesături. Cu toate acestea, sunt necesare mai multe date științifice pentru a determina rezistența pe termen lung a produselor textile fabricate din materiale reciclate la condițiile de mediu. În acest context, evidențierea efectelor intemperiilor naturale asupra proprietăților mecanice ale țesăturilor, prin compararea acestora cu țesăturile fabricate din fibre virgine, este foarte importantă atât din perspectiva alegerii corecte a materialelor, cât și a duratei de viață optime a produsului. Prezentul studiu a investigat și a comparat performanțele mecanice ale țesăturilor de tapițerie pentru exterior realizate din fire din amestec de bumbac/poliester complet și parțial reciclate, precum și din fire din amestec de bumbac/poliester virgine, care au fost expuse la intemperiile naturale timp de trei luni în timpul verii și trei luni în timpul toamnei. Rezultatele au arătat că țesăturile din fibre virgine își păstrează proprietățile mecanice mai eficient în condiții naturale de expunere la intemperii, în timp ce țesăturile semi-reciclate prezintă performanțe mecanice acceptabile, comparabile cu cele ale țesăturilor din fibre virgine. Aceste constatări evidențiază potențialul lor ridicat ca alternativă durabilă și promițătoare pentru aplicațiile textile de exterior.

Cuvinte-cheie*: bumbac reciclat, poliester reciclat, fire virgine și reciclate în amestec, țesătură pentru tapițerie, rezistență la tracțiune, intemperii naturale*

INTRODUCTION

Research in the textile industry has increasingly focused on sustainable solutions due to global environmental challenges such as climate change and limited natural resources. Textile products that are produced with recycled fibres have gained attention recently. One of these textile products is upholstery fabrics.

Upholstery fabrics are widely used in both indoor and outdoor furniture applications. Since they are in direct contact with users, they are expected to offer good aesthetic and comfort properties, along with mechanical durability under varying conditions. Woven fabrics are commonly preferred in the production of upholstery fabrics thanks to their durability, comfort, and good air and water permeability properties.

These fabrics are generally produced in main weave types, and plain weave is one of the most basic weaving structures in the textile industry [1].

Various natural and synthetic fibres are used in the production of upholstery fabrics. Cotton and synthetic fibres are among the most widely used raw materials due to their superior quality [2]. Additionally, the growing need for bio-based and recyclable materials is becoming even more apparent with new sustainability-related regulations expected [3].

The limited number of previous studies in the literature have examined the mechanical properties of woven upholstery fabrics made of recycled yarns. Results revealed that although slight decreases occur in mechanical properties, high-value-added and sustainable products can successfully be produced by using recycled textile wastes [4, 5]. Outdoor upholstery fabrics are exposed to various environmental stresses, including sunlight, moisture, and temperature fluctuations. Sunlight is a major source of energy for life on Earth and also a source of UV radiation, which consists of harmful UV rays [6]. When fabrics are exposed to UV radiation, both natural and synthetic fibres undergo photodegradation, which causes a decrease in mechanical properties, a loss in fabric flexibility, and colour [7, 8]. All these environmental factors can significantly impact the mechanical properties of fabrics, such as strength, durability, and appearance. Therefore, there is a rising interest in determining the performance of different types of recycled and virgin yarns under challenging outdoor conditions as a result of the need for sustainable raw material use.

Degradation in material structure caused by UV radiation and environmental factors is evaluated through weathering tests conducted in a laboratory or under natural environmental conditions. Natural environmental conditions provide more reliable and realistic data compared to accelerated laboratory tests. However, as a disadvantage, the weathering process under real-world conditions requires a longer time. Nevertheless, outdoor tests are considered one of the fundamental tools for predicting degradation, as they provide both quantitative and qualitative information [9]. Previous research has examined various aspects of outdoor fabric durability [10]. Outdoor exposures caused strength losses for all materials; cotton blends exhibited the smallest decreases. In another recent study, standard and recycled polyester sportswear knits under natural weathering were examined, and significant strength and moisture-management degradations were reported for recycled samples [11].

Despite the studies mentioned, there is still a knowledge gap concerning how fully and semi-recycled cotton/polyester blends perform as outdoor upholstery fabrics under natural weathering. Especially, data that compares mechanical property alteration across virgin, semi-recycled, and fully recycled yarns in a plain-weave construction after a specified period of natural weathering are insufficient. Addressing this gap is crucial for guiding manufacturers toward sustainable choices without compromising durability and also providing knowledge for researchers who study this subject. However, no previous study has systematically compared the mechanical deterioration of virgin, semi-recycled, and fully recycled cotton/polyester plain-weave upholstery fabrics under identical natural weathering durations.

This study aimed to provide science-based insights for recycled outdoor textiles in terms of sustainability and durability under outdoor conditions by comparing them with untreated fabrics. Therefore, the study investigated the impact of natural weathering on the mechanical properties of outdoor upholstery fabrics produced from three types of cotton/polyester blended yarns: virgin, semi-recycled, and fully recycled. In this direction, tensile strength, elongation at break, circular bending rigidity, and weight loss percentage after abrasion were measured, and fabric performance and yarn types were compared after different exposure durations. The findings will contribute to the development of upholstery fabrics that are sustainable with acceptable performance.

MATERIALS AND METHODS

Fabric production

In this study, three different types of cotton/polyester blended yarns were used as weft yarns to produce woven fabrics in plain weave construction. All purchased yarns were Ne 20/2 open-end yarns, and the recycled ones were produced from pre-consumer

Table 1

DETAILED INFORMATION OF YARNS AND FABRIC PRODUCTION

Yarn code	Yarn type	Weft yarn composition	Warp yarn composition	Weft density	Warp density	Fabric construction
FRY[1]	Recycled cotton/ recycled polyester	50% recycled cotton, 50% recycled polyester	100 % cotton	20 and 28 picks/cm	14 ends/cm	Plain weave
SRY[2]	Recycled cotton/ virgin polyester	50% recycled cotton, 50% virgin polyester				
VY[3]	Virgin cotton/virgin polyester	50% virgin cotton, 50% virgin polyester				

Note: [1]FRY: Full recycled blended yarn; [2]SRY: Semi recycled blended yarn; [3]VY: Virgin blended yarn.

textile wastes. The fabrics were woven on a Sulzer Ruti projectile weaving machine, and six types of plain fabrics with two different weft densities were produced. Information regarding the yarns and fabric production details is given in table 1.

Natural weathering of fabrics

Natural weathering was carried out in Izmir, Türkiye (38° 24' 09" N and 27° 09' 21" E). Fabrics were divided into three groups for testing. The first group was exposed to sunlight and natural outdoor conditions for three months during summer (June-August), while the second group was subjected to the same conditions for an additional three months during autumn (September-November) to ensure a total of 6 months' exposure. To ensure better exposure of the samples to sunlight, the fabrics were positioned at an angle of approximately 45° towards the south. Meteorological data, including temperature, relative humidity, UV index, cloud cover, and rainfall, were obtained from publicly available meteorological records and monitored at two-hour intervals throughout the exposure period. Table 2 summarises the natural weathering conditions.

All fabrics were greige fabrics and were not exposed to any finishing processes except home laundering. Home laundering was conducted to reduce the stresses formed during fabric production and to prevent possible shrinkage effects that may occur during the following washing processes [12, 13]. The laundering process was performed at 40°C for 90 minutes, using 50 g of colormatic detergent, followed by air-drying at room temperature. This procedure was repeated for all fabrics at the end of each month during the natural weathering process. The third group was the control group and was only exposed to a single laundering cycle once before mechanical tests.

The UV Index (UVI) is defined as an irradiance scale computed by multiplying the erythemally weighted UV irradiance, and is converted to erythemally weighted UV irradiance (E_{ery}, W/m^2) using the internationally accepted formula given in equation 1. This conversion factor of 40 m^2/W corresponds to the definition of the UV Index, which represents forty times the erythemally weighted irradiance [14–16]. Thus, UV Index values were consistently expressed as physical irradiance (W/m^2) to enable quantitative comparison with fabric exposure data and the calculated UV irradiance values for each month are presented in table 2.

$$E_{ery}\ (\mathrm{W/m^2}) = UVI/40 \qquad (1)$$

Mechanical tests

Various tests were conducted on both untreated and naturally weathered fabrics. Fabric weight (TS EN 12127) and fabric thickness (TS 7128 EN ISO 5084) were measured initially for untreated fabrics, and measurements were repeated after three and six months of natural weathering. All fabrics were subjected to abrasion on the James Heal Martindale device, following the TS EN ISO 12947-2 standard. In this study, sandpapers were used instead of standard wool fabric as an abradant to observe yarn breakage at lower cycle numbers and to perform the tests more efficiently and effectively [17–19]. Two different sandpaper grit sizes (Atlas P600C and P1200C) were selected to simulate the performance of fabrics under varying abrasive conditions, as reported in previous studies [17, 20, 21]. P600 sandpaper, providing a coarser and faster abrasion, and P1200 sandpaper, serving as a finer and milder abrasive, were used. After a specified number of cycles, the fabric weights were measured, and weight loss percentages were calculated. Tensile strength tests of fabric samples were carried out on a Lloyd tensile tester (TS EN ISO 13934-1), and circular bending rigidity was measured using a Shirley circular bending tester (ASTM D 4032).

Statistical analysis

The results obtained from the mechanical tests were statistically analysed using SPSS Statistics 25 software. The data collected from tests such as weight loss percentage after abrasion, tensile strength, elongation, and circular bending rigidity were first subjected to a normality test. Since the fabric tensile

Table 2

NATURAL WEATHERING CONDITIONS					
Months	**Temperature (°C) M±SD**	**Humidity (%) M±SD**	**UV Index M±SD**	**Cloud cover (%) M±SD**	**Rainfall amount (mm) M±SD**
1st Month	27.80±3.46	49.00±16.14	5.50±2.79	30.6±28.55	0.14±0.63
2nd Month	34.12±3.28	30.20± 8.32	6.07±2.85	9.30±11.73	0.00±0.00
3rd Month	32.64±2.83	42.84±10.39	5.25±2.80	9.26±11.50	0.00±0.00
4th Month	28.60±3.62	42.50±11.28	3.72±2.39	24.90±19.92	0.05±0.68
5th Month	23.20±4.02	41.36±10.51	2.23±1.67	25.17±25.57	0.00±0.00
6th Month	15.02±4.02	59.59±18.38	1.16±1.00	42.31±34.60	0.15±0.78
No rainfall was recorded during the 2nd, 3rd and 5th months.					

CALCULATED ERYTHEMALLY WEIGHTED UV IRRADIANCE VALUES						
Month	1	2	3	4	5	6
UV Irradiance (W/m²)	0.138	0.152	0.131	0.093	0.056	0.029

Table 3

FABRIC WEIGHT(g/m^2) AND FABRIC THICKNESS (mm) VALUES OF UNTREATED AND NATURALLY WEATHERED FABRICS						
Fabric code	**Untreated**		**3-month natural weathering**		**6-month natural weathering**	
	Weight	**Thickness**	**Weight**	**Thickness**	**Weight**	**Thickness**
1	232.833	0.729	233.667	0.781	235.500	0.790
2	306.833	0.815	310.137	0.831	306.333	0.803
3	225.333	0.690	228.333	0.745	227.000	0.738
4	290.833	0.757	297.833	0.814	297.333	0.794
5	225.333	0.703	228.667	0.728	227.833	0.717
6	290.500	0.727	302.000	0.792	301.167	0.759

strength values showed a normal distribution, a one-way ANOVA was performed. In contrast, the data obtained from the abrasion-induced weight loss and circular bending tests did not meet the normality assumption; therefore, the nonparametric Friedman test was conducted to evaluate the fabric properties measured in the untreated condition and after exposure to different natural weathering durations. The Wilcoxon signed rank test was used to compare two related samples, such as the effect of different sandpaper types on the same fabrics under various weathering conditions. The Bonferroni correction was applied in the post hoc tests.

RESULTS AND DISCUSSION

Fabric weight and thickness values of untreated fabrics and naturally weathered fabrics are given in table 3.

The fabric weight and thickness values slightly increased after natural weathering. This small increase may be explained by the moisture absorption of fabrics from the air, because the moisture in the structure of textiles directly affects the weight and thickness of the fabrics [22]. In addition, the monthly home laundering performed during the study may contribute to this minor change, as indicated in the literature [23]. Even though the values became slightly higher for some samples, the differences were not very noticeable. Therefore, it can be said that up to six months of natural weathering does not cause any serious damage to the structure of the woven fabrics.

Weight loss percentages of untreated and naturally weathered fabrics after 200 abrasion cycles with P1200 sandpaper are presented in table 4. The weight loss values of the fabrics slightly decreased after three months of natural weathering. This result indicates a temporary improvement in abrasion resistance. However, after six months, the values tended to increase again for some samples, especially for the 1st, 2nd, and 6th fabrics. According to this result, it can be said that long-term exposure to outdoor conditions weakened the fibres and reduced the abrasion resistance of fabrics. A similar trend was reported in a study on knitted cotton fabrics exposed to outdoor conditions [24]. Nevertheless, statistical analysis revealed no significant difference between the weight loss values of the samples abraded with P1200 sandpaper in the untreated condition and after three or six months of natural weathering ($p>0.05$).

Table 4

WEIGHT LOSS (%) AFTER 200 ABRASION CYCLES WITH P1200 SANDPAPER			
Fabric code	**Untreated**	**3-month natural weathering**	**6-month natural weathering**
1	1.4	1.2	1.4
2	1.2	0.2	1.4
3	0.4	1.0	0.6
4	1.8	1.2	0.8
5	1.2	1.6	1.0
6	1.8	1.0	1.2

Table 5 presents the weight loss of fabrics after 50 abrasion cycles with two different sandpapers. As expected, the fabrics tested with P600 showed slightly higher weight loss than those tested with P1200 due to its rougher surface. After three months of natural weathering, weight loss generally increased, especially for fabrics abraded with P600, which suggests that short-term outdoor exposure made the surface fibres slightly weaker, as mentioned above. After six months, however, the weight loss tended to decrease for several samples. Friedman test results indicate that the differences among the weight loss percentages of the same samples were not statistically significant for either P1200 or P600 sandpapers ($p>0.05$). In addition, the possible effect of sandpaper type on the same samples under different conditions (untreated, 3-month, and 6-month weathered) was also investigated. Based on the Wilcoxon test results, no statistically significant relationship was found between them ($p>0.05$). Some samples showed slightly negative weight loss values (e.g., –0.2% for samples 2 and 4). These values reflect the limits of experimental measurement, including the sensitivity of the precision balance, the low number of abrasion cycles, minor fibre accumulation remaining on the fabric surface, and possible static effects during weighing. Therefore, these small negative values are within acceptable measurement uncertainty and do not indicate an actual increase in fabric mass.

Table 5

COMPARISON OF WEIGHT LOSS % AFTER 50 ABRASION CYCLES WITH P600 AND P1200						
Fabric code	**Untreated**		**3-month natural weathering**		**6-month natural weathering**	
	P600	**P1200**	**P600**	**P1200**	**P600**	**P1200**
1	1.6	1.0	1.6	0.8	0.6	0.0
2	1.0	0.6	1.6	-0.2	0.6	1.0
3	0.8	0.2	1.8	0.6	0.4	1.0
4	0.8	0.8	–0.2	0.6	0.6	0.0
5	0.4	1.8	1.0	1.0	0.8	1.0
6	0.6	0.6	1.4	0.4	0.6	0.6

Fabric tensile strength and elongation at break values of fabric samples are given in table 6. For all samples and all conditions, the tensile strength values in the weft direction are higher than those in the warp direction, as expected, due to the presence of polyester fibres in the weft. Therefore, it can be concluded that polyester fibre's crystalline structure plays a decisive role in tensile behaviour [25]. Although tensile strength remained higher in the weft direction, the percentage reduction in strength after exposure to natural weathering was greater in the weft direction, which may be attributed to interfacial weakening between polyester and cotton fibres under prolonged UV and moisture exposure, as also emphasised in a previous study [26]. Nevertheless, the weft yarns still maintained higher overall tensile strength due to the inherent durability of polyester fibres against environmental stress.

The results also clearly demonstrate the effect of weft density (20 and 28 picks/cm) and yarn type (FRY, SRY, and VY) on the tensile strength of the fabrics. As expected, fabrics with higher weft densities exhibited significantly higher tensile strength, particularly in the weft direction [27]. When evaluated based on yarn type, fabrics containing VY exhibited the highest tensile strength, followed by SRY and FRY, as reported in [28]. The tensile strength of recycled yarns and fabrics was found to be lower than that of virgin ones. Additionally, when tensile strength and tensile elongation at break values of the same samples under different conditions were evaluated, a general decreasing trend was observed in both warp and weft directions from the untreated state to six months of outdoor exposure, as also reported in previous studies [29–31]. This trend was also statistically supported by the ANOVA results, showing significant differences among different time periods ($p<0.05$) in both warp and weft directions for all yarn types. Bonferroni pairwise comparisons revealed that the greatest decreases occurred between the untreated and weathered samples (Un–3M and Un–6M), with p-values mostly below 0.05, indicating significant strength loss after exposure. Conversely, the differences between 3-month and 6-month exposures (3M–6M) were statistically insignificant in most cases (p-values ranging from 0.13 to 0.86). This finding suggests that the majority of mechanical degradation occurred within the first three months of natural weathering. After this initial stage, the rate of degradation slowed because the most easily damaged fibre surfaces and weak fibre bonds had already separated from the fabric structure during the early exposure period.

In terms of elongation at break, a gradual decrease occurred in both warp and weft directions with increasing exposure time. This reduction indicates that fibres became more brittle and less flexible after natural weathering [31]. Additionally, elongation at break values were generally higher in the weft direction due to the presence of polyester fibres, which provide better elasticity and resilience compared to cotton [32]. Significant differences ($p<0.05$) were observed in elongation values for most weft directions,

Table 6

FABRIC TENSILE STRENGTH AND ELONGATION AT BREAK												
Fabric code	**Untreated**				**3-month natural weathering**				**6-month natural weathering**			
	Tensile strength (N)		**Elongation at break (mm)**		**Tensile strength (N)**		**Elongation at break (mm)**		**Tensile strength (N)**		**Elongation at break (mm)**	
	Warp	Weft	Warp	Weft	Warp	Weft	Warp	Weft	Warp	Weft	Warp	Weft
1	593.43	626.71	56.10	75.21	465.09	515.66	42.18	72.59	488.74	399.02	48.30	64.87
2	640.33	1004.13	38.60	89.13	505.85	832.52	30.21	85.66	581.15	747.61	34.99	82.10
3	587.85	918.02	56.59	77.45	504.33	580.14	53.80	63.59	426.60	443.73	51.62	60.53
4	614.44	1331.13	41.19	89.44	559.15	850.86	36.50	77.73	426.21	776.05	35.27	77.82
5	627.93	904.79	57.00	78.09	526.84	584.72	50.33	69.79	501.58	598.78	51.81	68.30
6	664.03	1354.33	40.14	91.60	613.21	1031.11	34.94	87.10	557.47	862.81	36.93	79.93

particularly between untreated and 6-month naturally weathered samples.

Statistical analysis showed clear differences in tensile strength among the same samples at different exposure times. These differences were consistent across all samples (1–6) with $p<0.05$.

Similarly, noticeable changes in elongation at break values were observed for most samples. Pairwise comparisons were conducted, and the outcomes of the ANOVA and Bonferroni tests are summarised in table 7. Overall, the statistical results confirm that both tensile strength and elongation at break were significantly influenced by exposure duration, fabric structure, and yarn composition, with the most obvious statistical significance for tensile strength observed in the weft direction ($p<0.001$).

Circular bending rigidity results of the fabric samples are presented in table 8. Generally, a slight increase in rigidity values was observed after natural weathering, indicating a moderate stiffening effect. This finding suggests that extended outdoor exposure may have slightly altered the fibre surfaces and increased the structural compactness of the fabrics due to monthly repeated home laundering. Thereby, it causes a decrease in fabric flexibility. The degree of this change seems to vary depending on the fabric structure and yarn composition. Rigidity values gradually increased from the untreated condition to the 6-month exposure for samples 4, 5, and 6. In contrast, samples 2 and 3 exhibited a minor increase for the first three-month period, followed by a minor decrease for the last three-month period. Fabric stiffness tends to increase with higher weft density. Minor differences between samples related to yarn type were also observed, but these can be considered negligible.

Table 7

ONE-WAY ANOVA RESULTS FOR TENSILE STRENGTH AND ELONGATION AT BREAK

Fabric code	Direction	Tensile strength			Elongation at break		
		F (2,6)	Sig. (p)	Post Hoc	F (2,6)	Sig. (p)	Post Hoc
1	Warp	22.611	**0.002**	Un–3M=**0.002** Un–6M=**0.006** 3M–6M=0.866	30.366	**0.001**	Un–3M=**0.001** Un–6M=**0.014** 3M–6M=**0.043**
	Weft	118.648	**<0.001**	Un–3M=**0.001** Un–6M=**0.000** 3M–6M=**0.001**	10.362	**0.011**	Un–3M=0.932 Un–6M=**0.014** 3M–6M=0.051
2	Warp	8.314	**0.019**	Un–3M=**0.020** Un–6M=0.371 3M–6M=0.189	67.951	**<0.001**	Un–3M=**0.000** Un–6M=**0.007** 3M–6M=**0.002**
	Weft	30.469	**0.001**	Un–3M=**0.006** Un–6M=**0.001** 3M–6M=0.133	4.741	0.058	-
3	Warp	13.557	**0.006**	Un–3M=0.107 Un–6M=**0.006** 3M–6M=0.138	1.779	0.247	-
	Weft	383.609	**<0.001**	Un–3M=**0.000** Un–6M=**0.000** 3M–6M=**0.001**	54.971	**<0.001**	Un–3M=**0.001** Un–6M=**0.000** 3M–6M=0.376
4	Warp	61.664	**<0.001**	Un–3M=0.058 Un–6M=**0.000** 3M–6M=**0.001**	15.707	**0.004**	Un–3M=**0.017** Un–6M=**0.005** 3M–6M=0.940
	Weft	84.363	**<0.001**	Un–3M=**0.000** Un–6M=**0.000** 3M–6M=0.474	35.542	**<0.001**	Un–3M=**0.001** Un–6M=**0.001** 3M–6M=**1.000**
5	Warp	59.813	**<0.001**	Un–3M=**0.001** Un–6M=**0.000** 3M–6M=0.253	24.450	**0.001**	Un–3M=**0.002** Un–6M=**0.006** 3M–6M=0.569
	Weft	100.293	**<0.001**	Un–3M=**0.000** Un–6M=**0.000** 3M–6M=1.000	15.060	**0.005**	Un–3M=**0.015** Un–6M=**0.007** 3M–6M=1.000
6	Warp	22.501	**0.002**	Un–3M=0.056 Un–6M=**0.002** 3M–6M=**0.038**	17.005	**0.003**	Un–3M=**0.004** Un–6M=**0.036** 3M–6M=0.206
	Weft	75.731	**<0.001**	Un–3M=**0.001** Un–6M=**0.000** 3M–6M=**0.018**	15.867	**0.004**	Un–3M=0.224 Un–6M=**0.004** 3M–6M=**0.042**

Pairwise comparisons: *Un–3M: Untreated-3 Month weathering, Un-6M: Untreated-6 Month weathering, 3M-6M: 3 Month weathering-6 Month weathering*

Nevertheless, differences between measurements of the same samples at different exposure times were also statistically evaluated. Statistical analysis revealed that significant differences were only observed between the measurement periods for samples 2 ($p=0.050$) and 6 ($p=0.050$). According to pairwise comparisons, significant differences were found for sample 2 (between 3-month and 6-month natural weathering periods), and for sample 6 (between untreated and 6-month natural weathering conditions) ($p<0.05$).

Table 8

CIRCULAR BENDING RIGIDITY			
Fabric code	**Untreated**	**3-month natural weathering**	**6-month natural weathering**
1	4.10	4.00	4.65
2	7.65	8.53	7.20
3	4.43	5.15	4.63
4	7.10	7.88	8.20
5	4.10	4.43	4.88
6	7.43	8.20	8.98

CONCLUSION

This study comprehensively evaluated how the mechanical performance of outdoor upholstery fabrics produced from virgin, semi-recycled, and fully recycled cotton/polyester yarns changed after exposure to natural weathering conditions such as UV radiation, temperature, and humidity in comparison with their untreated references. The study results clearly demonstrate that the mechanical stability of the fabrics is significantly affected by yarn type after exposure to natural weathering conditions.

Virgin fabrics demonstrated the highest durability across all measured properties and retained a significant portion of their tensile strength, flexibility, and abrasion resistance even after six months of outdoor exposure. Semi-recycled fabrics exhibited moderate but acceptable performance, although with some reductions in strength and elongation. Fully recycled fabrics exhibited the highest mechanical deterioration, although they are environmentally advantageous. The most apparent mechanical deterioration occurred during the first three months of natural weathering, after which the rate of degradation slowed considerably. Semi-recycled yarn blends demonstrated mechanical performance close to that of virgin fabrics, particularly in tensile strength retention, indicating their feasibility for outdoor applications.

Overall, the results confirm that fabric structure, yarn type and exposure time significantly affect the mechanical behaviour of outdoor upholstery fabrics. Additionally, the data obtained from the research reveals that recycled yarns are applicable for sustainable textile solutions when the raw material blend ratio of yarns is carefully optimised. Semi-recycled yarns, in particular, are clearly a sustainable and promising alternative to virgin yarns, demonstrating comparable performance to virgin yarns for outdoor applications.

In conclusion, this study provides valuable scientific data for the field of sustainable textiles, which has gained increasing importance in recent years, by examining and comparing the mechanical performance of recycled fabrics under natural weathering conditions.

REFERENCES

[1] Arshad, Z., Alharthi, S.S., *Enhancing the thermal comfort of woven fabrics and mechanical properties of fiber-reinforced composites using multiple weave structures*, In: Fibres, 2023, 11, 9, 73

[2] Levent, T., *Upholstery fabrics as a design element in interior space and selection criterias*, In: Muğla Journal of Science and Technology, 2016, 2, 2, 38–43

[3] Friant, M.C., Vermeulen, W.J., Salomone, R., *Analysing European Union circular economy policies: words versus actions*, In: Sustainable Production and Consumption, 2021, 27, 337–353

[4] Esi, B., Baykal, P.D., *Investigation of tensile strength and elongation properties of chenille upholstery fabrics including recycling polyester yarns*, In: Journal of Engineered Fibres and Fabrics, 2020, 15

[5] Özdil, N., Dalbaşı, E.S., Özgüney, A.T., Atiker, L., *Thermal comfort properties of woven upholstery fabrics*, In: AATCC Journal of Research, 2023, 10, 4, 223–231

[6] Nikafshar, S., Zabihi, O., Ahmadi, M., Mirmohseni, M., Taseidifar, M., Naebe, M., *Thermoplastic composites reinforced with natural fibres*, In: Materials, 2017, 10, 2, 180

[7] El Messiry, M., Mito, A.B., Issa, S., *Multi-criteria decision analysis for supporting the selection of car upholstery fabric under degradation due to UV exposure*, In: Journal of Engineered Fibres and Fabrics, 2022, 17

[8] Moezzi, M., Yekrang, J., Ghane, M., Hatami, M., *Mechanical behavior of industrial textiles*, In: Journal of Industrial Textiles, 2020, 50, 2, 240–260

[9] Aparicio-Ardila, M.A., Pedroso, G.O.M., Kobelnik, M., Valentin, C.A., da Luz, M.P., Lins da Silva, J., *Evaluating the degradation of a nonwoven polypropylene geotextile exposed to natural weathering for 3 years*, In: International Journal of Geosynthetics and Ground Engineering, 2021, 7, 1–11

[10] Tayyar, A.E., Alan, G., *Mechanical performance of woven fabrics*, In: The Journal of the Textile Institute, 2015, 106, 3, 303–310

[11] Katić Križmančić, I., Salopek Čubrić, I., Potočić Matković, V.M., Čubrić, G., *Changes in Mechanical Properties of Fabrics Made of Standard and Recycled Polyester Yarns Due to Aging*, In: Polymers, 2023, 15, 23, 4511
[12] Sohaib Anas, M.S.A., Abbas, A., Azam, Z., Tariq, Z., Gul, Z., Sarwar, M.E., *Mechanical performance of engineered fiber fabrics*, In: Journal of Engineered Fibres and Fabrics, 2022, 17, 1–10
[13] Ahmad, M., Sun, D., Hussain, T., *Influence of core spun yarn characteristics on shrinkage and stretch behavior of woven fabrics*, In: Journal of Natural Fibres, 2025, 22, 1, 2512395
[14] Tereszchuk, K.A., Rochon, Y.J., McLinden, C.A., Vaillancourt, P.A., *Atmospheric modeling of UV radiation*, In: Geoscientific Model Development, 2018, 11, 3, 1093–1113
[15] Fioletov, V., Kerr, J.B., Fergusson, A., *The UV index: definition, distribution and factors affecting it*, In: Canadian Journal of Public Health, 2010, 101, 4, I5–I9
[16] Schmalwieser, A.W., Lohr, M.A., Daly, S.M., Williams, J.D., *Advances in UV radiation research*, In: Photochemical and Photobiological Sciences, 2023, 22, 1, 1–20
[17] Avcu, Ö., Gürkan Ünal, P., *Mechanical properties of double-layered woven fabrics used in car seat upholstery*, In: The Journal of the Textile Institute, 2018, 109, 11, 1409–1417
[18] Özdil, N., Kanat, Z.E., Topuz, B.E., Özçelik, G., Mengüç, G.S., *Properties of the fabrics knitted from yarns with different slub parameters*, In: Industria Textila, 2025, 76, 1, 89–97, https://doi.org/10.35530/IT.076.01.202452
[19] Özdil, N., Kayseri, G.Ö., Mengüç, G.S., *Abrasion resistance of materials*, In: Abrasion Resistance of Materials, Adamiak, M. (Ed.), InTech, Rijeka, 2012, 119–146
[20] Jerkovic, I., Pallares, J.M., Capdevila, X., *Study of the abrasion resistance in the upholstery of automobile seats,* In: AUTEX Research Journal, 2010, 10, 1, 14–20
[21] Jerkovic, I., Pallarés, J.M., Ardanuy, M., Capdevila, X., *Abrasion behavior of upholstery fabrics*, In: Journal of Engineered Fibres and Fabrics, 2013, 8, 3, 1–10
[22] Garg, S., Midha, V.K., Sikka, M., *Studies on thermal comfort of multi-layered fabric assembly after wetting with sweat and distilled water*, In: Journal of Industrial Textiles, 2022, 52, 15280837221110105
[23] Demiryürek, O., Güleyüpoğlu, İ., Turhan, E., *Effects of repeated laundering on thermal comfort properties of cellulosic knitted fabrics*, In: Cellulose Chemistry and Technology, 2019, 53, 7
[24] Katogi, H., Tsunekawa, H., *Engineering performance of textile structures*, In: WIT Transactions on Engineering Sciences, 2021, 133, 47–54
[25] Akter, N., Repon, M.R., Pranta, A.D., Islam, S., Khan, A.A., Malik, A., *Effect of cotton–polyester composite yarn on the physico-mechanical and comfort properties of woven fabric*, In: SPE Polymers, 2024, 5, 4, 557–567
[26] Üzümcü, B., Sarı, B., Temel, E., *Mechanical performance of apparel textiles*, In: Textile and Apparel, 2024, 34, 1, 51–68
[27] Bedez Ute, T., *Analysis of mechanical and dimensional properties of the denim fabrics produced with double-core and core-spun weft yarns with different weft densities*, In: The Journal of the Textile Institute, 2019, 110, 2, 179–185
[28] Yuksekkaya, M.E., Celep, G., Dogan, G., Tercan, M., Urhan, B., *Mechanical properties of engineered fabrics*, In: Journal of Engineered Fibres and Fabrics, 2016, 11, 2, 1–10
[29] Potočić Matković, V.M., Skenderi, Z., *Mechanical performance of woven structures*, In: Fibres and Textiles in Eastern Europe, 2017, 25, 4, 124–130
[30] Asadi, H., Uhlemann, J., Stranghoener, N., Ulbricht, M., *Tensile strength deterioration of PVC coated PET woven fabrics under single and multiplied artificial weathering impacts and cyclic loading*, In: Construction and Building Materials, 2022, 342, 127843
[31] Jie, S.Y., Hoe, L.Z., Paul, S.C., Anggraini, V., *Mechanical and durability performance of applied science materials*, In: Applied Sciences, 2022, 12, 22, 11440
[32] Babaarslan, O., Shahid, M.A., Okyay, N., *Investigation of the performance of cotton/polyester blend in different yarn structures*, In: AUTEX Research Journal, 2023, 23, 3, 370–380

Author:

ELIF YILMAZ

Ege University, Emel Akın Vocational Training School, 35040, Izmir, Turkey

Corresponding author:

ELIF YILMAZ
e-mail: elif.yilmaz@ege.edu.tr